



**Fakultät für Medizin**

**Institut für Experimentelle Onkologie und Therapieforschung**

# **Immunological aspects of YB-1-dependent oncolytic virotherapy**

**Vroni Girbinger**

Vollständiger Abdruck der von der Fakultät für Medizin der Technischen Universität München zur Erlangung des akademischen Grades eines

**Doctor of Philosophy (Ph.D.)**

genehmigten Dissertation.

**Vorsitzende:** Univ.-Prof. Dr. Agnes Görlach

**Betreuer:** Priv.-Doz. Dr. Per Sonne Holm

**Prüfer der Dissertation:**

1. Univ.-Prof. Dr. Gabriele Multhoff
2. Priv.-Doz. Dr. Oliver Ebert

Die Dissertation wurde am 01.08.2013 bei der Fakultät für Medizin der Technischen Universität München eingereicht und durch die Fakultät für Medizin am 31.08.2013 angenommen.

## Table of Contents

<b>Table of Contents</b> .....	1
<b>Summary</b> .....	5
<b>1. Introduction</b> .....	7
1.1. The cancer problem and limitations of conventional cancer therapy.....	7
1.2. Current state of research in oncolytic virotherapy.....	8
1.3. Adenovirus biology.....	9
1.3.1. Adenoviruses.....	9
1.3.2. Adenoviral life cycle.....	10
1.3.3. Adenoviral gene regulation.....	11
1.4. Nature and application of oncolytic adenoviruses.....	12
1.4.1. Oncolytic adenoviruses.....	12
1.4.2. Arming of oncolytic viruses with immunostimulatory transgenes.....	14
1.5. The multifunctional cellular protein YB-1.....	15
1.6. YB-1-dependent oncolytic adenoviruses.....	17
1.7. Need for immunocompetent tumor models to test YB-1-dependent oncolysis.....	19
1.8. Immunogenicity of therapy-induced tumor cell death.....	20
1.9. Adenoviruses-host interactions.....	23
1.9.1. Immune defense against adenoviruses.....	23
1.9.2. Immune evasion strategies of adenoviruses.....	25
1.9.3. Cell death modulation by adenoviruses.....	27
1.10. Objective.....	28
<b>2. Materials and Methods</b> .....	29
2.1. Materials.....	29
2.1.1. Laboratory equipment.....	29
2.1.2. Software and web portals.....	31
2.1.3. Consumables.....	31
2.1.4. Chemicals.....	33
2.1.5. Commercially available buffers, standards, and other biochemical substances.....	34
2.1.6. Prepared buffers and solutions.....	35
2.1.7. Kits.....	36
2.1.8. Enzymes.....	36
2.1.9. Antibiotics and cytostatic drugs.....	37

## Table of Contents

---

2.1.10. Cytokines .....	38
2.1.11. Primers.....	38
2.1.12. Antibodies.....	39
2.1.13. Cell culture media and supplements.....	40
2.1.14. Cell lines.....	41
2.1.15. Viruses .....	42
2.1.16. Mice .....	43
2.2. Methods .....	44
2.2.1. Cell culture.....	44
2.2.2. Virus amplification and purification .....	44
2.2.3. Determination of viral titer, particle count, purity, size, and homogeneity .....	46
2.2.4. DNA isolation and PCR analysis of viral genes.....	47
2.2.5. Virus infection.....	48
2.2.6. Flt3L ELISA.....	48
2.2.7. Immunofluorescence staining of YB-1 expression .....	49
2.2.8. Cytotoxicity assay <i>in vitro</i> by SRB staining of infected cells .....	49
2.2.9. Monitoring of virus infection with quantitative real time PCR .....	49
2.2.10. Analysis of formation of new infectious virus particles.....	50
2.2.11. Cellular protein isolation and WB analysis .....	51
2.2.12. Flow cytometric analysis of <i>in vitro</i> samples .....	52
2.2.13. Apoptosis monitoring by caspase activity assay.....	53
2.2.14. Analysis of HMGB1 release into cell supernatants.....	53
2.2.15. Analysis of ATP release into cell supernatants .....	54
2.2.16. KLN205 <i>in vivo</i> model .....	54
2.2.17. Serum collection .....	55
2.2.18. Splenocyte isolation.....	56
2.2.19. Flow cytometric analysis of immune cell surface markers on blood cells and splenocytes .....	56
2.2.20. Immunohistological analysis of murine tumors .....	57
2.2.21. Anti-viral antibody detection by ELISA .....	58
2.2.22. Determination of HMGB1 and ATP in mouse serum.....	59
2.2.23. IFN $\gamma$ ELISpot analysis.....	59
2.2.24. Calcein release and retention assay .....	60

<b>3. Results</b> .....	61
3.1. Production and validation of YB-1-dependent oncolytic adenoviruses.....	61
3.1.1. Adenovirus production yields good quality viruses for <i>in vitro</i> and <i>in vivo</i> experiments .....	61
3.1.2. Verification of viral mutations critical for tumor specificity, oncolytic efficacy, and immune recognition .....	62
3.1.3. Flt3L is efficiently released in the supernatant of Ad-Delo3-RGD-Flt3L infected cells <i>in vitro</i> .....	63
3.2. KLN205 lung cancer cells as a murine model for YB-1-dependent oncolysis.....	64
3.2.1. Murine KLN205 and CMS-5 cells, and Syrian hamster HaK cells are infectable by adenoviruses.....	64
3.2.2. Non-human cell lines HaK, KLN205, and CMS-5 cells allow formation of viral particles . .....	66
3.2.3. Murine cell lines have sufficiently high expression of YB-1 to enable YB-1-dependent oncolysis .....	67
3.3. Replication of and tumor cell lysis by YB-1-dependent oncolytic adenoviruses <i>in vitro</i> ....	69
3.3.1. YB-1-dependent oncolytic adenoviruses replicate in tumor cells and form infectious progeny.....	69
3.3.2. Cytotoxicity of YB-1 dependent oncolytic adenoviruses.....	71
3.4. Induction of different modes of cell death by wild type and oncolytic adenoviruses.....	72
3.4.1. Replicating adenoviruses induce apoptosis in murine and human tumor cells.....	72
3.4.2. Adenoviruses cause no major induction of autophagy in murine and human tumor cells .....	75
3.4.3. YB-1-dependent oncolytic adenoviruses trigger exposure and release of several ICD molecules <i>in vitro</i> .....	76
3.5. Less interference of YB-1-dependent oncolytic adenoviruses than of Ad-wt with MHCI expression and IFN signaling .....	80
3.6. Use of immunocompetent KLN205 cells in DBA/2 mice to test efficacy of YB-1-dependent oncolytic adenoviruses <i>in vivo</i> .....	83
3.7. Reduction of tumor growth after oncolytic adenoviral treatment.....	84
3.8. Mediation of tumor inflammation by replicating adenoviruses .....	85
3.9. Adenovirus-mediated immune cell recruitment.....	87
3.9.1. Adenovirus treatment of tumors increases spleen weight and blood leukocyte counts. .....	87
3.9.2. Ad-wt and Ad-PSJL-K elicit increased recruitment of several immune cell populations into the blood .....	88
3.10. Efficient anti-virus host immune response .....	90

---

3.11. Anti-tumor immune reactions elicited by YB-1-dependent virotherapy .....	91
3.11.1. Replicating or conditionally replicating viruses induce exposure and release of ICD molecules in mice .....	91
3.11.2. Adenoviral treatment is able to trigger anti-tumor immune responses .....	93
<b>4. Discussion .....</b>	<b>98</b>
4.1. Purity and quality of adenoviruses are crucial for their application as virotherapeutics ....	98
4.2. Murine KLN205 cells express YB-1, can be infected by adenoviruses and allow viral particle formation <i>in vitro</i> .....	100
4.3. YB-1-dependent oncolytic viruses replicate in tumor cells and cause their lysis <i>in vitro</i> ..	102
4.4. Oncolytic adenoviruses cause apoptosis and immunogenic cell death .....	104
4.5. YB-1-dependent oncolytic adenoviruses do not suppress immunogenicity of tumor cells by downregulation of cellular MHC I expression and IFN signaling.....	108
4.6. YB-1-dependent oncolytic adenoviruses reduce tumor growth in immunocompetent mice .	110
4.7. Treatment of tumors with YB-1-dependent oncolytic adenovirus triggers immune cell recruitment .....	111
4.8. Adenoviral treatment elicits high anti-virus immune responses .....	113
4.9. Oncolytic adenovirus treatment enhances anti-tumor immune responses .....	116
4.10. Future prospects of oncolytic adenoviral therapy .....	121
<b>5. Appendix .....</b>	<b>123</b>
<b>Abbreviations.....</b>	<b>124</b>
<b>Figures.....</b>	<b>128</b>
<b>Tables .....</b>	<b>129</b>
<b>Bibliography.....</b>	<b>130</b>
<b>Acknowledgements .....</b>	<b>153</b>
<b>Statutory Declaration .....</b>	<b>154</b>
<b>Curriculum Vitae .....</b>	<b>155</b>

## Summary

Current treatments against cancer are lacking efficacy due to development of resistance towards cancer therapies. The cellular protein YB-1 is involved in resistance formation and maintenance. YB-1-dependent oncolytic adenoviruses thus present a promising approach to target resistant tumor cells. YB-1-dependent oncolytic adenoviruses, which are rendered YB-1- and tumor-specific by manipulation of the essential viral *E1A* region, have proven efficacy *in vitro* and in immunocompromised xenograft tumor models *in vivo*. However, a fully functional immune system can have an ambivalent impact on the efficacy of virotherapy *in vivo*. On the one hand, the immune system can hamper virus efficacy by clearance of viruses. On the other hand, it has been shown that immune cell recruitment and activity can support viral anti-tumor activity. To investigate whether the contribution of the immune system is beneficial or detrimental in the context of YB-1-dependent oncolysis, non-human cells were required, which could later be used in a syngeneic immunocompetent animal model. Murine KLN205 lung cancer cells were chosen after investigation of several non-human cells for general infectability by adenoviruses, adenovirus propagation, and YB-1 expression. YB-1-specific oncolytic adenoviruses, despite various manipulations in their genomes, were able to replicate in KLN205 cells, to produce viral progeny, and most importantly to lyse the tumor cells. Particularly viral *E1* and *E3* genes are involved in manipulation of host cell apoptosis and anti-viral immune functions. Since most of the *E1A* or *E3* genes are manipulated or deleted in the used oncolytic adenoviruses, it was investigated how cell death elicited by oncolytic adenoviral treatment differs from wild type adenovirus-mediated cell death *in vitro*, and how oncolytic viruses and immune system interact in an immunocompetent setting *in vivo*. Despite reduced capability of YB-1-dependent oncolytic adenoviruses to lyse tumor cells as compared to wild type adenovirus, oncolytic adenoviruses enhanced induction of apoptosis *in vitro*. Furthermore, the oncolytic viruses were able to trigger marked cell surface exposure or release of most of the danger molecules typically associated with an immunogenic cell death *in vitro* and *in vivo*. Oncolytic adenoviruses did not suppress tumor immunogenicity in terms of MHC I antigen presentation *in vitro* in contrast to wild type adenoviruses. Tumor growth was reduced upon administration of YB-1-specific oncolytic viruses as compared to PBS or wild type virus treatment. All replicating adenoviruses triggered inflammatory immune cell infiltration into tumors, an important prerequisite for attenuation of tumor-mediated immunosuppression. Moreover, adenoviral therapy led to recruitment of immune cells into blood and spleen. Particularly dendritic cell and T cell populations, which are known to be crucial for the *in vivo* success of adenoviral therapy, were enriched in the blood. The cellular and humoral immune reactivity was mainly directed towards the applied viruses. However, adenoviral treatment, particularly treatment with oncolytic adenoviruses, triggered

tumor-specific cytotoxic immune reactions, as assessed by measurement of splenocyte IFN $\gamma$  release, degranulation, and cytotoxicity against tumor cells. In contrast to previous reports, insertion of the immunostimulatory Flt3L transgene into one of the YB-1-dependent oncolytic adenoviruses did not improve immune cell recruitment into the blood. Surprisingly, treatment of tumors with this virus even decreased anti-viral immunity, while triggering efficient anti-tumor reactivity, as demonstrated by splenocyte IFN $\gamma$  release and splenocyte-mediated tumor cell lysis. These findings suggest that the presence of Flt3L caused a shift from anti-viral to anti-tumor immunity. In conclusion, treatment with *E1A*-deficient YB-1-specific adenoviruses was not sufficient for tumor elimination in the poorly immunogenic KLN205 cell model probably due to limited virus propagation. However, in a model that better resembles the natural human host environment for adenoviruses, or in combination with immunotherapeutic approaches, YB-1-dependent virotherapy could present a promising tool to target tumors by combined adenoviral oncolysis and adenovirus-mediated immune stimulation.

## 1. Introduction

### 1.1. The cancer problem and limitations of conventional cancer therapy

About 13% of all human deaths worldwide are accounted to cancer (Jemal et al. 2011). In western countries like in the USA 23% of deaths are cancer-related, which makes invasive cancer, next to heart diseases one of the leading causes of death in the western world (Heron 2012). Despite intensive research on the molecular mechanisms of tumor development, progression, and metastasis, as well as the development of new therapeutic options, cancer rates are still increasing (Hoyert 2012, Jemal et al. 2011). The worldwide increase is partly attributed to growth and aging of the world population, and a change of lifestyles in the economically developing countries (Jemal et al. 2011). However, the lack of decrease of cancer numbers despite intensive research also demonstrates the lack of major success in the development of new regimens. Conventional cancer therapies like surgery, radiation, and chemotherapy are still widely used despite their massive side effects, high overall toxicity, and a high frequency of recurrence due to insufficient clearing of tumor cells (Chabner and Roberts 2005). New treatment regimens such as targeted therapies like trastuzumab for breast cancer or erlotinib for non-small cell lung cancer are limited by lack of efficacy and low response rates (Chabner and Roberts 2005, McCormick 2011, Thirukkumaran and Morris 2009). Also resistances can develop against many of these therapies, as they largely do against traditional chemotherapy (Gottesman et al. 2002). Dose escalation and combination therapies designed to overcome resistance and metastasis formation and to increase efficacy are limited by a narrow therapeutic index (McCormick 2011). Targeting of either signal transduction networks or key oncogenes or even of metabolic enzymes that are commonly dysregulated in cancer can be effective. However, targeting of signal transduction networks often results in compensation through other closely related pathways (Butler et al. 2013, McCormick 2011). The ability of cancers to evade immune destruction has newly been defined as one important hallmark of cancer, which hampers therapeutic success and is not addressed by conventional and targeted therapy (Hanahan and Weinberg 2011). This ability includes the cancers' ability to survive and expand in a chronically inflamed microenvironment, their ability to evade immune recognition and their ability to actively suppress immune reactivity (Cavallo et al. 2011). Oncolytic viruses present a promising option to address existing limitations. They are highly specific to cancer cells, can reproduce and spread inside all target cells, even metastatic cells, and lyse them. Often, oncolytic viruses are even more effective in drug-resistant cells in comparison to sensitive cells due to molecular changes in resistant cells, such as elevated expression of the oncogenic Y-box binding protein 1 (YB-1), that favor viral replication.



Side effects of especially adenoviral therapy are lower than in most other therapeutic regimens, which are highly toxic to the whole organism (Parato et al. 2005, Thirukkumaran and Morris 2009).

## 1.2. Current state of research in oncolytic virotherapy

The concept of oncolytic virotherapy is especially in the focus lately, because of the first success in a clinical phase III trial, which is opening the field prominent new possibilities. Amgen's Talimogene laherparepvec<sup>1</sup>, also called T-VEC, is an oncolytic attenuated herpes simplex virus 1 (HSV-1) encoding the immunostimulatory molecule granulocyte macrophage colony-stimulating factor (GM-CSF). T-VEC is being tested for intratumoral injection into accessible melanoma lesions in patients with unresectable Stage IIIb, c and Stage IV melanoma (Kaufman and Bines 2010). Amgen announced the success of its study on 19th March 2013, when the study met its primary endpoint, the durable response rate, defined as "the rate of complete or partial response lasting continuously for at least six months". This goal was achieved in 16% of patients receiving T-VEC, compared to 2% in the control group given only GM-CSF. The second study criterion, which is said to demonstrate improved overall survival as compared to GM-CSF is expected in late 2013 (Amgen 2013). Besides the success in melanoma, T-VEC has also been successfully tested in combination with radiotherapy and cisplatin in head and neck squamous cell carcinoma (HNSCC) in clinical phase II trials (Harrington et al. 2010, Senzer et al. 2009) and is currently being tested in Phase I studies in pancreatic cancer, breast, and gastrointestinal cancers (Hu et al. 2006). T-VEC has been generally well tolerated, with most of the adverse events being mild to moderate. Side effects are mostly injection site reactions or mild flu-like symptoms (Harrington et al. 2010, Senzer et al. 2009). A selection of promising virotherapeutics that are currently tested in clinical trials is given in table 1-1.

**Table 1-1: Overview of selected currently tested virotherapeutics.**

Oncolytic virus	Application	Progress	Reference
T-VEC: modified HSV-1 with GM-CSF	Melanoma	Phase III ongoing	Kaufman and Bines 2010
T-VEC: modified HSV-1 with GM-CSF	HNSCC in combination with radiotherapy and cisplatin	Phase II completed	Harrington et al. 2010, Senzer et al. 2009
T-VEC: modified HSV-1 with GM-CSF	Breast cancer, gastrointestinal cancers	Phase I completed	Hu et al. 2006

<sup>1</sup> acquired as OncoVEX<sup>GM-CSF</sup> from BioVex Inc. in 2011

JX-594: modified vaccinia virus with GM-CSF	Hepatocellular carcinoma	Phase II completed	Heo et al. 2013, Park et al. 2008
JX-594: modified vaccinia virus with GM-CSF	Melanoma	Phase I completed	Hwang et al. 2011
Reolysin: unmodified reovirus	Melanoma	Phase II ongoing	Galanis et al. 2012
Modified measles viruses with imaging genes	Ovarian cancer, glioblastoma, myeloma	Phase I ongoing	Msaouel et al. 2012
Unmodified newcastle disease virus	Glioblastoma, solid tumors	Phase I/II completed	Freeman et al. 2006, Lorence et al. 2007
ONYX-015: modified adenovirus *	HNSCC with and without combination with conventional therapy, colorectal cancer	Phase II completed	Hamid et al. 2003, Khuri et al. 2000, Nemunaitis et al. 2001
Ad-D24: modified adenovirus	Ovarian cancer	Phase I completed	Kimball et al. 2010, Pesonen et al. 2012a
Modified adenovirus under control of a human telomerase reverse transcriptase (hTert) promoter	Solid tumors	Phase I completed	Nemunaitis et al. 2010

\*The identical vector, termed Oncorine (H101) has been approved for the therapy of head and neck cancer in China in 2005 (Frew et al. 2008, Garber 2006).

### 1.3. Adenovirus biology

#### 1.3.1. Adenoviruses

Human adenoviruses were first isolated from adenoids in 1953 (Rowe et al. 1953). They belong to the family of *Adenoviridae* and the genus of *Mastadenoviruses*. So far, about 60 human serotypes have been described, which are classified into seven species (A-G) (Robinson et al. 2013). Adenoviruses mainly cause respiratory infections, but depending on the serotype can also cause ocular, gastrointestinal, kidney, and urinary tract infections. Respiratory infections are mostly mild and self-limited due to an intact host defense in healthy patients, but can range up to severe acute respiratory disease with life-threatening viral dissemination mostly in immunologically or nutritionally compromised patients (Hierholzer 1992, Robinson et al. 2011, Robinson et al. 2013, Walsh et al. 2010).

Adenoviruses have a diameter of approximately 900 Å without their spikes and a mass of 150 MDa. They bear a linear, double-stranded (ds) DNA genome of about 36 kb (Harrison 2010,

Nemerow et al. 2012, Smith et al. 2010). In 2010, adenoviruses were visualized at nearly atomic resolution, at 3.5 Å by X-ray crystallography (Reddy et al. 2010), as well as at 3.6 Å by cryo-electron microscopy (Liu et al. 2010), establishing profound insights into adenoviral structure. The non-enveloped adenoviral particles are composed of two major structural elements, the outer capsid and the core (figure 1-1). The icosahedral shell of the virus is composed of 240 hexagon-shaped hexon homotrimers on the faces and edges of the capsid, as well as of 12 pentons on the 12 apices, each consisting of a pentagon-shaped penton base and a penton base-associated fiber trimer. Four minor capsid components (IIIa, VI, VIII, and IX) stabilize the virion capsid (Burnett 1985, Liu et al. 2010, Vellinga et al. 2005). Five out of six viral core proteins are associated with the viral genome (V, VII,  $\mu$ , the terminal protein, and IVa2). The sixth core protein, the 23K cysteine protease, is associated with virion assembly (Russell 2009, Smith et al. 2010).

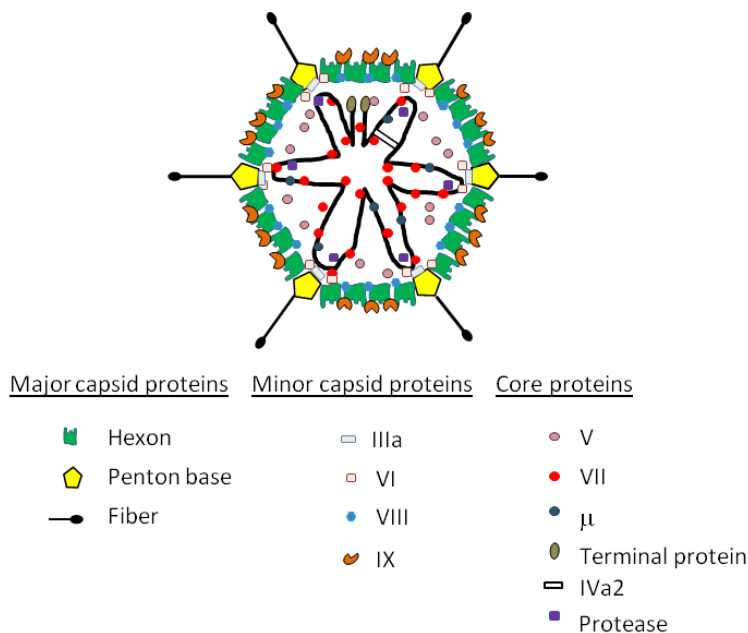


**Figure 1-1: Adenovirus assembly.** Adenoviral structural proteins are classified as capsid proteins and core proteins. The capsid proteins are two different major proteins hexon and penton (composed of penton base and fiber), and four minor capsid proteins IIIa, VI, VIII, and IX. The core proteins V, VII,  $\mu$ , the terminal protein, and IVa2 are associated with the viral DNA. The viral protease is also classified as a viral core protein (image modified from Russell 2009).

### 1.3.2. Adenoviral life cycle

Adenoviruses enter the target cells via contact of the viral fiber protein with the coxsackie virus and adenovirus receptor (CAR). However, depending on their species, adenoviruses can also interact with other receptors on the target cell surfaces like CD80, CD86, sialic acid receptors, or heparin sulfate glycosaminoglycans (Bergelson et al. 1997, Russell 2009). Accompanying the fiber-host receptor binding, an arginine-glycine-aspartic acid (RGD) peptide on the viral penton

base binds to cellular  $\alpha v\beta 3/\alpha v\beta 5$  integrins (Wickham et al. 1993). This interaction initiates the transport of bound viral particles towards clathrin-coated pits, where they get internalized by clathrin-mediated endocytosis (Meier and Greber 2004). Post endosomal acidification, the destabilized virions escape the endosome and are transported to the nuclear membrane (Leopold et al. 2000). After binding to the nuclear pore complex, the virions become disassembled and the DNA is transported into the nucleus, where DNA transcription is initiated (Russell 2009).

### **1.3.3. Adenoviral gene regulation**

The viral DNA comprises inverted terminal repeats at both genome ends and the packaging signal  $\Psi$ . The genome is built up of early and late transcription sequences, which are named after the time point of their transcription within the viral life cycle (Hay et al. 1995, Russell 2000) (figure 1-2). The early sequences (*E1-4*) are transcribed beginning 7 h after infection and code mostly for regulatory proteins. The early region 1 A (*E1A*) proteins are the first proteins of the virus that are produced. They initiate the viral replication cycle. On the one hand, they promote host cell proliferation, thus providing the appropriate cellular environment for viral replication. *E1A* proteins bind to host cell retinoblastoma proteins (pRb) and thereby disrupt pRb-E2F complexes. Consequently, the transcription factor E2F is released and mediates the host cell cycle entry from G0/G1 into the S phase (Fattaey et al. 1993, Frisch and Mymryk 2002). *E1A* proteins can also promote S phase entry via direct targeting of the phosphatase cell division cycle 25 homolog a (*cdc25a*) (Spitkovsky et al. 1996). On the other hand, *E1A* proteins transactivate the transcription of the following delayed early genes *E2-4*, as well as of cellular genes. The *E1A* transcript comprises different mRNAs generated by alternative splicing. Important for the major *E1A* functions are the 289 amino acid (aa) and 243 aa proteins, encoded by 13S and 12S mRNAs, respectively. Four conserved regions (CR1-4) exist in the *E1A* gene. The CR3 is only encoded by the 13S mRNA. The 46 aa, which are therefore only present in the 289 aa protein, contain a C-4 zinc finger motif that is crucial for the transactivation activity of *E1A* (Berk et al. 1979, Frisch and Mymryk 2002, Jones and Shenk 1979, Pelka et al. 2008). The *E1B* proteins prevent host cell death by apoptosis. The *E1B55K* protein, together with *E4orf6*, builds up an ubiquitin ligase complex that binds to p53 and inhibits p53-mediated cell cycle arrest and apoptosis (Querido et al. 2001). *E1B55K* and *E4orf6* also cause the favored export of viral mRNA into the cytoplasm for biosynthesis of viral proteins and competitive inhibition of host protein synthesis (Flint and Gonzalez 2003). The second *E1B* protein, *E1B19K*, a B cell lymphoma-2 (Bcl-2) homologue protein, has anti-apoptotic effects, too (Han et al. 1996). The *E2* gene products have prominent functions in DNA replication. *E2A* encodes the multifunctional DNA binding protein (DBP), which is involved

in replication initiation and DNA elongation. *E2B* encodes the viral DNA polymerase and the DNA 5'-terminal protein, which enables initiation of viral replication, protein priming, protection of viral DNA against degradation, and prevents DNA integration into the host cell genome (de Jong et al. 2003, Hay et al. 1995, Rekosh et al. 1977). *E3* proteins are important for modulation of the host immune response in favor of the viral life cycle as described in chapter 1.9.2. Final host cell lysis and release of virions is mediated by the adenovirus death protein (ADP), which is also encoded in the *E3* region (*E3* 11.6K) (Tollefson et al. 1996). *E4* proteins have diverse roles involving viral DNA replication, transcription, RNA splicing, DNA repair, and cell signaling (Weitzman 2005). 10 h after infection, the late adenoviral proteins encoded by the late regions *L1-4* are expressed, consisting of the above described structural proteins that build up the virions. The late region 3 (*L3*) 23K protease, besides its function in capsid maturation, destabilizes the host cell cytoskeleton and is thus responsible for the typical rounding of the cells, the cytopathic effect (CPE), just before release of the newly assembled viral particles. First host cell lysis and particle release can occur one to two days after infection (Russell 2000).

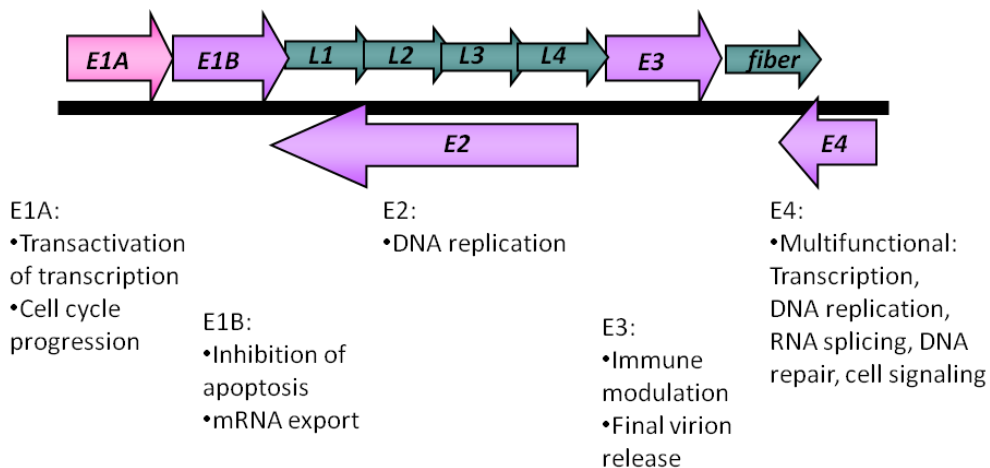


**Figure 1-2: Adenoviral gene functions.** Genome positions of the early region (*E*) and late region (*L*) genes and important viral gene functions. Late genes mostly code for structural proteins.

## 1.4. Nature and application of oncolytic adenoviruses

### 1.4.1. Oncolytic adenoviruses

The basic principle of oncolytic virotherapy is the use of viruses as therapeutic agents that selectively kill tumor cells without harming normal tissue. The viruses reproduce within the tumor in order to spread into all existing tumor cells and ideally eradicate the complete primary tumor, as well as potentially spread tumor metastatic foci. This, at least in theory, enhances the efficacy of the rather inefficient use of replication-deficient viral vectors in gene therapy (Alemany et al.

2000, Parato et al. 2005, Russell et al. 2012). Naturally occurring tumor selective viruses include dsRNA reoviruses (Hirasawa et al. 2003, Lal et al. 2009), as well as the single-stranded RNA viruses newcastle disease virus (Altomonte et al. 2010, Krishnamurthy et al. 2006, Zamarin and Palese 2012) and vesicular stomatitis virus (Balachandran and Barber 2004, Ebert et al. 2003, Stojdl et al. 2000, Wollmann et al. 2013). In contrast, human DNA viruses, including adenovirus, vaccinia virus, and herpes simplex virus need to be genetically modified in order to provide tumor selectivity. Especially adenoviruses have been under intensive investigation as anti-tumor virotherapeutics (Alemany et al. 2000, Curiel 2000, Pesonen et al. 2011). Adenoviruses have a natural lytic cycle, and a favorable safety profile due to their non-integrating genome, their genetic stability and low pathogenicity. They can be furthermore produced in high titers with high stability of viral particles (Nettelbeck 2003). The profound knowledge about the adenoviral genome, structure and infection cycle provides the basis for the possibility to imply changes into the virus, rendering it tumor-specific. Additionally, the experience from the relatively long history of use of adenoviruses as viral gene transfer vectors is beneficial. Two ways of rendering adenoviruses tumor-specific can be distinguished. One way is the partial or complete deletion of crucial viral functions, e.g. the *E1* genes, thereby eliminating the viral ability to replicate in healthy cells. In tumor cells however, the cell lysis ability is maintained due to the aberrant gene expression of oncogenes or mutated tumor suppressor genes, such as p53, pRb, or YB-1. The second strategy by which adenoviruses are rendered tumor-specific is the replacement of wild type viral promoters of genes involved in replication, such as the *E2* genes, with tumor-specific promoters, like for example the hTert promoter (Curiel 2000, de Gruijl and van de Ven 2012, Nettelbeck 2003). The majority of testing is performed with intratumoral virus administration, due to the high immunogenicity of adenoviruses and resultant delivery problems. Toxicity and safety profiles of oncolytic adenoviral therapy are favorable, the overall anti-tumor efficacy of single therapies has been limited though (Aghi and Martuza 2005, Pesonen et al. 2011). Limiting for successful oncolytic adenoviral delivery is, besides the high immunogenicity of the vectors (Haase et al. 1972), mostly the natural tropism of adenoviruses (Nettelbeck 2003, Vaha-Koskela et al. 2007). CAR receptors are often expressed in only low concentrations on tumor cell surfaces, limiting viral tumor cell targeting (Kim et al. 2002). Natural virus tropism can be altered by insertion of an additional integrin binding RGD motif into the viral fiber (Dmitriev et al. 1998, Kimball et al. 2010, Pesonen et al. 2012a) or by exchange of fiber proteins with fibers of other adenoviral serotypes binding to different cellular receptors (Douglas et al. 1996, Kim et al. 2011b, Koski et al. 2010, Stevenson et al. 1997). Anti-tumor efficacy of oncolytic viruses can be enhanced by addition of transgenes like the HSV-1 thymidine kinase gene, which has been shown to enhance cell killing by tumor-specific activation of the prodrug ganciclovir (Ahn et al. 2009, Wildner et al. 1999).

#### **1.4.2. Arming of oncolytic viruses with immunostimulatory transgenes**

The inherent immunogenicity of adenoviruses can be exploited in favor of oncolytic virotherapy. The anti-tumor immune reaction elicited by oncolytic viruses can be further augmented by arming of oncolytic adenoviruses with molecules that stimulate the immune system in diverse ways in order to support the virus in destroying the tumor cells (Cerullo et al. 2012). GM-CSF is an immunostimulatory cytokine secreted by macrophages, T cells, natural killer (NK) cells, and mast cells, as well as endothelial cells and fibroblasts. It promotes the differentiation of hematopoietic myeloid progenitor cells into granulocytes, dendritic cells (DCs) and macrophages (Hamilton and Anderson 2004). This leads to enhanced tumor antigen presentation by DCs with subsequently recruitment of cytotoxic T lymphocytes (CTLs). GM-CSF can thus mediate a protective immune environment against tumors (Dranoff et al. 1993, Lee et al. 1997). The relevance of virus-mediated immune stimulation in virotherapy, as well as particularly the benefit of GM-CSF as a virotherapy-supporting cytokine is demonstrated by the fact that the above mentioned most advanced oncolytic viruses in clinical trials, T-VEC and JX-594, both carry the GM-CSF gene. Accordingly, in adenoviral therapy, GM-CSF is used to support anti-tumor immunity. Treatment with Ad5-D24-GM-CSF elicits induction of virus-specific and tumor-specific immunity (Cerullo et al. 2010, Kanerva et al. 2013). Besides GM-CSF expression by oncolytic adenoviruses, also expression of other immunostimulatory factors like heat shock protein (Hsp) 70 (Li et al. 2009), tumor necrosis factors-related apoptosis-inducing ligand (TRAIL) (Bernt et al. 2005), CD40 ligand (Diaconu et al. 2012, Pesonen et al. 2012b), regulated on activation normal T cell expressed and secreted (RANTES) (Lapteva et al. 2009), interferon  $\gamma$  (IFN $\gamma$ ) (Sarkar et al. 2005), and interleukin-12 (IL-12) (Bortolanza et al. 2009) has been shown to improve oncolytic viral performance via stimulation of the immune system. Along these lines, the hematopoietic cytokine FMS-like tyrosine kinase-3 ligand (Flt3L) affects the development of multiple hematopoietic lineages and causes mobilization of progenitor cells. It thus triggers the *in vivo* expansion of B cells, T cells, NK cells and DCs (Maraskovsky et al. 1996, Matsumura et al. 2008, McKenna et al. 2000). Therefore, Flt3L has been shown to stimulate anti-tumor immune responses in hepatocellular carcinoma (Wang et al. 2005) and breast cancer (Braun et al. 1999) amongst others and to promote tumor regression (Lynch et al. 1997). An oncolytic adenovirus expressing macrophage inflammatory protein 1  $\alpha$  (MIP-1 $\alpha$ ) and Flt3L triggered DC and T cell infiltration. Besides anti-viral immunity, also the anti-tumoral immune response was enhanced by this approach (Edukulla et al. 2009).

### **1.5. The multifunctional cellular protein YB-1**

YB-1 is a multifunctional oncogenic transcription- and translation factor. It is a highly conserved nucleic acid binding protein, belonging to the family of cold-shock proteins (Kohno et al. 2003, Wu et al. 2007). YB-1 is a crucial factor in early embryonic development, being involved in neural tube formation and cell proliferation (Uchiumi et al. 2006). Whereas YB-1 is overexpressed in many sorts of cancer, mostly in the cell nucleus, it is not present in healthy tissue or only in small amounts in the cytoplasm (Bargou et al. 1997, Holm et al. 2002). However, upon cell entry into the G1/S phase (Jurchott et al. 2003), or when the cell is exposed to extrinsic stress like chemotherapy (Bargou et al. 1997), UV irradiation (Koike et al. 1997), or hyperthermia (Stein et al. 2001), YB-1 is translocated to the nucleus and accumulates there. Nuclear transfer of YB-1 is also elicited by adenoviruses, via a protein complex involving the adenoviral proteins E1B55K and E4orf6 (Holm et al. 2002, Mantwill et al. 2006). Localization of YB-1 either in the cytoplasm or in the nucleus of cells determines the multiple functions of YB-1. In the cytoplasm, YB-1 acts as a translation factor that regulates gene expression by association with mRNA and by regulation of mRNA transport (Evdokimova et al. 2006, Soop et al. 2003). In the nucleus, by binding to the so called Y-box, an inverted CCAAT element in the promoter region of multiple genes involved in tumor growth and drug resistance, YB-1 acts as a transcription factor (Goldsmith et al. 1993, Jurchott et al. 2003). Important nuclear roles of YB-1 in cell proliferation, drug resistance, and tumor relapse, amongst others, as well as the particular genes that are regulated by YB-1 in these contexts are summarized in table 1-2. Because of these multiple oncogenic roles of YB-1, elevated levels of preferentially nuclear localized YB-1 are an indicator for tumor aggressiveness and are often associated with bad response to certain chemotherapeutics, high rates of metastases and relapse, and therefore bad clinical prognosis. Correlations between high nuclear YB-1 expression and unfavorable clinical outcome have so far been shown for many cancers including amongst others breast cancer (Maciejczyk et al. 2012), HNSCC (Kolk et al. 2011), ovarian cancer (Oda et al. 2007), B cell lymphomas (Xu et al. 2009), and non-small cell lung cancer (Hyogotani et al. 2012, Shibahara et al. 2001). The central role of YB-1 can be utilized by stratification of patients by the degree of YB-1 expression and in consequence by the choice of adequate therapeutic regimen (Gluz et al. 2009, Kolk et al. 2011).



**Table 1-2: Summary of important oncogenic roles of nuclear YB-1 as a transcription factor.**

Effect of YB-1	Genes regulated by YB-1 in this context	Reference
Cell cycle progression, DNA replication, cell proliferation	Cyclin A and B1, topoisomerase-II $\alpha$ , DNA polymerase $\alpha$	En-Nia et al. 2005, Jurchott et al. 2003, Oda et al. 2003
Cell adhesion, motility, invasion, epithelial-mesenchymal transition, formation of metastases	Matrix metalloproteinases 2 and 13, collagen $\alpha 1$ , E-cadherin	Evdokimova et al. 2009, Mertens et al. 1997, Norman et al. 2001, Samuel et al. 2007
Tumorigenesis	Epidermal growth factor receptor, human epidermal growth factor receptor 2	Wu et al. 2006
Genome instability and mutation	Human endonuclease III	Marenstein et al. 2001
Drug resistance	Multidrug resistance related protein 1 (MRP1), multidrug resistance gene 1 (MDR1)	Bargou et al. 1997, Goldsmith et al. 1993, Stein et al. 2001
Tumor growth and relapse	CD44, CD49b	Fotovati et al. 2011, To et al. 2010

Activation of YB-1 itself is a complex process involving different interconnected pathways. YB-1 has been shown to be phosphorylated by Akt (Basaki et al. 2007, Sutherland et al. 2005), a serine/threonine kinase in the phosphoinositide 3-kinase (PI3K)/Akt signaling pathway and by the extracellular signal-regulated kinase (ERK) 2 (Coles et al. 2005) and ribosomal S6 kinases (RSK) 1 and 2 (Stratford et al. 2008) of the mitogen-activated protein kinases (MAPK)/ERK pathway. Phosphorylation of YB-1 thereby promotes nuclear translocation (Basaki et al. 2007). Mainly in cisplatin-resistant cells, a possible activation of YB-1 by other transcription factors involved in tumorigenesis, e.g. Twist (Shiota et al. 2008) and c-Myc (Uramoto et al. 2002) has been observed. The histone acetyltransferase p300/CBP-associated factor acetylates Twist, and by this possibly activates YB-1 transcription (Shiota et al. 2010). So besides YB-1 phosphorylation, acetylation might also play a role in YB-1 activation and nuclear translocation. Moreover, YB-1 interacts with other transcription factors like for example p53 (Lasham et al. 2003, Okamoto et al. 2000), the activator proteins (AP) AP1 and AP2 (Mertens et al. 1998, Samuel et al. 2005), SMA/mothers against decapentaplegic homology 3 (Smad3) (Higashi et al. 2003), and signal transducer and activator of transcription 3 (Stat3) (Lee et al. 2008). It can thus also indirectly regulate gene expression. This short summary illustrates the central role of YB-1 in many signaling pathways associated with tumorigenesis, growth regulation, metastasis formation, and survival of malignant cells, rendering it an ideal target for cancer therapy (Wu et al. 2007).

### **1.6. YB-1-dependent oncolytic adenoviruses**

Adenoviral replication depends mainly on proteins encoded by the adenoviral *E2* region, namely, as mentioned above, DBP, DNA polymerase, and terminal protein. The expression of these proteins is controlled by the *E2*-early and *E2*-late promoters (Swaminathan and Thimmapaya 1995). The CR1 and CR2 encoded regions of *E1A* proteins activate the *E2*-early promoter, following *E1A*-dependent release and promoter binding of the host cell factor *E2F* (Frisch and Mymryk 2002, Kovetski et al. 1987) (figure 1-3). For full adenoviral replication though, activation of the *E2*-late promoter is necessary, which is independent of cellular *E2F* (Mantwill et al. 2006). The *YB-1* protein is able to activate the *E2*-late promoter by binding to *Y*-boxes within the promoter. In wild type adenovirus infected cells, the adenoviral *E1B55K* and *E4orf6* proteins, which are expressed following transactivation by *E1A* 289 aa, cause translocation of *YB-1* into the nucleus leading to adenoviral replication (Frisch and Mymryk 2002, Holm et al. 2002, Mantwill et al. 2006). *YB-1* is present in the cell nucleus in many types of cancer (Bargou et al. 1997). Thus, *YB-1* is able to initiate viral replication and subsequent host cell lysis independently of *E1B55K* and *E4orf6*-mediated *YB-1* transfer into the nucleus in tumor cells infected with adenoviruses lacking the CR3-mediated *E1A* transactivation function (Holm et al. 2002, Mantwill et al. 2006). In healthy cells, though, *YB-1* is rarely expressed at all and is not present in the nucleus (Bargou et al. 1997). The *E2*-late promoter is therefore not initially activated in healthy cells infected with viruses that are not able to express *E1A* 289 aa with the CR3 region. Consequently, *YB-1*-dependent oncolytic adenoviruses can only replicate in tumor cells with nuclear *YB-1* expression, and are not able to destroy healthy cells. In stressed cells, for example after chemotherapeutic treatment, *YB-1* localization towards the nucleus is even enhanced (Bargou et al. 1997), making *YB-1*-dependent oncolytic adenovirus treatment a potent weapon to target drug-resistant cells (Holm et al. 2004, Mantwill et al. 2006) and possibly even stem-like cells (Fotovati et al. 2011, To et al. 2010). Furthermore, treatment of drug-resistant cells with a *YB-1*-dependent oncolytic adenovirus has led to downregulation of *MRP1* and *MDR1* (Mantwill et al. 2006), known mediators of drug resistance (Gottesman et al. 2002). In consequence, *YB-1*-dependent virotherapy restored the sensitivity of cancer cells towards chemotherapy, pointing out the potential benefit of combination therapies involving *YB-1*-based viruses and conventional therapies (Bieler et al. 2008, Mantwill et al. 2006, Rognoni et al. 2009).

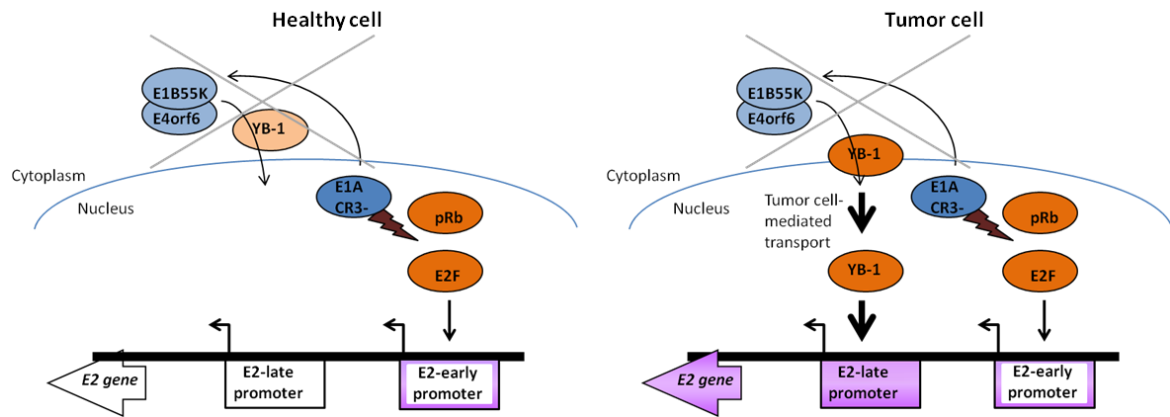


**Figure 1-3: Concept of tumor specificity of YB-1-dependent adenoviruses.** Adenoviral E1A proteins activate the E2-early promoter by causing separation of the pRb-E2F complex and subsequent promoter binding of E2F. E2-early promoter activity however is not sufficient for activation of full adenoviral replication in contrast to the YB-1-dependent E2-late promoter. In healthy cells (left), YB-1 is rarely expressed at all and not expressed within the nucleus. Adenoviruses lacking E1A 289 aa and thus the E1A CR3-dependent transactivation of E1B55K and E4orf6, and in consequence transport of cytoplasmatic YB-1 transport into the nucleus, can not activate E2-late promoter-induced E2 gene transcription and the following DNA replication. In tumor cells (right), YB-1 is expressed in the nucleus of the cells. It can activate the E2-late promoter and subsequent E2 protein-dependent DNA replication (image modified from Mantwill et al. 2006).

One realization of this concept is the YB-1-dependent oncolytic adenovirus Ad-Delo3-RGD (Mantwill et al. 2006, Rognoni et al. 2009). It has an 11 bp deletion in CR3 of *E1A*, a mutation which has already been described in 1984 by Haley et al. (Haley et al. 1984). An adenovirus that carries this mutation can only express the 243 aa E1A 12S protein product and not the 289 aa E1A 13S protein containing the CR3, which is the major factor for transactivation. This deletion provides the above mentioned YB-1-specificity (Holm 02). Besides the *E1A* mutation, Ad-Delo3-RGD also comprises a partial deletion of the *E1B19K* gene (Mantwill et al. 2006, Rognoni et al. 2009). Deletion of the anti-apoptotic Bcl-2 homologue protein E1B19K has been shown to induce faster and more efficient cell lysis, and to enhance viral spread (Liu et al. 2004, Sauthoff et al. 2000). Ad-Delo3-RGD also comprises a deletion of most of the *E3* region in order to improve immune detection. An additional RGD motif has been inserted into the viral fiber region in order to improve tumor cell infection (Mantwill et al. 2006, Rognoni et al. 2009). Ad-Delo3-RGD has already proven to be YB-1-specific and to be able to selectively kill cancer cells *in vitro* and *in vivo* in a xenograft pancreatic cancer model, especially in combination with paclitaxel (Rognoni et al. 2009) and in a xenograft glioma model, particularly in combination with temozolomide (Holzmüller et al. 2011).

### **1.7. Need for immunocompetent tumor models to test YB-1-dependent oncolysis**

Ad-Delo3-RGD has thus far only been tested in xenograft models (Holzmuller et al. 2011, Rognoni et al. 2009). Also in general, most of the currently used models to test oncolytic adenoviruses are xenograft systems (Russell et al. 2012). Although xenograft models are well established and allow the use of many of the common cancer cell lines, the mice need to have a compromised immune system in order to not reject the transplanted human tumor cells (Rygaard and Povlsen 1969). The gained xenograft tolerance allows relatively easy generation of xenograft tumor models and has therefore been the standard for use in testing of drug- or virus-mediated anti-tumor toxicity (Russell et al. 2012). However, adenoviral vectors are naturally detected and eradicated by their host's immune system (Haase et al. 1972). Contrariwise, there is increasing evidence that the effect of oncolytic viruses can be dramatically reinforced by synergistic interactions of virus-mediated cell lysis on the one hand, and immune recognition of viruses and immune cell-mediated tumor cell destruction on the other hand (Boozari et al. 2010, Diaconu et al. 2012, Edukulla et al. 2009). To include these factors in the evaluation of the anti-tumor effect of an oncolytic virus, it is necessary to find an adequate immunocompetent tumor model. The inherent difficulty in finding an immunocompetent model to test adenoviral oncolysis is the strict species specificity of the human adenoviruses. Apart from liver cells, CAR is not expressed in high levels in most murine cells (Tomko et al. 2000) and moreover, adenoviral infection allows no or only minor assembly of functional viral particles in other than human hosts (Youngusband et al. 1979). Still, there are some models of, amongst others, Syrian hamsters (Thomas et al. 2006, Wold and Toth 2012), cotton rats (Steel et al. 2007), dogs (Ternovoi et al. 2005), and mice (Boozari et al. 2010, Hallden et al. 2003, Wang et al. 2012) available that permit adenovirus replication.

### **1.8. Immunogenicity of therapy-induced tumor cell death**

Cancer cell death has always been classified into different modes of cell death ranging from apoptosis, over necrosis, to autophagy-related cell death, and mitotic catastrophe. These modes of cell death are grouped according to morphological and molecular events after cell death induction (Galluzzi et al. 2012, Okada and Mak 2004). During the past few years though, it became evident that apparently similar cell death morphotypes are still highly heterogeneous concerning distinct functional, biochemical, and mostly immunological characteristics (Galluzzi et al. 2012, Green et al. 2009). Hence, the focus in research on therapy-mediated cell death has largely changed towards including the immunogenicity of the dying cells into the assessment, distinguishing between tolerogenic or non-immunogenic and immunogenic cell death (ICD) (Green et al. 2009, Kroemer et al. 2013, Krysko et al. 2012). The immunogenic characteristics of ICD are mediated mainly by molecules called damage-associated molecular patterns (DAMPs) that function as danger signals or adjuvants for the innate immune system (Krysko et al. 2012). The spatio-temporal interplay of these molecules (Green et al. 2009, Kroemer et al. 2013), which are described in more detail in the next paragraphs, together with the presence of adequate interaction partners on the immune side (DeNardo et al. 2011, Denkert et al. 2010, Halama et al. 2011), allows an effective anti-tumor immune response (Kroemer et al. 2013, Zitvogel et al. 2011) (figure 1-4). Tumor-specific immune responses elicited by cells dying an ICD after a certain treatment have been found to be highly correlated with efficacy and even long-term success of the therapeutic agent (Kroemer et al. 2013, Zitvogel et al. 2011). Apart from chemotherapy with distinct agents like anthracyclines (Apetoh et al. 2007, Casares et al. 2005, Fucikova et al. 2011) or oxaliplatin (Ghiringhelli et al. 2009, Michaud et al. 2011, Tesniere et al. 2010), the concept of ICD has also been proven for other therapeutic approaches, such as proteasome inhibition by bortezomib (Spisek et al. 2007), ultraviolet C light (Panaretakis et al. 2009),  $\gamma$ -irradiation (Obeid et al. 2007a), and hypericin-based photodynamic therapy (PDT) (Garg et al. 2012c). In some cases, like in PDT, involved signaling pathways are slightly different from those, discovered for anthracyclines, which are described in the following (Krysko et al. 2012). In the context of virotherapy, the virus-mediated triggering of ICD has been only rarely examined so far, for example for measles virus (Donnelly et al. 2013), coxsackievirus B3 (Miyamoto et al. 2012), and adenovirus (Diaconu et al. 2012, Liikanen et al. 2013, Schierer et al. 2012). Therefore, little is known about the connections between viral lytic potency, elicited classical cell death modes, and the immunogenicity of the virus-mediated cell death.

Early molecular changes typical for ICD involve the cell surface exposure of Hsps (Hsp70 or Hsp90) (Fucikova et al. 2011, Spisek et al. 2007) and calreticulin (CRT) (Obeid et al. 2007b, Panaretakis et al. 2009). Hsps are intracellular proteins that participate in protein folding and stabilization during non-stress conditions (De Maio 1999). The stress-inducible chaperone Hsp70 can be translocated to the surface of tumor cells, but is not found on healthy cell surfaces (Multhoff et al. 1995). Hsps can increase immunogenicity of dying tumor cells by capturing of cellular antigens, including tumor antigens, and facilitation of their cell surface presentation (Binder et al. 2001). Also the crosspresentation of Hsp-chaperoned exogenous tumor peptides on antigen-presenting cells (APCs) enhances the immunogenicity of the peptides and attracts antigen-specific CTLs (Binder et al. 2001, Binder and Srivastava 2005). Moreover, Hsps contribute to the immunogenicity of dying cells by participation in the interaction between the membrane of dying cells and that of DCs over interaction of Hsp70 and the DC surface receptor CD91 (Basu et al. 2001). Cell surface exposed Hsp70 has also shown to enhance NK cell-mediated tumor cell lysis (Gross et al. 2003). Especially following PDT, in the course of which Hsp70 and Hsp90 are prominent markers of ICD (Garg et al. 2012a), Hsps have been found to be secreted and act as danger signals in the extracellular space (Krysko et al. 2012). The second protein, which is exposed on the cell surface of dying cells in the course of ICD, is CRT, a soluble protein normally localized in the lumen of the endoplasmic reticulum (ER). Its primary functions are regulation of calcium homeostasis and ER chaperone functions (Gelebart et al. 2005). CRT exposure in the context of ICD and anti-cancer activity is often a pre-apoptotic process (Obeid et al. 2007b, Panaretakis et al. 2009). Cell surface exposure of CRT is dependent on the ER stress response and associated with reactive oxygen species (ROS) production (Garg et al. 2012b, Panaretakis et al. 2009). PDT actively induces ER stress as a prerequisite for CRT exposure (Garg et al. 2012a, Garg et al. 2012c). But also during the process of ICD induction by other agents, ER stress is induced as a secondary or collateral effect (Martins et al. 2011, Panaretakis et al. 2009). Protein kinase RNA-like endoplasmic reticulum kinase (PERK), an ER-sensible kinase, gets activated and phosphorylates eukaryotic translation initiation factor 2 subunit  $\alpha$  (eIF2 $\alpha$ ) that activates the ER stress response and leads to translational arrest, as well as autophagy. Activation of the ER stress-mediated apoptotic pathway via caspase 8, Bcl-2 homologous antagonist killer (Bak), and Bcl-2-associated X protein (Bax) is required for CRT exposure. Upon activation of the ER stress response, CRT is transported from the ER to the Golgi apparatus and exposed on the cell surface (Martins et al. 2010, Martins et al. 2011, Panaretakis et al. 2009). Cell surface exposed CRT acts as a potent “eat me” signal. Cell surface CRT has been shown to dictate the immunogenicity of cancer cell death (Obeid et al. 2007b). Like Hsp70, CRT binds to CD91 on DC surfaces and enables the engulfment of dying cells by DCs (Basu et al. 2001, Gardai et al. 2005, Obeid et al. 2007b).

Later in the process of ICD, the DAMPs adenosine-5'-triphosphate (ATP) (Elliott et al. 2009, Martins et al. 2011) and high mobility group box 1 protein (HMGB1) (Apetoh et al. 2007, Scaffidi et al. 2002) are released from dying cells. Extracellular localization of the cellular coenzyme ATP serves as an important danger signal and as a chemoattractant, a so called "find me" signal. As a response to stress, ATP can be released passively or through active exocytosis (Krysko et al. 2012). Usually, ATP release, such as CRT exposure is a pre-apoptotic process (Chekeni et al. 2010, Elliott et al. 2009, Martins et al. 2009). Autophagy is required but not sufficient for the optimal release of ATP from dying cells following anthracycline therapy (Martins et al. 2012, Michaud et al. 2011). In addition, phosphatases and ectonucleotidases determine the equilibrium of extracellular immunostimulatory ATP and immunosuppressive adenosine (Stagg and Smyth 2010). Extracellular ATP regulates DC migration (Elliott et al. 2009), binds to purinergic P2RX<sub>7</sub> receptors on DCs, and triggers inflammasome activation. Subsequent IL-1 $\beta$  secretion from DCs activates CTL-mediated anti-tumor immune reactions (Ghiringhelli et al. 2009). The alarmin HMGB1 represents the most abundant non-histone chromatin protein with roles in genome stabilization and the promotion of transcription in the nucleus. It can be actively secreted as a cytokine by immune cells or stressed tumor cells, and can also be released by injured cells following loss of plasma membrane integrity (Guo et al. 2013, Krysko et al. 2012, Scaffidi et al. 2002). HMGB1 has been reported to be released by cells undergoing necrosis (Rovere-Querini et al. 2004, Scaffidi et al. 2002), secondary necrosis (Apetoh et al. 2007), apoptosis (Bell et al. 2006), and even autophagy (Thorburn et al. 2009). Extracellular HMGB1 acts as a potent ICD signal operating as a pro-inflammatory stimulus (Guo et al. 2013, Scaffidi et al. 2002). Recent findings implicate the relevance of the redox state of HMGB1 in determining its role in chemoattractance or in pro-inflammatory cytokine induction (Venereau et al. 2012). HMGB1 binds to various immune cell receptors including Toll-like receptor 4 (TLR4) (Apetoh et al. 2007), or TLR2 (Curtin et al. 2009) on DCs and in consequence promotes antigen processing and presentation (Apetoh et al. 2007). Following ICD-mediated activation of antigen-presenting DCs, these DCs promote CTL activation, IFN $\gamma$  release, and cytotoxicity directed against the residual tumor cells (Kroemer et al. 2013).

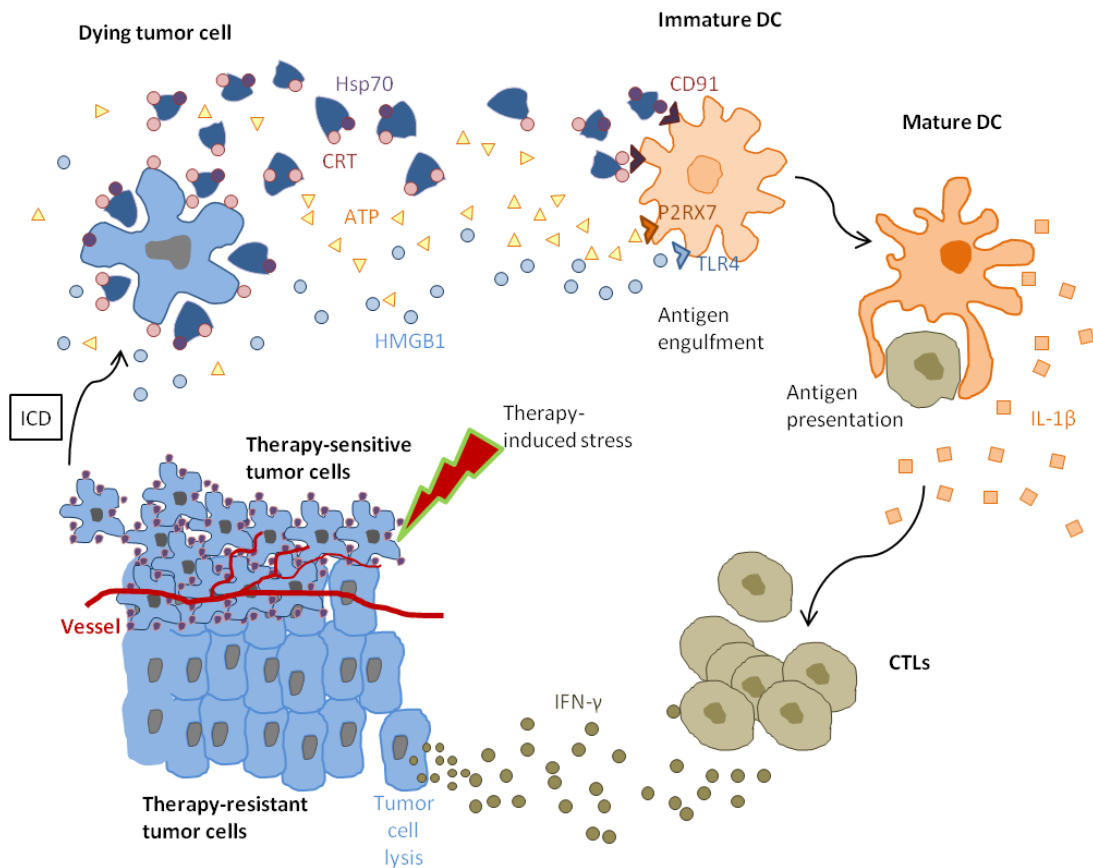


**Figure 1-4: Therapy-induced induction of ICD elicits potent anti-tumor immune responses.** Following therapy-induced ICD, Hsp70 and CRT are exposed on the cell surface of the dying cells. They bind to CD91 receptors on DCs. Cells dying an ICD release ATP and HMGB1, which bind to P2RX7 and TLR4 receptors, respectively. The ICD parameters trigger DC recruitment, maturation, antigen presentation, and IL-1 $\beta$  secretion. CTLs are activated, release IFN $\gamma$  and destroy remaining tumor cells (image modified from Kroemer et al. 2013).

## 1.9. Adenoviruses-host interactions

### 1.9.1. Immune defense against adenoviruses

The high immunogenicity of adenoviruses and the high percentage of preexisting immunity against adenoviruses, leading to rapid virus clearance and tissue damage by inflammation (Haase et al. 1972, Zaiss et al. 2009), present significant obstacles in the application of adenoviral vectors in gene therapy and for oncolytic virus delivery, especially when viruses are administered intravenously (de Gruijl and van de Ven 2012, Parato et al. 2005). Moreover, also complement factors in the blood stream in the presence or absence of preexisting anti-viral immunity recognize the viruses and trigger an inflammatory response (Cichon et al. 2001, Kiang et al. 2006). Innate immune recognition of capsid proteins (Borgland et al. 2000, Bowen et al. 2002, Molinier-Frenkel et al. 2003) and cellular recognition of fiber binding to CAR (Tamanini et al. 2006), or RGD-



integrin interaction (Liu et al. 2005a) lead to DC activation, neutrophil recruitment and triggering of inflammatory immune pathways. Pro-inflammatory cytokines, in the first line IL-1, but also for example tumor necrosis factor  $\alpha$  (TNF $\alpha$ ), IL-6, IL-18, or RANTES are released in a nuclear factor 'k-light-chain-enhancer' of activated B cells (NF $\kappa$ B)-dependent way by macrophages and DCs. These effectors in consequence cause a wide range of inflammatory immune responses like attraction and activation of various immune cells, including NK cells and T cells that mediate target cell death (Di Paolo et al. 2009, Muruve et al. 1999, Thaci et al. 2011). Moreover, adenovirus infected macrophages release ROS following mitochondrial membrane destabilization, leading to additional innate immune activation (McGuire et al. 2011). Nucleic acids of internalized adenoviruses are recognized in a cell type-dependent manner (Zhu et al. 2007). In plasmacytoid DCs, the foreign DNA is recognized by TLR9 in endosomes, also resulting in an inflammatory response or in the secretion of type 1 IFN (Barlan et al. 2011, Cerullo et al. 2007, Muruve et al. 2008). In conventional DCs, macrophages, and fibroblasts, in contrast, viral DNA is sensed independently of TLRs in the cytoplasm of infected cells, followed by activation of type 1 IFN and inflammation responses (Nociari et al. 2007). Type 1 IFN secretion elicits recruitment and phosphorylation of Stat1 and Stat2. Phosphorylated Stats together with interferon regulatory factor 9 (IRF9) form the IFN-stimulated gene factor 3 (ISGF3) complex, which activates a wide range of IFN-stimulated genes (Garcia-Sastre and Biron 2006, Stark and Kerr 1992). IFN-stimulated anti-viral genes include protein kinase RNA-activated (PKR) and IFN-induced guanosine triphosphate-binding protein myxovirus resistance A (MxA). PKR promotes phosphorylation of eIF2 $\alpha$  and regulation of protein synthesis, whereas MxA blocks viral replication (Sadler and Williams 2008, Thaci et al. 2011). Type 1 IFN expression is critical for innate, as well as for adaptive immune responses (Zhu et al. 2007). It promotes NK cell recruitment and activation (Biron et al. 1999, Zhu et al. 2008) and DC maturation (Hensley et al. 2005). Mature APCs, primarily DCs, presenting adenoviral peptides, elicit potent adaptive immune responses including IFN $\gamma$ -mediated CTL killing of virus infected cells (Schagen et al. 2004, Yang et al. 1995). Anti-viral antibodies, targeted mainly against the viral capsid proteins hexon and fiber, strengthen both inflammatory and IFN-mediated innate immune responses (Bradley et al. 2012).

### 1.9.2. Immune evasion strategies of adenoviruses

Adenoviruses are able to modulate the immune system in multiple ways in order to support their own replication and spread. Mainly the adenoviral *E1* and *E3* encoded proteins are involved in adenovirus-mediated immune escape. *E1A* proteins, as mentioned above, play major roles in the adenoviral life cycle being the first molecules that are activated and that transactivate all other adenoviral genes in succession (chapter 1.3.3). Besides their roles in cell cycle progression and transactivation, *E1A* proteins have been shown to play critical roles in the interplay between adenoviruses and the host immune system (Berhane et al. 2011, Leonard and Sen 1996). As mentioned above, the *E3* region encodes several proteins involved in immune modulation (Ilan et al. 1997, Schagen et al. 2004, Thaci et al. 2011). Adenoviral genes involved in immune modulation and regulation of cell death (chapter 1.9.3) are depicted in figure 1-5.

Adenoviral *E1* and *E3* proteins for example interfere with IFN signaling and major histocompatibility complex class I (MHC I) presentation of viral antigens in multiple ways. The *E1A* proteins 289 aa and 243 aa are able to downregulate IFN $\alpha$  (Kalvakolanu et al. 1991) and IFN $\gamma$  signaling (Leonard and Sen 1996). In both pathways, *E1A* reduces Stat1 expression and thus Stat1 phosphorylation, which is needed for functional complex formation of ISGF3 and gamma-interferon activation factor (GAF). Thus, *E1A* promotes downregulation of IFN-stimulated genes (Kalvakolanu et al. 1991, Leonard and Sen 1996), including multiples genes involved in antigen processing and MHC I-mediated antigen presentation. Effective presentation of intracellular antigens on MHC I is an important prerequisite for the immunogenicity of cells and for CTL-mediated cell killing (Zhou 2009). Proteasomes are the major non-lysosomal way to degrade proteins and are responsible for MHC I-specific peptide processing (Coux et al. 1996, Glickman and Maytal 2002). In cells of hematopoietic origin, or during an immune response in the context of for example IFN $\gamma$  stimulation, the constitutive catalytic S26 proteasome components  $\beta$ 1,  $\beta$ 5, and  $\beta$ 2 are replaced by the immunoproteasome components low molecular mass polypeptide 2 (LMP2), LMP7, and multicatalytic endopeptidase complex-like 1 (MECL1), respectively (Basler et al. 2013, Hisamatsu et al. 1996). Due to structural changes in the proteasome substrate binding pockets and an altered cleavage pattern of the multicatalytic complex, the immunoproteasome improves quality and quantity of generated peptides for presentation on MHC I molecules (Basler et al. 2013). Immunoproteasome formation is inhibited by viral *E1A* proteins by interference with IFN $\gamma$  signaling. Immunoproteasome formation however is not completely abrogated by adenoviral infections. For that reason, viral *E1A* proteins can also interfere with immunoproteasome activity directly. *E1A* binds to and specifically downregulates the expression of the exclusive immunoproteasome component MECL1 (Berhane et al. 2011) and inhibits Stat1-dependent LMP2

transcription over binding to Stat1 (Chatterjee-Kishore et al. 2000). Hence, by inhibition of immunoproteasome-mediated protein degradation in multiple ways, E1A interferes with processing and presentation of adenoviral antigens by MHCI. Importantly, the E3 glycoprotein 19K (E3gp19K) inhibits peptide presentation of MHCI directly by retargeting of MHCI to the ER (Sester et al. 2013). Infection of the cell is thus not recognized by cytotoxic immune cells and is left alive for the virus to be able to persist (Andersson et al. 1985, McSharry et al. 2008). Besides the functions of E1A proteins in regulation of IFN signaling, also adenoviral non-coding virus-associated RNA molecule I (VA RNAI) has been shown to inhibit IFN-induced PKR activity amongst others and thus eIF2 $\alpha$ -mediated ICD (Galluzzi et al. 2010, Kitajewski et al. 1986). Phosphorylation of eIF2 $\alpha$  is also limited by the viral E1B55K and E4orf6 protein complex during the late phase of adenoviral infection (Spurgeon and Ornelles 2009).

An alternative way of viral interference with innate anti-viral immune responses and of enabling of viral persistence is the inhibition of production of the anti-viral innate immune effector nitric oxide (NO). The viral E1A proteins have been shown to decrease expression of inducible NO synthase (iNOS), the enzyme that is responsible for anti-viral NO production (Cao et al. 2003).

Several E3 proteins further protect virus infected cells from immune effects. E3 14.7K blocks NF $\kappa$ B function and thus NF $\kappa$ B-mediated anti-viral inflammation and immune response (Carmody et al. 2006), whereas a complex of E3 10.4K and 14.5K inhibits TNF, TRAIL and Fas ligand (FasL)-induced cell death by internalization and degradation of Fas and TRAIL receptors (Lichtenstein et al. 2002, Tollefson et al. 1998).

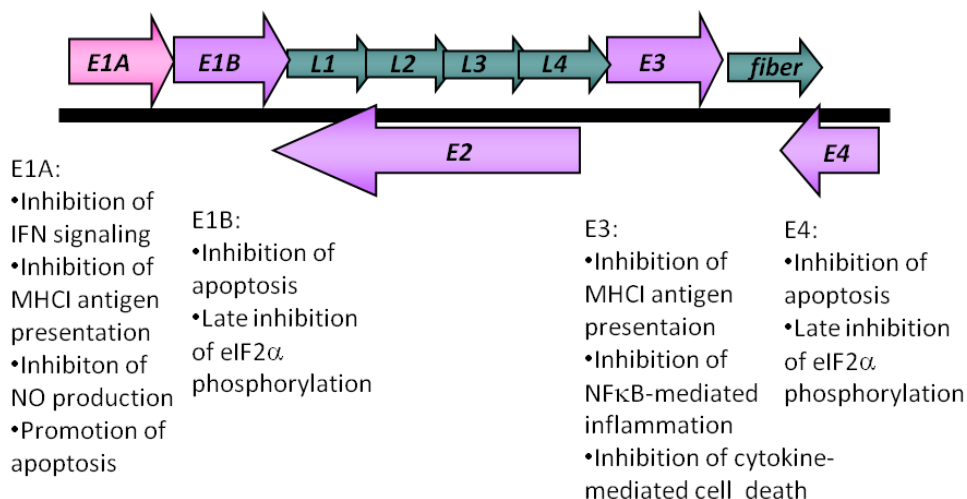


**Figure 1-5: Interference of adenoviral proteins with anti-viral immune response and cell death.** Genome positions of the early region (E) and late region (L) genes and important viral gene functions in manipulation of host immune responses and apoptosis.

### 1.9.3. Cell death modulation by adenoviruses

Adenoviral proteins are capable of regulating apoptosis induction to their favor depending on the status of virus life cycle (figure 1-5). E1A proteins generally sensitize cells to apoptosis, while E1A-mediated apoptosis is prevented by E1B proteins. As mentioned in chapter 1.3.3 E1A stimulates entry into the S phase to create the appropriate host cell environment for productive DNA replication. The cellular factors involved in cell cycle deregulation, namely pRb and the transcriptional coactivator p300 simultaneously promote apoptosis as a cellular defense mechanism to antagonize major cell growth deregulation (Berk 2005, White 2001). E1A thus sensitizes tumor cells to apoptosis in response to injuries by for example macrophages via TNF $\alpha$  (Cook et al. 2002) or NO (Radke et al. 2008). E1A moreover stabilizes p53 and sensitizes cells to p53-mediated apoptosis (Hong et al. 2008, Lowe and Ruley 1993). Since early cell death is not favorable for virus production, E1A is coexpressed during cellular infection with the E1B proteins E1B55K and E1B19K, which counteract the pro-apoptotic effects of E1A and prevent early host cell death with limited viral production (Berk 2005, White 2001). The Bcl-2 homologue protein E1B19K binds to and inhibits the pro-apoptotic Bcl-2 family members Bax and Bak that promote apoptosis (Han et al. 1996). E1B19K also binds to and inhibits p53 directly, and indirectly via association with Bak (Lomonosova et al. 2005). Of note, Bax and Bak are also involved in the late apoptotic module of ICD, which is therefore inhibited by E1B19K (Galluzzi et al. 2010). As mentioned in chapter 1.3.3, also the *E1B* encoded protein E1B55K has anti-apoptotic functions. E1B55K sequesters p53 into aggresomes and promotes its proteasome degradation following ubiquitination by an ubiquitin ligase complex involving E1B55K and E4orf6 (Liu et al. 2005c). As mentioned in chapter 1.3.3, towards the end of the infectious cycle, the *E3* encoded ADP protein directly promotes cell lysis (Tollefson et al. 1996), demonstrating that multiple viral proteins are involved in the regulation of cell death at multiple time points during infection. In addition, adenoviruses have also been shown to mediate cell death via involvement in the damage response pathway leading to cell death due to overreplication and accumulation of genomic DNA damage (Connell et al. 2011).

### 1.10. Objective

Oncolytic viruses present a promising way to target the currently existing limitations of anti-cancer therapy. Oncolytic viruses that selectively replicate in tumor cells that express the oncogenic protein YB-1 have already proven efficacy *in vitro* and in xenograft tumor models *in vivo* (Holzmuller et al. 2011, Rognoni et al. 2009) However, a fully functional immune system can on the one hand compromise viral efficacy *in vivo* by clearance of viruses (de Gruijl and van de Ven 2012, Haase et al. 1972) and on the other hand support the viral anti-tumor activity (Boozari et al. 2010, Edukulla et al. 2009, Melcher et al. 2011). It was thus one of the objectives within this work to find appropriate non-human cells that allow adenoviral infection, propagation, and virus-mediated cell lysis. These cells should then be used in an immunocompetent tumor model.

Viral proteins, especially the E1A proteins, have multiple functions that modulate host cell cycle, cell death, and also anti-viral immune defense mechanisms (Frisch and Mymryk 2002, Schagen et al. 2004). It was thus of great interest to investigate whether YB-1-dependent viruses that can not or only in part express the E1A proteins are still able to replicate in tumor cells, lyse infected cells, and how cell death elicited by them differs from wild type adenovirus-mediated cell death. The aim of the present study was to investigate whether changes in the genomes of the oncolytic viruses are able to trigger a cell death that is more immunogenic as compared to wild type adenovirus-caused cell death and whether this has an impact on, not only anti-viral, but rather anti-tumor immune responses in an immunocompetent model *in vivo*. Since attraction of DCs and T cells has shown to be crucial for the success of adenoviral therapy *in vivo* (Diaconu et al. 2012, Woller et al. 2011), the attraction of these immune cell populations should also be investigated.

Immune activity directed against the viruses was tried to be further capitalized on by insertion of a murine Flt3L transgene into one of the oncolytic vectors to investigate an improvement of the anti-tumor effect by possible Flt3L-mediated recruitment and activation of APCs (Edukulla et al. 2009). Moreover, it should be investigated whether anti-viral immune responses triggered by viral infections can be used to break the immunotolerance evolved in tumors and to redirect elicited anti-viral immune responses towards the tumor cells.

## 2. Materials and Methods

### 2.1. Materials

#### 2.1.1. Laboratory equipment

**Table 2-1: Laboratory equipment.**

Laboratory equipment	Manufacturer
Balances: PCE-LSM 2000 Research RC210P	PCE Deutschland GmbH, Meschede, GER Sartorius AG, Göttingen, GER
Caliper, digital, 0-100 mm	Hoffmann GmbH Qualitätswerkzeuge, Munich, GER
Centrifuges: Mini centrifuge MCF-2360 Table centrifuge 5417R Megafuge 2.0R Ultracentrifuge Optima LE-80K, rotor SW32 Ti	LMS Consult GmbH & Co. KG, Brigachtal, GER Eppendorf AG, Hamburg, GER Heraeus Instruments GmbH, Hanau, GER Beckman Coulter GmbH, Krefeld, GER
CO <sub>2</sub> incubator HERAcCell 150i	Thermo Fisher Scientific Inc., Waltham, MA, USA
Counting chamber, Neubauer	Brand GmbH & Co. KG, Wertheim, GER
Dynamic light scattering device: Zetasizer Nano	Malvern Instruments GmbH, Herrenberg, GER
Ear punch	Bioscape EBECO, Castrop-Rauxel, GER
Enzyme linked immunosorbent assay (ELISA) washer ImmuWash Model 1575	Bio-Rad Laboratories, Munich, GER
Enzyme linked immuno spot assay (ELISpot) reader Bioreader 3000	BIO-SYS GmbH, Karben, GER
Flow cytometer FACS Canto II (FACS: fluorescence-activated cell sorting)	BD Biosciences, Heidelberg, GER
Freezing container Mr. Frosty	Thermo Fisher Scientific Inc., Waltham, MA, USA
Incubator shaker TH15	Edmund Bühler GmbH, Hechingen, GER
Multilabel counter for fluorescence, luminescence, photometry: Wallac Victor <sup>2</sup> 1420	PerkinElmer LAS GmbH, Rodgau, GER
Microscopes: Axiovert 25 and 135 with AxioCam MRc AxiomagerZ1 with ApoTome (Fluorescence) Microscope Eclipse te2000-5 (Fluorescence) Microscope Leica DMR (Immunohistology)	Carl Zeiss Jena GmbH, Jena, GER Carl Zeiss Jena GmbH, Jena, GER Nikon GmbH, Düsseldorf, GER Leica Camera AG, Solms, GER
Microtome Microm HM 355	Thermo Fisher Scientific Inc., Waltham, MA, USA

Materials and Methods

Polymerase chain reaction (PCR) gel electrophoresis unit Mini horizontal submarine unit HE33	Hoefer, Inc, Holliston, MA, USA
Photometer for cuvettes: Biophotometer	Eppendorf AG, Hamburg, GER
Pipettes: Eppendorf Research: 10, 20, 200, 1000 $\mu$ L Multichannel pipette Eppendorf Research Repetitive pipette Multipette plus	Eppendorf AG, Hamburg, GER Eppendorf AG, Hamburg, GER Eppendorf AG, Hamburg, GER
Pipette controller Accu-jet <sup>®</sup> pro	Brand GmbH & Co. KG, Wertheim, GER
Power supply for PCR and Western blot (WB) systems PowerPac 300	Bio-Rad Laboratories, Munich, GER
Sequence detection system ABI PRISM <sup>®</sup> 7900HT	Applied Biosystems, Life Technologies GmbH, Darmstadt, GER
Shakers: Microtiter shaker MTS 2/4 Mini rocker MR-1 Vortex shaker Minishaker MS2	IKA Werke GmbH & Co. KG, Staufen, GER G.Kisker GbR, Steinfurt, GER IKA Werke GmbH & Co. KG, Staufen, GER
Sterile bench HERAsafe	Thermo Electron Corporation, Waltham, MA, USA
Thermal cycler for PCR Robocycler Gradient 40	Agilent Technologies Deutschland GmbH, Böblingen
Thermomixer <sup>®</sup> compact	Eppendorf AG, Hamburg, GER
Tissue embedding molds	Medite Medizintechnik, Burgdorf, GER
Tissue embedding system TBS 88	Medite Medizintechnik, Burgdorf, GER
Tissue floating bath TFB 35	Medite Medizintechnik, Burgdorf, GER
Tissue processor Shandon Excelsior ES	Thermo Fisher Scientific Inc., Waltham, MA, USA
Tissue stretching table OTS 40	Medite Medizintechnik, Burgdorf, GER
Ultraviolet (UV) image station for PCR analysis	LTF-Labortechnik GmbH & Co. KG, Wasserburg, GER
Water bath	Memmert GmbH & Co. KG, Schwabach, GER
Western blot electrophoretic transfer cell Criterion <sup>™</sup> Blotter	Bio-Rad Laboratories, Munich, GER
WB gel casting chamber Multiple Gel Caster	Bio-Rad Laboratories, Munich, GER
WB gel electrophoresis system Mini PROTEAN Tetra System	Bio-Rad Laboratories, Munich, GER
WB imager ChemiDoc <sup>™</sup> MP System	Bio-Rad Laboratories, Munich, GER

### 2.1.2. Software and web portals

**Table 2-2: Software and web portals.**

Software	Application	URL or company
EndNote	Literature management	Thomson Reuters, New York City, NY, USA
FACSDiva	Flow cytometry	BD Biosciences, Heidelberg, GER
FlowJo	Flow cytometry	Tree Star, Inc., Ashland, OR, USA
Image Lab™	WB software	Bio-Rad Laboratories, Munich, GER
ImageJ	Image processing	National Institutes of Health, Bethesda, MD, USA ( <a href="http://rsbweb.nih.gov/ij/">http://rsbweb.nih.gov/ij/</a> )
MS Office	Calculations, figures, text	Microsoft Deutschland GmbH, Unterschleißheim, GER
PubMed	Literature research	<a href="http://www.ncbi.nlm.nih.gov/pubmed">http://www.ncbi.nlm.nih.gov/pubmed</a>
ReaderFit	Curve fitting, ELISA	<a href="http://www.readerfit.com">http://www.readerfit.com</a>
SDS2.2	Real time PCR	Life Technologies GmbH, Darmstadt, GER
Universal Protein Resource Knowledgebase (Uniprot)	Protein database	<a href="http://www.uniprot.org">http://www.uniprot.org</a>
VectorNTI	Gene analysis	Life Technologies GmbH, Darmstadt, GER

### 2.1.3. Consumables

**Table 2-3: Consumables.**

Consumable	Manufacturer
Cell culture dishes: 10 x 2 cm, 15 x 2 cm	TPP AG, Trasadingen, Switzerland
Cell culture flasks: 25 cm <sup>2</sup> , 75 cm <sup>2</sup> , 150 cm <sup>2</sup>	TPP AG, Trasadingen, Switzerland
Cell culture test plates: 6-well, 12-well, 24-well, 96-well flat and round bottom	TPP AG, Trasadingen, Switzerland
Cell scraper, 30 cm	TPP AG, Trasadingen, Switzerland
Cell strainer, 40 µm, nylon	BD Biosciences, Heidelberg, GER
Cover slips, 24 x 50 mm	Gerhard Menzel GmbH, Braunschweig, GER
Cuvettes: UVette® 50-2000 µL Cuvettes, disposable, for dynamic light scattering, semi-micro, 1.5 mL	Eppendorf AG, Hamburg, GER Brand GmbH, Wertheim, GER
Desalting columns PD-10 Columns, sephadex	GE Healthcare GmbH, Munich, GER
Filters: Steritop filter units, 0.22 µm Sterile filter, 0.2 µm	Millipore, Merck KGaA, Darmstadt, GER Josef Peske GmbH & Co. KG, Aindling, GER
Forceps, polystyrene	J. Söllner GmbH, Deggendorf, GER
Microscope slides Menzel Superfrost Plus	Gerhard Menzel GmbH, Braunschweig, GER



Materials and Methods

Pasteur pipettes: 150, 230 mm	Hirschmann Laborgeräte GmbH & Co.KG, Eberstadt, GER
Pipette tips: 0.5-10, 2-200, 100-1000 µL Filter tips Multi Guard Barrier Tips: 10, 10-200, 100-1000 µL Multipipette tips Combitips plus: 1, 2.5, 5, 10 mL	Josef Peske GmbH & Co. KG, Aindling, GER Sorenson BioScience, Inc., Salt Lake City, UT, USA Eppendorf AG, Hamburg, GER
Reaction plates: ELISA plates Nunc Immuno™ Plates, polystyrene, MaxiSorp ELISA plate sealers  ELISpot plates MultiScreen HTS-IP Filter Plate, hydrophobic, polyvinylidenfluorid (PVDF) Real time PCR plates Reaction Plate Micro Amp®, optical, 96-well and Optical Adhesive Film	Thermo Fisher Scientific Inc., Waltham, MA, USA R&D Systems GmbH, Wiesbaden-Nordenstadt, GER Millipore, Merck KGaA, Darmstadt, GER  Life Technologies GmbH, Darmstadt, GER
Scalpel, disposable	Pfm medical Ag, Köln, GER
Serological pipettes, sterile: 1, 2, 5, 10, 25, 50 mL	BD Biosciences, Heidelberg, GER
Syringes and needles: Inject® Luer Solo: 5, 10 mL Omnifix-F Solo, 1 mL Omnican 40 U-40 Insulin, 30G x ½'' Hypodermic injection needles Sterican®: 27G x ¾'', 24G x 1'', 20G x 1½''	B.Braun Melsungen AG, Melsungen, GER B.Braun Melsungen AG, Melsungen, GER B.Braun Melsungen AG, Melsungen, GER B.Braun Melsungen AG, Melsungen, GER
Tissue embedding cassettes	Medite Medizintechnik, Burgdorf, GER
Tubes: Centrifuge tubes, conical, 15, 50 mL FACS tubes, 5 mL, round bottom, polystyrol Reaction tubes: 0.5, 1.5, 2 mL Trucount Tubes BD Trucount Tubes Ultracentrifuge tubes Ultra-Clear 25 x 89 mm	TPP AG, Trasadingen, Switzerland BD Biosciences, Heidelberg, GER Josef Peske GmbH & Co. KG, Aindling, GER BD Biosciences, Heidelberg, GER Beckman Coulter GmbH, Krefeld, GER
WB membranes: nitrocellulose: Amersham Hybond™ ECL™ and PVDF: Amersham Hybond™-P	GE Healthcare GmbH, Munich, GER
Whatman paper	Schleicher & Schuell Bioscience GmbH, Dassel, GER

## 2.1.4. Chemicals

Table 2-4: Chemicals.

Chemical	Manufacturer
Acetic acid	Merck KGaA, Darmstadt, GER
Acetone	Merck KGaA, Darmstadt, GER
Agarose, peqGold universal	PEQLAB Biotechnologie GMBH, Erlangen, GER
Ammonium acetate (NH <sub>4</sub> C <sub>2</sub> H <sub>3</sub> O <sub>2</sub> )	Merck KGaA, Darmstadt, GER
Ammonium chloride (NH <sub>4</sub> Cl)	Merck KGaA, Darmstadt, GER
Ammonium persulfate (APS)	Sigma-Aldrich Chemie GmbH, Steinheim, GER
Bromophenol blue	Feinbiochemica GmbH, Heidelberg, GER
Cesium chloride (CsCl)	MP Biomedicals Europe, Illkirch, FRA
Chloroform	Merck KGaA, Darmstadt, GER
Cresol red	Sigma-Aldrich Chemie GmbH, Steinheim, GER
Dimethyl sulfoxide (DMSO)	Sigma-Aldrich Chemie GmbH, Steinheim, GER
Dithiothreitol (DTT)	Sigma-Aldrich Chemie GmbH, Steinheim, GER
Ethanol	Merck KGaA, Darmstadt, GER
Ethidium bromide (EtBr)	Boehringer Mannheim, GER
Ethylenediaminetetraacetic acid (EDTA)	Merck KGaA, Darmstadt, GER
Formalin 10%, neutral buffered	Sigma-Aldrich Chemie GmbH, Steinheim, GER
Glycerin	Merck KGaA, Darmstadt, GER
Glycin	Merck KGaA, Darmstadt
Glycogen	Sigma-Aldrich Chemie GmbH, Steinheim, GER
Hydrochloric acid (HCl)	Merck KGaA, Darmstadt, GER
Hydrogen peroxide (H <sub>2</sub> O <sub>2</sub> ) solution, 30%	Sigma-Aldrich Chemie GmbH, Steinheim, GER
Isopropyl alcohol	Merck KGaA, Darmstadt, GER
Magnesium chloride (MgCl <sub>2</sub> )	Merck KGaA, Darmstadt, GER
Methanol	Merck KGaA, Darmstadt, GER
Nonidet P 40	Fluka Chemie AG, Buchs, Switzerland
Phenol:chloroform:isoamyl alcohol 25:24:1	Sigma-Aldrich Chemie GmbH, Steinheim, GER
Polyacrylamide(PAA): Rotiphorese® Gel 40: 40% Acrylamide-, bisacrylamide solution (19:1)	Carl Roth GmbH & Co. KG, Karlsruhe, GER
Ponceau S solution	Sigma-Aldrich Chemie GmbH, Steinheim, GER
Potassium chloride (KCl)	Sigma-Aldrich Chemie GmbH, Steinheim, GER
Potassium dihydrogen phosphate (KH <sub>2</sub> PO <sub>4</sub> )	Merck KGaA, Darmstadt, GER
Potassium hydrogen carbonate (KHCO <sub>3</sub> )	Sigma-Aldrich Chemie GmbH, Steinheim, GER
Sodium carbonate (Na <sub>2</sub> CO <sub>3</sub> )	Fluka Chemika AG, Buchs, Switzerland
Sodium chloride (NaCl )	Sigma-Aldrich Chemie GmbH, Steinheim, GER
Sodium citrate	Merck KGaA, Darmstadt, GER
Sodium dodecyl sulfate (SDS)	SERVA Electrophoresis GmbH, Heidelberg, GER
Sodium hydrogen carbonate (NaHCO <sub>3</sub> )	Fluka Biochemika, Buchs, Switzerland

Sodium hydroxide (NaOH)	Merck KGaA, Darmstadt, GER
Sodium phosphate dibasic (Na <sub>2</sub> HPO <sub>4</sub> )	Sigma-Aldrich Chemie GmbH, Steinheim, GER
Sulforhodamine B (SRB), sodium salt	Sigma-Aldrich Chemie GmbH, Steinheim, GER
Tetramethylethylenediamine (TEMED)	Carl Roth GmbH & Co. KG, Karlsruhe, GER
Trichloroacetic acid (TCA)	Sigma-Aldrich Chemie GmbH, Steinheim, GER
Tris HCl and tris base	Roche Diagnostics GmbH, Mannheim, GER
Triton X-100	Sigma-Aldrich Chemie GmbH, Steinheim, GER
Tween 20	Sigma-Aldrich Chemie GmbH, Steinheim, GER
Xylene	Sigma-Aldrich Chemie GmbH, Steinheim, GER

### 2.1.5. Commercially available buffers, standards, and other biochemical substances

**Table 2-5: Commercially available buffers, standards, and other biochemical substances.**

Substance	Manufacturer
Albumin bovine Fraction V (BSA)	SERVA Electrophoresis GmbH, Heidelberg, GER
Antibody diluent	Dako Deutschland GmbH, Hamburg, GER
Antibody diluent with background reducing components	Dako Deutschland GmbH, Hamburg, GER
Calcein-acetoxymethyl (AM) ester	Sigma-Aldrich Chemie GmbH, Steinheim, GER
Caspase substrate Acetyl-Asp-Glu-Val-Asp-7-amino-4-methylcoumarin (Ac-DEVD-amc)	Bachem AG, Bubendorf, Switzerland
3,3'-diaminobenzidine (DAB) substrate: Liquid DAB+ Substrate Chromogen System	Dako Deutschland GmbH, Hamburg, GER
Deoxyribonucleotide 4dNTP mix (10mM)	Fermentas GmbH, St. Leon Rot, GER
DNA ladder mix Gene ruler™	Fermentas GmbH, St. Leon Rot, GER
DNA loading buffer (6x)	PEQLAB Biotechnologie GMBH, Erlangen, GER
Eosin solution	Sigma-Aldrich Chemie GmbH, Steinheim, GER
FACS lysing solution	BD Biosciences, San Jose, CA, USA
FcR blocking reagent	Miltenyi Biotec GmbH, Bergisch Gladbach, GER
Fixation buffer Cytotfix	BD Biosciences, Heidelberg, GER
Hemalum solution acid acc. to Mayer	Carl Roth GmbH & Co.KG, Karlsruhe, GER
Hoechst 33342 trichloride, trihydrate	Life Technologies GmbH, Darmstadt, GER
Lumi-Light Western Blotting Substrate	Roche Diagnostics GmbH, Mannheim, GER
Mammalian cell lysis reagent ProteoJET	Fermentas GmbH, St. Leon Rot, GER
Milk powder, nonfat, dried	AppliChem GmbH, Darmstadt, GER
Mounting medium for fluorescence Vectashield	Vector laboratories Burlingame, CA, USA
Mounting medium Permount	Thermo Fisher Scientific Inc., Waltham, MA, USA
Phosphatase inhibitor cocktail tablets PhosSTOP	Roche Diagnostics GmbH, Mannheim, GER

Protease inhibitor cocktail Complete Mini	Roche Diagnostics GmbH, Mannheim, GER
Protein ladder : Spectra™ Multicolor Broad Range Protein Ladder	Fermentas GmbH, St. Leon Rot, GER
Real time PCR master mix MESA GREEN Plus for SYBR® Assay	Eurogentec Deutschland GmbH, Köln, GER
Serum, rabbit	Santa Cruz Biotechnology, Inc., Heidelberg, GER
Serum, swine	Santa Cruz Biotechnology, Inc., Heidelberg, GER
Streptavidin- horseradish peroxidase (HRP) for ELISpot	BD Biosciences, Heidelberg, GER
Taq buffer with ammonium sulfate (10x)	Fermentas GmbH, St. Leon Rot, GER
Tissue embedding medium Surgipath Paraplast Regular	Leica Microsystems, Wetzlar, GER
3,3',5,5'-Tetramethylbenzidine (TMB) substrate reagent set BD OptEIA™	BD Biosciences, Heidelberg, GER
WB incubation buffer for microtubule-associated protein light chain 3 (LC3) detection: Blot Incubation Buffer CPPT	Nanotools GmbH, Munich, GER

### 2.1.6. Prepared buffers and solutions

**Table 2-6: Prepared buffers and solutions.**

Buffer or solution	Composition
Cell freezing medium	90% fetal bovine serum (FBS), 10% DMSO
Citrate buffer	10 mM sodium citrate, pH 6.0
CsCl light solution $\rho = 1.33 \text{ g/cm}^3$	454.2 g/L CsCl in 10 mM Tris (pH 7.8)
CsCl heavy solution $\rho = 1.45 \text{ g/cm}^3$	609.0 g/L CsCl in 10 mM Tris (pH 7.8)
Digestion buffer for DNA isolation	100 mM NaCl, 25m M EDTA (pH 8.0), 10mM Tris (pH 8.0), 0.5% SDS
FACS Puffer	1% FBS in Phosphate Buffered Saline (PBS)
ELISA coating buffer	200 mM NaHCO <sub>3</sub> , 80 mM Na <sub>2</sub> CO <sub>3</sub> , pH 9.5
Erythrocyte lysis buffer	150 mM NH <sub>4</sub> Cl, 10 mM KHCO <sub>3</sub> , 0.1 mM EDTA
Lysis buffer for caspase assay	50 mM Tris (pH 8.0), 130 mM NaCl, 0.5% Nonidet P 40, 5 mM EDTA (pH 8.0)
20x PBS	200 mM Na <sub>2</sub> HPO <sub>4</sub> , 2.8 M NaCl, 36 mM KH <sub>2</sub> PO <sub>4</sub> , 54 mM KCl, pH 7.4
PCR master mix	1x Taq buffer, 10% glycerin, 1.5 mM MgCl <sub>2</sub> , 0.5 mM dNTPs, 0.1 mM cresol red
Precipitation buffer for DNA isolation	588 mM NH <sub>4</sub> C <sub>2</sub> H <sub>3</sub> O <sub>2</sub> in 94% ethanol
SDS-PAGE collection gel 5% (PAGE: polyacrylamide gel electrophoresis)	125 mM Tris (pH 6.8), 5% PAA, 0.1% SDS, 0.1% TEMED, 0.1% APS
SDS-PAGE separation gel 10-14%	375 mM Tris (pH 8.6), 10-14% PAA, 0.1% SDS, 0.1% TEMED, 0.1% APS

SDS-PAGE 10x electrophoresis buffer	250 M Tris, (pH 8.6), 1.92 M glycine, 1% SDS
SDS-PAGE 10x sample buffer	62.5 mM Tris (pH 6.8), 0.5 M DTT, 10% glycerol, 2% SDS, 0.01% bromophenol blue
SRB staining solution	0.5% SRB solution in 1% acetic acid
SRB solubilization solution	10 mM Tris, pH 10.0
Tris acetate EDTA buffer (TAE) for PCR	40 mM Tris (pH 8.0), 1 mM EDTA (pH 8.0), 0.1% acetic acid
10x Tris Buffered Saline (TBS)	200 mM Tris (pH 7.6), 1.5 M NaCl
Virus sample buffer	20 mM Tris, 25 mM NaCl, pH 7.8
Virus storage buffer	20 mM Tris, 25 mM NaCl, 2.5% Glycerol, pH 7.8
WB blotting buffer	5 mM Tris (pH 6.8), 192 mM glycine, 0.05% SDS, 20% methanol
WB washing solution TBS-T	0.1% Tween 20 in 1x TBS

### 2.1.7. Kits

**Table 2-7: Kits.**

Kit	Manufacturer
ATP determination kit	Life Technologies GmbH, Darmstadt, GER
Gel extraction kit QIAquick	Qiagen GmbH, Hilden, GER
HMGB1 ELISA	IBL International GmbH, Hamburg, GER
Mycoplasma PCR detection kit MycoTrace	PAA Laboratories GmbH, Cölbe, GER
Mouse Flt3L Quantikine Immunoassay	R&D Systems GmbH, Wiesbaden-Nordenstadt, GER
Protein assay kit Bicinchoninic acid (BCA)	Thermo Fisher Scientific Inc., Waltham, MA, USA

### 2.1.8. Enzymes

**Table 2-8: Enzymes.**

Enzyme	Manufacturer
Endonuclease Benzonase Nuclease	Merck KGaA, Darmstadt, GER
Proteinase K	QIAGEN GmbH, Hilden, GER
Taq polymerase	Fermentas GmbH, St. Leon Rot, GER

### **2.1.9. Antibiotics and cytostatic drugs**

Cycloheximide (CHX) was used as a positive control for apoptosis in combination with FasL. It acts as an antibiotic inhibitor of protein biosynthesis by blockage of translational elongation at the ribosomes (Martin et al. 1990). CHX was kindly provided by PD Dr. Ulrike Naumann, Hertie-Institute for Clinical Brain Research, Tübingen, GER.

Daunorubicin or daunomycin belongs to the group of anthracyclines. It inhibits nucleic acid biosynthesis as a result of its DNA intercalation (Mizuno et al. 1975). Within this thesis, daunorubicin was used to maintain the drug-resistant phenotype of the HeLaRDB cells. Daunorubicin was purchased from Sigma-Aldrich Chemie GmbH, Steinheim, GER.

Mitoxantrone (MTX) is an anthracenedione, but not an anthracycline antineoplastic agent. It acts as a topoisomerase II inhibitor and intercalates into the DNA. It disrupts DNA synthesis and DNA repair in both healthy cells and cancer cells (Mazerski et al. 1998). MTX was used as a positive control for induction of ICD within this work. MTX was purchased from Baxter Oncology GmbH, Unterschleißheim, GER.

Monensin is polyether antibiotic that acts as an ionophore. It blocks intracellular protein transport (Mollenhauer et al. 1990) and was therefore used within this thesis to detect CD107a on cell surfaces by flow cytometry. 1000x monensin was purchased from eBioscience, Frankfurt, GER.

Mitomycin C is an aziridine-containing cytotoxic antibiotic. It is a potent DNA crosslinker, inhibiting DNA replication and transcription. It is used to inhibit cell growth in tumor cells in cocultures with splenocytes (Kuroda and Furuyama 1963). Mitomycin C was purchased from SERVA Electrophoresis GmbH, Heidelberg, GER.

Penicillin and streptomycin (PS) were used to avoid bacterial infections in the freshly isolated splenocytes. Penicillin antibiotics are  $\beta$ -lactam antibiotics that are used in the treatment of bacterial infections caused by susceptible, usually Gram positive, organisms (Garrod 1960). They inhibit the formation of peptidoglycan cross-links in the bacterial cell wall by binding to a bacterial enzyme that catalyzes formation of these cross-links. Streptomycin is an antibiotic aminoglycoside (Singh and Mitchison 1954). It acts as a protein synthesis inhibitor by binding to the 16S rRNA of the bacterial ribosome leading to codon misreading. Penicillin and streptomycin were purchased from Merck KGaA, Darmstadt, GER.

Phorbol 12-myristate 13-acetate (PMA) and ionomycin were used within this thesis as a positive control for T cell activation in the ELISpot assay. PMA activates the signal transduction enzyme protein kinase C (Niedel et al. 1983). Ionomycin is an ionophore that raises the intracellular level of calcium ( $Ca^{2+}$ ) (Liu and Hermann 1978).

PMA and ionomycin act together to stimulate T cell activation, proliferation, and cytokine production like IFN $\gamma$ . PMA was purchased from Sigma-Aldrich Chemie GmbH, Steinheim, GER and ionomycin from Calbiochem, Merck KGaA, Darmstadt, GER.

### 2.1.10. Cytokines

**Table 2-9: Cytokines.**

Cytokine	Manufacturer
FasL	FasL was kindly provided by PD Dr. Ulrike Naumann, Hertie-Institute for Clinical Brain Research, Tübingen, GER
IL-2	Peptotech GmbH, Hamburg, GER
IFN $\gamma$ , human, murine	Peptotech GmbH, Hamburg, GER

### 2.1.11. Primers

All primers were purchased from Eurofins MWG Operon, Ebersberg, GER and dissolved in 10 mM Tris (pH 7.8) to a final stock concentration of 100  $\mu$ M.

**Table 2-10: Primer sequences.**

Target gene	Sequence	Application
Adenovirus E1A	Fw: 5'-AATGGCCGCCAGTCTTTT-3' Rev: 5'-GCCATGCAAGTTAAACATTATC-3'	PCR
Adenovirus E1A CR3	Fw : 5'-GGCATGTTTGTCTACAGTAAG-3' Rev : 5'-GCCATGCAAGTTAAACATTATC-3'	PCR
Adenovirus E1B19K	Fw: 5'-CGTGAGAGTTGGTGGGCGT-3' Rev: 5'-CTTCGCTCCATTATCCT-3'	PCR
Adenovirus E3	Fw: 5'-GAACAATTCAAGCAACTCTAC-3' Rev: 5'-CTCGAGGAATCATGTCTC-3'	PCR
RGD peptide in adenovirus fiber	Fw: 5'-CTGCCGCGGAGACTGTTTC-3' Rev: 5'-CTGCAATTGAAAAATAAACACG-3'	PCR
Adenovirus hexon	Fw: 5'-GGCCATTACCTTTGACTCTTC-3' Rev: 5'-GCATTTGTACCAGGAACCGTC-3'	Real time PCR
$\beta$ -Actin	Fw: 5'TAAGTAGGTGCACAGTAGGTCTGA-3', Rev: 5'-AAAGTGCAAAGAACACGGCTAAG-3'	Real time PCR

## 2.1.12. Antibodies

Table 2-11: Antibodies.

Target protein	Isotype (clone)	Conjugate	Company	Application
Actin	Rabbit polyclonal		Sigma-Aldrich Chemie GmbH, Steinheim, GER	WB
CRT	Rabbit polyclonal		Abcam plc, Cambridge, UK	FACS
CD3	Rat IgG2b $\kappa$ (17A2)	eF450	eBioscience, Frankfurt, GER	FACS
CD8a	Rat IgG2b $\lambda$ (5H10)	FITC	Caltag, Life Technologies GmbH, Darmstadt, GER	FACS
CD11c	Armenian hamster IgG (N418)	FITC	BioLegend, Fell, GER	FACS
CD19	Rat IgG2a $\kappa$ (eBio1D3)	APC-eF780	eBioscience, Frankfurt, GER	FACS
CD45	Rat IgG2b $\kappa$ (30-F11)	PerCP-Cy5.5	eBioscience, Frankfurt, GER	FACS
CD49b	Rat IgM $\kappa$ (DX5)	APC	eBioscience, Frankfurt, GER	FACS
CD49b	Rat IgM $\kappa$ (DX5)	PE	BioLegend, Fell, GER	FACS
CD107a	Rat IgG2a $\kappa$ (1D4B)	APC	BioLegend, Fell, GER	FACS
F4/80	Rat IgG2a $\kappa$ (BM8)		eBioscience, Frankfurt, GER	IHC
Hexon	Mouse IgG		Applied Biological Materials Inc., Richmond, BC, CAN	ICC
Hsp70	Mouse IgG1 (cmHsp70.1)	FITC	*	FACS
IFN $\gamma$	Rat IgG1 $\kappa$ (AN-18)		eBioscience, Frankfurt, GER	ELISpot
IFN $\gamma$	Rat IgG1 $\kappa$ (R4-6A2)	Biotin	eBioscience, Frankfurt, GER	ELISpot
LC3	Mouse IgG1 (5F10)		nanoTools Antikörpertechnik GmbH & Co. KG, Teningen, GER	WB
MHC Class I	Mouse IgG2b (2G5)		AbDSerotec, Düsseldorf, GER	FACS
Poly ADP-ribose polymerase 1 (PARP1)	Rabbit polyclonal		Cell Signaling Technology, Inc., Danvers, MA, USA	WB
Phospho (P)-eIF2 $\alpha$ (Ser51)	Rabbit polyclonal		Cell Signaling Technology, Inc., Danvers, MA, USA	WB
P-Stat1 (Tyr701)	Rabbit polyclonal		Cell Signaling Technology, Inc., Danvers, MA, USA	WB
YB-1 **	Rabbit polyclonal			IF, WB
Isotype antibody	Rabbit polyclonal		BD Biosciences, Heidelberg, GER	FACS
Isotype antibody	Mouse IgG2b $\kappa$		BD Biosciences, Heidelberg, GER	FACS
Isotype antibody	Mouse IgG1	FITC	Southern Biotech, Birmingham, AL, USA	FACS



Mouse	Goat polyclonal	HRP	Dako Deutschland GmbH, Hamburg, GER	ICC, ELISA, WB
Mouse	Rabbit polyclonal	PE	Dako Deutschland GmbH, Hamburg, GER	FACS
Rabbit	Swine polyclonal	FITC	Dako Deutschland GmbH, Hamburg, GER	IF, FACS
Rabbit	Goat polyclonal	HRP	Dako Deutschland GmbH, Hamburg, GER	WB
Rat	Rabbit polyclonal	HRP	eBioscience, Frankfurt, GER	IHC

So far undefined abbreviations within this table: Allophycocyanin (APC), Cyanine (Cy), eFluor (eF), Fluorescein isothiocyanate (FITC) Peridinin chlorophyll protein (PerCP), Phycoerythrin (PE). Immunocytochemistry (ICC), immunohistochemistry (IHC), immunofluorescence (IF). Abbreviation FACS stands for flow cytometric analysis here.

\* The cmHsp70.1 antibody (Stangl et al. 2011) was kindly provided by Prof. Gabriele Multhoff, Klinikum rechts der Isar, Munich, GER.

\*\* The polyclonal anti-YB-1 antibody used within this thesis was custom produced by Eurogentec Deutschland GmbH, Köln, GER with their 28 d program. The sequence used for immunization is depicted in appendix A.

### 2.1.13. Cell culture media and supplements

**Table 2-12: Cell culture media and supplements.**

Cell culture medium, supplement	Manufacturer
Eagle's Minimum Essential Medium (MEM) containing 2 mM L-glutamine, 1 mM sodium pyruvate, 1% MEM non-essential amino acids (NEAA) and 10% FBS	CLS Cell Lines Service GmbH, Eppelheim, GER
PBS, Dulbecco	Biochrom AG, Berlin, GER
MEM NEAA	Gibco, Life Technologies GmbH, Darmstadt, GER
Dulbecco's Modified Eagle's Medium (DMEM)	Biochrom AG, Berlin, GER
Roswell Park Memorial Institute RPMI 1640	Biochrom AG, Berlin, GER
FBS Sera Plus	PAN-Biotech GmbH, Aidenbach, GER
Glutamine, L-glutamine	Biochrom AG, Berlin, GER
Sodium pyruvate	Gibco, Life Technologies GmbH, Darmstadt, GER
Trypsin/EDTA solution	Biochrom AG, Berlin, GER
TrypLE™ Express	Gibco, Life Technologies GmbH, Darmstadt, GER
OptiMEM® I + GlutaMAX™ I	Gibco, Life Technologies GmbH, Darmstadt, GER
Trypan blue solution (0.4%)	Sigma-Aldrich Chemie GmbH, Steinheim, GER

KLN205 cells were cultured in readily supplemented MEM from CLS GmbH. CT26 cells were cultured in RPMI medium containing 5% FBS, 2 mM L-glutamine, 2 mM sodium pyruvate, 1% MEM NEAA. All other cell lines were cultured in DMEM supplemented with 10% FBS and 2 mM L-glutamine.

#### **2.1.14. Cell lines**

Human cell lines include HEK293 (American Type Culture Collection (ATCC) number CRL-1573) cells. HEK293 cells are human embryonic kidney cells that are frequently used for adenovirus titration and production. They are permissive for adenovirus serotype 5 infection and are able to transcomplement the *E1* region because 4.5 kb of the left end of the adenovirus 5 genome including the *E1* region have been stably integrated into their genome (Graham et al. 1977). Therefore, all viruses, including replication-deficient viruses can be produced and viral titer can be determined in this cell line. HEK293 cells were kindly provided by Dr. Martina Anton, Klinikum rechts der Isar, Munich, GER. A549 (ATCC CCL-185) is an adenocarcinomic alveolar basal epithelial cell line (Giard et al. 1973). The lung carcinoma cells were used as a human control cell line. The other human control cells used were HeLa cells (ATCC CCL-2). They are named after Henrietta Lacks, from whose cervical adenocarcinoma the malignant epithelial cells were isolated 1951. It was the first permanent human cell line ever established (Scherer et al. 1953). HeLaRDB (resistant to daunoblastin) entitles the drug-resistant sub-cell line, which was rendered resistant by multiple passages in daunorubicin supplemented culture medium. To maintain the drug-resistant status that is characterized by overexpression of P-glycoprotein, 0.25 µg/mL daunorubicin were added to the culture medium at each passaging. A549 and HeLa cells were provided by Prof. Hermann Lage, Charité, Berlin, GER. Human foreskin fibroblast cells HS68 (ATCC CRL-1635) were used as a non-tumor control for YB-1 expression (Dawes et al. 1993). HS68 cells were kindly provided by Dr. Martina Anton, Klinikum rechts der Isar, Munich, GER.

Murine cell lines used within this thesis were KLN205, SCCVII, CMS-5, CT26, and SMA560. KLN205 (ATCC CRL-1453), are murine squamous cell carcinoma cells of the lung that spontaneously developed in DBA/2 (H2-d) mice (Kaneko and LePage 1978). DBA/2 or BDF1 mice injected with this low immunogenic cell line develop tumors and lung metastases. The cells were purchased from CLS Cell Lines Service GmbH, Eppelheim, GER. SCCVII is a poorly immunogenic murine squamous cell carcinoma cell line that spontaneously arose from the skin of a C3H/HeJ mouse (Hirst et al. 1982, Khurana et al. 2001). SCCVII cells were kindly provided by Jan Alsner, Aarhus University Hospital, Aarhus, Denmark. CMS-5, a fibrosarcoma cell line originating from

a methylcholanthrene-induced tumor in BALB/c mice, is also weakly immunogenic (DeLeo et al. 1977). CMS-5 cells were provided by Prof. Bernd Gänsbacher, Klinikum rechts der Isar, Munich, GER. CT26 (ATCC CRL-2638) is a murine N-nitroso-N-methylurethane-induced, undifferentiated colon carcinoma cell line of BALB/c origin (Wang et al. 1995). CT26 cells were kindly provided by Prof. Gabriele Multhoff, Klinikum rechts der Isar, Munich, GER. SMA560 are non-immunogenic to low immunogenic spontaneous VM/Dk murine astrocytoma cells (Serano et al. 1980). The cell line was kindly provided by PD Dr. Ulrike Naumann, Hertie-Institute for Clinical Brain Research, Tübingen, GER.

HaK (ATCC CCL-15) are Syrian golden hamster epithelial cells. Although HaK cells were originally derived from normal kidneys, these cells injected subcutaneously into the flanks of Syrian hamsters have been shown to develop tumors in the animals (Thomas et al. 2006). HaK tumors metastasize to multiple sites and are histologically characterized as adenocarcinomas. HaK cells were provided by Prof. Hermann Lage, Charité, Berlin, GER.

#### **2.1.15. Viruses**

The wild type adenovirus Ad-wt is a human serotype 5 adenovirus of the species C. The well characterized virus is replication-competent and holds no genomic alterations. It therefore served as a positive control for replication, particle formation, and cell lysis. All other oncolytic viruses used in this thesis are derived from this virus. Ad-dl703 has a 3.2 kb deletion in the *E1* region (Bett et al. 1994). It is replication-deficient at low to medium multiplicity of infection (MOI), and thus serves as a negative control for replication in the experiments within this thesis. Ad-eGFP is a replication-deficient adenovirus with an enhanced green fluorescent protein (eGFP) gene insertion under the control of a cytomegalovirus (CMV) promoter in the *E1* region. It was used within this thesis to monitor the infectability of cells.

The oncolytic adenovirus Ad-Delo3-RGD (figure 2-1 A) has an 11 bp deletion in CR3 region of the *E1A* gene resulting in the lack of expression of the transactivating 289 aa E1A protein by this virus (Mantwill et al. 2006, Rognoni et al. 2009). E1B19K protein expression is disabled by a partial deletion of the *E1B19K* gene, but without influence on the open reading frame of *E1B55K*. The *E3* region is largely deleted in Ad-Delo3-RGD and an additional RGD motif has been inserted into the viral fiber knob.

The following oncolytic virus vectors were constructed and kindly provided for this work by Klaus Mantwill, Klinikum rechts der Isar, Munich, GER. In Ad-Delo3-RGD-Flt3L (figure 2-1 B), an additional murine Flt3L (mFlt3L) gene is inserted into the *E3* region of Ad-Delo3-RGD replacing the wild type *E3gp19K* gene under the control of the natural major late promoter. In the oncolytic adenovirus Ad-PSJL-K (figure 2-1 C), most of the *E1* region, including *E1A* and the anti-apoptotic gene *E1B19K* is deleted and replaced by *E1B55K* under the control of a CMV promoter to enhance cytoplasmatic YB-1 transport into the nucleus. A part of the *E3* region, including the immunosuppressive glycoprotein gene *E3gp19K* is deleted and the *E4* promoter is replaced by a YB-1 promoter to further enhance tumor cell specificity and to render besides *E1B55K* also *E4orf6* independent of adenoviral promoters and adenoviral replication. As in the other oncolytic viruses, an additional RGD motif is inserted into the fiber knob domain of the protein fiber.

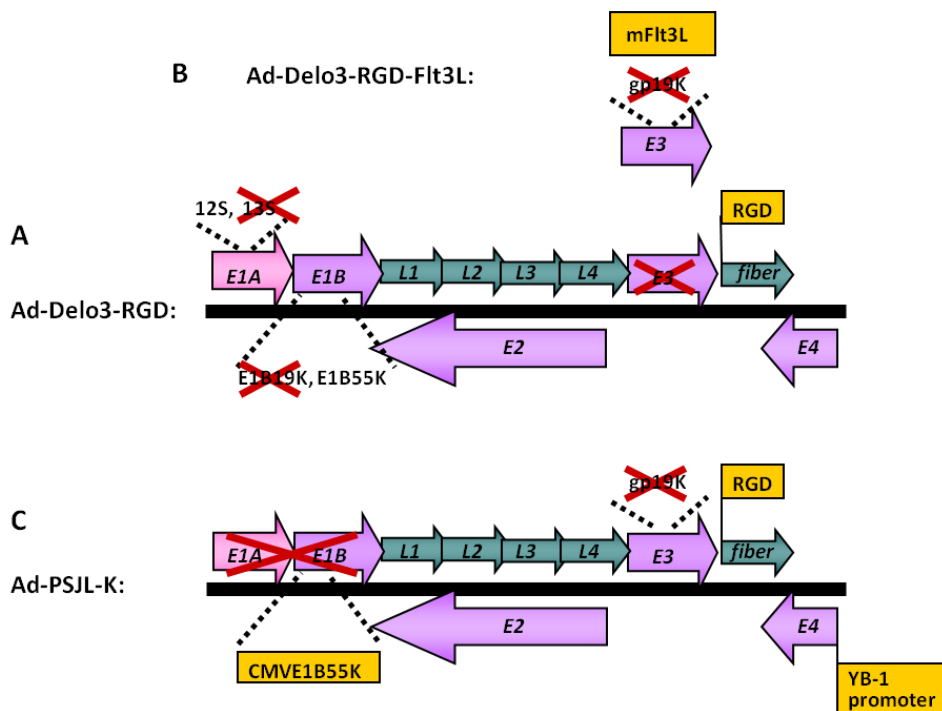


**Figure 2-1: Mutations in YB-1-dependent oncolytic adenoviruses.** Mutations are described in the text in chapter 2.1.15. A. Ad-Delo3-RGD. B. Ad-Delo3-RGD-Flt3L: Ad-Delo3-RGD-Flt3L is constructed like Ad-Delo3-RGD with exception for the *E3* region which is separately depicted here. C. Ad-PSJL-K.

### 2.1.16. Mice

DBA/2 mice (haplotype H-2<sup>d</sup>) were used for the *in vivo* experiments. The DBA inbred mouse strain was established as the first inbred mouse strain in 1909 from C.C. Little (Carter 1952). DBA/2 mice are syngeneic for the tumor cell line KLN205 used within this thesis. Eight week old DBA/2 mice were purchased from Janvier, Le Genest Saint Isle, Saint Berthevin Cedex, France.

## **2.2. Methods**

### **2.2.1. Cell culture**

Shortly after arrival in the laboratory, all cell lines were routinely tested for mycoplasma infections with the mycoplasma PCR detection kit according to the manufacturer's instructions. All cells were incubated at 37 °C in a humidified atmosphere containing 5% CO<sub>2</sub>. Cells were maintained as subconfluent monolayers in their particular culture medium (chapter 2.1.13) by passaging them twice a week at appropriated dilutions. For this purpose, cells were washed with PBS and detached with trypsin. For KLN205 cells, TryLE™ Express was used instead of trypsin. The cell pellet was collected by centrifugation at 1200 rpm for 5 min at room temperature (RT), cells were resuspended in fresh medium, and adequate amounts of cells were applied to new culture flasks or dishes. For freezing of cells, they were collected as described above and the pellet was resuspended in cell freezing medium. Cells were cooled down in a freezing container with isopropyl alcohol at -80 °C and after 24 h transferred to liquid nitrogen for long time storage. Cryo-conserved cells were thawed in a 37 °C water bath and immediately but carefully supplemented with fresh medium to prevent cell damage by DMSO, a component of the freezing medium. Cell pellets were collected as described above, resuspended in appropriate volumes of fresh medium, and further cultivated as described above. For plating of cells, they were collected as described above and counted in cell counting chambers. The number of cells per volume was calculated as average number of cells per big square x 10<sup>4</sup> x dilution factor, resulting in the number of cells per mL. To control the viability of the cells, the cell suspension was mixed with trypan blue solution before counting. If cells appear blue, their cell membrane is leaky and the anionic diazo dye can accumulate within the cell. Only non-colored cells account for the actual cell number. Cells were plated in dishes or multi-well plates™ according to the assay and incubated at 37 °C in 5% CO<sub>2</sub> for 24 h to adhere.

KLN205 cell lysate for immune cell stimulation in immunological assays was prepared by three steps of thawing and freezing of 4x10<sup>7</sup> cells in 3 mL PBS and subsequent centrifugation at 3000 rpm for 15 min at 4 °C. The sterile filtered supernatant was used to stimulate the cells.

### **2.2.2. Virus amplification and purification**

All experiments involving viruses were conducted in a S2 facility according to the present guidelines of the German Act on Genetic Engineering. All contaminated materials and solutions

were collected, inactivated, and disposed following the official guidelines. Genetic engineering was approved by the local authorities (Regierung von Oberbayern, Munich, GER).

Viruses were produced in large scale in, depending on the virus, 20-45 15 cm culture dishes in HEK293 cells. When difficulties arose during virus production, the amplification was performed in smaller steps, starting with for example one 15 cm culture dish. Either seed viral lysate or readily purified virus were used as starting points for the production. The amount of virus to be used for the amplification was determined by infection of smaller plate formats with various volumes of lysate or infectious units (IFU)/cell of purified virus. After 48 h, the first well with almost complete lysis was assessed and from that, the amount of virus needed to infect a 15 cm dish was calculated by scaling up the plate area. At a confluency of 90-100%, the cells in the 15 cm dishes were infected with the determined amount of virus in 4 mL OptiMEM including 2% FBS. During 1 h of incubation at 37 °C and 5% CO<sub>2</sub>, medium and virus have to be evenly distributed, so the dish was tilted every 15 min. After 1 h, 14 mL of complete culture medium containing 10% FBS were added to the infection dish and the infected cells were further incubated at 37 °C and 5% CO<sub>2</sub>. After 48 h of incubation, the cells have to show signs of advanced CPE, ideally shortly before budding off of the viral particles. The cells can then be easily detached from the dish surface by gently tapping on the rim of the plate. Cells were rinsed off the plate, collected and centrifuged at 1500 rpm for 10 min at RT. The cell pellet was resuspended in 10 mL sample buffer per 20 plates and repeatedly frozen and thawed three times to release the virions from the cells. The virions were separated from the cell debris by centrifugation at 3000 rpm for 15 min at 4 °C. 12.5 U/mL Benzonase Nuclease was added to the supernatant in the presence of 1 mM MgCl<sub>2</sub>. The endonuclease was activated for 5 min at 37 °C and degraded the remaining cellular nucleic acids during 1 h at RT with shaking steps every 15 min. The debris was separated from the virus solution by another 3000 rpm centrifugation step for 15 min at 4 °C. The virus solution was purified by a CsCl density gradient. The gradient was built in ultracentrifuge tubes with one layer (17 mL) of light and one layer (9 mL) of heavy CsCl solution. The adenovirus solution was carefully added on top of the gradient and the tubes were centrifuged in an ultracentrifuge at 20,000 rpm for 3 h at 10 °C. The viral band was taken by a syringe without touching the above band with the fragmentary particles and cell remains. For further purification, a second centrifugation step was performed like the previous one but for 18 h. The purified virus band was carefully taken from the gradient and the remaining salts were removed from the solution by sephadex PD-10 columns according to manufacturer's instructions. Storage buffer containing glycerin was used to equilibrate the columns. 2.5 mL of virus solution was applied onto each column. The virus solution was stored at -80 °C in aliquots until use.

### 2.2.3. Determination of viral titer, particle count, purity, size, and homogeneity

Within this thesis, viral titers are all indicated as IFU/mL. They were determined with an ICC assay directed towards the essential adenoviral capsid protein hexon in HEK293 cells. The assay was conducted according to Agilent Technology's titer protocol AdEasy Viral Titer Kit. 10-fold serial dilutions in duplicates were prepared in fully supplemented DMEM medium and 50  $\mu$ L per well were applied to 24-well plates together with  $2.2 \times 10^5$  HEK293 cells in 500  $\mu$ L per well. 48 h after infection, cells were fixed with cold methanol and washed twice with PBS containing 1% BSA. The hexon protein was detected by staining with a primary anti-hexon antibody 1:500 and a secondary HRP-conjugated antibody 1:1000, each diluted in 150  $\mu$ L PBS with 1% BSA, for 1 h each with two washes with PBS with 1% BSA after each antibody incubation. Hexon positive spots were visualized by the colorimetric conversion of DAB substrate by HRP. Brownish spots per microscope field were counted using a 20x microscope objective and the titer was calculated as IFU/mL = (average number of positive cells per field x 314 fields per well)/(volume of diluted virus used in each field (mL) x dilution factor).

The amount and purity of viral particles (VP) were determined via the optical density of the solution. The virus solution was diluted 1:20 and 1:10 in equal amounts of storage and sample buffer. Dilutions and blank buffer were incubated at 100 °C for 10 min in a heating block. After heating, the samples were chilled on ice for 1 min and the optical density (OD) was measured. The amount of VP/mL was calculated as  $OD_{260} \times 1.1 \times 10^{12}$  VP/mL (Maizel et al. 1968). The  $OD_{260\text{nm}}/OD_{280\text{nm}}$  ratio was monitored for assessment of virus purity.

Aggregate formation in the adenovirus preparation can be excluded by particle size measurement using dynamic light scattering. Dynamic light scattering is an optical method to study Brownian motion of sub-micron sized particles in solution. Brownian motion is dependent on temperature, viscosity, and ionic strength of the solvent, and also on the size of the particles. By recording the scattering pattern of the light from a sample, conclusions can be drawn concerning the size and dispersity of the particles within the sample.  $4 \times 10^{10}$  VP in a total of 800  $\mu$ L of freshly prepared 10 mM NaCl solution were applied to the Zetasizer under constant solvent, temperature and measurement conditions (attenuator 8). The Cumulants analysis-determined hydrodynamic diameter (Z-average) and the polydispersity index (Pdl) depict the average diameter of the viral molecules in the solution and the grade of dispersity, respectively. Both values were monitored for each virus sample. Absence of virus aggregation is determined by acquisition of a single peak with an average diameter of  $110 \pm 20$  nm representing the adenovirus particles and a Pdl smaller than 0.1 indicates that the virus is homogeneous. Count rates per second higher than 250 are

necessary in order to obtain valid results (Malvern\_Instruments 2011, Dr. P.S. Holm personal communication).

#### **2.2.4. DNA isolation and PCR analysis of viral genes**

To analyze the viral genome and verify the vector mutations, DNA was isolated from the viruses by phenol chloroform extraction. 200  $\mu\text{L}$  digestion buffer was added to 200  $\mu\text{L}$  of purified virus solution. 100  $\mu\text{g}$  proteinase K was added to degrade proteins within the cell digest. After incubation overnight at 50  $^{\circ}\text{C}$ , an equal volume of phenol chloroform isoamyl alcohol was added to the cell digest. The mixture was shaken and phases were separated by centrifugation at 13,000 rpm for 5 min at 4  $^{\circ}\text{C}$ . The upper aqueous phase containing the DNA was added to another equal volume of chloroform for disposal of the remaining phenol. Phases were mixed again and separated by another equal centrifugation step. The DNA in the upper phase was gained by ethanol precipitation by addition of 425  $\mu\text{L}$  precipitation buffer per 100  $\mu\text{L}$  of DNA solution. By mixing, the polar DNA is precipitated with positive ions in the solution. 35  $\mu\text{g}/\text{mL}$  glycogen was added as a carrier that helps to maximize DNA recovery. The pellet that results from centrifugation for 40 min at 13,000 rpm at 4 $^{\circ}\text{C}$  was resuspended in 70% ethanol to wash out remaining salts, centrifuged 7 min at 9000 rpm at RT and air dried. The pellet was resuspended in 10 mM Tris (pH 7.8) and the DNA concentration was determined using a photometer. Following the Beer Lambert law, the absorbance value at 260 nm equals the product of the extinction coefficient, which is  $0.020 (\mu\text{g}/\text{ml})^{-1} \text{cm}^{-1}$  for dsDNA, the concentration of the substance in  $\mu\text{g}/\text{mL}$ , and the length of the light path in cm that equals 1 for a usual spectrophotometer. So the dsDNA concentration was calculated as  $50 \mu\text{g}/\text{mL} \times \text{OD}_{260\text{nm}} \times \text{dilution factor}$ . Purity of the DNA was controlled via the  $\text{OD}_{260\text{nm}}/\text{OD}_{280\text{nm}}$  and  $\text{OD}_{260\text{nm}}/\text{OD}_{230\text{nm}}$  ratios (Barbas et al. 2007). Viral genes of interest were amplified via PCR using PCR master mix, 0.5  $\mu\text{M}$  of each forward and reverse primer (table 2-10), 0.1 U/ $\mu\text{L}$  Taq polymerase and 1-10 ng/ $\mu\text{L}$  template DNA in a total volume of 25  $\mu\text{L}$ . DNA was amplified on a thermal cycler as follows: after a 1 min activation step at 95  $^{\circ}\text{C}$ , the DNA products were amplified in 30 cycles of each 40 sec denaturation at 95  $^{\circ}\text{C}$ , annealing at 52  $^{\circ}\text{C}$  and DNA synthesis at 72  $^{\circ}\text{C}$ . PCR was terminated by a 5 min step at 72  $^{\circ}\text{C}$ . PCR products were supplemented 1:6 with 6x DNA loading dye and run at 80-100 V on gels of 1% agarose in TAE buffer containing 2  $\mu\text{L}$  EtBr per 50 mL gel. DNA bands were visualized with UV light.



### **2.2.5. Virus infection**

For virus infection of cells *in vitro*, cells were plated the day before the assay in appropriate cell numbers and plate or dish formats, depending on the specific assay. Usually cells should have a confluency of 70-90% at the time of the infection. For infection, the cultivation medium was removed and replaced by a thin layer of infection medium, just covering the cell layer. OptiMEM without FBS was used as infection medium. It contained the particular adenovirus with a MOI given as IFU/cell in this work. During the incubation period of 1 h at 37 °C and 5% CO<sub>2</sub>, the plate was tilted every 15 min for equal distribution of the virus and to prevent drying of the cell layer with this low infection medium volume. After the hour of infection, the infection medium was replaced by fresh complete medium. Control wells were “mock” infected, meaning they were treated exactly like the infected cells (OptiMEM for 1 h and then exchange of medium) but without addition of virus. The infected cells were incubated at 37 °C 5% CO<sub>2</sub> for the desired time depending on the experiment. Dying adenovirus infected cells undergo typical morphological changes called CPE, characterized by rounding of the cells and subsequent detachment. This process was monitored under a light microscope and pictures were taken for documentation.

### **2.2.6. Flt3L ELISA**

To verify the expression of murine Flt3L protein in Ad-Delo3-RGD-Flt3L infected cells, an ELISA specific for this protein was performed according to the manufacturer’s instructions. Supernatant of virus infected cells in 6-well plates was analyzed 48 h after infection. 50 µL of the supernatant was applied per well. Samples were analyzed in duplicates, background values were subtracted, and the mFlt3L concentration was determined according to a standard curve resulting from a 4-parameter analysis using the software ReaderFit.

### **2.2.7. Immunofluorescence staining of YB-1 expression**

To stain the cells for YB-1 expression, cells were grown on microscope slides in 10 cm dishes. 24 h after infection, cells were fixed with 1:1 acetone and methanol for 20 min at -20 °C. Cells were rinsed with PBS and blocked with 150 µL 5% swine serum (the secondary antibody was raised in swine) in PBS for 30 min at RT. After another wash with PBS, the YB-1 antibody was added 1:100 in 150 µL antibody diluent with background reducing components at 4 °C overnight. After another wash with PBS, cells were incubated with the secondary FITC-conjugated antibody 1:20 in 1% swine serum in PBS for 45 min at RT. After another wash with PBS, cells were counterstained with 2 µg/mL Hoechst 33342 in 200 µL water for 5 min. Finally, slides were rinsed with PBS, let dry and mounted with mounting medium. Stained cells were observed on an AxioImager microscope with ApoTome and analyzed with ImageJ software.

### **2.2.8. Cytotoxicity assay *in vitro* by SRB staining of infected cells**

Virus-mediated cytotoxicity was determined by staining of the adherent cells with SRB solution 6 d after virus infection of cells in 96-well plates (Skehan et al. 1990). Before the staining performed in triplicates of each viral concentration, cells were carefully washed with PBS. Subsequently, cells were fixed with cold 10% TCA solution overnight at 4 °C. Cells were thereafter washed five times with distilled water before they were stained with the pink fluorescent aminoxanthene dye SRB staining solution for 10 min at RT. Under the mild acetic conditions, the anionic fluorescent dye binds to basic amino acids of the cellular proteins. After the staining, cells were rinsed five times with 1% acetic acid for excess dye to be washed away and let dry. Plates can then be scanned in a commercial scanner for storage of images. For quantitative analysis, the protein bound dye was solved under basic conditions with 100 µL of SRB solubilization solution for 1 h and its optical density at 590 nm was measured on a photometer with subtraction of background values. Since SRB binding is stoichiometric, the amount of dye extracted from the stained cells is directly proportional to cell density. Cell survival, here in the form of remaining adherent cells, was calculated as percentage of mock infected cells:  $100\% \times OD_{\text{sample}}/OD_{\text{mock infection}}$ .

### **2.2.9. Monitoring of virus infection with quantitative real time PCR**

To monitor the replication of particular adenoviruses in particular cells, the cells were infected in 6-well plates and DNA was extracted at desired time points by phenol chloroform extraction as

described in chapter 2.2.4. Cells were washed with PBS first and 400  $\mu\text{L}$  digestion buffer was added to the cells. Virus replication was obtained by quantitative real time PCR with adenoviral hexon gene-specific primers. The cellular gene  $\beta$ -actin was used for normalization (table 2-10). To quantify the hexon and  $\beta$ -actin copies, standards were produced by running a PCR (chapter 2.2.4) with the above mentioned primers and extracting the amplified gene products from the agarose gel with the QIAquick gel extraction kit according to the manufacturer's instructions. Standard dilutions in DNA copies per  $\mu\text{L}$  were prepared according to the DNA concentration and molecular weight of the products. The real time PCR was performed with a SYBR green-based system (Bengtsson et al. 2003). The fluorescent cyanine dye SYBR green binds to the minor groove of dsDNA. The bound SYBR green has a 1000 fold stronger fluorescent signal at 520nm after excitation with 497 nm than the unbound dye which makes it suitable to detect accumulation of ds PCR products. 0.5  $\mu\text{M}$  of each forward and reverse primer and 12.5  $\mu\text{L}$  real time PCR master mix, containing the hotstart enzyme Meteor Taq, a passive reference dye and a specific buffer, were added to 100 ng DNA in a total reaction volume of 25  $\mu\text{L}$ . The PCR was performed on a sequence detection system, where, after a 15 min polymerase activation step at 95  $^{\circ}\text{C}$ , the DNA product was amplified in 40 cycles of each 15 sec denaturation at 95  $^{\circ}\text{C}$ , annealing at 60  $^{\circ}\text{C}$  and DNA synthesis at 72  $^{\circ}\text{C}$ . A melting curve was generated to monitor product specificity and purity at 0.5  $^{\circ}\text{C}$  steps at temperatures from 60  $^{\circ}\text{C}$  to 95  $^{\circ}\text{C}$ . After each cycle, the amount of dsDNA was measured in real time via the bound SYBR green at an acquisition step at a temperature of 80  $^{\circ}\text{C}$  for 30 sec. By analysis with the SDS2.2 software, initial hexon and  $\beta$ -actin copies in the samples can be quantified according to the standard curve that correlated initial copy numbers with the cycle threshold (ct) values measured. The ct value is defined as the cycle in which the measured fluorescence signal of the sample exceeds a threshold fluorescence level during the exponential phase of the reaction. It is inversely proportional to the logarithm of the initial copy number in the sample (Heid et al. 1996). Results were indicated as copy numbers of hexon normalized to copy numbers of  $\beta$ -actin.

#### **2.2.10. Analysis of formation of new infectious virus particles**

For measurement of formation of new infectious particles, cells and supernatants from infected cells in 6-well plates were collected by scraping off the cell layer from the well bottom surface after 72 h. The suspension was frozen and thawed three times in a row to release the virions from the cells and centrifuged at 3000 rpm for 15 min at 4  $^{\circ}\text{C}$ . The virus titer in the supernatant was

determined according to the protocol of the hexon protein-based titer test (chapter 2.2.3). The formed infectious particles were indicated as IFU/mL.

#### **2.2.11. Cellular protein isolation and WB analysis**

For protein analysis, cells were grown in 6-well plates or 10 cm dishes. At indicated time points, cells were washed in PBS and scrapped off the plates in PBS. If cells were already detached from the plates, they were collected in centrifuge tubes first and washed afterwards. Ten times the estimated cell volume of mammalian cell lysis reagent supplemented with protease inhibitors, as well as phosphatase inhibitors if necessary, was added to the cell pellet. The suspension was incubated 10 min at RT on a shaker (1100 rpm) and subsequently centrifuged at 13,000 rpm for 15 min at 4 °C. Protein containing supernatants were stored at -80 °C or used for WB analysis directly. Protein concentrations were determined by a BCA-based assay, which is based on the reduction of copper ions by proteins in an alkaline medium (biuret reaction) (Smith et al. 1985). Reduced ions are then complexed with the purple colored salt of BCA. The absorbance at 562 nm is nearly linear with increasing protein concentration and can therefore be used for photometric determination of protein concentrations. 10 µL of prepared BSA standards or samples were mixed with 200 µL of the working reagent. The plate was read on a photometer at 590 nm after 30 min of incubation at 37 °C. The blank well value was subtracted from all sample values and the protein concentration was calculated according to the standard curve.

Protein samples (40 µg) were supplemented 1:10 with 10x sample buffer containing anionic SDS to create a negative loading of the samples and DTT to destroy disulfide bonds by reduction and heated to 95 °C for 5 min to break protein hydrogen bonds and secondary and tertiary structures. The denatured samples were separated according to their size on a PAA gel containing SDS in an electric field of 20 mA for 3 h (Laemmli 1970). The separation gel had an acrylamide content according to the size of the expected band, ranging from 10% for almost all samples within this thesis, to 14%, resulting in narrower PAA net pores for the relatively small LC3 proteins. Protein transfer onto a nitrocellulose membrane or a PVDF membrane for LC3 antibody staining, was conducted electrophoretically for 1 h at 100 V (Burnette 1981). To verify a successful blotting procedure, nitrocellulose membranes can be stained with Ponceau S for 10 min (Salinovich and Montelaro 1986). Through rinsing the blot with TBS-T, the dye was removed again. Unspecific binding sites on the membrane were blocked with 5% BSA in TBS-T for 1.5 h. For the LC3 blot, commercial blot incubation buffer was used instead of TBS-T, and milk powder instead of BSA. The following washing steps, as well as all subsequent washing steps, were conducted by

three times 10 min washing with TBS-T. The primary antibody was incubated in 2.5% BSA in TBS-T for 1.5 h at RT or depending on the antibody overnight at 4 °C. Antibodies were diluted as follows: actin 1:250, LC3 1:200, YB-1 1:400, others 1:1000. After washing away the excess antibody, the secondary HRP-conjugated antibody was added 1:1000 in 2.5% BSA in TBS-T for 1.5 h at RT. Bound antibodies were visualized with Lumi-Light substrate. The oxidation of the luminol in this enzyme substrate solution is catalyzed by the HRP and the emitted chemiluminescence of the bands positive for the protein of interest can be detected by an image station. The intensity of the signals was quantified with ImageJ software.

### **2.2.12. Flow cytometric analysis of *in vitro* samples**

To determine cellular surface protein expression by flow cytometric analysis, infected cells from 6-well plates were collected in FACS tubes at indicated time points after treatment by scraping off the cell layer. During the immunofluorescent staining process up to the point of analysis, the cells were kept at 4 °C and stained cells were protected from light. All washing steps were conducted with FACS buffer. Cells were washed before primary antibody and corresponding isotype controls diluted in 10 µL FACS buffer, were added to the cells. Antibodies were diluted as follows: CRT 1:10, MHCI 1:50, Hsp70 1:2 and isotype controls correspondingly. After 35 min incubation, the cells were washed again, and if necessary, the secondary fluorophore-conjugated antibody was applied diluted 1:20 in FACS buffer for 35 min. After washing, the cells were fixed by addition of 250 µL fixation buffer, containing 2% paraformaldehyde (PFA). The original fixation buffer, which contains 4% PFA, was diluted 1:2 with FACS buffer because some of the used cells, e.g. KLN205 cells were very sensitive regarding the fixation buffer. Cells were washed after incubation with fixation buffer for 20 min, resuspended in FACS buffer and analyzed on a flow cytometer with FACSDiva software. Results were analyzed with FlowJo software. The fluorescence was indicated as the median of the fluorescence intensity with subtraction of isotype fluorescence values. When cells were infected with Ad-eGFP, the cells only had to be washed and subsequently fixed to be ready for flow cytometric analysis. Fluorescence emitted by the eGFP protein can be measured in the same channel as FITC stained cells due to the fact that the excitation and emission spectra of both fluorescent molecules overlap significantly. The percentage of eGFP positive cells was indicated. For analysis of MHCI exposure, cells of indicated samples were incubated with IFN $\gamma$  overnight before staining. Flow cytometric analysis was performed as described above.

### **2.2.13. Apoptosis monitoring by caspase activity assay**

Apoptosis occurring in cells can be measured with a caspase activity assay. The assay is based on the cleavage of the Ac-DEVD-amc substrate by several caspases including caspases 3 and 7. The amino acid sequence Ac-DEVD corresponds to the upstream sequence of the caspase cleavage site Asp<sup>216</sup> within PARP1, a DNA repair enzyme also involved in the apoptotic caspase cascade (Nicholson et al. 1995). During apoptotic cell death, the sequence Ac-DEVD is cleaved off the Ac-DEVD-amc molecule by the caspases according to the natural target and the fluorogenic amc moiety is released, leading to fluorescence signals corresponding to the caspase cleavage activity.  $1 \times 10^4$  cells in 96-well plates were infected with virus or treated with control agents in triplicates. Stimulation with 100 ng/mL FasL and 1  $\mu$ g/mL CHX 3 h before cell lysis served as positive control. 50  $\mu$ L 1x lysis buffer per well was given to the carefully washed cells at indicated time points after virus infection and incubated for 10 min at 37 °C for the cells to lyse. Ac-DEVD-amc in 50  $\mu$ L PBS per well was added to the lysed cells to a final concentration of 12.5  $\mu$ M. The samples were excited at 355 nm and the emitted fluorescence was measured at 460 nm after 20 min incubation at 37 °C. Caspase activity depicts the resulting optical density as percentages of the optical density in mock treated cells.

### **2.2.14. Analysis of HMGB1 release into cell supernatants**

HMGB1 release into the cell culture supernatant of infected cells was assayed with a sandwich ELISA kit according to the manufacturer's instructions of the normal range ELISA. In brief, 10  $\mu$ L liquid nitrogen shock frozen samples from the supernatants of virus infected cells in 6-wells plates were applied to the assay plates in triplicates. The wells of the provided microtiter strips are precoated with purified anti-HMGB1 antibody. HMGB1 in the samples was allowed to bind to the immobilized antibody during a 24 h incubation. A peroxidase-conjugated secondary anti-HMGB1 antibody was applied and after substrate reaction the optical density was determined 45 min after stop of the color reaction with a photometer at 450 nm. The measurement at a reference wave length of 630 nm was subtracted. After subtraction of the blank value, HMGB1 concentrations were calculated from the standard curve.

### **2.2.15. Analysis of ATP release into cell supernatants**

ATP release into the cell culture supernatant of infected cells was determined with the help of a recombinant firefly luciferase-based bioluminescence assay. The luciferase enzyme needs energy in the form of ATP and oxygen to convert D-luciferin into oxyluciferin. The electronically excited oxyluciferin releases a photon of light while returning to its ground state. This luminescence can be monitored on a luminometer. When ATP is the limiting component in the luciferase reaction, the intensity of the luminescence is proportional to the ATP concentration (Lundin and Thore 1975). An ATP determination kit was used according to the manufacturer's instructions. In brief, 90  $\mu$ L of the reaction mixture containing 0.5 mM D-luciferin, 1.25  $\mu$ g/mL firefly luciferase, 25 mM tricine buffer, pH 7.8, 5 mM MgSO<sub>4</sub>, 100  $\mu$ M EDTA and 1 mM DTT was measured as background luminescence and subtracted from the luminescence of reaction mixture containing 10  $\mu$ L of supernatant samples or ATP standards in duplicates. As for the HMGB1 assay, samples from the supernatant of virus infected cells in 6-well plates had been shock frozen in nitrogen before. Luminescence was measured after sample addition and ATP concentrations were calculated from the standard curve or given as percentage of mock infected controls like in the HMGB1 assay.

### **2.2.16. KLN205 *in vivo* model**

DBA/2 mice were kept at the animal facility of the Technical University of Munich, the Zentrum für präklinische Forschung at the Klinikum rechts der Isar, Munich, GER in individually ventilated cages in groups of five animals per cage in a pathogen-free environment. Mice were left to adjust to their new environment for 7-10 d so that they were 9-9.5 weeks old at the start of the experiments. All *in vivo* experiments were approved by the local authorities (Regierung von Oberbayern, Munich, GER) and conducted according to the German legal animal welfare requirements (Tierschutzgesetz TierSchG). Well-being of mice and tumor sizes were monitored every day. Animals were excluded from the experiment and sacrificed, accordingly to the guidelines of the German society of laboratory animal science (Gesellschaft für Versuchstierkunde GV-SOLAS), when tumors grew bigger than 1.5 cm in diameter or grew invasive, after ulcerations or automutilations, when mice lost weight, or when they had abnormal clinical or behavioral symptoms.

KLN205 cells were tested for mycoplasma as described in chapter 2.2.1 before each animal experiment. KLN205 cells were washed with PBS and detached by a 10 min incubation with TrypLE Express. 15 mL fresh medium were added per 15 cm plate or 150 cm<sup>2</sup> flask, the cell pellet was collected by centrifugation according to normal cell culture and resuspended in 5 mL fresh medium including FBS to recover the cells from the detachment agent. The cells were washed two times with 5 mL PBS each, to wash away the animal FBS. Cells in PBS were counted with trypan blue to verify the viability of the cells. Cells injected into mice had to have a viability of at least 90%. Cells were adjusted to 10<sup>7</sup> cells/mL. 2x10<sup>6</sup> cells were injected subcutaneously into the right flank of the animals in 200µL PBS. Tumor growth and mouse well-being was controlled thereafter as described above. When tumors reached an average diameter of 0.5 cm, 10<sup>9</sup> IFU adenoviruses per mouse were injected in 50µL PBS intratumorally. Only virus that passed through two CsCl gradient centrifugations and a desalting process was used for *in vivo* experiments. But since also the virus for the *in vitro* experiments was purified like this, the same viruses were used for *in vitro* and *in vivo* experiments. Mice received Ad-wt, Ad-Delo3-RGD, Ad-Delo3-RGD-Flt3L, Ad-PSJL-K, or Ad-dl703, and control mice received injections of PBS only. Group sizes were 4-8 mice per group depending on the experiment. For monitoring of anti-viral responses and treatment efficacy, two mice per group were given a second dose of virus 7 d after the first injection. To analyze the impact of the different oncolytic viruses on the immune response towards virus and tumor, mice were sacrificed by CO<sub>2</sub> inhalation 3 and 7 d after virus injection and blood, tumor, and spleen were isolated. To assess tumor growth curves, the diameter of the tumors was measured in two directions by a digital caliper every third day over a time course of 28 d. The volume was calculated as 0.52 x (width)<sup>2</sup> x length. The tumor growth experiment was terminated after 28 d and mice were sacrificed as described above.

#### **2.2.17. Serum collection**

Blood was taken from the mice 14 d after treatment from the tail veins. On day 3 and 7, when mice were sacrificed, blood was taken from the posterior vena cava. To get serum, the blood was allowed to clot at RT for up to 2 h. Serum was then separated from the clotted blood by centrifugation at 2000 g for 15 min at 15 °C.



### **2.2.18. Splenocyte isolation**

After weighing of the spleens, the splenocytes were isolated from the mouse spleens mechanically. Therefore, freshly isolated spleens were placed onto a cell strainer that was located upon a centrifugation tube. 5 mL of RPMI medium were added onto the spleens and the spleens were crushed through the cell strainer with the stamp of a syringe. Additional 5 mL of medium were added and the crushing step was repeated. Cells and spleen remains were vortexed shortly and centrifuged at 1200 rpm for 10 min at 4 °C. The supernatant was discarded thereafter and the pellet was vortexed again. 12 mL of erythrocyte lysis buffer was added per mL of pellet. After shaking the suspension it was left at RT no more than 5 min for the erythrocytes to be lysed and the immune cells not to be impaired. After a subsequent centrifugation at 1200 rpm for 7 min at 4 °C, the pellet was resuspended in 15 mL of RPMI supplemented with 2% FBS and PS. After shaking, the cell suspension was purified by another passage through a new cell strainer and collected in a new centrifugation tube. Splenocytes were counted with trypan blue as described in chapter 2.2.1.

### **2.2.19. Flow cytometric analysis of immune cell surface markers on blood cells and splenocytes**

Blood cell surface marker expression was analyzed in Trucount tubes for assessment of absolute cell numbers (Schnizlein-Bick et al. 2000). Blood was taken from the killed mice as described for serum (chapter 2.2.17). EDTA was added 1:6 to prevent clotting of the blood. 20 µL of antibody mix containing all fluorophore-conjugated antibodies used within the particular panel in the particular dilutions (as stated at the bottom of this paragraph) was added to 50 µL of EDTA blood and vortexed carefully (Baumgarth and Roederer 2000). After the staining for 15 min at RT in the dark, 450 µL of 1x FACS lysing solution was added to the cells, vortexed, and incubated in the dark for 30 min for erythrocytes to be lysed. The stained cells were diluted 1:10 with FACS buffer 10 min before flow cytometric analysis. Blood cell staining was analyzed by FlowJo software. The absolute blood cell count of a distinct population per volume was calculated as (number of events of the population/number of events in the absolute count bead region) x (number of beads per test/test volume).

Degranulation of splenocytes was measured by flow cytometric analysis of CD107a surface exposure and subsequent staining of immune cell surface markers. Therefore,  $2 \times 10^5$  splenocytes in RPMI medium with 2% FBS were incubated with 20  $\mu$ L of tumor cell lysate, 5  $\mu$ L of anti-CD107a antibody (1:20) and 0.12  $\mu$ L 1000x monensin for 4 h at 37 °C. Monensin thereby prevents reinternalization and degradation of cell surface CD107a (Alter et al. 2004). After centrifugation, cells were resuspended in 100  $\mu$ L FACS buffer and stained by addition of 20  $\mu$ L of antibody mix containing fluorophore-conjugated antibodies in the particular dilutions, as stated at the bottom of this paragraph, as well as 1  $\mu$ L FcR block to block unspecific binding. After vortexing, the staining procedure was conducted for 15 min at RT in the dark. The cells were fixed by addition of 200  $\mu$ L Cytofix for 15 min at RT in the dark. After addition of 3 mL of FACS buffer, the cells were centrifuged and resuspend in 300  $\mu$ L of fresh FACS buffer. The readily stained cells were measured on a flow cytometer and analyzed by FlowJo software.

**Blood:** CD45 PerCP-Cy5.5 (1:200), CD3-eF450 (1:100), CD11c-FITC (1:167), CD49b-APC (1:40), CD19-APC-eF780 (1:200)

**CD107a splenocyte staining:** CD45-PerCP-Cy5.5 (1:200), CD3-eF450 (1:100), CD8-FITC (1:100), CD49b-PE (1:80)

#### **2.2.20. Immunohistological analysis of murine tumors**

For histological analysis of tumors, the tumor samples were fixed in 10% neutral buffered formalin for 24 h. They were then dehydrated in a tissue processor and embedded into paraffin blocks with the help of a paraffin embedding system. Paraffin blocks were cut with a microtome into sections of 2  $\mu$ m, mounted onto microscope slides, and left to adhere to the glass surface overnight at 60 °C. Before IHC staining, the sections were deparaffinized and rehydrated. They were therefore put in xylene three times for 10 min each, followed by two steps in isopropanol for 5 min each, and subsequently 96% and 70% ethanol for 5 min each. Sections were subsequently rinsed in distilled water three times. For antigen retrieval, slides were cooked in citrate buffer in a commercial pressure cooker for 7 min. This process serves to break the methylene bridges formed during fixation and exposes the antigenic sites in order to allow the antibodies to bind. After the sections were cooled to RT in the buffer, they were washed. This washing process, as well as the subsequent ones, was performed by three washes with TBS buffer. Sections were thereafter incubated with 3% H<sub>2</sub>O<sub>2</sub> for 15 min at RT to suppress endogenous peroxidase activity and thus reduce background staining. Open binding sites were blocked with 5% rabbit serum (the

secondary antibody was raised in rabbit) in antibody diluent in a moisture chamber for 30 min at RT. The F4/80 macrophage-specific antibody diluted 1:500 in antibody diluent was added and the slides were incubated at 4 °C in a moisture chamber overnight. After washing, sections were incubated with the secondary HRP-conjugated antibody diluted 1:100 in antibody diluent for 30 min in a moisture chamber at RT. After another washing step, DAB substrate was added and incubated until optimal color development. After washing with water, cells were counterstained with Mayer's hemalum solution for 3 min and blued with tap water until the process was stopped with distilled water. After dehydration with an ascending alcohol series and xylene, the sections were mounted with cover slips and mounting medium and dried before microscopic investigation. Tumor morphology was analyzed by staining of the section with hematoxylin and eosin (H&E). Therefore, sections were deparaffinized and rehydrated as described above. Sections were then rinsed with tap water, stained with Mayer's hemalum solution for 3 min and rinsed with tap water. Sections were then dipped into 0.1% HCl three times, followed by rinsing with tap water again. Sections were stained with 0.5% eosin solution for 3 min and then rinsed in tap water before performance of the ascending alcohol series and mounting as mentioned above.

#### **2.2.21. Anti-viral antibody detection by ELISA**

Anti-virus antibodies in the serum of virus injected mice were measured by ELISA. Therefore,  $10^9$  adenoviral particles in 100  $\mu$ L ELISA coating buffer per well were incubated in MaxiSorp 96-well plates overnight at 4 °C. Unbound viral particles were washed away with PBS the next day and open binding sites were blocked with 300  $\mu$ L 4% milk powder in PBS per well for 2 h at RT. Wells were washed with PBS two times. Serum samples were diluted in 2-fold steps from 1:250 up to 1:32000 in 2% milk powder and 100  $\mu$ L per well in triplicates were incubated for 2 h at RT. After four washing steps with PBS, bound anti-virus antibodies were detected by addition of 100  $\mu$ L per well of HRP-conjugated anti-mouse antibody reacting with all classes of mouse immunoglobulins (Igs) in 2% milk powder in PBS (1:2000) and incubated for 1.5 h at RT. After a final wash, 150 $\mu$ L TMB substrate was added and the color reaction was stopped by addition of 50  $\mu$ L of 0.8 M H<sub>2</sub>SO<sub>4</sub> per well after 20 min. The optical density was measured with a photometer at 450 nm with subtraction of background measurement at 590nm. Results were indicated as  $OD_{450nm} - OD_{590nm}$ .

### **2.2.22. Determination of HMGB1 and ATP in mouse serum**

HMGB1 and ATP were determined from the serum samples according to the corresponding protocols in the *in vitro* section with the exception that HMGB1 from *in vivo* serum samples was determined with the sensitive range protocol after addition of 50  $\mu$ L sample.

### **2.2.23. IFN $\gamma$ ELISpot analysis**

The ability of the splenocytes to recognize viral or tumor antigens and in consequence release IFN $\gamma$  was tested by an IFN $\gamma$  ELISpot (Janetzki et al. 2005). The Immobilon-P PVDF membranes of the ELISpot plates were activated with 15  $\mu$ L 35% ethanol per well for no longer than 1 min. Wells were washed shortly after three times with 200  $\mu$ L PBS. The plate was coated with 0.5  $\mu$ g of the IFN $\gamma$  capture antibody in 100  $\mu$ L ELISA coating buffer per well at 4  $^{\circ}$ C overnight. The next day, the plates were washed three times with 200  $\mu$ L PBS and unspecific binding sites were blocked with 300  $\mu$ L of 10% FBS in RPMI medium per well for at least 2 h at RT. After another washing step, the freshly isolated splenocytes were stimulated by addition of 2  $\mu$ g peptide or 200  $\mu$ L KLN205 cell lysate to  $5 \times 10^6$  cells in 1 mL RPMI containing 2% FBS and PS. As a positive control,  $5 \times 10^6$  cells in 1 mL were stimulated with 50 ng PMA and 1  $\mu$ g ionomycin. After mixing,  $5 \times 10^5$  cells were applied to the plates in triplicates. IFN $\gamma$  was released from the stimulated cells during the 18 h incubation at 37  $^{\circ}$ C 5% CO $_2$  and was detected after six washings with PBS including 0.01% Tween 20, with the 100  $\mu$ L of sterile filtered biotin-conjugated IFN $\gamma$ -specific detection antibody diluted 1:1000 in PBS with 1% FBS per well. After incubation for 1.5 h, plates were washed six times with PBS including 0.01% Tween 20 and streptavidin-HRP diluted 1:100 in PBS with 10% FBS was applied for 45 min. Plates were washed extensively three times with PBS including 0.01% Tween 20 and three times with only PBS, and 100  $\mu$ L DAB substrate were applied per well. Developing spots were monitored closely in order to receive an optimal background to noise ratio. The color reaction was stopped by washing with ice cold tap water for 10 min. Spots of the dried plate, each correlating to one IFN $\gamma$  secreting, and thus antigen recognizing immune cell were counted on an ELISpot reader.

#### 2.2.24. Calcein release and retention assay

Lymphocyte-mediated anti-tumor cytotoxicity was measured by a fluorometric assay. Target tumor cells were loaded with calcein-AM, a non-fluorescent vital dye that passively enters the cell membrane of viable cells (Lichtenfels et al. 1994). Inside the cell, the dye is converted by AM ester hydrolysis by intracellular esterases into the green fluorescent calcein, which is retained inside cells with intact membranes. Analogous to the classical  $^{51}\text{Cr}$  release assay, the calcein release assay is based on the release of the marker into the supernatant following membrane permeabilization, which can here be measured by a fluorescence reader. It correlates with the number of lysed cells. Alternatively, one can measure the retention of calcein within the cells (Matza et al. 2009). KLN205 cells as target cells were washed with RPMI medium without FBS.  $1 \times 10^6$  cells/mL in serum- and phenol red-free OptiMEM were incubated with  $10 \mu\text{M}$  DMSO dissolved calcein-AM for 30 min at  $37^\circ\text{C}$  for the dye to enter the cells. Tumor cells were washed carefully and resuspended in RPMI without FBS to  $10^5$  cells/mL.  $10^4$  stained target cells in  $100 \mu\text{L}$  were mixed with splenocytes in various concentrations resulting in different effector cell to target cell (E:T) ratios of (100:1, 30:1, 10:1, 3:1, 1:1) in  $100 \mu\text{L}$  OptiMEM with 10% FBS added in round bottom 96-well plates in triplicates. Spontaneous release was determined in six wells by addition of only medium to the tumor cells. After centrifugation at 200 g for 2 min, the assay was incubated at  $37^\circ\text{C}$  for 4 h. Maximal release was determined by addition of 1% Triton X-100 for 15 min before the end of the incubation time. After incubation, cells were centrifuged for 5 min at 500 g and the fluorescence of  $100 \mu\text{L}$  supernatant excited at 485 nm was read at an emission wavelength of 520 nm. Percentage of effector-mediated target cell lysis was calculated as  $100\% \times (F_{\text{experiment}} - F_{\text{spontaneous}}) / (F_{\text{maximal}} - F_{\text{spontaneous}})$ . To determine the remaining dye retained in the cells, cells were washed and the fluorescence of the cells read. Percentage of effector-mediated target cell lysis was calculated as  $100\% \times (F_{\text{spontaneous}} - F_{\text{experiment}}) / (F_{\text{spontaneous}} - F_{\text{maximal}})$ .

The calcein assay was also conducted after coculture of splenocytes and growth arrested KLN205 cells. Growth arrest was induced by incubation of  $2 \times 10^6$  cells/mL with  $50 \mu\text{g/mL}$  mitomycin C for 30 min in OptiMEM at  $37^\circ\text{C}$ . After washing two times with PBS, the cells were resuspended in 10% FBS in RPMI and PS to a concentration of  $3.2 \times 10^5$  cells/mL. 1 mL of these tumor cells were mixed with 1 mL splenocytes containing  $8 \times 10^6$  cells also in 10% FBS RPMI with PS resulting in a tumor cell to splenocyte ratio of 1:25. The cytokine IL-2 was added at a final concentration of  $100 \text{ U/mL}$  for general immune cell stimulation. Cocultures were incubated for 5 d at  $37^\circ\text{C}$  5%  $\text{CO}_2$  (Schirmacher et al. 1979). Cells were thereafter collected and counted. The calcein assay after the coculture was conducted as described above in 10% FBS OptiMEM with E:T ratios of 100:1 and 1:1 in triplicates.

### 3. Results

#### 3.1. Production and validation of YB-1-dependent oncolytic adenoviruses

##### 3.1.1. Adenovirus production yields good quality viruses for *in vitro* and *in vivo* experiments

In order to prevent variance in results due to batch to batch variations of virus preparations, the same stock of each YB-1-dependent oncolytic adenovirus and control virus was used for all experiments within this thesis work. Therefore, viruses were produced in large amounts in  $4 \times 10^8$ - $1 \times 10^9$  HEK293 cells. The amplified viruses were purified by two CsCl gradient ultracentrifugation steps and desalted with sephadex columns because viruses purified this way can also be used for *in vivo* animal experiments. Results for determination of virus titers and quality of virus production are summarized in table 3-1. Virus production was very efficient, reaching 19,000-38,000 viral particles per cell, as determined by optical density measurement at 260 nm and calculation of VP concentrations. Virus titers were determined by ICC staining of the viral essential capsid protein hexon after infection of HEK293 cells. Hexon positive spots can be counted after staining with a secondary HRP-conjugated antibody and subsequent DAB substrate conversion. The spots were counted and the viral titers in IFU/cell were calculated. Viruses had high titers (from  $2 \times 10^{11}$  IFU/mL) so that reasonable volumes could be applied in each experiment and that viruses were suitable for application in all *in vitro* and *in vivo* experiments within this thesis. Resulting VP to IFU ratios (4-25) were also within the required range even for the use in clinical trials (Bauer 2000). Adenoviruses were obtained in high purity with  $OD_{260nm}/OD_{280nm}$  ratios ranging from 1.36 to 1.40. Particle size measurement by dynamic light scattering resulted in clear single peaks and ideal sizes of hydrodynamic diameters (indicated as Z-average) of the adenoviruses of  $110 \pm 20$  nm. Pdl values, denoting the grade of dispersity, were equal to or smaller than 0.1, which indicates a lack of aggregate formation and homogeneous sizes of virus particles. Count rates for dynamic light scattering measurements ranged between 250 and 700 counts per seconds, signifying that all dynamic light scattering measurements were valid (Malvern\_Instruments 2011, Dr. P.S. Holm personal communication). Viruses were thus all suitable to be used for the following experiments after verification of the viral genome mutations.

**Table 3-1: Adenoviruses have ideal physical conditions to be used.**

	Production [VP/cell]	Titer [IFU/mL]	VP/IFU	OD <sub>260nm</sub> / OD <sub>280nm</sub>	Z-Average [nm]	PdI
Ad-dl703	27,500	$2 \times 10^{11}$	11	1.36	111.3	0.048
Ad-wt	25,000	$2 \times 10^{11}$	10	1.38	109.0	0.047
Ad-Delo3-RGD	27,778	$2 \times 10^{11}$	25	1.38	133.5	0.119
Ad-Delo3-RGD-Flt3L	37,806	$2 \times 10^{12}$	4	1.40	114.0	0.079
Ad-PSJL-K	19,267	$2 \times 10^{11}$	17	1.39	106.9	0.049

### 3.1.2. Verification of viral mutations critical for tumor specificity, oncolytic efficacy, and immune recognition

The modified genome structure of the used oncolytic adenoviruses (figure 2-1) and the maintenance of mutations during virus production were verified at the beginning of this work. For this purpose, DNA was isolated from the produced purified viruses and the most important viral regions were analyzed by PCR analysis. All expected PCR signals are summarized in appendix B and the observed PCR signals are shown in figure 3-1. Ad-dl703 is rendered replication-deficient by deletion of most of the *E1* region. Faint residual bands resulted from the E1A and the CR3-specific E1A PCRs and the E1B19K PCR was completely negative (figure 3-1). Presence of the *E3* gene was verified by the E3 PCR. A small residual band was detected for the RGD PCR in the viral fiber. As expected, Ad-wt comprised all signals except for the artificially integrated RGD motif. However, like in Ad-dl703, a small residual band was visible in the RGD PCR, which was fainter though as compared to the oncolytic viruses with integrated RGD motif. Ad-Delo3-RGD and Ad-Delo3-RGD-Flt3L have an 11 bp deletion in CR3 of the *E1A* gene (Mantwill et al. 2006, Rognoni et al. 2009), which is the basis for the YB-1-dependency of these viruses (Holm et al. 2002). Hence, as expected, the PCR for the *E1A* gene, which allows transcription of the 12S mRNA, was positive for both viruses, whereas the PCR in which the forward primer binds within the CR3 sequence was negative for both viruses. 209 bp of the anti-apoptotic *E1B19K* gene are deleted in order to increase target cell lysis (Liu et al. 2004, Sauthoff et al. 2000). Indeed, the PCR specific for this region gave a shorter signal for both viruses, which confirms the deletion (378 bp instead of 587 bp). The fainter band for Ad-Delo3-RGD was just an artifact in the PCR shown here, maybe due to addition of a smaller amount of DNA in this particular experiment. Following experiments resulted in thick bands like the one seen here for Ad-Delo3-RGD-Flt3L (data not shown). Deletion of *E3gp19K* is intended to enhance viral immune recognition, since E3gp19K suppresses MHCII-mediated tumor antigen presentation (Sester et al. 2013). The E3 PCR forward and reverse primers bind upstream of the *E3gp19K* and within the *ADP* gene, respectively. Thus

Ad-Delo3-RGD, in which most of the *E3* region (2.7 kb) including *E3gp19K* and *ADP* is deleted, showed no signal for this region, and Ad-Delo3-RGD, in which *E3gp19K* is deleted and replaced by an *mFlt3L* gene gave the expected signal of 1394 bp. Ad-Delo3-RGD and Ad-Delo3-RGD-Flt3L, as mentioned above, both comprise the RGD motif in the fiber knob, as confirmed by the RGD PCR. In Ad-PSJL-K, most of the *E1* region, including *E1A* and *E1B19K* is deleted, as confirmed by *E1A* and *E1B19K* PCRs. Only a small residual band resulted from the *E1A* PCR comparable to the residual band in Ad-dl703, but with no signal for the CR3 PCR. In the *E3* region, the *E3gp19K* gene is deleted, leading to the shorter product of 646 bp instead of 1248 bp in the *E3* PCR. Also Ad-PSJL-K, as mentioned above, comprises the RGD peptide sequence in the viral fiber knob, as confirmed by the RGD PCR. To sum up, all viral mutations that are essential for functionality of the oncolytic viruses were verified and viruses were therefore suitable to be used for the following experiments.

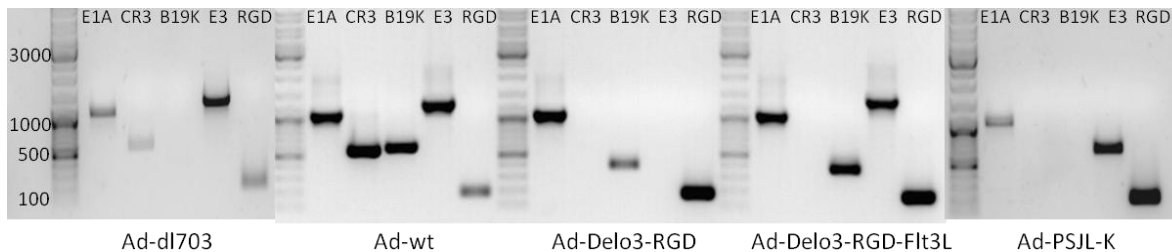


**Figure 3-1: The amplified adenoviruses contain the expected mutations.** DNA from purified indicated viruses was isolated by phenol chloroform extraction. DNA was analyzed by PCR with primers specific for the adenoviral *E1A*, *E1A* CR3 (indicated as CR3), *E1B19K* (indicated as B19K), and the *E3* region, as well as a primer pair for the artificial RGD insertion into the viral fiber knob. PCR products were separated on a 1% agarose gel. Sizes of important marker bands are indicated at the left side as size in bp.

### 3.1.3. Flt3L is efficiently released in the supernatant of Ad-Delo3-RGD-Flt3L infected cells *in vitro*

In order to enhance DC attraction and thus the anti-tumor efficacy of the virus *in vivo* (Edukulla et al. 2009), the transgene *mFlt3L* has been inserted into the *E3* region of the Ad-Delo3-RGD viral vector, resulting in the virus Ad-Delo3-RGD-Flt3L. The presence of the gene in the *E3* region was verified by PCR (figure 3-1). The correct orientation of the inserted gene and the transcription and expression of the protein were verified by a mFlt3L-specific ELISA. mFlt3L release into the supernatant of murine KLN205 cells (squamous cell carcinoma cells of the lung) and human A549 cells (adenocarcinomic alveolar basal epithelial cells) was determined 48 h after infection of the cells with either Ad-Delo3-RGD-Flt3L or its transgene-free counterpart Ad-Delo3-RGD. mFlt3L proteins were selectively released into the supernatant of Ad-Delo3-RGD-Flt3L virus infected cells



(figure 3-2). In both KLN205 and A549 cells, 2000-4000 pg/mL mFlt3L was released into the supernatant, compared to 10-30 pg/mL detected in Ad-Delo3-RGD and mock infected supernatants. Infection of A549 cells with Ad-Delo3-RGD-Flt3L already reached 2000 pg/mL mFlt3L after infection with 10 IFU/cell, whereas in KLN205 cells, 100 IFU/cell were needed. This shows that Ad-Delo3-RGD-Flt3L was able to secrete sufficient amounts of its carried transgene into the supernatant of infected cells thus allowing the use of this armed YB-1-dependent oncolytic virus in the *in vivo* experiments. Of note, results for Ad-Delo3-RGD-Flt3L infection are not shown in all following *in vitro* experiments because results were similar to the results after Ad-Delo3-RGD infection.

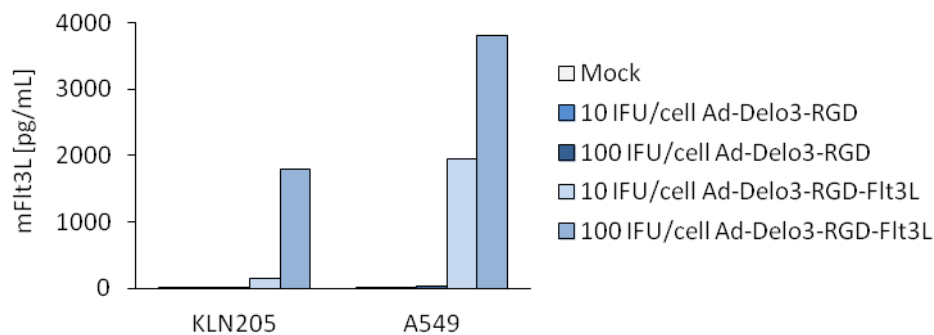


**Figure 3-2: Ad-Delo3-RGD-Flt3L effectively releases its transgene Flt3L into the supernatant of infected cells.** KLN205 cells (left) and A549 cells (right) were infected with 10 or 100 IFU/cell of either Ad-Delo3-RGD or Ad-Delo3-RGD-Flt3L as indicated. An ELISA specific for the mFlt3L protein was performed 48 h after infection. mFlt3L release is indicated as concentration of mFlt3L in pg/mL (n=1).

### 3.2. KLN205 lung cancer cells as a murine model for YB-1-dependent oncolysis

#### 3.2.1. Murine KLN205 and CMS-5 cells, and Syrian hamster HaK cells are infectable by adenoviruses

YB-1-dependent oncolytic adenoviruses have so far only been tested in human cell lines *in vitro* and in immunocompromised xenograft models *in vivo* (Holzmuller et al. 2011, Rognoni et al. 2009). However, the immune system on the one hand interferes with the viral infection (Parato et al. 2005) and is on the other hand said to augment oncolytic virus performance (Boozari et al. 2010, de Gruijl and van de Ven 2012). It is not possible to analyze these important influences on viral efficacy in immunocompromised human tumor cell models *in vivo*. Therefore, in an attempt to identify adequate non-human tumor cells for the use in immunocompetent animals *in vivo*, a number of murine and Syrian hamster cell lines were analyzed regarding their infectability by human adenoviruses and their capability of YB-1-specific oncolysis *in vitro*. Positive tested cells could subsequently be used in a syngeneic immunocompetent host to study the influence of the

immune system on YB-1-dependent oncolysis *in vivo*. Several weakly immunogenic mouse cell lines, as well as one Syrian hamster cell line were tested for adenovirus infectability (figure 3-3), adenoviral particle formation (figure 3-4) and YB-1 expression (figure 3-5). To analyze whether the non-human cell lines can be infected by adenoviruses, they were infected with a replication-deficient Ad-eGFP virus. Human cells with known virus propagation were included as positive controls.

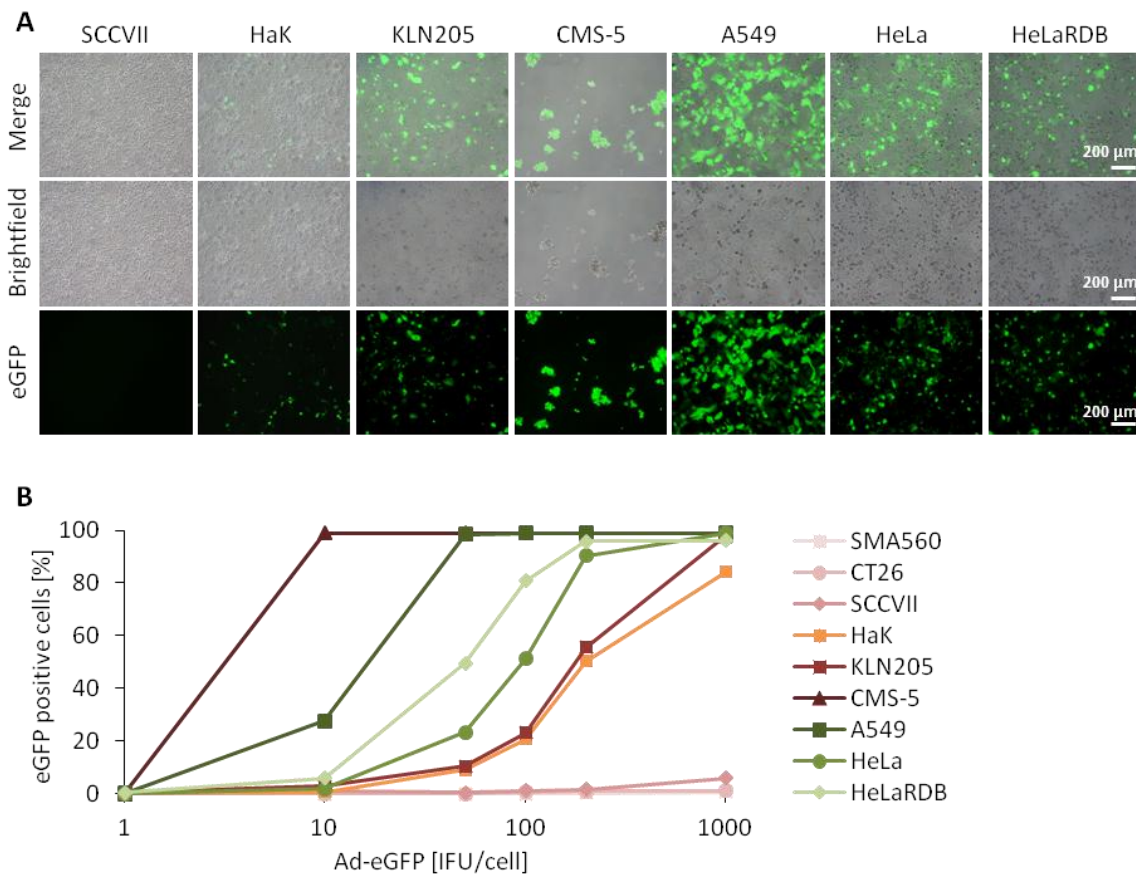


**Figure 3-3: Murine KLN205 and CMS-5 cell, as well as Syrian hamster HaK cells are infectable by human adenoviruses.** A. Indicated cell lines were infected with 100 IFU/cell Ad-eGFP. Immunofluorescent images were taken 72 h after infection. From top to bottom: merge, brightfield, eGFP. Bars=200 $\mu$ m. B. Indicated cells were infected with indicated MOI of Ad-eGFP and the percentage of eGFP positive cells was assessed by flow cytometric measurement in the FITC channel 72 h after infection (n=1-2).

Assessment of the rate of infection 72 h post viral infection by fluorescence microscopy (figure 3-3 A) and flow cytometric analysis (figure 3-3 B) of eGFP positive cells verified that human cell lines were efficiently infected by adenoviruses. Human A549 cells showed the best infectability with eGFP expression in 100% of the cells after infection with 50 IFU/cell Ad-eGFP (figure 3-3 B). To reach similar results in human cervix carcinoma cells HeLa and HeLaRDB, about 200 IFU/cell Ad-eGFP were needed. Murine cells SCCVII (squamous cell carcinoma), CT26 (colon carcinoma), and SMA-560 (astrocytoma) were almost not infectable by Ad-eGFP, at 100 IFU/cell, less than 1% of the cells expressed eGFP. Syrian hamster HaK cells (adenocarcinoma) and murine KLN205 cells

were both infectable by Ad-eGFP. Infection was not very efficient and inferior to all human cell lines tested, but still sufficient. Infection with 100 IFU/cell Ad-eGFP resulted in eGFP expression in 23% of both KLN205 and HaK cells and 1000 IFU/cell resulted in eGFP expression in 85% of HaK cells and almost 100% of KLN205 cells after 3 d. CMS-5 cells could be infected very efficiently by Ad-eGFP with infection rates even higher than in the human cell line A549. However, replication-deficient Ad-eGFP lysed the cells at viral concentrations starting from less than 10 IFU/cell, an effect that was not observed in any of the human cell lines, which were stable to Ad-eGFP infection up to 1000 IFU/cell (for 100 IFU/cell see figure 3-3 A). In summary, HaK, KLN205, and CMS-5 cells showed sufficient infectability and were therefore further analyzed for their applicability as non-human target cells for YB-1-dependent oncolysis.

### **3.2.2. Non-human cell lines HaK, KLN205, and CMS-5 cells allow formation of viral particles**

Non-human cell lines HaK, KLN205, and CMS-5 could be infected successfully by adenoviruses (figure 3-3). However, an additional important criterion for the use in adenoviral oncolysis is whether these cells allow formation of functional viral progeny. Younghusband et al. have reported that only early and not late adenoviral proteins are expressed and that in consequence assembly of functional viral particles is ineffective in non-human cells (Younghusband et al. 1979). To test whether formation of new infectious particles is possible from HaK, KLN205, and CMS-5 cells, the cells were infected with 100 IFU/cell of Ad-wt. Viral particles were released from the cells 72 h after infection and the amount of released particles able to infect HEK293 cells was tested by ICC staining of the viral hexon protein. While  $10^{10}$ - $10^{11}$  IFU/mL Ad-wt were formed in human control cell lines,  $3 \times 10^9$  IFU/mL were formed in CMS-5 cells and about  $10^7$  IFU/mL in HaK and KLN205 cells (figure 3-4). The infectious viral particles present within replication-deficient virus Ad-dl703 infected cells served as a negative control for new particle formation. About  $1 \times 10^4$ - $5 \times 10^5$  particles were present within Ad-dl703 infected cells. Only in CMS-5 cells, new particles were formed from the usually replication-deficient virus at this MOI, resulting in  $10^9$  IFU/mL after 3 d, which are almost as many particles as after Ad-wt infection. Moreover, CMS-5 cells were efficiently killed by the replication-deficient adenovirus Ad-dl703, as already seen for the replication-deficient virus Ad-eGFP (figure 3-3 A). This sensitivity towards adenoviral infections makes CMS-5 cells no confident model system to test the effects of virus replication- and particle formation-dependent oncolysis. Adenoviral particle formation was similar in KLN205 and HaK cells. In both cell lines about 400-500 times more particles were present after Ad-wt infection than after Ad-dl703 infection, which was considered as a sufficient precondition for testing of adenoviral oncolysis.

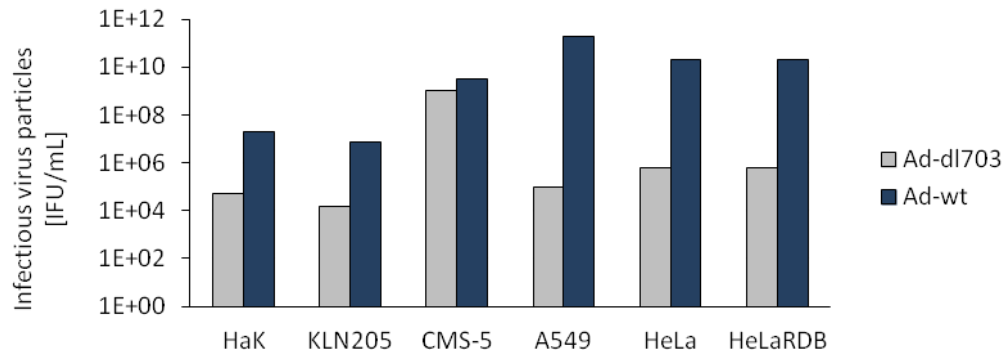


**Figure 3-4: HaK, KLN205, and CMS-5 cells are able to form infectious progeny.** Indicated cells were infected with 100 IFU/cell Ad-wt or Ad-dl703. 72 h after infection, cells were isolated, viruses were released from the cells and the viral particles in the supernatant were tested for infectivity in a hexon-based ICC assay in HEK293 cells. Infectious progeny is depicted as IFU/mL on a logarithmic scale (n=1).

### 3.2.3. Murine cell lines have sufficiently high expression of YB-1 to enable YB-1-dependent oncolysis

In order to constitute an adequate model for YB-1-dependent virotherapy, suitable cells need to have a sufficiently high expression level of YB-1, to allow YB-1-specific replication of viruses lacking the E1A transactivating domain CR3. The oncogenic factor YB-1, when present in the nucleus of the tumor cells, can activate the viral E2-late promoter and thus compensate for the lack or mutation of E1A in the used oncolytic viruses (Holm et al. 2002, Mantwill et al. 2006). The YB-1 status of the animal cell lines was assessed by WB analysis and immunofluorescence staining of the YB-1 protein. For both methods, an anti-human YB-1-directed antibody was used that specifically binds to the first 12 N-terminal amino acids of the protein. Since the epitope is conserved in human and in murine YB-1 (appendix A), the antibody crossreacts with murine YB-1. The Syrian hamster YB-1 structure has not been investigated so far, but as the 12 aa sequence is conserved in human, mouse, rabbit, rat, neat, and Guinea pig (appendix A) according to information in the UniProt database, the antibody was expected to bind also to the Syrian hamster protein. YB-1 was differently high expressed in the human control cell lines, with the highest expression in HeLa cells and lower expressions in HeLaRDB and A549 cells (figure 3-5 A). Human HS68 cells (foreskin fibroblasts) were included as a non-cancer control cell line with low YB-1 expression. In the murine cell line CMS-5, YB-1 expression was as high as in HeLa cells. In murine KLN205, and also in Syrian hamster HaK cells, YB-1 expression was 50-60% of HeLa and CMS-5 cell expression but similar to A549 cell YB-1 expression, and should thus be sufficient to allow viral E2-late promoter activation and subsequent tumor-specific replication of YB-1-dependent oncolytic adenoviruses. YB-1 was found mostly perinuclear in the cytoplasm, but also in low amounts in the nucleus (figure 3-5 B). In the drug-resistant cell line HeLaRDB in contrast, as

expected, YB-1 was found predominantly in the cell nucleus (Bargou et al. 1997, Mantwill et al. 2006). However, nuclear YB-1 amounts were slightly higher in HaK cells as compared to HeLa cells, and comparable between KLN205 and HeLa cells, thus signifying that levels of nuclear YB-1 should be sufficient for initiation of viral transcription.

In conclusion, HaK and KLN205 cells seem to be equally good models for the YB-1-dependent oncolysis. Knowledge about immune cell populations is further advanced in mice and all assays and antibodies are available for mouse-specific proteins or at least validated for them, in contrast to Syrian hamster proteins. KLN205 cells were therefore used for all further *in vitro* experiments, as well as injected into syngeneic DBA/2 mice to obtain an immunocompetent *in vivo* tumor model.

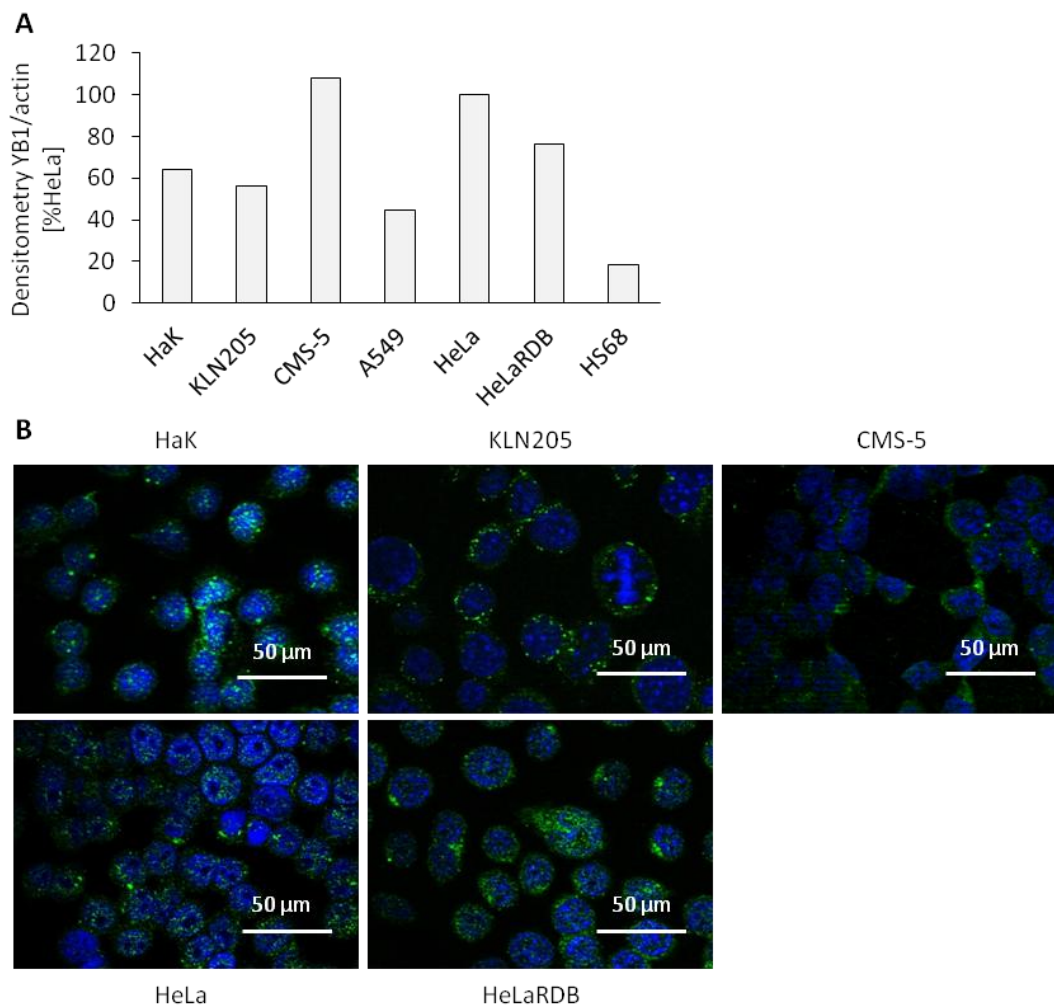


**Figure 3-5: Cell lines all have efficient YB-1 expression to allow YB-1 dependent adenoviral activity.** A. Proteins were isolated from indicated cell lines 72 h after seeding of the cells and were subjected to WB analysis with an antibody specific for the YB-1 N-terminal region. Densitometry of WB bands of YB-1 and cellular actin control was performed. The ratio of YB-1 and actin is depicted normalized to HeLa cells, which were set to 100% (n=1-2). B. Immunofluorescent staining of YB-1 with an antibody specific for the YB-1 N-terminal region and a FITC-conjugated secondary antibody (green). Nuclei were stained with Hoechst 33342 (blue). Bars=50 µm.

### **3.3. Replication of and tumor cell lysis by YB-1-dependent oncolytic adenoviruses *in vitro***

#### **3.3.1. YB-1-dependent oncolytic adenoviruses replicate in tumor cells and form infectious progeny**

The ability of the adenoviruses to produce new progeny and lyse its target cells is dependent on their ability to efficiently replicate in the host system. Mutations within the original adenoviral genome mostly interfere with the adenoviral ability to efficiently replicate. Thus, the replication of YB-1-dependent oncolytic adenoviruses was assessed in comparison to Ad-wt in murine KLN205 and human A549 control cells. After infection with 10 IFU/cell of the different adenoviruses, DNA was isolated and viral replication was analyzed by real time PCR with primers specific for the viral hexon gene. Hexon DNA copies were normalized to copies of cellular  $\beta$ -actin. In murine KLN205 cells, 130 Ad-wt copies per  $\beta$ -actin copy were present in the cells after 48 h as compared to 0.1 copies after 3 h, depicting a 1000-fold increase (figure 3-6 A). Replication of oncolytic viruses also peaked 48 h after infection. 7 hexon copies of Ad-PSJL-K were produced and only 0.7 copies of Ad-Delo3-RGD both per  $\beta$ -actin copy, corresponding to a 100-fold and 10-fold increase of starting values, respectively. Ad-dl703 DNA amount did not increase during these 4 d, in contrast, it even decreased slightly over time, confirming the replication-deficiency of the vector. In human A549 cells, viral replication reached almost 3700 viral DNA copies after 4 d, starting from 0.1 copies 3 h after virus infection both per  $\beta$ -actin copy, which is a 40,000-fold increase (figure 3-6 B). Oncolytic adenoviral replication reached similar DNA concentrations as Ad-wt after 4d, however, after 12-72 h, the difference between oncolytic viruses and Ad-wt was still more prominent with about 10 times higher DNA amounts for Ad-wt. This indicates that both oncolytic viruses were able to replicate in human cells but that replication kinetics were changed due to the introduced vector modifications. Also in this cell line, the DNA amount of Ad-dl703 was nearly unchanged over the whole time course of the infection. In conclusion, Ad-wt replication was, as expected, superior to replication of Ad-Delo3-RGD and Ad-PSJL-K, but these oncolytic viruses were still able to replicate in both murine and human cells.

The formation of new viral progeny following viral replication is a prerequisite for viral spread and effective target cell lysis. Since it is reported that assembly of functional viral particles rather than viral replication is impaired in non-human cells (Youngusband et al. 1979), formation of infectious virus particles from oncolytic and wild type adenoviruses was assessed next. Cells were harvested 72 h after virus infection with 100 IFU/cell and viral particles were released from the cells by repeated cycles of freezing and thawing. The supernatant including the released viral particles was examined for infective particles via a hexon protein-based ICC assay in HEK293 cells.

The ability of the oncolytic adenoviruses to reproduce was diminished in contrast to Ad-wt in all examined cell lines, about 10-fold in murine KLN205 and 100-fold in human cell lines (figure 3-6 C). In HeLa cells, markedly fewer particles were produced from Ad-Delo3-RGD as compared to Ad-PSJL-K (100 times). In A549 and KLN205 cells, in contrast to HeLa cells, comparable amounts of Ad-PSJL-K and Ad-Delo3-RGD amounts were produced. In comparison to replication-deficient Ad-dl703, over 10 times more particles were produced after oncolytic virus infection in KLN205 cells, in contrast to 10,000 times more particles after oncolytic virus infection in A549 cells, and 5 or 500 times more IFU of Ad-Delo3-RGD or Ad-PSJL-K, respectively in HeLa cells. Hence, infection with YB-1-dependent oncolytic adenoviruses resulted in efficient replication and particle formation in murine and human cells, even though replication and particle formation were less effective than after Ad-wt infection.

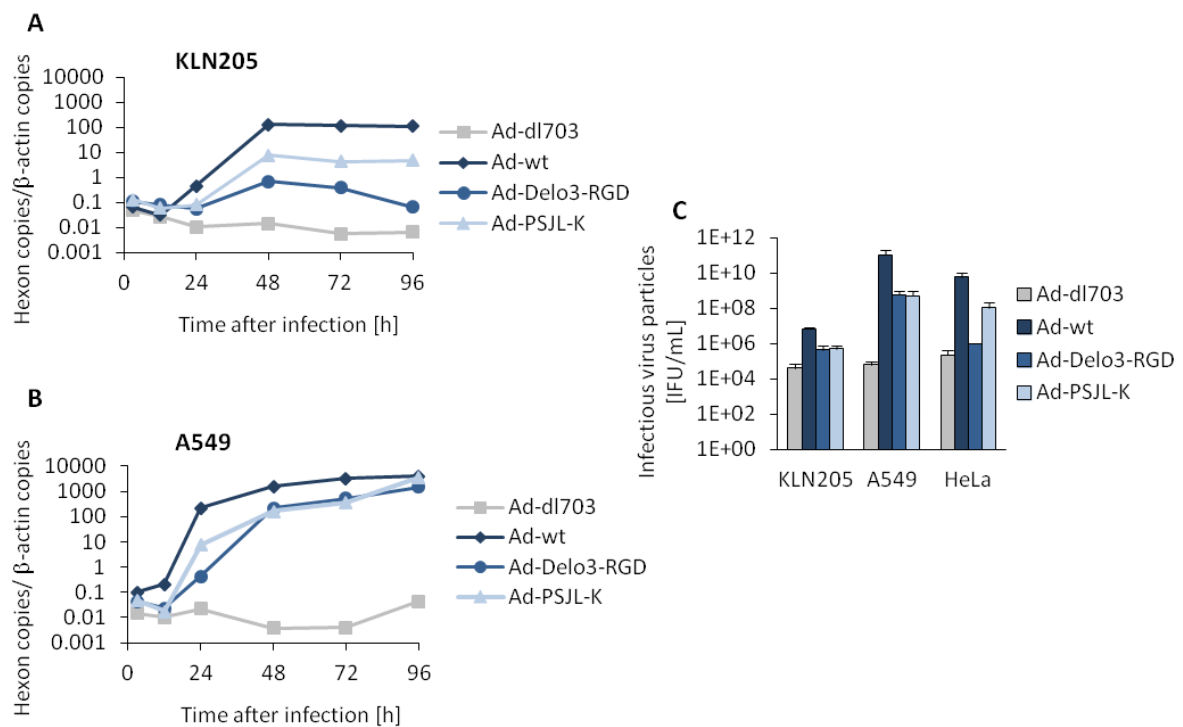


**Figure 3-6: YB-1-dependent oncolytic adenoviruses replicate in murine and human tumor cells and form infectious progeny.** A,B. After infection of KLN205 (A) and A549 (B) cells with 10 IFU/cell of the different adenoviruses, DNA was isolated by phenol chloroform extraction at indicated time points after infection. 100 ng DNA were analyzed for viral replication by real time PCR with primers specific for viral hexon and cellular  $\beta$ -actin. Results are depicted as hexon copies per  $\beta$ -actin copies on a logarithmic scale ( $n=1$ ). C. For assessment of viral infectious particle formation, cells were isolated 72 h after infection with 100 IFU/cell and viruses were released from the cells by three cycles of thawing and freezing. Viral particles in the supernatant were tested for infectivity with a hexon-based immunohistochemical assay in HEK293 cells. Infectious progeny is depicted as IFU/mL on a logarithmic scale (mean $\pm$ SEM,  $n\geq 2$ ).

### 3.3.2. Cytotoxicity of YB-1 dependent oncolytic adenoviruses

Adenoviruses capitalize on their hosts cell cycle, transcription, and translation machineries in order to allow their own survival. When enough viral progeny has been developed in one cell, this cell is killed by the virus in order to release the virions. The virus thereby spreads to neighboring cells and further reproduces there (Russell 2009). Replication and particle formation by YB-1-specific oncolytic adenoviruses was shown (figure 3-6). The cytotoxicity mediated by oncolytic viruses was measured by staining of proteins of adherent cells with the pink aminoxanthene dye SRB.

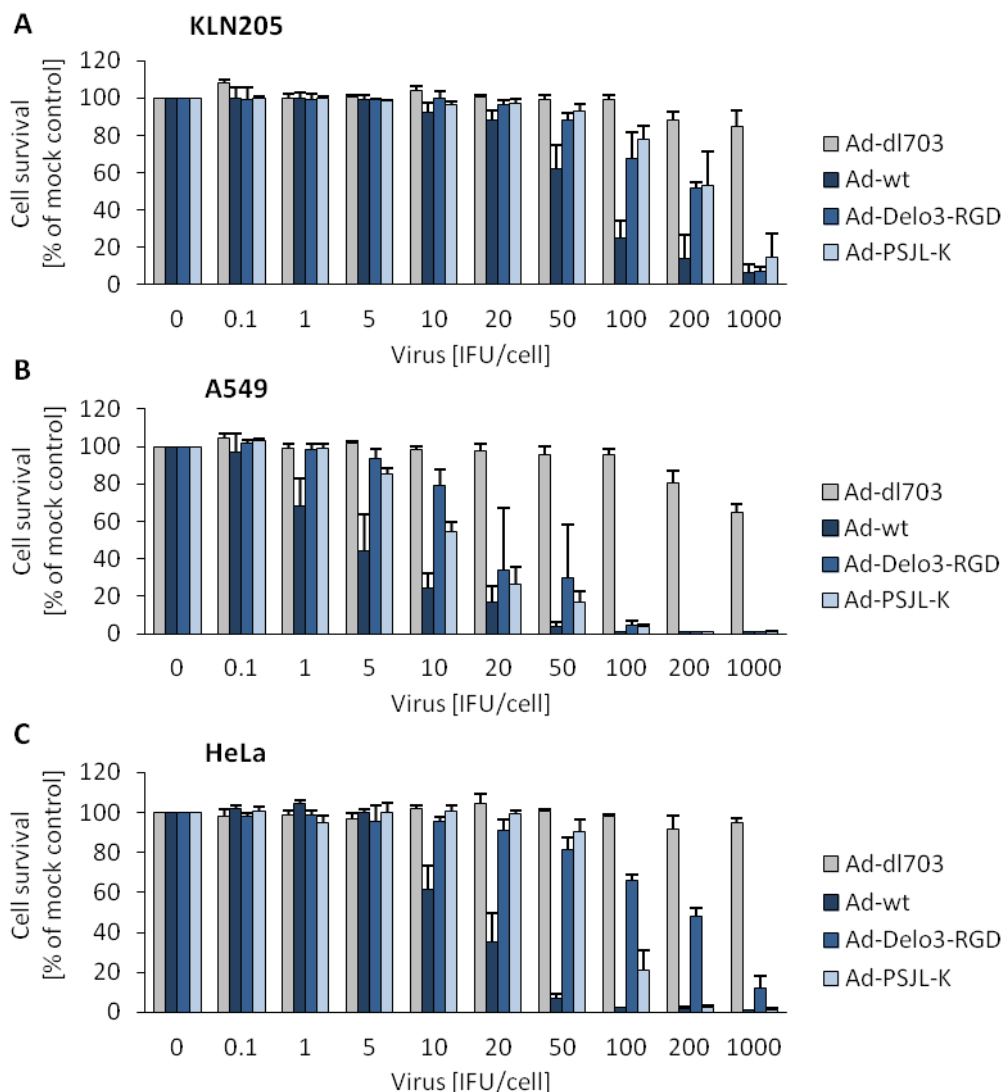


**Figure 3-7: YB-1-dependent oncolytic viruses lyse murine and human tumor cells.** SRB assay of virus-infected KLN205 (A), A549 cells (B), and HeLa cells (C). Cells were fixed 6 d after infection with indicated viruses with indicated MOI and stained with SRB. The solved dye was analyzed by photometry. The results are indicated as cell survival as explained in the Materials and Methods section and normalized to the mock control, which was set to 100% (mean±SEM, n≥3).



As observed in SRB stained cells, about 10-fold higher MOI were needed to reach the same killing potential in murine KLN205 than in human A549 cells and about 2-5 times higher MOI than HeLa cells (figure 3-7). These results are in accordance with the reduced replication and particle formation capability as discussed in the previous section (figure 3-6). About 2-5 times higher MOIs of YB-1-dependent oncolytic viruses were needed to reach the same killing activity like after Ad-wt infection in all cell lines (figure 3-7). Ad-PSJL-K was slightly less potent in KLN205 cells as compared to Ad-Delo3-RGD, whereas it was contrariwise in A549 cells. In HeLa cells, Ad-Delo3-RGD was markedly less cytotoxic than Ad-PSJL-K, reaching only the killing potential that it had in murine KLN205 cells, especially at higher MOIs, which was in accordance with the results for viral infectious particle formation (figure 3-6). Ad-dl703 started to lyse the tumor cells at about 200 IFU/cell, but with 1000 IFU/cell still 70-95% of the cells were viable (figure 3-7). In conclusion, YB-1-dependent oncolytic viruses were able to lyse even murine KLN205 cells, even though relatively high MOIs of about 200 IFU/cell had to be applied for 50% lysis.

### **3.4. Induction of different modes of cell death by wild type and oncolytic adenoviruses**

#### **3.4.1. Replicating adenoviruses induce apoptosis in murine and human tumor cells**

Many adenoviral proteins like E1A, E1B19K, and E3 proteins influence apoptosis, depending on the progression in the adenoviral life cycle (Berk 2005, Lichtenstein et al. 2002, White 2001). As the used YB-1-dependent viruses carry different combinations of mutations of these genes, it seemed reasonable to investigate how these genetic changes would influence the induction of apoptosis by these viruses. To examine the degree of apoptosis occurring in the cells dying due to oncolytic adenovirus infections, a caspase activity assay was conducted using the substrate Ac-DEVD-amc. The peptide sequence Ac-DEVD has homology to the caspase cleavage site of PARP1, which is recognized by the effector caspases 3 and 7. During apoptosis, caspases cleave the nuclear DNA repair enzyme and thereby disable the DNA repair function of PARP1. Cleavage of PARP1 is a necessary event in the late phase of the apoptotic signaling cascade ultimately leading to programmed cell death (Decker and Muller 2002, Nicholson et al. 1995). In the assay used within this thesis, the fluorogenic amc moiety is cleaved from the Ac-DEVD-amc substrate and the resulting amc fluorescence can be measured. In KLN205 cells, after 24 h, almost no activity was observed as compared to mock infected cells, whereas caspase activity was highest after infection with 100 IFU/cell Ad-wt and Ad-Delo3-RGD as compared to mock infected cells 48 h past virus infection (figure 3-8 A). Caspase activity decreased again after the 48 h time point. Ad-wt and Ad-Delo3-RGD reached almost twice the caspase activity of mock treated cells after

48 h, whereas Ad-dl703 showed no additional activity. Caspase activity in Ad-PSJL-K treated cells was slightly elevated to 130%, comparable to FasL and CHX treatment, which served as a positive control for induction of apoptotic cell death. In A549 cells, Ad-wt infection resulted in the highest caspase activity 72 h after infection, with values 1.3-fold as high as mock infected cells (figure 3-8 B). Ad-Delo3-RGD infected cells showed only slightly enhanced caspase activity as compared to mock infected cells after 48 h and no increase was seen for Ad-PSJL-K injected cells. Also in this cell line, as expected, Ad-dl703 treatment did not show caspase activity induction. The results seen in the caspase activity assay show effector caspase activation and indicate cleavage of PARP1. The actual cleavage of PARP1 was verified by WB analysis of KLN205 and A549 cell lysates 48 h post infection, which was the time of the highest caspase activity in KLN205 cells as stated above (figure 3-8 A). In this cell line, the relatively high caspase activity after infection with replicating and conditionally replicating oncolytic viruses could also be observed in the WB for the PARP1 cleavage, whereas PARP1 cleavage was observed, but was not very high in A549 cells (figure 3-8 C). After infection with 100 IFU/cell of the viruses, WB analysis confirmed high caspase activity in Ad-Delo3-RGD treated KLN205 cells and proved the actual PARP1 cleavage. PARP1 cleavage was also markedly enhanced after infection with Ad-PSJL-K and Ad-wt as compared to PARP1 in mock treated cells. In replication-deficient Ad-dl703 virus infected cells, as well as in mock infected cells, only minimal PARP1 cleavage was observed. In A549 cells, PARP1 cleavage activity was highest for Ad-Delo3-RGD as monitored by WB analysis. Thus in both assays and for both cell lines, Ad-Delo3-RGD infections showed the highest induction of apoptosis, probably due to the manipulations in the viral *E1B19K* and *E3* regions. The observed induction is consistent with the reported induction of apoptosis by Ad-Delo3-RGD *in vivo* in a xenograft glioma model (Holzmuller et al. 2011).

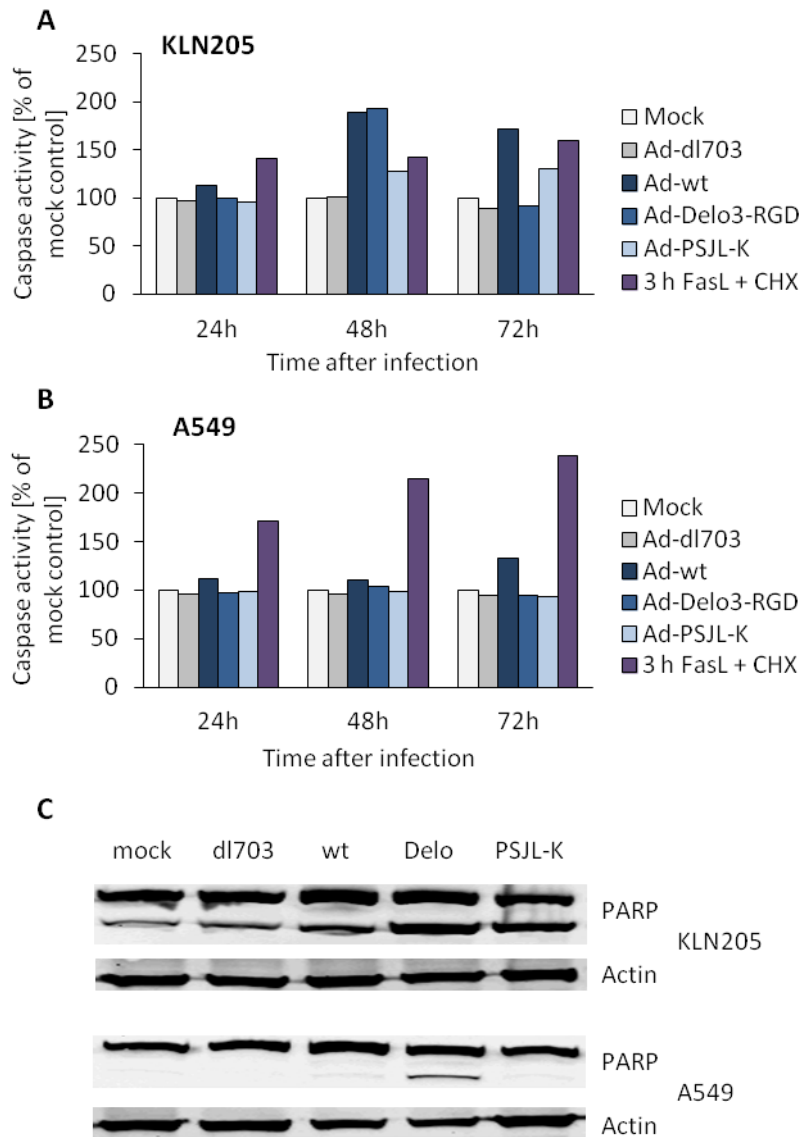


**Figure 3-8: Replicating adenoviruses trigger apoptosis in murine and human tumor cells.** A,B. KLN205 (A) and A549 (B) were infected with 100 IFU/cell of depicted adenoviruses. At indicated time points, a caspase assay using the substrate Ac-DEVD-amc was conducted after lysis of the cells. 3 h before cell lysis, indicated cells (purple) were treated with 100 ng/mL FasL and 1  $\mu$ g/mL CHX as a positive control for induction of apoptosis. Caspase activity is indicated as percentages of caspase activity in mock treated cells (mean $\pm$ SEM, n=1-2). C. WB analysis of PARP1 cleavage in KLN205 (top) and A549 cells (bottom). WB analysis was conducted 48 h after infection with no virus (mock), or 100 IFU/cell of Ad-dl703 (dl703), Ad-wt (wt), Ad-Delo3-RGD (Delo), Ad-PSJL-K (PSJL-K). Bands constitute full length PARP1 (top, 116 kDa) and cleaved PARP (middle, 89 kDa), and the bottom row depicts the actin control (42 kDa).

### 3.4.2. Adenoviruses cause no major induction of autophagy in murine and human tumor cells

Besides apoptotic cell death, also induction of macroautophagy has been reported after infection with adenoviruses and is said to positively (Ito et al. 2006, Rodriguez-Rocha et al. 2011) or negatively (Botta et al. 2012) influence oncolytic cell killing, possibly depending on the degree of autophagy induction (Kroemer and Levine 2008). Macroautophagy or “self-eating”, in the following indicated as autophagy, is a conserved self-degradative process involved in survival, development, and homeostasis, in which proteins and organelles are captured in autophagosomes and are subsequently directed to and proteolytically degraded in lysosomes. Autophagy is important for the maintenance of energy sources during development and in response to stress, such as nutrient deprivation, but also for example viral infection. Cells that undergo excessive autophagy die in a non-apoptotic, non-necrotic manner (Klionsky and Emr 2000, Levine and Klionsky 2004). In order to analyze whether YB-1-specific oncolytic adenoviruses induce autophagy, WB analysis of the LC3 protein was conducted. Following translation, the unprocessed form of LC3 (proLC3) is proteolytically cleaved, resulting in the LC3-I form. Upon induction of autophagy, LC3-I is conjugated with highly lipophilic phosphatidylethanolamine (PE) by the interplay of several autophagy-related proteins (Atgs), which control the autophagic process. LC3-I is thereby turned into its active form LC3-II. LC3-II in contrast to LC3-I is essential for autophagy. It gets localized in the lipid autophagosomal membranes, where it is supposed to play a role in membrane fusion with the lysosome. Later in the process, LC3-II gets delipidated again by another Atg protein, Atg4 and is recycled along with other Atg proteins (Kabeya et al. 2000, Levine and Deretic 2007). This process is illustrated in figure 3-9 A. Guidelines in autophagy research suggest the comparison of the amount of LC3-II relative to actin rather than the LC-II/LC-I ratios in interpretation of WBs (Klionsky et al. 2008, Mizushima and Yoshimori 2007). In KLN205 cells, the signal intensity for LC3-II was very strong in all samples, strongest in mock, Ad-dl703, and Ad-Delo3-RGD infected cells in relation to actin expression as assessed by WB analysis 48 h post adenoviral infection with 100 IFU/cell (figure 3-9 B). Thus, no relevant virus-mediated accumulation of LC3-II was observed in KLN205 cells. In A549 cells, lipidated LC3-II expression was by far highest in Ad-Delo3-RGD infected cells and slightly enhanced after Ad-dl703 treatment, indicating that the treatment causes accumulation of autophagosomes. However, it has to be considered that also the expression of LC3-I was high in the case of Ad-Delo3-RGD infection. In summary, Ad-Delo3-RGD besides apoptosis induction (figure 3-8), showed also the highest induction of autophagy (figure 3-9), which in the case of KLN205 cells was only a very slight increase and is not supposed to influence the outcome of the cell, in contrast to apoptosis induction.

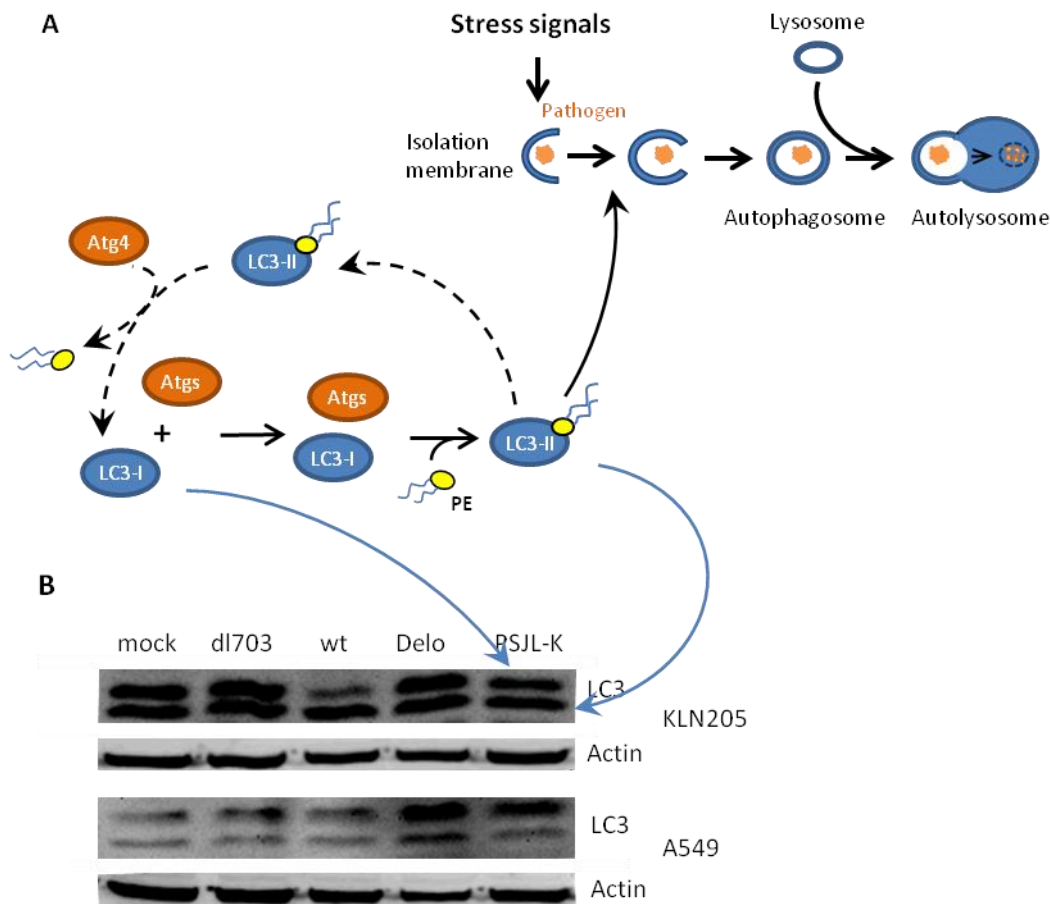


**Figure 3-9: No major induction of autophagic activity after infection with adenoviruses.** A. Depiction of LC3 modification (left) in the process of autophagy (right). After stress signals like starvation, isolation membranes form around pathogens or damaged or dispensable cellular components (orange). Expressed proLC3 proteins are rapidly converted into LC3-I. LC3-I is processed and conjugated with PE (yellow) by Atg proteins (orange) to LC3-II. LC3-II is a unique component of the formed autophagosomal membrane. Upon lysosome fusion, the disposable component is degraded in the autolysosome. Later in the autophagic process, LC3-II is delipidated again by Atg4 and is recycled (image modified from Levine and Deretic 2007). B. LC3-II is in WB analysis detected as the lower band (around 14 kDa) and LC3-I as the upper band (around 17kDa). WB analysis of virus infected KLN205 (top) and A549 (bottom) cells 48 h after infection with 100 IFU/cell with no virus (mock), Ad-dl703 (dl703), Ad-wt (wt), Ad-Delo3-RGD (Delo), Ad-PSJL-K (PSJL-K). The actin control (42 kDa) for each sample is shown beneath LC3.

### 3.4.3. YB-1-dependent oncolytic adenoviruses trigger exposure and release of several ICD molecules *in vitro*

For *in vivo* application of the oncolytic adenoviruses it is important to predict, to what extent the mode of cell death induced by the YB-1-dependent oncolytic viruses can trigger immune responses. The different modes of cell death like apoptosis or autophagy-related cell death can be either immunogenic or tolerogenic (Galluzzi et al. 2012). The immunogenicity of dying cells has been shown to depend on several distinct events during their dying process (Kroemer et al. 2013,

Krysko et al. 2012). Early events in ICD, which are usually determined about 24 h after cell death induction, include cell surface exposure of Hsp70 (Fucikova et al. 2011) and CRT (Obeid et al. 2007b), which are required for efficient antigen presentation and engulfment of dying cells by DCs. Hsp70 cell surface exposure was markedly enhanced in KLN205 cells infected with Ad-PSJL-K and Ad-wt to 1.6 and 1.3 times the uninfected value, respectively, as determined by flow cytometric analysis of the median fluorescence intensity (MFI) 24 h post adenoviral infection with 100 IFU/cell (figure 3-10 A). Treatment with MTX, a topoisomerase II inhibitor and DNA intercalating cytostatic agent (Mazerski et al. 1998), is known to potently activate ICD (Michaud et al. 2011). Hsp70 exposure after infection with Ad-PSJL-K or Ad-wt was higher than in 1  $\mu$ M MTX treated cells. In contrast, Hsp70 exposure was not upregulated, but rather downregulated in Ad-Delo3-RGD infected cells. The flow cytometric analysis of CRT surface exposure resulted in a 3-fold increase in CRT exposure in the 1 $\mu$ M MTX treated positive control, as assessed by measurement of the MFI (figure 3-10 B). Infection with Ad-wt resulted in almost twice the CRT exposure of the mock control, and also the exposure in all other adenovirus infected cells was increased in comparison to mock treated cells to about 130%. To sum up, infection with most adenoviruses slightly enhanced the cell surface exposure of both Hsp70 and CRT *in vitro*. The cell surface exposure of both ICD parameters was particularly high after Ad-wt infection and the exposure of Hsp70 was even further enhanced after Ad-PSJL-K treatment.

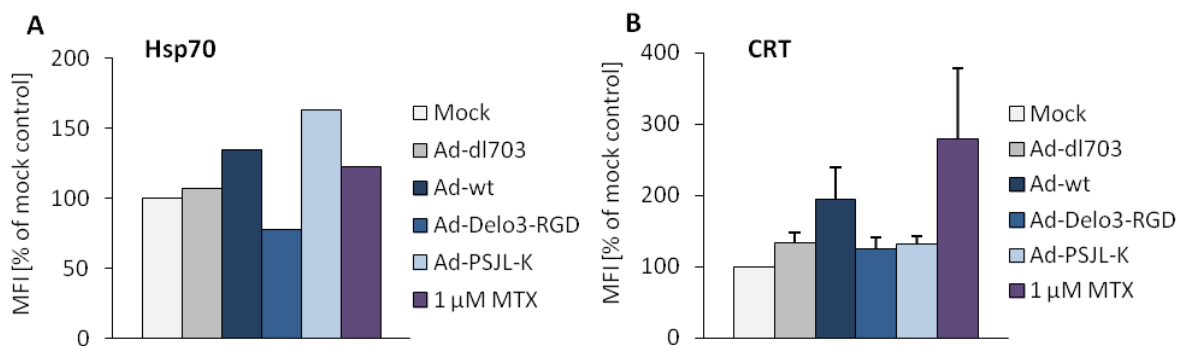


**Figure 3-10: Adenovirus injection stimulates tumor cell surface exposure of ICD parameters Hsp70 and CRT.** KLN205 cells were treated with 100 IFU/cell of indicated adenoviruses and with 1  $\mu$ M MTX as positive control (purple) both for 24 h. A. Hsp70 surface expression was analyzed by Hsp70 immunostaining and subsequent flow cytometric analysis. Results are indicated as MFI in percentage of the mock treated control (n=1). B. CRT surface expression was analyzed by CRT immunostaining and subsequent flow cytometric analysis. Results are indicated as MFI normalized to the mock treated control, which was set to 100% (mean $\pm$ SEM, n=2).

Induction of ICD, and particularly cell surface recruitment of CRT was reported to strongly depend on phosphorylation of the translation initiator eIF2 $\alpha$  by PERK following ER stress (Panaretakis et al. 2009). P-eIF2 $\alpha$  expression, as determined by WB analysis was highest for Ad-wt infected KLN205 cells 48 h post infection (figure 3-11), which is in accordance with the observation of high CRT surface exposure after Ad-wt treatment (figure 3-10 B). Expression of P-eIF2 $\alpha$  was also markedly increased in Ad-PSJL-K infected cells and slightly increased in Ad-Delo3-RGD and Ad-dl703 infected cells as compared to mock infected control cells (figure 3-11). These results indicate that adenovirus-mediated induction of ICD, or at least of CRT cell surface exposure, is indeed dependent of ER-stress response-induced phosphorylation of eIF2 $\alpha$ .

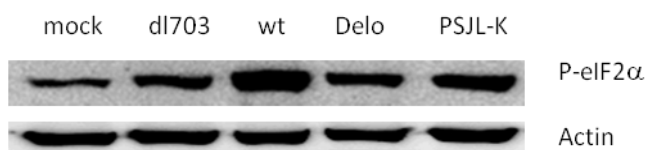


**Figure 3-11: Adenoviruses induce an ER stress response involving phosphorylation of eIF2 $\alpha$ .** WB analysis of P-eIF2 $\alpha$  expression in KLN205 cells 48 h after infection with no virus (mock), or 100 IFU/cell of Ad-dl703 (dl703), Ad-wt (wt), Ad-Delo3-RGD (Delo), Ad-PSJL-K (PSJL-K). P-eIF2 $\alpha$  (top, 38 kDa) and actin (bottom, 42 kDa) proteins were detected by the respective antibodies.

Later events in the course of ICD include release of ATP (Michaud et al. 2011) and HMGB1 (Apetoh et al. 2007), which result in DC attraction, activation and antigen presentation. ATP release into the supernatant of injected cells was measured by a luciferase assay, in which the luminescence signal is based on the ATP-dependent conversion of D-luciferin. As ATP is the limiting factor in the assay, the intensity of the emitted luminescent light is proportional to the ATP concentration. ATP release into the supernatant of infected cells was lower than 0.05 nM. It was therefore hard to assess by the standard curve and was indicated normalized to the mock control. Release of ATP into the supernatant was strongest from Ad-Delo3-RGD infected cells with 1.7-fold increase as compared to the release in the mock treated control, followed by Ad-wt and Ad-dl703 infection 24 h after infection with 100 IFU/cell adenoviruses (figure 3-12 A). ATP release of all other virus infected cells and also of 1  $\mu$ M MTX treated cells only slightly exceeded the value of mock treated cells. HMGB1 release into the supernatant of all adenovirus infected cells was enhanced as compared to mock treated cells as determined by a sandwich ELISA assay after 24 h and still after 6 d after infection (figure 3-12 B). About 8 ng/mL HMGB1 was released into the supernatants of the virus infected cells and more than 100 ng/mL were found in the supernatants of replicating virus or conditionally replicating oncolytic virus infected cells. After 24 h, HMGB1 release was highest from Ad-wt infected cells and lowest from Ad-dl703 infected cells. After 6 d, HMGB1 release from oncolytic virus, especially PSJL-K infected cells was almost as high as from

Ad-wt infected cells. The increase as compared to mock infected cells was 2.7-, 2.3-, and 1.7-fold for Ad-wt, Ad-Delo3-RGD, and Ad-PSJL-K. In summary, adenoviral infection caused exposure and release of all examined ICD parameters. Ad-wt strongly induced exposure or release of all key molecules. YB-1-dependent oncolytic viruses, even though they were less cytotoxic at the same MOI as compared to Ad-wt caused comparable levels of mostly Hsp70, ATP, and HMGB1 exposure or release. Hsp70 exposure was even higher after Ad-PSJL-K infection as compared to Ad-wt infection, and ATP release was higher after Ad-Delo3-RGD infection as compared to Ad-wt infection. These findings indicate that oncolytic adenoviruses, because of their altered genetic structure induce a cell death with slightly different molecular features, i.e. higher induction of apoptosis and higher or different exposure and release of ICD molecules as compared to Ad-wt (figure 3-8 to 3-12). These differences might even, regarding the immunogenicity of the cell death, compensate for the weaker induction of cell killing (figure 3-7).

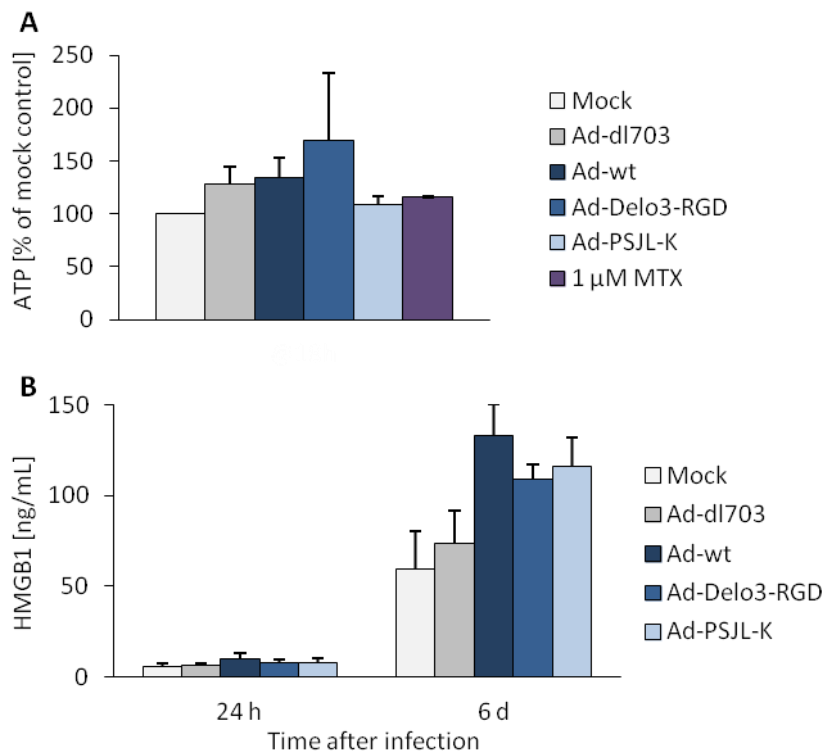


**Figure 3-12: Adenoviral treatment is able to elicit release of the ICD parameters ATP and HMGB1.** Cells were infected with 100 IFU/cell of indicated adenoviruses. A. 24 h after adenoviral infection or treatment with 1 μM MTX positive control (purple), release of ATP into the supernatant was analyzed. ATP was analyzed by a luciferase-based assay. ATP release is indicated as percentage of mock treated control (mean±SEM, n=3). B. HMGB1 release into the cell supernatant was analyzed 24 h and 6 d after adenoviral infection by a HMGB1-specific ELISA. HMGB1 in the supernatant is indicated as ng/mL (mean±SEM, n=3).



### 3.5. Less interference of YB-1-dependent oncolytic adenoviruses than of Ad-wt with MHC I expression and IFN signaling

Besides the immunogenicity of dying cells, also the immune recognition of viable virus infected tumor cells is important for an efficient immune response against the tumor *in vivo*. Presentation of antigens by MHC I complexes is the major requirement for immune recognition of tumor cells and infected cells. Therefore, a sufficiently high presentation of viral and tumor antigens by MHC I is indispensable for an effective anti-tumor immune response. However, besides the general downregulation of MHC I expression by tumor cells (Cavallo et al. 2011), also adenoviral E1A interferes with antigen presentation on MHC I by inhibition of IFN $\gamma$  signaling (Leonard and Sen 1996) and by downregulation of at least two of the three exclusive immunoproteasome subunits, LMP2 and MECL1 (Berhane et al. 2011, Chatterjee-Kishore et al. 2000). Moreover, adenoviral E3gp19K directly inhibits MHC I antigen presentation by retargeting of MHC I to the ER (Sester et al. 2013). It was thus of interest to determine whether KLN205 tumor cells, as described for tumor cells in the literature, have suppressed levels of MHC I exposure and how infection with YB-1-specific oncolytic adenoviruses impaired in *E1A* and *E3gp19K* influences the cell surface expression of MHC I. MHC I cell surface expression was detectable on KLN205 cells as monitored by flow cytometric analysis (figure 3-13). IFN $\gamma$  is known to upregulate antigen processing and MHC I presentation by activation of several IFN-stimulated genes involved in these events, for example by initiation of immunoproteasome expression (Zhou 2009). It was therefore investigated whether IFN $\gamma$  stimulation could induce MHC I expression on the surface of tumor cells. Indeed, addition of IFN $\gamma$  upregulated the cell surface expression of MHC I in a concentration-dependent manner (figure 3-13 A). By addition of 200 U/mL IFN $\gamma$ , the MFI increased about 3.5-fold as compared to unstimulated cells and doubled after treatment with 5 U/mL. Different levels of MHC I cell surface exposure were observed in KLN205, A549, and HeLa cells. In A549 cells (data not shown), MHC I was expressed on a relatively low number of cells and could not be significantly enhanced by exposure to IFN $\gamma$ , whereas addition of 2-200 U/mL IFN $\gamma$  to HeLa cells increased the MFI to up to 1.7 times the intensity in unstimulated cells (figure 3-13 A). Addition of 2 U/mL was sufficient because application of higher concentrations showed no additional increase of MHC I expression.

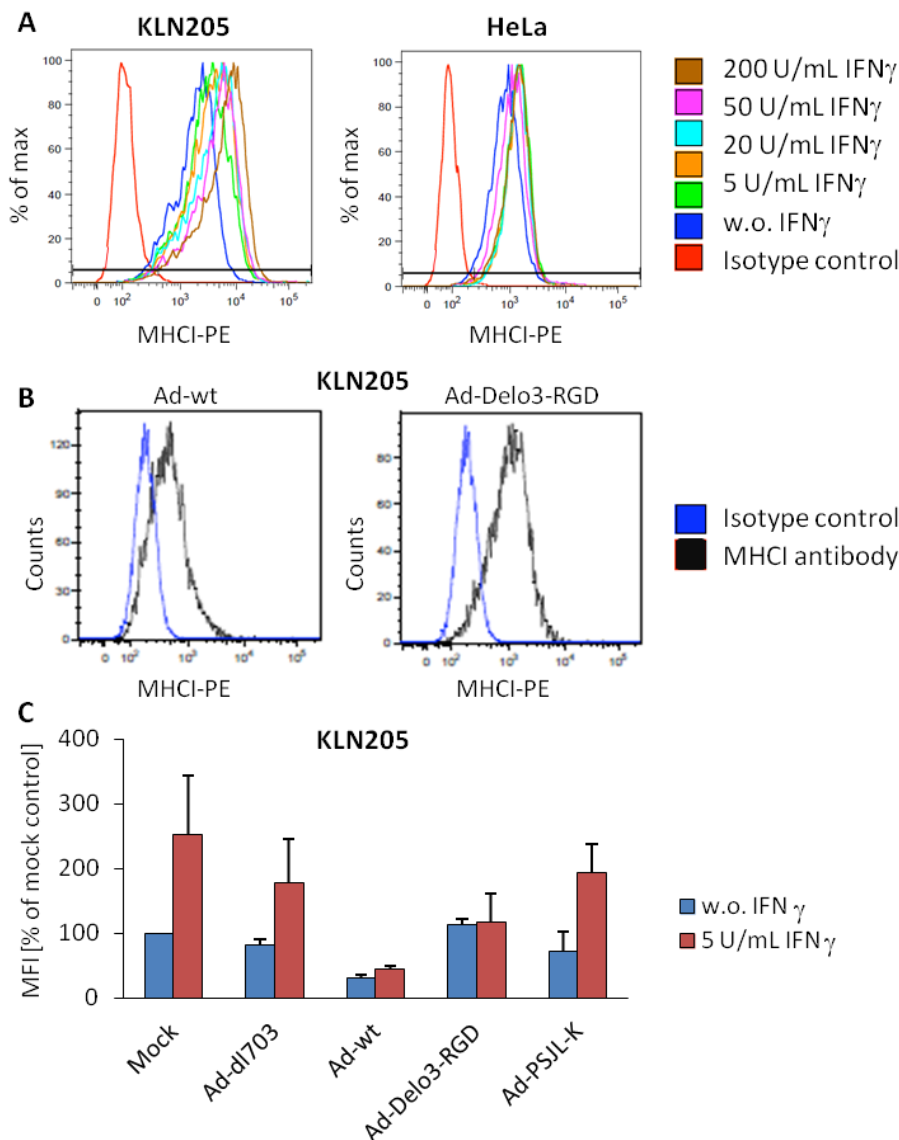


**Figure 3-13: YB-1-dependent oncolytic adenoviruses do not downregulate MHCI surface exposure in contrast to Ad-wt.** A. KLN205 (left) and HeLa (right) cells were treated with different amounts of IFN $\gamma$  overnight. Cells were then stained for MHCI expression. Fluorescence intensity (PE) is indicated on the x-axis with a logarithmic scale against the percentage of maximal counts on the y-axis. The isotype control is depicted in red and untreated cells in blue. B. Flow cytometric analysis of MHCI cell surface expression in KLN205 cells was conducted 24 h after infection with 100 IFU/cell Ad-wt (left) and Ad-Delo3-RGD (right). MHCI stained cells are shown in black and the isotype control is depicted in blue. Fluorescence intensity (PE) is indicated on a logarithmic scale (x-axis) against the number of cell counts (y-axis). C. Flow cytometric analysis of MHCI cell surface expression in KLN205 cells was conducted 24h after infection with 100 IFU/cell of indicated viruses. To stimulate MHCI expression, indicated cells (red) were treated with 5 U/mL IFN $\gamma$  overnight before analysis. MFI was measured and values are depicted as percentage of mock treated not IFN $\gamma$  treated cells (mean $\pm$ SEM, n=2).

The influence of adenoviral infection on MHCI exposure in KLN205 cells was examined next. As expected, infection with 100 IFU/cell Ad-wt, which contains both *E1A* and *E3gp19K*, downregulated the MHCI surface exposure to 30% as compared to uninfected cells 24 h after infection (figure 3-13 B,C). Overnight IFN $\gamma$  treatment of cells before flow cytometric

measurement, was not able to rescue the diminished exposure significantly, which was still 44% as high as the fluorescence intensity measured in mock infected cells (figure 3-13 C). All the other viral constructs, namely Ad-dl703, Ad-PSJL-K, and Ad-Delo3-RGD, all of which have mutations in *E1* and or *E3*, were not able to downregulate MHCI expression (figure 3-13 B,C), and IFN $\gamma$  was always able to enhance MHCI expression in contrast to uninfected unstimulated cells (figure 3-13 C). Ad-dl703 and Ad-PSJL-K treatment slightly decreased MHCI surface exposure (to 72-82%). In contrast to Ad-wt treatment, this effect was completely rescued by stimulation with IFN $\gamma$ , reaching almost twice the mock value of MHCI expression after stimulation. After Ad-Delo3-RGD infection, MHCI was not downregulated, however, addition of IFN $\gamma$  did not have a stimulatory effect on MHCI exposure, in contrast to IFN $\gamma$ -stimulated increase of MHCI cell surface expression after other treatments. Thus, MHCI presentation of virus and tumor antigens was higher after oncolytic virus infection than after Ad-wt infection, suggesting that tumor cells treated with YB-1-specific oncolytic adenovirus should be more susceptible to MHCI-dependent recognition by the immune system *in vivo*.

IFN $\gamma$ -regulated antigen processing and MHCI presentation is dependent on Stat1 expression and phosphorylation (Zhou 2009). IFN $\gamma$  signaling is also generally regulated by phosphorylation and homodimerization of Stat1. Adenoviral E1A has shown to downregulate IFN $\gamma$  by inhibition of Stat1 expression (Leonard and Sen 1996). Monitoring of P-Stat1 by WB analysis 48 h post infection with 100 IFU/cell of different adenoviruses resulted in P-Stat1 dimers observed in virus infected cells as well as mock treated control cells (figure 3-14). By the size of the dimers, dimers were defined as P-Stat1 homodimers. As expected, P-Stat1 expression was markedly reduced in *E1A* gene positive Ad-wt infected KLN205 cells, which is also consistent with the downregulation of MHCI after Ad-wt infection in KLN205 cells and with the lack of further stimulation of MHCI expression by addition of IFN $\gamma$  (figure 3-13). P-Stat1 expression was also reduced in oncolytic virus infected cells, but to a smaller extent than after Ad-wt infection (figure 3-14). Infection with replication-deficient Ad-dl703 did not influence P-Stat1 expression. In conclusion, oncolytic viruses in addition to the enhanced MHCI expression as compared to Ad-wt also showed enhanced IFN $\gamma$  signaling thus further enabling *in vivo* immune activity.

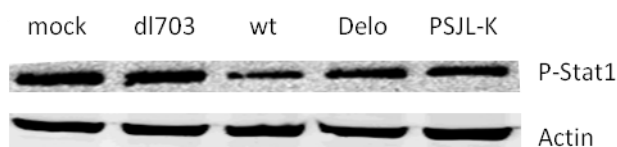


**Figure 3-14: Ad-wt downregulates P-Stat1 expression.** WB analysis of KLN205 cells 48 h after infection with no virus (mock), or 100 IFU/cell of Ad-dl703 (dl703), Ad-wt (wt), Ad-Delo3-RGD (Delo), Ad-PSJL-K (PSJL-K). P-Stat1 (top) and actin (bottom, 42 kDa) proteins were detected by specific antibodies. P-Stat1 usually results in bands of 84 and 91 kDa, the bands in the presented WB depict dimers of approximately 180 kDa.

### 3.6. Use of immunocompetent KLN205 cells in DBA/2 mice to test efficacy of YB-1-dependent oncolytic adenoviruses *in vivo*

YB-1-dependent oncolytic adenoviruses were shown lyse murine KLN205 tumor cells *in vitro* (figure 3-7). Moreover, a reduction in tumor growth after infection of human xenograft tumors in immunocompromised mice with Ad-Delo3-RGD has been described before (Holzmuller et al. 2011, Rognoni et al. 2009). However, the immune system has been shown to hamper oncolytic adenoviral efficacy by clearing of viruses (Parato et al. 2005), but also to enhance tumor destruction by immune-mediated cytotoxicity against the tumor cells (Boozari et al. 2010, Woller et al. 2011). Therefore, the influence of YB-1-dependent oncolytic viruses on tumor growth and anti-virus and anti-tumor immunity was examined in an immunocompetent mouse model. DBA/2 mice were injected with syngeneic KLN205 cells with viabilities of 92-95%.  $2 \times 10^6$  cells were injected subcutaneously into the flank of the animals, whereupon tumor take was 100%. When tumors reached an average diameter of 0.5 cm after about 14 d,  $10^9$  IFU adenoviruses per mouse were injected intratumorally. Mice received YB-1-dependent oncolytic adenoviruses Ad-Delo3-RGD, Ad-Delo3-RGD-Flt3L, or Ad-PSJL-K, replication-competent control virus Ad-wt, or replication-deficient control virus Ad-dl703. Control mice received injections of PBS only. Group sizes were 4-6 mice per group depending on the experiment. The conduction of the *in vivo* experiments within this work is summarized in figure 3-15.

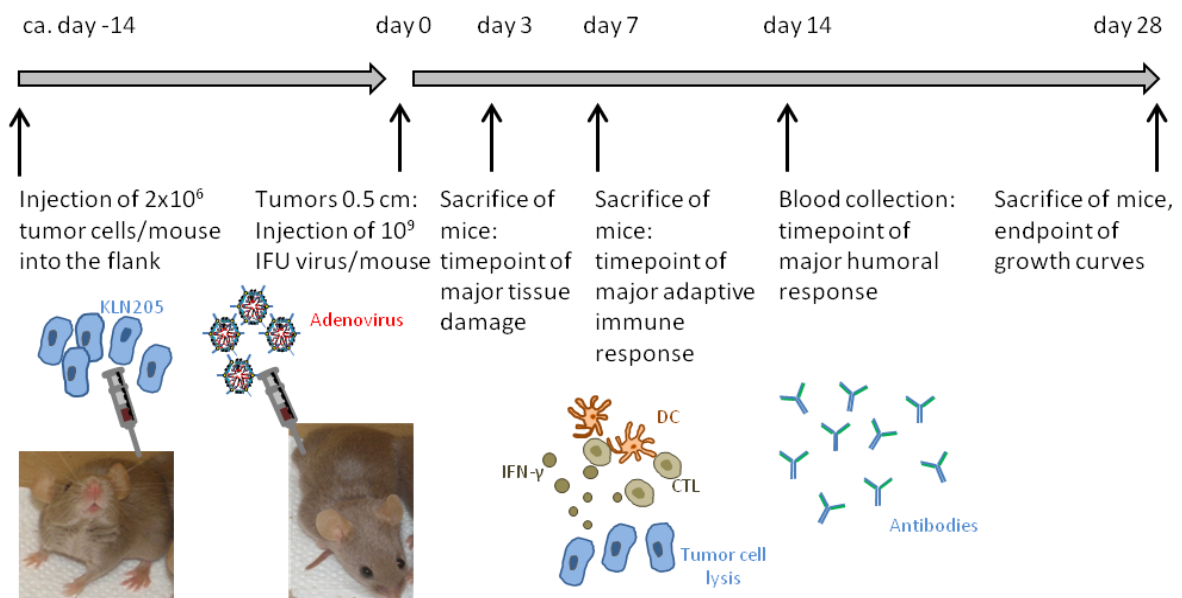


**Figure 3-15: Schematic depiction of *in vivo* experiments.**  $2 \times 10^6$  cells were injected subcutaneously into the flank of DBA/2 mice. When tumors reached an average diameter of 0.5 cm after about 14 d,  $10^9$  IFU adenoviruses per mouse were injected intratumorally at day 0. Mice were sacrificed 3 d after virus injection to assess the virus-mediated tissue damage and 7 d after treatment to assess the maximal adaptive immune response, which is mediated by DCs and subsequent CTL-mediated IFN $\gamma$  secretion and tumor cell killing. Blood was taken from the mice 14 d after virus injection to assess the humoral anti-virus response. Tumor sizes were monitored for 28 d and mice were sacrificed thereafter.

### **3.7. Reduction of tumor growth after oncolytic adenoviral treatment**

Adenoviral therapy has been shown to successfully reduce tumor growth of KLN205 cell tumors in DBA/2 mice (Edukulla et al. 2009, Woller et al. 2011). KLN205 tumors in this study after injection into the flank of DBA/2 mice grew very differently, showing great variances between mice within each treatment group. Tumor growth was slightly slowed down in oncolytic virus infected mice, particularly in Ad-Delo3-RGD treated mice (figure 3-16). Especially after 4-11 d, tumors treated with oncolytic viruses or Ad-dl703 grew very slowly, whereas tumors grew faster in PBS and Ad-wt treated mice. After 11 d, also oncolytic and Ad-dl703 treated tumors began to grow faster, with Ad-dl703 treated tumor growing fastest, especially after about 20 d. For all tested groups, tumor volumes increased about 7- to 8-fold on average during the 28 d course of the experiment. A second injection of virus 7 d after the first injection, as performed for two animals per group, did not result in further decrease of tumor growth (data not shown). Three out of seven PBS injected mice had to be excluded from the experiment due to tumor sizes, tumor ulcerations, lack of weight gain, or signs of morbidity, according to the animal welfare guidelines. Two mice were taken out of the experiment 14 d after treatment and one mouse after 22 d. One Ad-wt treated mouse was excluded from the experiment 14 d after treatment because of a big tumor and signs of morbidity. One Ad-Delo3-RGD-Flt3L mouse had to be taken out of the experiment because of an ulcerated tumor after 22 d. The experiment was terminated after 28 d, when most tumors reached critical sizes. To summarize, treatment with YB-1-dependent oncolytic adenoviruses slowed down tumor growth in comparison to treatment with Ad-wt or Ad-dl703 and resulted in improved overall state of health of the treated mice.

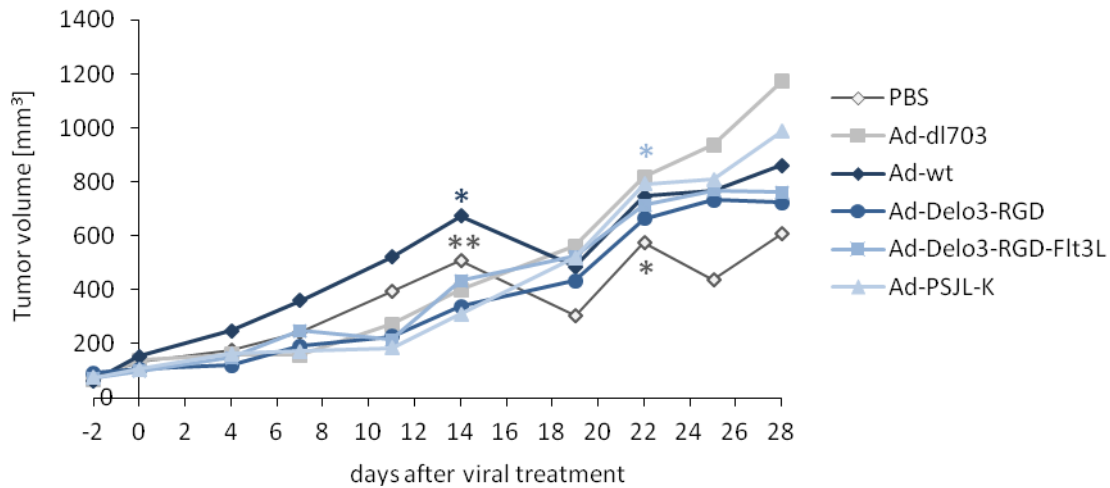


**Figure 3-16: Reduced tumor growth after oncolytic virotherapy.** Tumor growth was measured 2 d before virus treatment, at the day of virus treatment and then every 3 d in average in two dimensions. Tumor volume was calculated as  $0.52 \times (\text{length} \times \text{width}^2)$  and is depicted in  $\text{mm}^3$ . Asterisks denote mice that were excluded from the experiment at that time point. They are thus not included to calculate the mean group tumor size after that time point. 14 d after viral treatment, two PBS treated mice were excluded and one Ad-wt treated mouse. After 22 d, one Ad-Delo3-Flt3L injected mouse was taken out of the experiment and one PBS treated mouse. N at the beginning of the experiment = 6 mice per group, n(PBS)=7 mice per group at the beginning of the experiment. Error bars are not included into the figure to facilitate figure reading.

### 3.8. Mediation of tumor inflammation by replicating adenoviruses

Oncolytic adenoviruses are reported to induce strong inflammation in tumors 3 d after infection (Woller et al. 2011). Therefore, tumor tissues were analyzed for changes in morphology and infiltration of inflammatory immune cells 3 and 7 d after intratumoral virus injection. Paraffin embedded tumor tissue sections of  $2 \mu\text{m}$  were stained with H&E, a classical stain for analysis of histological samples. Histopathology revealed that all tumors grew undifferentiated (figure 3-17), a sign for particularly aggressive tumor growth (Brabletz 2012). In tumors of all groups, necrotic areas could be observed within the tumor mass (figure 3-17 A), which is a typical consequence of insufficient oxygen and nutrient supply due to rapid tumor growth (Grivennikov et al. 2010, Zong and Thompson 2006). Additional major tumor lysis resulting from adenoviral infection was not observed. In all tumors, the tumor-host interface was infiltrated with inflammatory immune cells (figure 3-17 B). In replicating virus infected cells, foci of inflammation were visible within the tumors, containing mostly cells with nuclei resembling granulocytes (figure 3-17 C), an effect that was not observed in PBS and Ad-dI703 treated tumors (figure 3-17 D). This inflammation could be observed 3 as well as 7 d after virus treatment. Tumors were stained with the macrophage marker F4/80 to further assess innate immune cell recruitment. As seen in the H&E sections (figure 3-17 B), rims of the tumors were highly infiltrated by macrophages (figure 3-17 E). Within

the central tumor mass however, no macrophage infiltration was observed (figure 3-17 F). Thus, in accordance with literature reports (Woller et al. 2011), also YB-1-dependent oncolytic adenoviruses were able to trigger infiltration of tumors by immune cells, most likely granulocytes.

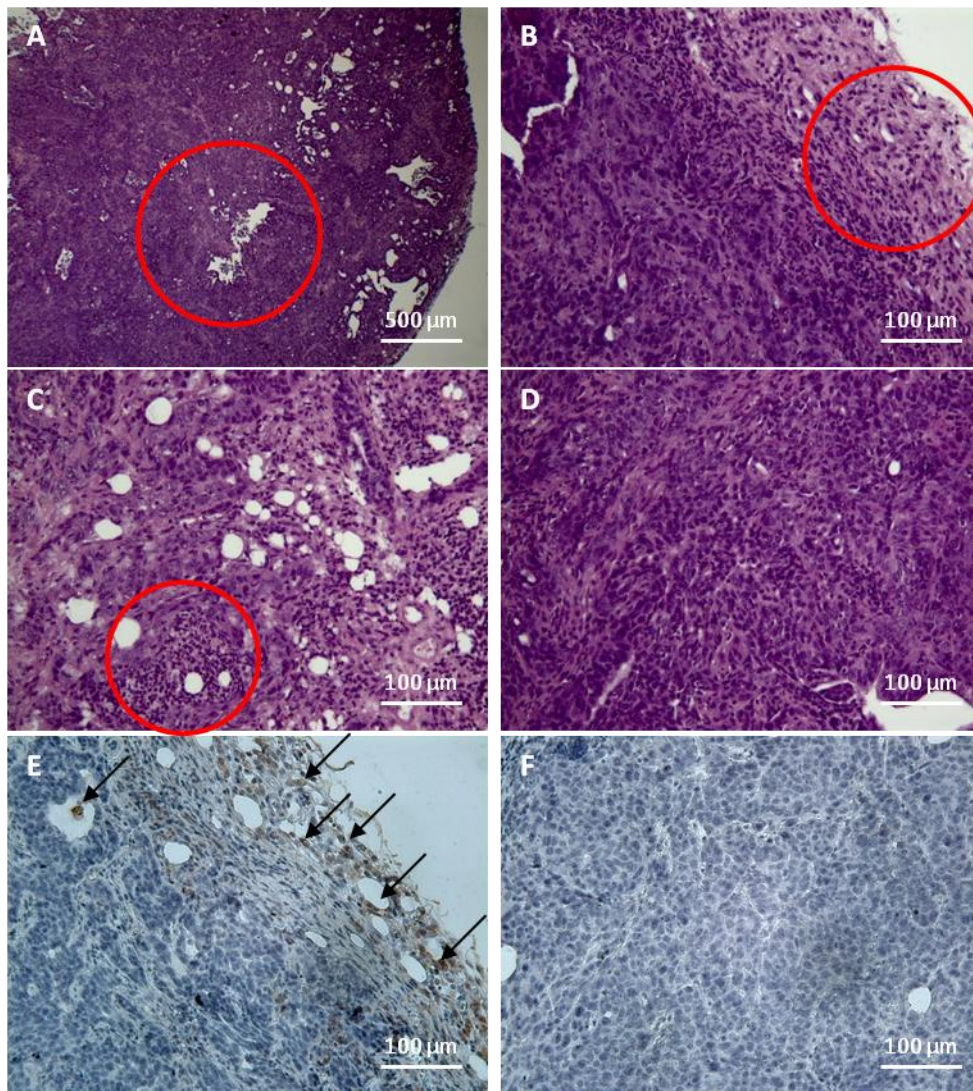


**Figure 3-17: Treatment with replicating adenoviruses triggers infiltration of tumors by innate immune cells.** A-D. 2  $\mu\text{m}$  paraffin sections of tumors were stained with H&E. Bars=500  $\mu\text{m}$  (A), 100  $\mu\text{m}$  (B-D). Tumor necrosis in the central area was assessed 7 d after treatment with Ad-Delo3-RGD. One necrotic area is encircled (red) (A). Immune cell infiltration in the rim areas was assessed 3 d after PBS treatment (B) and infiltration in central areas 3 d after treatment with Ad-wt (C) or PBS (D). Examples for immune cells and foci of inflammation are encircled (red). E,F. 2  $\mu\text{m}$  paraffin sections of tumors 3 d after Ad-Delo3-RGD treatment were stained for macrophage infiltration with an anti-F4/80 antibody. HRP-catalyzed substrate development is indicated (brown). Cells were counterstained with hemalum solution (blue). Depiction of one rim (E) and one middle (F) area. Arrows point to examples of stained F4/80 positive cells (E). Bars=100  $\mu\text{m}$ .

### **3.9. Adenovirus-mediated immune cell recruitment**

#### **3.9.1. Adenovirus treatment of tumors increases spleen weight and blood leukocyte counts**

Adenoviruses infection triggers a broad range of immune cell recruitment and activation including recruitment of innate and adaptive immune cells, as well as of humoral immune responses (chapter 1.9.1). To assess the overall immune activation after adenoviral treatment, spleens of virus treated cells were weighed. Spleens of healthy mice had a weight of about 95 mg, whereas spleens of tumor bearing mice weighed 120 to 200 mg 3-7 d post virus treatment and 160 to 260 mg 28 d post virus treatment (figure 3-18 A). Over the whole time course, spleen weight was about 160 mg in PBS treated tumor mice. 3 d after virus injection, the spleen weight was about the same with or without virus treatment (120-160 mg), but spleens of virus treated mice were grown 7 d after treatment to over 180 mg for Ad-wt, Ad-PSJL-K, and Ad-dl703 treated mice, but not in mice with Ad-Delo3-RGD and Ad-Delo3-RGD-Flt3L therapy. 28 d after virotherapeutic treatment, spleens of virus infected cells were grown significantly to about 240-260 mg whereas PBS treated mice still had 160 mg spleens. Only in Ad-Delo3-RGD-Flt3L treated mice, average spleen weight was 210 mg, and thus slightly lower than in all other virus treated animals. General leukocyte recruitment in the blood was assessed by flow cytometric analysis 3 and 7 d after treatment of tumors (figure 3-18 B). In the blood, numbers of leukocytes were increased after infection with all used viral variants, with highest numbers of leukocytes present in the blood after Ad-wt, Ad-PSJL-K, and Ad-dl703 treatment, demonstrating that adenoviruses efficiently trigger leukocyte recruitment into spleen and blood.



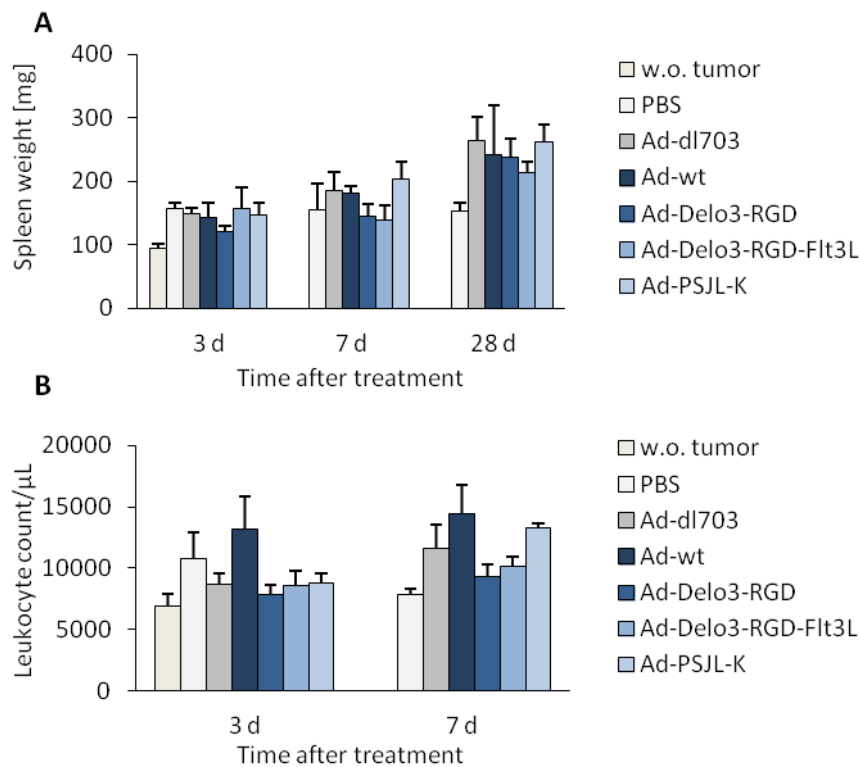


**Figure 3-18: Adenovirus-mediated increase in spleen weight and blood leukocyte counts.** A. Spleens of virus treated tumor bearing mice and non-tumor bearing control mice (w.o. tumor) were isolated at indicated time points after virus treatment and weighed. Spleen weight in mg is depicted (mean±SEM, n≥4 mice per group). B. The leukocyte count in the blood of virus treated tumor bearing mice and non-tumor bearing control mice (w.o. tumor) was determined by flow cytometric analysis of CD45 expression 7 d after virus treatment. CD45 positive leukocytes are depicted as counts per μL, which were calculated from the population counts as stated in the Materials and Methods section (mean±SEM, n≥4 mice per group).

### 3.9.2. Ad-wt and Ad-PSJL-K elicit increased recruitment of several immune cell populations into the blood

Successful oncolytic viral treatment and anti-tumor immune activity depends mostly on DC recruitment and T cell activation (Diaconu et al. 2012, Edukulla et al. 2009, Huang et al. 2010), while the role of B cells (Candolfi et al. 2011, Diaconu et al. 2012) and NK cells (Alvarez-Breckenridge et al. 2012a, Alvarez-Breckenridge et al. 2012b, Choi et al. 2012) in virotherapy is discussed controversially. Possible contributions of these immune cells to the observed anti-tumor effect of the administered adenoviruses should be investigated. Therefore, concentrations of these immune cell populations in the blood were examined by flow cytometric analysis 7 d after viral tumor treatment. Ad-wt and Ad-PSJL-K treatment of tumor bearing mice induced strong recruitment of all analyzed immune cell populations into the blood (figure 3-19). T cell recruitment was particularly high after Ad-PSJL-K infection and B cell counts were highest in blood

from Ad-wt infected mice. Replication-deficient Ad-dl703 treatment caused no additional recruitment of T cells and B cells as compared to PBS treatment, whereas the DC count was enhanced after Ad-dl703 treatment. Ad-dl703 triggered recruitment of more NK and natural killer T (NKT) cells at the same level as Ad-wt and Ad-PSJL-K. Treatment with Ad-Delo3-RGD and Ad-Delo3-RGD-Flt3L resulted in similar immune cell recruitment patterns. As opposed to the knowledge that Flt3L as a transgene recruits DCs (Edukulla et al. 2009), no additional DC recruitment was observed after Ad-Delo3-RGD-Flt3L treatment of tumors. Both DC and T cell recruitment were even slightly lower than after Ad-Delo3-RGD treatment without Flt3L transgene. Only B cell, NK, and NKT cell recruitment was slightly enhanced by the additional Flt3L transgene as compared to Ad-Delo3-RGD. In summary, Ad-wt and Ad-PSJL-K induced recruitment of total immune cells (figure 3-18), as well as recruitment and differentiation of all immune cell populations that are supposed to play a role in immune reactions against tumors following oncolytic virotherapy. Mainly DCs and T cells are said to be important for the success of virotherapy and these immune cell populations were even stronger recruited by Ad-PSJL-K treatment than by treatment with Ad-wt (figure 3-19).

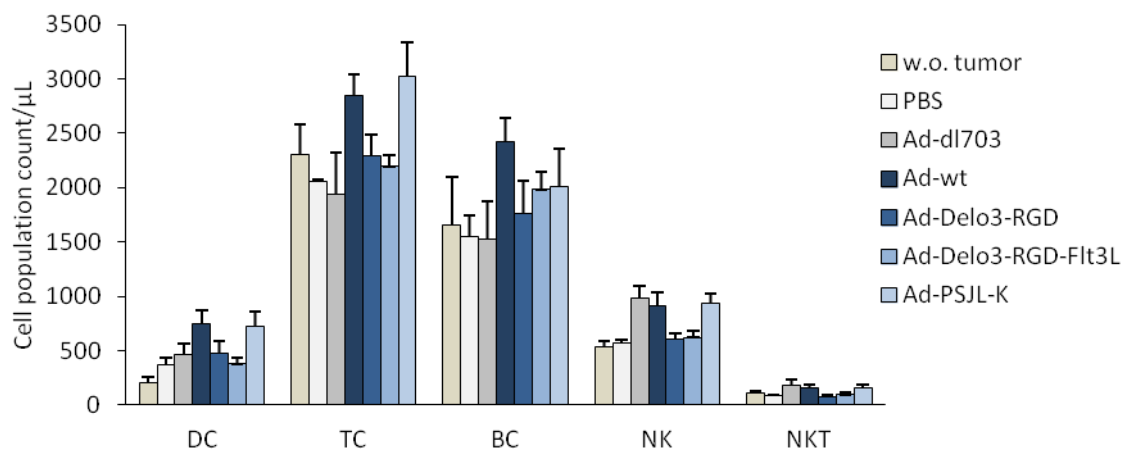


**Figure 3-19: Adenoviruses, especially Ad-wt and Ad-PSJL-K, trigger recruitment of DCs and immune effector cells.** Blood of virus and PBS treated tumor bearing mice and non-tumor bearing control mice (w.o. tumor) was analyzed for immune cell populations 7 d after virus injection. Immune cells were stained with antibodies specific for CD45, CD11c, CD3, CD49b, and CD19 and analyzed by flow cytometry in the presence of Trucount beads. Cell population counts per  $\mu\text{L}$  are depicted. They were calculated from the population counts as stated in the Materials and Methods section. Immune cell populations were gated and defined as follows: DCs (DC) (CD45+/CD11c+/CD3-), T cells (TC) (CD45+/CD11c-CD49b-/CD3+), B cells (BC) (CD45+/CD11c-CD49b-/CD19+), NK cells (NK) (CD45+/CD49b+/CD3-), NKT cells (NKT) (CD45+/CD49b+/CD3+) (mean $\pm$ SEM, n=5 mice per group, n(w.o. tumor)=4 mice per group).

### 3.10. Efficient anti-virus host immune response

Recruitment of total immune cells and distinct immune cell populations by adenovirus treatment of tumors has been shown before (figures 3-18 and 3-19). Since adenoviruses are very immunogenic naturally (de Gruijl and van de Ven 2012), high immune responses against the injected agents were expected. However, adenoviral treatment can also enhance anti-tumor immune responses (Boozari et al. 2010). Hence, in order to be able to discriminate between contributions of anti-virus and anti-tumor effect to the recruitment of immune cells after YB-1-dependent oncolytic virus treatment of tumors, the anti-virus and anti-tumor immune responses were examined. First, humoral anti-viral responses in the serums of the mice were analyzed by ELISA 14 d after adenovirus treatment of tumors (Woller et al. 2011). Total Igs were efficiently produced against administered adenoviruses (figure 3-20 A). Most antibodies were produced against Ad-Delo3-RDG, more than against Ad-wt and Ad-PSJL-K. Surprisingly, markedly less antibodies were produced against Ad-Delo3-RGD-Flt3L viruses than against all other adenoviruses, even less than against replication-defective Ad-dl703 viruses. A second virus treatment, 7 d after the first one, augmented anti-viral antibody responses in all groups (figure 3-20 B). Responses after repeated adenovirus delivery rose least in Ad-wt infected mice and most in Ad-dl703 treated mice. In Ad-Delo3-RGD-Flt3L, since only two mice per group were treated twice and since one mouse had highly elevated antibody responses and responses in the other mouse remained low, conclusions are hard to draw. Cellular anti-virus responses were determined by an IFN $\gamma$ -specific ELISpot assay. 3 d after virus treatment, no upregulation of IFN $\gamma$  expression after stimulation with viral peptide DBP was seen in splenocytes of treated mice (ca. 1 spot per  $5 \times 10^5$  splenocytes). 7 d after viral injection into tumor bearing mice, splenocyte recognition of the viral peptide and following IFN $\gamma$  release was very high (figure 3-20 C). PMA and ionomycin-stimulated positive controls resulted in 120-220 spots per  $5 \times 10^5$  splenocytes, whereas the immune effector cell recognition was highest against Ad-wt, reaching 210 spots per  $5 \times 10^5$  cells, all spots resembling one IFN $\gamma$  secreting cell. Ad-PSJL-K and Ad-Delo3-RGD infection resulted in 200 and 170 spots per  $5 \times 10^5$  cells, respectively. Ad-Delo3-RGD-Flt3L, as observed for the humoral response, elicits a response that is, with about 70 spots per  $5 \times 10^5$  cells, significantly smaller than for the other viruses. After Ad-dl703 treatment of tumor bearing mice, splenocyte IFN $\gamma$  release was minimal, reaching less than 9 spots per  $5 \times 10^5$  cells. PBS treated mice reached 2 spots per  $5 \times 10^5$  cells in average. Collectively, treatment of tumors with YB-1-dependent oncolytic adenoviruses induced strong anti-viral humoral and cellular immune responses comparable to Ad-wt treatment. The anti-virus immune responses in general, and particularly the cellular response, were strongly dependent on viral replication.

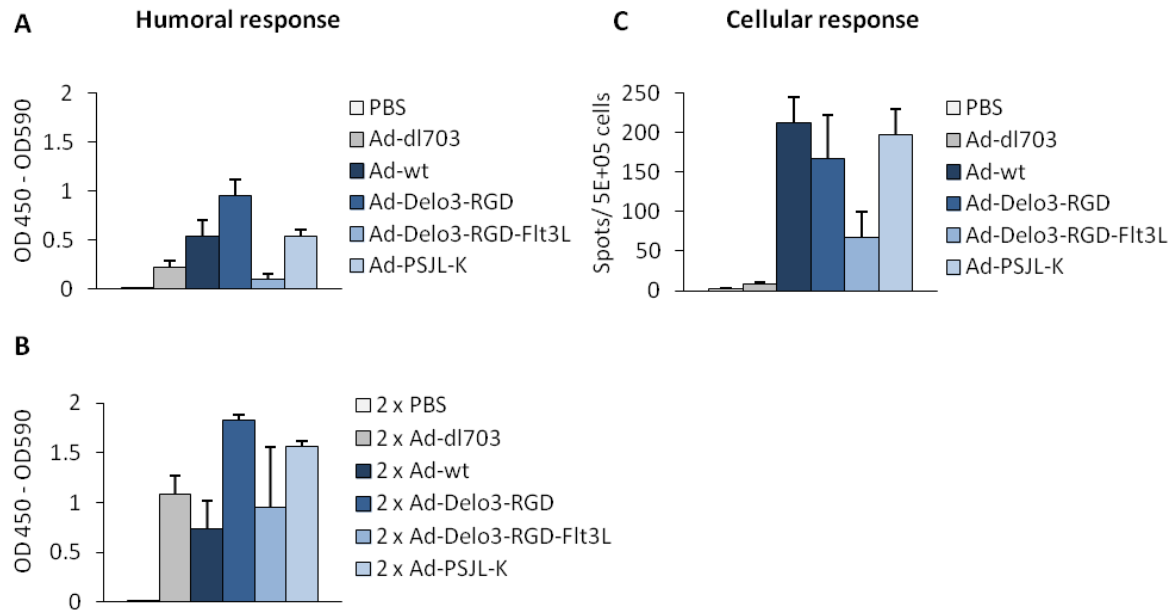


**Figure 3-20: Replicating adenoviruses trigger efficient humoral and cellular host anti-virus responses.**

A. Analysis of anti-viral antibody response. Blood was taken from virus injected tumor bearing mice 14 d after virus injection. The serum was analyzed for virus-specific total Ig antibodies by ELISA and is depicted as OD<sub>450nm</sub> – OD<sub>590nm</sub> (mean±SEM, n=5 mice per group). B. Analysis of anti-viral antibody response after treatment of tumor bearing mice after two consecutive virus injections, at day 0 and day 7. Blood was taken 14 d after the first virus injection. The serum was analyzed for virus-specific total Ig antibodies by ELISA and is depicted as OD<sub>450nm</sub> – OD<sub>590nm</sub> (mean±SEM, n=2 mice per group). C. Analysis of anti-viral cellular response. Splenocytes were isolated from virus injected tumor bearing mice 7 d after virus injection. 5x10<sup>5</sup> splenocytes per well were stimulated with 0.2 µg viral DBP peptide. The number of virus-specific IFNγ-secreting splenocytes was analyzed by ELISpot assay and is depicted as spots per 5x10<sup>5</sup> cells (mean±SEM, n=5 mice per group).

### 3.11. Anti-tumor immune reactions elicited by YB-1-dependent virotherapy

#### 3.11.1. Replicating or conditionally replicating viruses induce exposure and release of ICD molecules in mice

*In vitro* analysis of ICD parameters after YB-1-dependent oncolytic virus infection of tumor cells, particularly of molecules released during the later stages of ICD, namely ATP and HMGB1 (figure 3-12), provided an indication that treatment with oncolytic viruses could enhance the immunogenicity of the cells dying due to the viral therapy. Hence, ATP and HMGB1 were also analyzed after *in vivo* application of YB-1-dependent oncolytic viruses, in the serum of tumor bearing mice 7 d after treatment with adenoviruses. Both ATP and HMGB1 release were highly variable between the animals, also within one group. In the ATP assay, the mean serum ATP concentrations were smaller in animals without tumors, PBS treated mice, and Ad-dl703 treated mice (all around 1000 nM) as compared to ATP levels in animals treated with any of the other

viruses (figure 3-21 A). Mean ATP serum values were around 1800 nM after Ad-PSJL-K and Ad-Delo3-RGD treatment and around 1400 nM after Ad-wt and Ad-Delo3-RGD-Flt3L treatment. The high ATP release after Ad-Delo3-RGD treatment is in accordance with the high ATP release after Ad-Delo3-RGD infection *in vitro* (figure 3-12 A). Serum release of HMGB1 from mice without tumors and PBS injected control mice was as high as after treatment with Ad-wt or oncolytic viruses (figure 3-21 B). Only the HMGB1 serum concentrations after replication-deficient Ad-dl703 treatment were particularly low (4 ng/mL). Mean HMGB1 concentrations were highest for Ad-wt and Ad-Delo3-RGD-Flt3L (9 ng/mL), in contrast to 7 ng/mL in Ad-Delo3-RGD and Ad-PSJL-K treated animals, but because of the high variations no big differences were visible between all groups. Because of the high variability of ATP and HMGB1 serum concentrations, differences are hard to analyze. However, treatment with YB-1-specific oncolytic adenoviruses triggered the same or even higher release of ICD-specific molecules than treatment with Ad-wt, suggesting, like the *in vitro* results, a high immunogenicity of tumor cells dying because of oncolytic virus treatment.

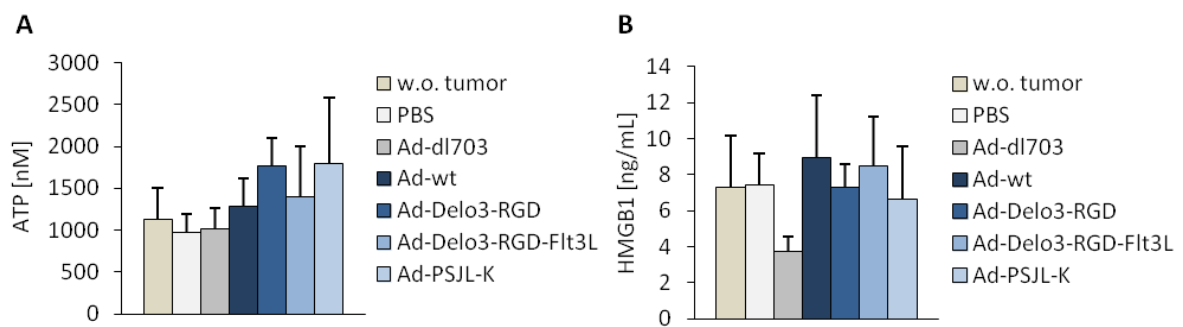


**Figure 3-21: Adenoviral therapy with replicating viruses elicits release of ICD parameter ATP and HMGB1 *in vivo*.** A. Released ATP in serum of virus or PBS treated tumor bearing mice and non-tumor bearing mice (w.o. tumor) was analyzed by a luminescence-based assay 7 d after virus injection. Serum ATP is depicted in nM (mean $\pm$ SEM, n=5 mice per group, n(w.o. tumor)=3 mice per group). B. Release of HMGB1 in serum of virus or PBS treated tumor bearing mice and non-tumor bearing mice (w.o. tumor) was analyzed by ELISA 7 d after virus injection. Serum HMGB1 is depicted in ng/mL (mean $\pm$ SEM, n=5 mice per group, n(w.o. tumor)=3 mice per group).

### 3.11.2. Adenoviral treatment is able to trigger anti-tumor immune responses

The key question for the applicability of the viruses as anti-tumor therapeutics is whether the oncolytic adenovirus infection can trigger an immune response that is not only directed towards the virus (figure 3-20), but rather towards the tumor (Woller et al. 2011). To address this question, the splenocytic immune cells were tested regarding different aspects of cytotoxic activity. Their potential to recognize tumor antigens and in consequence secrete IFN $\gamma$  was assayed by IFN $\gamma$ -specific ELISpot (figure 3-22 A). Their potential to show degranulation and in consequence degranulation-mediated release of cytotoxic molecules like granzymes and perforin should be further tested. Degranulation as a consequence of tumor antigen stimulation was assayed by flow cytometric analysis of the degranulation marker CD107a (figure 3-22 B). Finally, the potential of the immune effector cells to lyse tumor cells was tested by cell-mediated cytotoxicity assay with calcein-AM assay (figure 3-22 C).

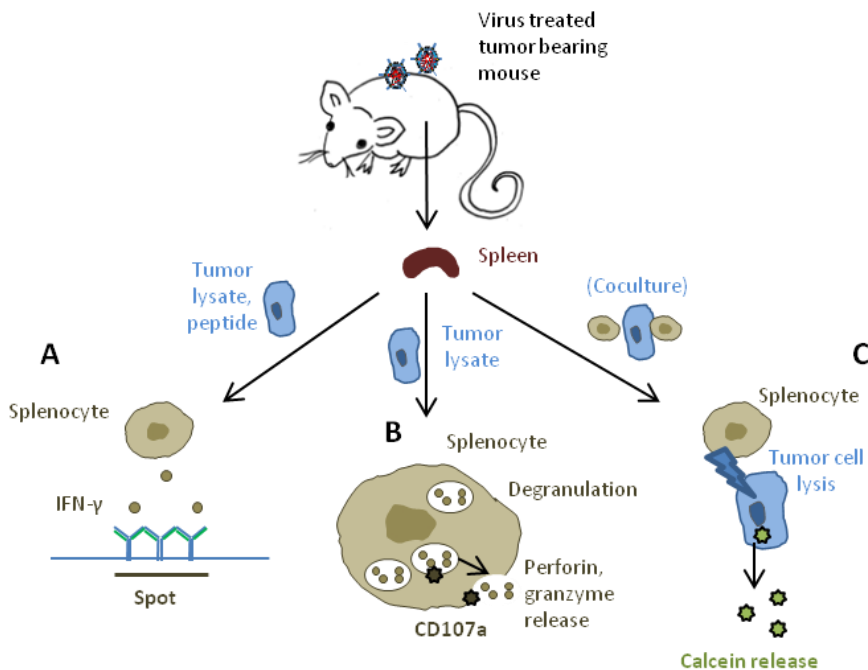


**Figure 3-22: Schematic overview over analysis of anti-tumor immune responses.** A. Tumor lysate- or tumor peptide-triggered splenocyte IFN $\gamma$  secretion was analyzed by an IFN $\gamma$ -specific ELISpot analysis. B. Tumor lysate-triggered degranulation of splenocytes resulting in perforin and granzyme release. Degranulation of splenocytes was analyzed by flow cytometric analysis of the degranulation marker CD107a on the splenocyte surfaces. C. Splenocyte-mediated tumor cell lysis was assessed by a calcein release assay. Calcein loaded tumor cells release calcein following splenocyte-mediated cell lysis. The assay was conducted with or without prior coculture of splenocytes with tumor cells.

The tumor-specific release of IFN $\gamma$  was monitored by an IFN $\gamma$ -specific ELISpot assay after stimulation of splenocytes with tumor peptide (hTert) or KLN205 cell lysate (figure 3-22 A). 3 d after virus injection, when no adaptive immune response was expected, IFN $\gamma$  responses did not exceed 2-3 spots per  $5 \times 10^5$  cells (data not shown). 7 d after adenovirus treatment, following stimulation with either of the tumor antigens, splenocytes of virus infected mice showed higher IFN $\gamma$  responses as compared to PBS treated mice (figure 3-23). Animals without tumor had IFN $\gamma$  responses of less than or equal to 1 spot per  $5 \times 10^5$  splenocytes, which resembles the background levels of the measurement. IFN $\gamma$  release was strongest in Ad-PSJL-K treated animals, exceeding 4 spots for both peptide and lysate stimulation in four out of five animals and even 6 spots in two or three out of five animals, respectively. IFN $\gamma$  release from splenocytes of PBS treated animals in contrast reached an average of 1-2 spots per  $5 \times 10^5$  splenocytes. Responses were also slightly elevated after Ad-dl703 treatment as compared to the other viruses, and following tumor lysate stimulation also for Ad-Delo3-RGD-Flt3L (figure 3-23 B). The increased anti-tumor response following Ad-Delo3-RGD-Flt3L treatment was in contrast to the reduced anti-virus response after treatment with this virus (figure 3-20). Negative controls without stimulation or with stimulation with the negative control lacZ peptide showed 1-3 spots per  $5 \times 10^5$  cells and PMA and ionomycin-stimulated positive controls resulted in 120-220 spots per  $5 \times 10^5$  splenocytes, indicating the general functionality of the assay. IFN $\gamma$  release following stimulation with either of the tumor antigens was thus enhanced by viral treatment, especially after Ad-PSJL-K treatment, indicating a slight stimulation of anti-tumor responses by adenoviral treatment.

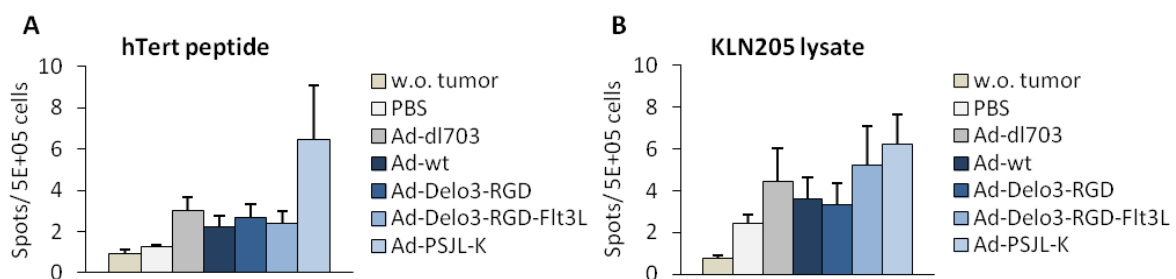


**Figure 3-23: Ad-PSJL-K treatment augments the anti-tumor immune response.** ELISpot analysis from tumor bearing mice treated with indicated viruses or PBS and non-tumor bearing mice (w.o. tumor). Splenocytes were isolated 7 d after treatment of animals and  $5 \times 10^5$  freshly isolated splenocytes per well were stimulated with 0.2  $\mu\text{g}$  hTert peptide (A) or 20  $\mu\text{L}$  tumor lysate cell lysate (B). Results are indicated as spots per  $5 \times 10^5$  cells (mean  $\pm$  SEM, n=5 mice per group, n(w.o. tumor)=4 mice per group).

Cytotoxic activity of CTL and NK cells, mediated by release of cytokines and release of cytotoxic molecules like granzymes or perforin, requires degranulation of the cytotoxic cells. Degranulation following stimulation is marked by cell surface exposure of the membrane glycoprotein lysosomal-associated membrane protein-1 or CD107a (figure 3-22 B) (Aktas et al. 2009, Alter et al. 2004). Splenocytes of virus infected tumor bearing mice were stimulated with tumor antigens of KLN205 cell lysates for 4 h. During this time, they were coincubated with CD107a antibody, as well as monensin, which prevents the acidification of endocytic vesicles. It thereby avoids reinternalization and degradation of cell surface exposed CD107a proteins, and thus enables visualization of this marker following stimulation (Alter et al. 2004). Tumor cell lysate stimulation was able to stimulate degranulation, as visualized by flow cytometric analysis of CD107a cell surface exposure of splenocytes from tumor bearing virus treated mice (figure 3-24 A). 4% of CD8+ CTLs of non-tumor bearing control animals were positive for CD107a surface expression following tumor antigen stimulation (figure 3-24 B). The same percentage was seen in PBS treated tumor bearing animals. Treatment of tumor bearing mice with adenoviruses augmented CD107a surface exposure following tumor antigen stimulation to more than 5% of CD8+ CTLs. Treatment with Ad-wt and Ad-PSJL-K showed a 1.5-fold increase as compared to 6.5% of CD8+ CTLs upon PBS treatment. NK cell CD107a surface expression following tumor antigen stimulation was elevated by adenovirus treatment of mice from 70% of NK cells in non-tumor bearing control mice or tumor bearing PBS treated animals to 75% of NK cells after virus treatment (figure 3-24 C). Only Ad-wt treatment was not able to augment CD107a surface exposure. NKT cell surface expression of CD107a was augmented after virus treatment of animals from 65% of NKT cells in PBS treated animals to 75% of NKT cells. Hence, in accordance with IFN $\gamma$  release measured in total splenocytes (figure 3-23) also degranulation of CTLs, NK cells, and NKT cells was enhanced following adenoviral treatment (figure 3-24). The strongest degranulation in CTLs was seen after Ad-wt and Ad-PSJL-K treatment, which is in concert with the generally enhanced immune cell recruitment by these viruses (figures 3-18 and 3-19) and with the increased IFN $\gamma$  release after Ad-PSJL-K treatment (figure 3-23).



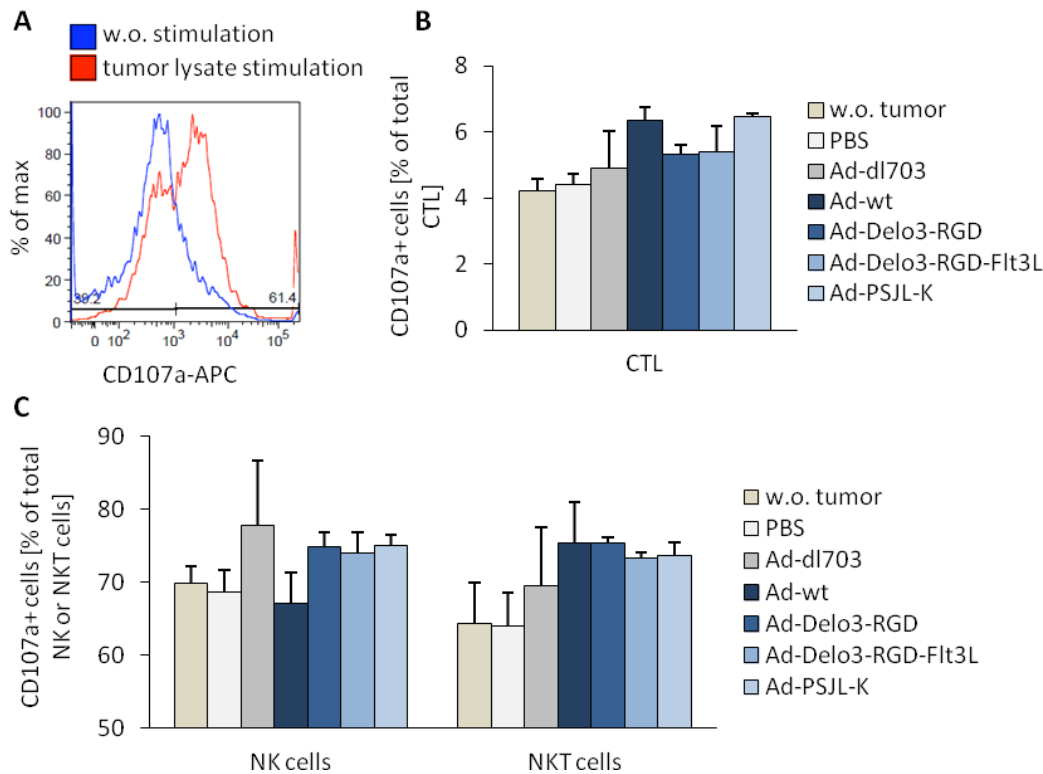


**Figure 3-24: Adenovirus-mediated degranulation of cytotoxic immune effector cells after stimulation with tumor cell lysate.** Splenocytes from virus treated tumor bearing mice and non-tumor bearing mice (w.o. tumor) were isolated 7 d after virus injection.  $2 \times 10^5$  freshly isolated splenocytes were stimulated with 20  $\mu$ L tumor cell lysate for 4 h at 37 °C with presence of monensin and anti-CD107a antibody. A. Splenocytes of Ad-Delo3-RGD injected tumor bearing mice were stimulated with tumor cell lysate (red) or left without stimulus (blue). Fluorescence intensity (APC) was analyzed by flow cytometric analysis and is indicated on a logarithmic scale (x-axis) against the percentage of the maximal cell count (y-axis). B, C. After stimulation and CD107a staining of splenocytes, they were in addition stained with immune cell population-specific antibodies (CD45, CD3, CD49b, CD8) and analyzed by flow cytometry. Results are depicted as CD107a positive cells in percentage of total CTL (CD45+/CD3+/CD49b-/CD8+) population (B) or NK cell (CD45+/CD49b+/CD3-) cell or NKT cell (CD45+/CD49b+/CD3+) populations (C). For C, the y-axis is displayed starting from 50% (mean $\pm$ SEM,  $n \geq 3$  mice per group,  $n(\text{w.o. tumor})=2$  mice per group).

The direct effector cell-mediated cytotoxicity towards the tumor cells was measured by application of a calcein assay (figure 3-22 C). KLN205 tumor cells were stained with the non-fluorescent dye calcein-AM, which is converted within living cells to fluorescent calcein. The effector cells, here the splenocytes were added to the stained KLN205 cells in different effector cell to target cell ratios. The release of the fluorescent dye from damaged tumor cells or the retention within cells with intact cell membranes can be measured. The effector-mediated cytotoxicity was calculated as described in the Materials and Methods section. Changes in cell-mediated toxicity were, as described in the literature, hard to identify in freshly isolated unstimulated effector cells (data not shown) (Schirmacher et al. 1979). Therefore, freshly isolated splenocytes were additionally cocultured with mitomycin C treated, growth arrested KLN205 tumor cells (Kuroda and Furuyama 1963, Schirmacher et al. 1979). After 5 d of coculture,

splenocytes were collected and subjected to a calcein-based cell-mediated cytotoxicity assay. The remaining calcein in the tumor cells gave more precise results as compared to the fluorescence measured in the supernatant of the assay cells (data not shown). E:T ratios of 1:1 showed cell lysis of around 0-10%, but with very high variability between animals (figure 3-25). The lysis potential of all splenocytes reached a relatively high level of 40% effector-mediated lysis, also in mice that had not seen tumor antigens before the coculture. The lysis was not augmented in tumor bearing animals or in animals treated with replication-deficient Ad-dl703 and wild type adenovirus. Cocultured splenocytes of Ad-Delo3-RGD-Flt3L treated mice showed the highest lysing potential with about 60% specific lysis by addition of 100 effector cells per target cell, which was about 1.5-fold the lysis observed for PBS treatment. The other oncolytic viruses Ad-Delo3-RGD and Ad-PSJL-K also showed markedly increased lytic activity with 52% and 54% effector-mediated lysis, respectively, which was a 1.2-fold increase as compared to PBS treatment. Therefore, despite the high, probably rather unspecific lysis, oncolytic virus treatment further enhanced the tumor cell killing, indicating a specific therapy-mediated anti-tumor effect. This effect was lower after Ad-wt treatment, correlating with the reduced efficacy of this vector concerning tumor growth reduction (figure 3-16), with the lower NK cell degranulation (figure 3-24 C), and with the reduced MHCI presentation (figure 3-13), but in contrast to the general immune stimulation (figures 3-18 to 3-24). Ad-Delo3-RGD-Flt3L, like observed for splenocyte IFN $\gamma$  release (figure 3-23) showed increased anti-tumor efficacy as compared to the reduced anti-virus efficacy (figure 3-20). In summary, oncolytic adenoviruses were able to trigger not only anti-virus, but also anti-tumor immune responses, which might have contributed to the reduced tumor growth observed after oncolytic virus treatment of tumors.

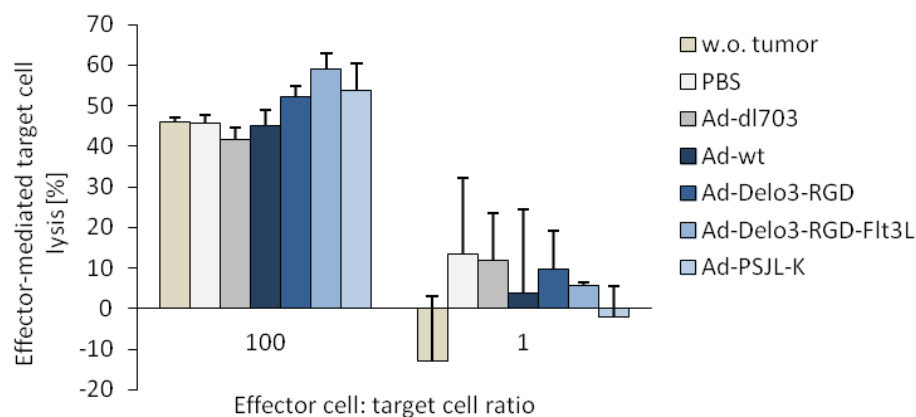


**Figure 3-25: YB-1-dependent oncolytic adenoviruses augment effector cell-mediated tumor cell cytotoxicity.** Freshly isolated splenocytes from tumor bearing mice treated with indicated viruses or PBS and non-tumor bearing mice (w.o. tumor) 7 d after virus treatment were cocultured with growth arrested tumor cells 25:1 in the presence of 100 U/mL IL-2 for 5d. These splenocytes were thereafter incubated with calcein-AM loaded tumor cells 100:1 and 1:1 and the retention of calcein was measured after a 4 h incubation. Percentage of effector-mediated target cell lysis is indicated and was calculated as stated in the Materials and Methods section (mean $\pm$ SEM, n=3-5 mice per group, n(w.o. tumor)=2 mice per group).

## 4. Discussion

### 4.1. Purity and quality of adenoviruses are crucial for their application as virotherapeutics

Current concepts to treat cancer are lacking efficacy due to cancer-associated resistance towards therapeutic regimens. Treatment resistance may be a consequence of changes in signal transduction, active removal of therapeutic agents, or tolerance against immune recognition, thus disabling therapeutic eradication of resistant tumor cells and hampering the whole therapeutic regimen (Gottesman et al. 2002). The oncogenic protein YB-1 is a prominent mediator of resistance formation and maintenance (Bargou et al. 1997, Stein et al. 2001, Wu et al. 2007). Oncolytic viruses that replicate specifically in YB-1 positive tumor cells represent promising new agents, because they specifically favor the targeting and destruction of cells that are not accessible by classical therapeutic regimens (Holm et al. 2004, Mantwill et al. 2006). Their YB-1 specificity makes the oncolytic viruses highly tumor-specific, which comes along with the low overall toxicity of adenoviral therapy (Liikanen et al. 2013, Rognoni et al. 2009). The use of oncolytic viruses might additionally help to overcome immunotolerance mechanisms evolved in the tumors by provision of danger signals and lysis-associated release of tumor antigens. The applicability of YB-1-dependent oncolytic adenoviruses and possible effects of YB-1-dependent oncolytic adenoviruses on immunotolerance and immune activation *in vitro* and *in vivo* were addressed in this work.

The first important requirement for the applicability of oncolytic adenoviruses in virotherapeutic approaches is the effective production of viruses in large amounts. Production of the viruses used within this thesis was very efficient. About 20,000-40,000 viral particles per cell were produced. These amounts lay within the reported range of successful virus production, which varies from  $10^4$  to  $10^5$  adenovirus particles per cell. For example bioreactor production by Kamen et al. using HEK293 cells in serum-free medium resulted in a production of 9400 VP and 3500 IFU per cell (Kamen and Henry 2004). Titers of all viruses within this thesis were high enough to use with at least  $2 \times 10^{11}$  IFU/mL, and VP to IFU ratios were reasonable for all produced viruses. Food and Drug Administration (FDA) guidelines necessitate that the ratio of total physical particles to infectious viral units does not exceed 30 VP/IFU for adenovirus preparations for use in clinical trials (Bauer 2000). Viruses used within this study all had VP/IFU ratios lower than or equal to 25. Further critical parameters for the application of adenoviruses in animals and humans are the homogeneity and purity of the production. Viruses produced for this study all had good quality concerning lack of aggregation and homogeneous size of the viral particles as investigated by

dynamic light scattering, and were pure as monitored by measurement of the optical density.  $OD_{260nm}/OD_{280nm}$  ratios ranged between 1.36 and 1.40 (table 3-1). Standard  $OD_{260nm}/OD_{280nm}$  values found in the literature for highly purified adenoviruses also range between 1.20 and 1.40 (Riske et al. 2013). Higher or lower ratios would indicate DNA or protein contamination, respectively. Vectors for application in mice were purified by two steps of CsCl gradient purification and in the following desalted via sephadex columns. Purification performed this way is save to be used in mice and indeed, no virus application-mediated acute reaction was observed, even not after repeated administration of the viruses.

The YB-1-dependent oncolytic adenoviruses used within this work are rendered tumor-specific by manipulation of the essential adenoviral *E1A* region. Ad-Delo3-RGD carries an 11 bp mutation, which results in lack of expression of the 289 aa *E1A* protein (Haley et al. 1984, Rognoni et al. 2009). Ad-PSJL-K has most of the viral *E1A* region deleted so that none of the *E1A* proteins can form. In both cases, the lack of *E1A* 289 aa results in a lack of viral replication in healthy cells. In tumor cells, in which the oncogenic factor YB-1 is overexpressed in the nucleus, but not in healthy cells, these adenoviruses can replicate based on a mechanism involving YB-1 binding to the *E2*-late promoter (Holm et al. 2002). During production of these *E1A*-mutant or *E1A*-deficient adenoviruses, residual viral *E1* region sequences can recombine with the inherent *E1* region of the producing cell line HEK293. The presence of *E1* in HEK293 cells is a prerequisite for production of all adenoviruses, because the inherent *E1* transcomplements the lack of *E1A* in replication-deficient viruses. However, homologous recombination can result in replication-competent adenoviruses (RCA), which represents a central challenge in the large scale production of adenoviruses for clinical application. Since safety is the key factor and a major concern in the application of natural products like viruses, the FDA limits RCA to less than one RCA per  $3 \times 10^{10}$  viral particles (Bauer 2000). In the present study, the occurrence of major RCA was excluded by PCR analysis of the *E1A* region. The PCR that confirms the lack of *E1A* CR3 was indeed negative for Ad-Delo3-RGD, Ad-Delo3-RGD-Flt3L, and Ad-PSJL-K, whereas it was positive for the wild type virus (figure 3-1). The PCR for the complete *E1A* gene resulted in clear thick bands for Ad-wt, Ad-Delo3-RGD, and Ad-Delo3-RGD-Flt3L. The *E1A* PCR should not result in any products for Ad-PSJL-K and Ad-dl703. However, faint bands were seen for both viruses. The question is whether this observation was a result of RCA, or whether the PCR was not completely specific. However, some facts rather support the lack of RCA in this case: PCRs were equally positive for Ad-PSJL-K and Ad-dl703, and the adjacent *E1B19K* region, as confirmed by the *E1B19K*-specific PCR was negative for both viruses. The CR3 PCR, in which the same reverse primer was used as in the PCR for the complete *E1A* gene, was completely negative for Ad-PSJL-K. It is not possible, that only parts of the *E1* gene, which lie within the deletion, have recombined into the adenoviral

viruses. Therefore, it is more likely, that the PCR gave false positive results due to unspecific primer binding. Other PCRs or expression analyses would be necessary to thoroughly exclude the generation of RCA. In addition to the *E1A* mutations, all other important mutations within the genomes of the oncolytic viruses, i.e. *E1B19K*, *E3gp19K*, and RGD, which are meant to improve virus spread, oncolytic efficacy and immune recognition, were verified by PCR (figure 3-1).

#### **4.2. Murine KLN205 cells express YB-1, can be infected by adenoviruses and allow viral particle formation *in vitro***

YB-1-dependent oncolytic adenoviruses have so far only been tested in human cell lines *in vitro* and in xenograft models *in vivo* focusing on the direct cytotoxic effect of YB-1-dependent adenoviral oncolysis (Holzmuller et al. 2011, Rognoni et al. 2009). However, these models do not take into account that the interaction between viruses and immune system may be important in a real *in vivo* situation in cancer patients (Liikanen et al. 2013). It was thus of interest to find a non-human cell line that could be used as a syngeneic *in vivo* model in succession. Several low immunogenic mouse cell lines and one Syrian hamster cell line, suitable for the use in syngeneic immunocompetent *in vivo* model systems, were tested in order to identify whether they can be infected by adenoviruses and whether they allow formation of new infectious viral particles *in vitro*. Next, cellular YB-1 expression was analyzed to find out whether the tested cells can serve as suitable models for YB-1-specific virotherapy. Infectability of non-human cells is hampered by the high species specificity of the human viruses depending on for example low expression of human adenovirus receptors like CAR in non-human cell lines (Tomko et al. 2000). Indeed, the analysis of infectability of the cells revealed that murine SCCVII, SMA560, and CT26 cells were hard to infect by adenoviruses at all, as assessed by infection with Ad-eGFP and flow cytometric and fluorescence microscopic analysis (figure 3-3). CMS-5 cells in contrast were very efficiently infectable. However, they were also very sensitive to adenovirus infection. They were killed by infection with replication-deficient viruses Ad-eGFP and Ad-dl703 already at relatively low MOI (chapter 3.2). Also others have reported a fast detachment of CMS-5 cells after infection with replication-deficient adenoviruses at MOIs at which standard human cell lines are still stably attached to the plate surface (Wirth 2009). Since CMS-5 cells were found to be very sensitive towards replication-deficient viruses, and infectious particles were found to be formed from replication-deficient adenoviruses in this cell line (figure 3-4), CMS-5 cells were not considered a suitable model to monitor replication- and virus propagation-related effects of tumor cell lysis. Besides CMS-5, also Syrian hamster HaK cells, as well as murine KLN205 and CMS-5 cells were sufficiently infectable by Ad-eGFP (figure 3-3). Although particle formation has been reported

to be impeded (Younghusband et al. 1979), about  $10^7$  IFU/mL were produced from Ad-wt in both Syrian hamster HaK cells and murine KLN205, 1000-10,000 times less than in human cells (figure 3-4). Regarding infectability and particle formation in HaK and KLN205 cells, both cell lines showed comparable results to other non-human cell lines in the literature that were considered adequate models for adenoviral oncolysis. One example are canine cells, in which  $10^4$ - $10^6$  IFU/mL adenoviruses were assessed after 4 d of infection (Ternovoi et al. 2005).

In terms of YB-1 expression all cell lines showed eligible results. YB-1 was predominantly found perinuclear in the cytoplasm in HaK and KLN205 cells, but also low amounts were present in the nucleus (figure 3-5 B). Nuclear YB-1 expression in HaK cells was even a bit higher than in HeLa cells and similar in KLN205 and HeLa cells. Due to the fact that HeLa cells allow sufficient priming of YB-1-dependent oncolysis (Mantwill et al. 2006), nuclear YB-1 expression in both non-human cell lines was supposed to be sufficient to allow viral E2-late promoter activation and oncolytic virus replication. Since HaK, as well as KLN205 cells, showed overall YB-1 expression that was comparable to human A549 cells, which are a very good model for adenovirus propagation (Glockzin et al. 2006), YB-1 should not represent the limiting factor for YB-1-dependent oncolysis in these models (figure 3-5 A). Stable transduction of the tested non-human cell lines with YB-1 did not result in superior tumor cell lysis as compared to eGFP transduced control cells, confirming the assumption that endogenous YB-1 expression in these cells is sufficient for YB-1-dependent oncolysis (data not shown).

Collectively, the non-human cell lines KLN205 and HaK were found to be equally suitable for the application of YB-1-dependent oncolytic adenoviruses with respect to infectability by adenovirus, adenovirus propagation, and YB-1 expression. After consideration of additional criteria like knowledge about immune cell populations as well as availability of assays and antibodies for mice versus Syrian hamster model systems, it was decided to perform all subsequent *in vitro* and *in vivo* experiments with KLN205 cells.

### **4.3. YB-1-dependent oncolytic viruses replicate in tumor cells and cause their lysis *in vitro***

YB-1-dependent oncolytic adenoviruses are able to replicate selectively in tumor cells with nuclear YB-1 expression due to mutations in the viral *E1A* region. Ad-Delo3-RGD is rendered tumor-specific by an 11 bp mutation in *E1A*, which results in lack of expression of the 289 aa E1A protein (Haley et al. 1984, Rognoni et al. 2009). Ad-PSJL-K has most of the viral *E1A* region deleted so that none of the E1A proteins can form. Since it was shown that YB-1 is present in KLN205 cells, even in low amounts in the nucleus (figure 3-5), YB-1-dependent viruses should be able to replicate in KLN205 cells and in succession form adenovirus particles and lyse the tumor cells. Indeed, replication of YB-1-dependent oncolytic adenoviruses was possible in KLN205 cells (figure 3-6 A). However, Ad-PSJL-K replication was 17-fold decreased as compared to Ad-wt infection and the replication of Ad-Delo3-RGD was about 10-fold less than of Ad-PSJL-K. In human A549 cells, replication of the tested oncolytic adenoviruses, namely Ad-Delo3-RGD and Ad-PSJL-K, resulted in only slightly decreased DNA amounts as compared to Ad-wt, but replication kinetics in oncolytic viruses were delayed by 1-2 d as compared to Ad-wt (figure 3-6 B). Moreover, Ad-PSJL-K replication started to increase slightly earlier than Ad-Delo3-RGD replication. The enhanced ability of Ad-PSJL-K to replicate in KLN205 cells and the earlier replication start in A549 cells, could be explained by the fact that for replication of Ad-Delo3-RGD, YB-1 has to be present in the nucleus of the cell (Holm et al. 2002), whereas Ad-PSJL-K over virus-independent expression of the tumor-specific YB-1 promoter-driven E4 region and CMV promoter-driven E1B55K expression can possibly transport YB-1 into the nucleus independently of viral replication.

Besides being able to efficiently replicate in hosts cells, the applicability of oncolytic adenoviruses is largely dependent on their capability to successfully form new infectious particles, in order to allow the spread of viral particles within the host and efficient host cell lysis. The ability of the oncolytic adenoviruses to form new infectious particles was reduced in contrast to Ad-wt in all examined cell lines, about 10-fold in KLN205 cells (figure 3-6 C). The differences in DNA replication between Ad-wt and oncolytic adenoviruses as well as between Ad-PSJL-K and Ad-Delo3-RGD in KLN205 cells were not reflected at the level of particle formation, possibly due to a limited number of particles that could be formed. This discrepancy in the efficacy of DNA replication versus particle formation might also depend on different starting concentrations of viruses and virus-specific differences regarding transcription, translation, and assembly of functional virus particles due to the alterations in the viral genomes. The difference in particle formation between Ad-wt and oncolytic viruses was even about 100-fold in human cell lines. In A549 cells, replication of oncolytic viruses was comparable to replication of Ad-wt, indicating that the reduced ability to

form new particles like in KLN205 cells might be a question of kinetics or of saturation. In HeLa cells, far less particles were formed from Ad-Delo3-RGD as compared to Ad-PSJL-K (100 times).

Efficient virus particle formation is an important prerequisite for oncolytic adenovirus-mediated host cell lysis. In order to monitor the efficacy of adenovirus-mediated oncolysis, SRB staining of surviving cells was performed. 2-5 times higher MOIs of YB-1-dependent oncolytic adenoviruses were needed to reach the same killing activity as after Ad-wt infection (figure 3-7). Ad-PSJL-K was slightly less potent in KLN205 as compared to Ad-Delo3-RGD (figure 3-7 A), as opposed to replication potential in KLN205 cells (figure 3-6 A). In A549 cells in contrast, Ad-PSJL-K was slightly more cytotoxic than Ad-Delo3-RGD (figure 3-7 B). In HeLa cells, as already seen for particle formation, Ad-Delo3-RGD was far less potent than Ad-PSJL-K (figure 3-7 C). In general, the reduced oncolytic performance of the YB-1-dependent viruses as compared to the wild type viruses can be explained by the multiple modifications in the YB-1-dependent oncolytic adenoviruses, for example by the deletion of *E1A* and thus the different ways of replication initiation. While wild type adenoviruses have naturally evolved for optimal host cell infection, replication, progeny formation, and spread, these functions might be impaired in the modified oncolytic adenoviruses. However, the mutations within the genome of the YB-1-dependent oncolytic adenoviruses are intended to counteract the derogated efficacy of oncolytic viruses. For example the deletion of the anti-apoptotic *E1B19K* gene, as in all used YB-1-dependent oncolytic adenoviruses has been shown to not only increase TNF $\alpha$ -enhanced cancer selectivity due to genetic blocks in apoptosis pathways in cancer cells, but also to counteract the attenuation of the virus. It has thus been shown to result in enhanced viral spread and oncolytic performance in tumor cells (Liu et al. 2004). Another way to enhance oncolytic virus performance is the insertion of an additional RGD sequence into the viral fiber knob, as implemented in all tested oncolytic adenoviruses. This mutation has been shown to enhance infection of tumor cells by increase of integrin-dependent cell entry even in cells with low CAR expression (Dmitriev et al. 1998, Kimball et al. 2010, Pesonen et al. 2012a). In Ad-Delo3-RGD, the *ADP* gene, which provides efficient host cell lysis and spread (Tollefson et al. 1996), is deleted. Thus for Ad-Delo3-RGD, the reduced cell lysis of human cell lines A549 and HeLa as compared to the other oncolytic vector Ad-PSJL-K could, at least in part, depend on the lack of the *ADP* gene. Consistently, Tollefson et al. found that virus mutants that lack *ADP* can replicate as well as wild type *ADP* viruses, but cell lysis and virus release from the cell is retarded (Tollefson et al. 1996). At the time point of the SRB assays performed in this thesis work, after 6 d, they found that *ADP* mutants have already caused the typical CPE with rounding up of A549 cells, but viruses have just begun to effectively lyse the cells (Tollefson et al. 1996). Thus, differences in cell lysis caused by Ad-Delo3-RGD might partly be due to the shift in lysis kinetics caused by the deletion of the *ADP* gene. Tollefson et al. furthermore



found that viral proteins were synthesized like for Ad-wt (Tollefson et al. 1996), but whether functional lytic virion assembly kinetics are changed was not addressed by this group and can not be taken into account as an explanation of reduced infectious particle numbers of Ad-Delo3-RGD in HeLa cells after 3 d. Moreover, Liu et al. found that combined deletion of *E1B19K* and the also anti-apoptotic region *E3B*, as in Ad-Delo3-RGD, was deleterious regarding cancer selectivity and viral efficacy (Liu et al. 2005b). In conclusion, tumor cell killing by oncolytic viruses was possible with sufficient efficacy, also in murine KLN205 cells, despite decreased replication and cell lysis potential of the oncolytic viruses as compared to Ad-wt *in vitro*. However, relatively high amounts of virus, about 200 IFU/cell for 50% lysis had to be applied.

#### **4.4. Oncolytic adenoviruses cause apoptosis and immunogenic cell death**

Regarding the application of YB-1-dependent oncolytic viruses *in vivo*, not only the replication efficacy and progeny formation of the viruses is important, but rather their ability to lyse cells (figure 3-7) and particularly the type of tumor death the viruses can trigger (Zitvogel et al. 2008a). Oncolytic adenoviruses have been reported to eradicate tumor cells by apoptosis (Boozari et al. 2010), autophagy (Ito et al. 2006), and additionally by ICD (Diaconu et al. 2012). The investigation of apoptosis was of special interest, since many of the deleted or manipulated genes within the YB-1-dependent oncolytic viruses play a role in induction or inhibition of apoptosis (*E1A*, *E1B19K*, *E3*). Ad-wt, Ad-Delo3-RGD, and Ad-PSJL-K showed the highest caspase-dependent cleavage activity of an artificial PARP-1 peptide as well as of the cellular PARP-1 protein, as measured 48 h after treatment by a fluorimetric caspase activity assay and by a WB assay, respectively (figure 3-8). In KLN205 cells, Ad-Delo3-RGD-mediated cell death was highest in both assays, closely followed by Ad-wt in the caspase activity assay, and followed by Ad-PSJL-K in the WB. Differences between both assays might result from different substrate availability of the artificial versus the cellular PARP1. Substrate availability was not assessed in the fluorimetric assay, whereas the uncleaved PARP1 is detected by the antibody as the upper band in the WB. As seen after Ad-PSJL-K infection, the concentration of uncleaved PARP1 was smaller, suggesting increased cleavage or decreased de novo expression of PARP1. In A549 cells, overall virus-elicited caspase activity was not very high. The cells might have different cell killing kinetics and killing did not occur in the assayed time frame. The fact that no caspase activity was observed after Ad-dl703 infection is explained by the actual lack of cell death induction by the replication-deficient virus (figure 3-7). Residual PARP1 cleavage was also observed for mock treated cells in the WB (figure 3-8 C) and can be attributed to cells that are dying without virus contribution. The increased apoptosis induction after oncolytic virus infection did probably result from the deletion

of the anti-apoptotic *E1B19K* gene, at least in part. The observed induction of apoptosis following Ad-Delo3-RGD infection reported here, has also been seen after Ad-Delo3-RGD infection in an *in vivo* xenograft glioma model (Holzmuller et al. 2011) and apoptosis has also been identified as the main mechanism of virus-mediated cell death for other oncolytic adenoviruses (Boozari et al. 2010).

Besides apoptosis, autophagy-related cell death is another mechanism, by which adenoviruses are able to induce cell death (Ito et al. 2006). Induction of autophagy following stress signals leads to the capture of intracellular components or pathogens into autophagosomes and to their delivery into lysosomes for degradation (figure 3-9 A). The amount of LC3-II correlates with the number of autophagosomes, however, LC3-II is degraded again later in the process of autophagy (Levy and Thorburn 2011). This fact makes interpretation of autophagy on the basis of LC3-II detection by WB analysis very complex even though it is one of the standard methods for assessment of autophagy (Klionsky et al. 2012, Mizushima and Yoshimori 2007). Within this study, no relevant virus-mediated accumulation of autophagosomes was observed in KLN205 cells as assessed by WB analysis of autophagy-related LC3 processing (figure 3-9 B). In A549 cells, lipidated LC3-II expression was highest in Ad-Delo3-RGD infected cells, indicating accumulation of autophagosomes. Accumulation of LC3-II could be either a consequence of upregulated autophagosome formation or of reduced autophagosome turnover. It needs to be considered however, that also the expression of LC3-I was highest for Ad-Delo3-RGD infected cells. Along the lines of the complexity of investigation of LC3 conversion, according to guidelines given by experts in autophagy research, the pattern of LC3-I to LC3-II conversion has been shown to be strongly dependent on the cell type (Klionsky 12). This fact was also observed for KLN205 and A549 cells within this work (figure 3-9 B). Moreover, changes in LC3 amounts can be hard to identify if LC3-II amounts are particularly low as seen here in A549 cells or particularly high as seen in KLN205 cells. Conversely, detectable LC3-II formation is not in any case sufficient evidence for autophagy and moreover, LC3-II can also associate with the membranes of non-autophagic structures, like for example apoptotic cell-containing phagosome membranes (Klionsky et al. 2012). Applying this knowledge to the results seen in figure 3-9 B, maybe a small induction of autophagy can be inferred for Ad-Delo3-RGD. Additional analyses of autophagy, e.g. electron microscopy, immunofluorescent monitoring of GFP-LC3 constructs, or WB analysis in the absence and presence of lysosomal protease or fusion inhibitors are required to be able to make a profound statement about induction of autophagy by oncolytic adenoviruses (Klionsky et al. 2012). Like seen in this study for Ad-Delo3-RGD (figure 3-9 B), many groups observe and induction of autophagy following oncolytic adenoviruses (Botta et al. 2012, Ito et al. 2006, Rodriguez-Rocha et al. 2011). However the consequences of autophagy induction by oncolytic adenoviruses are

discussed controversially. Botta et al. have observed that autophagy induction protects cells from virus-induced cell death. Autophagy in this case rather acts as a survival mechanism of the tumor cells following viral infection in order to inhibit virus-mediated cell death (Botta et al. 2012). Contrariwise, other groups claim that virus-mediated autophagy induction enhances viral replication (Rodriguez-Rocha et al. 2011) and tumor cell death (Ito et al. 2006). This can be probably explained by the fact that, if even upon autophagy induction cell survival can not be maintained, the cell is induced to die (Levine and Deretic 2007, Levy and Thorburn 2011). Adding to the complexity, Jiang et al. showed, that oncolytic adenovirus-induced autophagy can also trigger the extrinsic caspase pathway of apoptosis (Jiang et al. 2011). Induction of the extrinsic caspase pathway in the course of autophagy might be one of the reasons why induction of apoptosis was particularly high after infection with Ad-Delo3-RGD (figure 3-8), for which also autophagy induction was observed (figure 3-9 B). Thus, treatment with Ad-Delo3-RGD might be able to induce both apoptosis and autophagy at the same time. Others claim that oncolytic adenoviruses elicit a model of cell death that can not be characterized by one of the traditional models of cell death (Baird et al. 2008). Hence, it is not completely clear whether apoptosis or autophagy or a combination is important for virus-mediated cell death. Moreover, there is no stringent connection between the mode of cell death and therapeutic success in all cases (Galluzzi et al. 2012, Green et al. 2009).

Recently, the immunogenicity of dying cells has emerged as an additional criterion for classification of the different modes of cell death including apoptosis, autophagy and necrosis. The classical modes of cell death like apoptosis can, depending on the cell death stimulus, differentially induce exposure or secretion of ICD molecules and can in concert be either immunogenic or tolerogenic (Galluzzi et al. 2007). Therefore, exposure or release of these danger signals has been identified as the major discriminating factor in the distinction of immunogenic versus non-immunogenic modalities of cell death (Green et al. 2009). Consequently, induction of ICD results in immune cell recruitment *in vivo* and is thus highly associated with therapeutic success (Kroemer et al. 2013). The most important molecular factors associated with ICD are Hsps and CRT, which are exposed on the cell surface of dying cells during the early stages of ICD, and ATP and HMGB1, which are released from dying cells later in the process of ICD (Krysko et al. 2012). In the present study, treatment of KLN205 cells with adenoviruses augmented cell surface exposure of ICD parameters CRT and Hsp70 (figure 3-10). Only after Ad-Delo3-RGD infection the exposure of Hsp70 was reduced (figure 3-10 A). However, Hsp70 exposure following Ad-Delo3-RGD-Flt3L infection rather resembled mock infection (data not shown) and Hsp70 exposure was rather enhanced after Ad-Delo3-RGD infection of A549 cells (data not shown). Therefore, since analysis of Hsp70 surface exposure was only conducted once, this result may just

present an outlier. Surface exposure of Hsp70 and CRT was particularly high in Ad-wt infected cells, and surface exposure of Hsp70 was even higher in Ad-PSJL-K infected cells as compared to Ad-wt infected cells and also as compared to the 1  $\mu$ M MTX treated positive control.

Exposure of ICD-related DAMPs following chemotherapy, and especially cell surface recruitment of CRT during ICD, is induced by ER stress and subsequent phosphorylation of eIF2 $\alpha$  by PERK (Panaretakis et al. 2009). P-eIF2 $\alpha$  expression was enhanced after adenoviral infection, particularly after infection with Ad-wt (figure 3-11). These results are consistent with the observed CRT surface exposure (figure 3-10 B), suggesting an ER stress-dependent and P-eIF2 $\alpha$ -mediated activation of CRT also in the context of adenoviral infection. In accordance, oncolytic adenovirus-mediated induction of an ER stress response involving PERK and eIF2 $\alpha$  phosphorylation has been described earlier, even though CRT exposure was not addressed in this study (Boozari et al. 2010). Release of the ICD danger signals ATP and HMGB1 was also generally augmented after virus infection (figure 3-12). Release of ATP was highest from Ad-Delo3-RGD infected cells, followed by Ad-wt infected cells and also higher than release after 1  $\mu$ M MTX treatment of cells (figure 3-12 A). HMGB1 release from replication-competent or conditionally replicating adenoviruses was markedly enhanced as compared to replication-deficient Ad-dl703 (figure 3-12 B). Release was highest from Ad-wt infected cells, followed closely by Ad-PSJL-K infected cells and Ad-Delo3-RGD infected cells. This graduation of HMGB1 release concentrations after virus infection implies a replication or at least lysis dependency of HMGB1 release. Both ATP and HMGB1 release were within the range observed by others after adenoviral treatment *in vitro* (Diaconu et al. 2012).

The overall results of ICD molecule exposure and release are astonishing, since oncolytic adenoviruses were far less potent in lysing tumor cells as compared to wild type adenoviruses (figure 3-7). Still, exposure or release of ICD parameters after oncolytic virus infection was almost as high as after Ad-wt infection, or even higher depending on the respective molecule (figures 3-10 and 3-12). This might be due to the fact that the modes of cell death were differentially induced due to the alterations in the adenoviral genome (figures 3-8 and 3-9). Presence of all ICD parameters indicates immune induction and therapeutic success *in vivo* (Green et al. 2009, Kroemer et al. 2013, Zitvogel et al. 2008b). However, the analysis of parameters in this work showed that not all parameters were simultaneously up- or downregulated for the same virus, which is in accordance with differences observed for other therapeutic treatment modalities (Kroemer et al. 2013). Still, most danger molecules typical for ICD were exposed or released after infection with YB-1-dependent oncolytic adenoviruses *in vitro*, suggesting immunogenic apoptosis as the main tumor cell death mechanism triggered by YB-1-dependent oncolytic adenoviruses.

#### 4.5. YB-1-dependent oncolytic adenoviruses do not suppress immunogenicity of tumor cells by downregulation of cellular MHCI expression and IFN signaling

It is known, that tumors suppress presentation of self antigens by interfering with MHCI-mediated antigen presentation (Cavallo et al. 2011), for example by downregulation or functional impairment of the immunoproteasome subunits LMP2 and LMP7 (Heink et al. 2006, Igney and Krammer 2002). This suppression of MHCI-mediated antigen presentation leads to impaired tumor antigen presentation, making tumor cells difficult to be recognized by the immune system. The multifunctional immune activating cytokine IFN $\gamma$  is involved in the upregulation of antigen processing and MHCI cell surface presentation by Stat1-mediated expression of IFN-stimulated genes like the exclusive immunoproteasome subunits (Zhou 2009). In order to test the immunogenicity of the used tumor cells, MHCI cell surface expression was analyzed, as a measure of efficient tumor antigen presentation. MHCI cell surface expression was still detectable on the tested cell lines with different levels of MHCI cell surface exposure depending on the cell line (figure 3-13). Low concentrations of IFN $\gamma$  could further upregulate the expression of MHCI in KLN205 and HeLa cells, and IFN $\gamma$ -mediated upregulation of MHCI occurred in a concentration-dependent manner, at least in KLN205 cells (figure 3-13 A). Also adenoviruses have been shown to suppress MHCI regulation in terms of immune escape via their *E1A* and *E3gp19K* gene products. *E1A* interferes with viral antigen presentation on MHCI by inhibition of IFN $\gamma$  signaling (Leonard and Sen 1996) and by downregulation of at least two of the three exclusive immunoproteasome subunits, LMP2 and MECL1 (Berhane et al. 2011, Chatterjee-Kishore et al. 2000). *E3gp19K* inhibits peptide presentation on MHCI by retargeting of MHCI to the ER (Rawle et al. 1989, Sester et al. 2013) and thereby inhibits CTL-mediated target cell lysis (Rawle et al. 1989). Indeed, Ad-wt, carrying the complete *E1A* and the complete *E3gp19K* gene was efficient in inhibition of MHCI surface expression of KLN205 cells (figure 3-13 B,C). As expected, Ad-Delo3-RGD and Ad-PSJL-K, both of which have either a mutation or deletion of the *E1A* gene and additionally both a deleted *E3gp19K* gene, were not able to downregulate expression of MHCI on tumor cells, which is in accordance with the above described findings from the literature (Berhane et al. 2011, Chatterjee-Kishore et al. 2000, Leonard and Sen 1996, Sester et al. 2013). Cellular MHCI presentation could still be enhanced by IFN $\gamma$  application after infection with Ad-Delo3-RGD and Ad-PSJL-K in contrast to after infection with Ad-wt. The ability to increase MHCI surface exposure by addition of IFN $\gamma$  was limited after Ad-Delo3-RGD treatment though, which could be due to the presence of the complete *E1A* 243 aa protein in contrast to Ad-dl703 and Ad-PSJL-K, confirming that presence of *E1A* inhibits IFN $\gamma$  signaling (Leonard and Sen 1996) and IFN $\gamma$ -mediated antigen presentation via the immunoproteasome (Berhane et al. 2011, Chatterjee-Kishore et al. 2000).

As seen in Ad-dl703 infected cells, already the deletion of *E1A* seems to be sufficient to disable adenovirus-mediated downregulation of MHC I. Since E3gp19K inhibits target cell lysis by immune cells (Rawle et al. 1989), deletion of the immunosuppressive *E3gp19K* gene should have negative influence on viral propagation *in vivo* due to enhanced clearance of viruses by the immune system. Surprisingly, *E3gp19K* deletion showed increased viral replication *in vivo*, although the mechanisms behind this observation are not understood so far (Rawle et al. 1989, Wang et al. 2003).

IFN $\gamma$  signaling, which is involved in MHC I-associated antigen presentation, can be inhibited by viral E1A by inhibition of Stat1 expression (Leonard and Sen 1996). It is surprising, that even without administration of IFN $\gamma$ , Stat1 phosphorylation and dimerization was very prominent also in mock infected cells (figure 3-14). Dimerization has been reported to be maintained by deficient phosphatase activity or by maintenance of parallel oriented P-Stat1 dimers (Mertens et al. 2006). Adenoviruses have also been shown to inhibit Stat1 dephosphorylation, resulting in constitutively activated Stat1 signaling (Sohn and Hearing 2011). As expected, P-Stat1 expression was markedly reduced in *E1A* gene positive Ad-wt infected KLN205 cells and also after Ad-Delo3-RGD and Ad-PSJL-K infection. This is consistent with the findings that E1A suppresses IFN $\gamma$  signaling via downregulation of Stat1 (Leonard and Sen 1996). It is also consistent with the downregulation of MHC I antigen presentation after Ad-wt infection in KLN205 cells and the reduced ability of IFN $\gamma$ -mediated upregulation of MHC I exposure after Ad-Delo3-RGD infection as discussed before (figure 3-13). Infection with replication-deficient adenoviruses resulted in the same cellular P-Stat1 expression as in mock infected cells (figure 3-14), which can be explained by the lack of the *E1A* gene in this virus. Thus, at least in theory, IFN $\gamma$ -mediated immune activation and MHC I-dependent presentation of viral and tumor antigens should still be possible on the surface of tumor cells after infection with the here used YB-1-specific oncolytic adenoviruses, in contrast to many other oncolytic adenoviral systems in research that mostly express the full *E1A* gene (Boozari et al. 2010, Diaconu et al. 2012). Still it is difficult to predict whether efficient immune activation is possible by MHC I-dependent presentation of tumor and virus antigens *in vivo*, or whether antigen presentation is successfully suppressed by tumor cells. In this case, efficient antigen presentation would only be possible as a result of oncolytic adenovirus-mediated target cell lysis and subsequent release of tumor antigens.

#### **4.6. YB-1-dependent oncolytic adenoviruses reduce tumor growth in immunocompetent mice**

Oncolytic adenoviruses are used as efficient anti-cancer agents. They have been shown to reduce tumor growth *in vivo*, either by direct tumor cell lysis (Holzmuller et al. 2011) or by acting in concert with the immune system (Boozari et al. 2010, Prestwich et al. 2009). In the immunocompetent KLN205 tumor model, oncolytic adenoviral therapy has been shown to slow down tumor growth and to even reduce tumor sizes in combination with immune stimulation after multiple injections of the viruses (Edukulla et al. 2009). However, multiple injections were expected to enhance anti-virus immunity rather than anti-tumor immunity (de Gruijl and van de Ven 2012). Therefore, a single injection of one of the YB-1-dependent oncolytic adenoviruses Ad-Delo3-RGD, Ad-Delo3-RGD-Flt3L, or Ad-PSJL-K, or the replication-deficient Ad-dl703 or wild type Ad-wt as controls was administered to KLN205 tumors that grew from tumor cells injected into the flanks or syngeneic DBA/2 mice (figure 3-15). The influence of a second virus injection was tested in a small subset of mice. Variations in the growth of tumors observed within this study (chapter 3.7) are an issue that can have an immense influence on the growth curve results and also the different positions of the tumors within the flank determine the outcome of the tumor. Tumor microenvironments are known to play an important role in tumor formation and growth. For example the distance to vessels and the resulting kinetics of new vessel formations play important roles in ability of tumor growth, but also for immune cell infiltration (Egeblad et al. 2010). Hence, the difference in growth characteristics and tumor positions can in part explain why differences between virus treatment groups were hard to obtain but differences in each treatment group were very prominent. Tumors grew undifferentiated in all groups (figure 3-17), which is a sign for high aggressiveness of tumors (Brabletz 2012) and reached 7-8 times their starting volume (day 0) within the 28 d of the experiment (figure 3-16). Tumor growth was slightly slowed down after treatment with oncolytic viruses, especially in Ad-Delo3-RGD treated mice. About half the mice injected with PBS only had to be excluded from the experiment during these 28 d due to tumor sizes, ulcerations, or signs of morbidity. Besides PBS treated tumors, also tumor growth in Ad-wt treated animals was higher than after oncolytic adenovirus treatment. This could, at least in part, be explained by the downregulation of MHC1 expression in tumor cells after Ad-wt infection (figure 3-13), so that Ad-wt infected tumor cells would be protected from recognition by the immune system.

In tumors of all groups, necrotic areas were seen within the tumor mass (figure 3-17 A), a phenomenon that is often accompanying rapid tumor growth (Grivennikov et al. 2010, Zong and Thompson 2006). There was no evidence that adenoviral infection of tumors caused direct major

tumor cell lysis (figure 3-17). Since even *in vitro*, relatively high concentrations of adenoviruses had to be applied to reach sufficient cell killing in the murine KLN205 cells (figure 3-7), comparably low virus amounts that could be retained within the tumor may be a possible explanation why efficacy of YB-1-dependent virotherapy was limited in this model *in vivo*. One has to consider that generally higher viral amounts are needed due to fast clearance even after intratumoral injection of viruses *in vivo* (de Gruijl and van de Ven 2012). Thus maybe the adenovirus amounts applied here, under consideration of toxicity of extremely high virus concentrations, were too low to elicit sufficient initial killing of KLN205 cells.

#### **4.7. Treatment of tumors with YB-1-dependent oncolytic adenovirus triggers immune cell recruitment**

Inflammatory immune reactions are commonly elicited by adenoviruses (Thaci et al. 2011) and have also been reported after oncolytic adenoviral treatment of tumors (Woller et al. 2011). As seen in the KLN205 tumors within this work, the rims of the tumor at the tumor-host interface were highly infiltrated with inflammatory immune cells (figure 3-17 B). These immune cells constituted mainly macrophages as observed by IHC staining (figure 3-17 E). Inflammatory immune cell infiltration at the rims of the tumors was seen in all treatment groups, also in PBS treated mice and is no virus-mediated effect. Inflammations at the tumor-host interface can be caused in this case by the artificial implantation of the tumor, but is also a common phenomenon at the interfaces between tumor and tumor bed in established tumors or during tumorigenesis (Grivennikov et al. 2010). These inflammatory immune cells, mostly macrophages, can have a tumor-suppressive effect by mediating antigen presentation and cytokine release, but are mostly associated with tumor promotion due to triggering of immunosuppression, angiogenesis, invasion, and metastasis (Condeelis and Pollard 2006, Grivennikov et al. 2010). After treatment with Ad-wt or oncolytic viruses but not with Ad-dl703 or PBS, foci of inflammation were seen within the tumors (figure 3-17 C,D). Cells within these inflammatory infiltrates had the typical nuclear morphology of granulocytes and moreover, no macrophage infiltration was observed within the central tumor mass (figure 3-17 F). Granulocytes, mostly neutrophils within the tumor can play both anti-tumor and tumor-promoting roles, depending on their differentiation status and the presence of transforming growth factor  $\beta$  (TGF $\beta$ ) (Fridlender et al. 2009). Tumor-suppressive neutrophils can directly promote cytolysis or regulate CTL responses against the tumor (Grivennikov et al. 2010). Occurrence of tumor inflammation has been reported by others following application of adenoviral therapy and has been associated with virus-mediated danger



signaling for the immune system and in consequence success of the oncolytic adenovirus treatment (Woller et al. 2011).

The question arose whether oncolytic adenoviruses can attract immune cells into the tumor via either their immunogenic nature or via tumor cell killing, which might be immunogenic. Consequently, the attracted immune cells should then be able to attack and eradicate the tumor cells. A prerequisite for immune cell attraction into tumors is the recruitment of immune cells into the blood and the spleen (Takeichi et al. 2012). The recruitment of immune cells as assessed by spleen weights and blood leukocyte counts was elevated after oncolytic viral treatment starting 7 d after treatment (figure 3-18). Immune cell recruitment was strongest after Ad-wt, Ad-PSJL-K, and Ad-dl703 treatment of tumors with spleen weights and leukocyte counts comparable to results observed by other groups after oncolytic adenoviral treatment (Bernt et al. 2005, Edukulla et al. 2009). In spleens, activation after virus treatment was sustained and even enhanced 28 d after treatment. Concerning the recruitment of distinct immune cell populations, Ad-wt and Ad-PSJL-K treatment of tumor bearing mice induced strong recruitment of all analyzed immune cell populations, including DCs and T cells (figure 3-19). DCs and T cells are highly associated with success of virotherapeutic treatments (Diaconu et al. 2012, Edukulla et al. 2009). T cell recruitment was particularly high after Ad-PSJL-K infection, suggesting therapeutic efficacy of this vector as seen by slightly reduced tumor sizes as compared to Ad-wt or PBS treatment (figure 3-16). NK cells and NKT cells were also recruited into the blood by Ad-wt and Ad-PSJL-K, but also by Ad-dl703 (figure 3-19). However, even though some reports claim an association of NK cell recruitment and therapeutic success (Alvarez-Breckenridge et al. 2012a, Choi et al. 2011), others report that NK cells rather enhance viral clearance and thereby hamper the success of oncolytic virotherapy (Alvarez-Breckenridge et al. 2012a, Alvarez-Breckenridge et al. 2012b). B cell recruitment was mainly caused by Ad-wt infection. The contribution of B cells to virotherapy is discussed controversially. In the context of glioma therapy, B cells have been shown to be indispensable for T cell-mediated anti-tumor activity (Candolfi et al. 2011). Others see no B cell activation despite therapeutic success (Diaconu et al. 2012). The immunostimulatory cytokine Flt3L is reported to trigger *in vivo* expansion of DCs, T cells, as well as of NK cells and B cells (Maraskovsky et al. 1996, Matsumura et al. 2008, McKenna et al. 2000), also as a transgene in adenoviral virotherapy (Edukulla et al. 2009). However, no additional DC and T cell recruitment was observed after Ad-Delo3-RGD-Flt3L treatment of tumors as compared to Ad-Delo3-RGD. B cell, NK cell, and NKT cell recruitment was indeed slightly enhanced by the additional Flt3L transgene. Immune stimulation, mainly concerning anti-viral immunity after Ad-Delo3-RGD-Flt3L treatment is discussed in more detail in chapter 4.8.

#### **4.8. Adenoviral treatment elicits high anti-virus immune responses**

Adenoviruses are highly immunogenic and are able to stimulate multiple arms of the immune system: They elicit potent innate and adaptive, humoral and cellular immune reactions that are targeted to eliminate the viral infection (de Gruijl and van de Ven 2012, Thaci et al. 2011). Intratumoral injection of wild type adenovirus and conditionally replicating oncolytic adenoviruses within this work confirmed this high immunogenicity on humoral and cellular level (figure 3-20). Already after a single virus injection into tumors of naive mice, high humoral as well as cellular anti-viral responses were observed (figure 3-20 A). Concerning the humoral response, most virus-specific antibodies were produced against Ad-Delo3-RDG, more than against wild type adenovirus and Ad-PSJL-K. The antibody response against Ad-dl703 was weaker than against replicating viruses, which is in accordance with findings from others (Woller et al. 2011). Out of all tested oncolytic adenoviruses Ad-Delo3-RGD-FIt3L was the only exception, which triggered even lower virus-specific antibody responses than Ad-dl703. Possible reasons for this observation are discussed in the next passage. Since antibody formation against adenoviruses is primarily directed against viral capsid proteins (Bradley et al. 2012), the diminished amount of antibodies against Ad-dl703 might be a sign for decreased presence of Ad-dl703 as a consequence of decreased replication and progeny formation. Concerning the cellular anti-virus defense, as expected, no increase in adaptive T cell responses was seen 3 d after virus treatment of mice. 7 d after viral injection into tumor bearing mice, a high number of splenocytes released IFN $\gamma$  following stimulation with the viral DBP peptide (figure 3-20 C). The degree of overall virus-elicited immune responses, as analyzed by ELISpot assay was for most viruses as high as observed after stimulation with PMA and ionomycin, which served as positive controls. Moreover, found immune responses were comparable to IFN $\gamma$  responses towards oncolytic adenoviruses observed by others (Gurlevik et al. 2010). Virus antigen stimulation did not trigger an effective IFN $\gamma$  response in splenocytes from mice treated with the replication-defective adenovirus Ad-dl703, in contrast to virus antigen stimulation of splenocytes from mice treated with replicating or conditionally replicating adenoviruses. Therefore, IFN $\gamma$  secretion by virus antigen-specific splenocytes seemed to depend on the replication of or the lysis mediated by the respective adenoviruses. The finding that highest IFN $\gamma$  responses were observed to Ad-wt indicates that in fact replication of the viruses is required to induce effective IFN $\gamma$  responses.

The markedly impaired humoral as well as cellular immune response towards Ad-Delo3-RGD-Flt3L as compared to the Flt3L transgene-free virus Ad-Delo3-RGD and also as compared to all other viruses (figure 3-20) were not expected, because Flt3L is usually described as an efficient stimulator of the immune response (Wang et al. 2005), including the immune response towards viral vectors carrying Flt3L as a transgene (Edukulla et al. 2009). Moreover, B cell levels in the blood were rather increased after Ad-Delo3-RGD-Flt3L treatment as compared to Ad-Delo3-RGD treatment, while T cell levels decreased very slightly (figure 3-19). To understand this unexpected result, functionality of the secreted mFlt3L and *in vitro* DC expansion would be required to be tested for the secreted transgene product. However, at least *in vitro*, mFlt3L was efficiently released from Ad-Delo3-RGD-Flt3L infected murine KLN205 and human A549 control cells (figure 3-2) with concentrations comparable to observation of other groups in similar *in vitro* settings (Lee et al. 2006, Zhu et al. 2012). Chavan et al. see a lack of anti-viral antibodies and CD8+ T cell responses from modified vaccinia viruses expressing Flt3L, whereas other transgenes like GM-CSF provided this effect (Chavan et al. 2006). However, the sole lack of functional expression from the otherwise not significantly altered viruses in contrast to Ad-Delo3-RGD or Ad-PSJL-K is not sufficient to explain the decline in anti-viral responses following Ad-Delo3-RGD-Flt3L administration. Also, there was no hint concerning impeded functionality of the viruses considering other than anti-viral immune responses as for example immune cell recruitment (figures 3-18 and 3-19) or anti-tumor efficacy (figures 3-23 to 3-25). Hence, expression of the Flt3L transgene might also actively reduce anti-viral responses, whereas anti-tumoral responses are maintained. This would be a beneficial aspect concerning problems with vector clearance and with unfavorably balanced anti-virus to anti-tumor immune responses, which are frequently observed in adenoviral therapy (de Gruijl and van de Ven 2012). To my knowledge, a reduction in anti-viral responses upon administration of Flt3L has never been observed in the context of adenoviral therapy before. However, in the context of vaccination, several groups have observed a negative influence of Flt3L administration on humoral and cellular antigen-specific responses. They see impeded immune responses after transcutaneous (Baca-Estrada et al. 2002) or oral (Viney et al. 1998) vaccination and hypothesize that immature DCs in the skin or mucosa, which are recruited by intraperitoneally administered Flt3L, might limit harmful immune responses and induce antigen tolerance. Kwon et al. showed that naked virus antigen DNA vaccination coadministered intramuscularly at the same site and time with Flt3L plasmid suppressed anti-virus antibody responses despite DC activation (Kwon and Park 2002). This is a scenario that resembles the intratumoral injection of virus armed with the Flt3L transgene so that indeed Ad-Delo3-RGD-Flt3L could trigger DC-mediated anti-viral tolerance but likely without influence on anti-tumor immunity.

Already a single adenoviral injection elicited high anti-viral responses (figure 3-20). One of the emerging questions in this context is whether multiple adenoviral administrations are favorable or detrimental concerning oncolytic viral performance. Generally, secondary injections function like booster vaccine injections and lead to more rapid neutralization by the enhanced virus-specific immune response (de Gruijl and van de Ven 2012). Also in this work, a second virus injection into tumor bearing animals 7 d after the first one had the effect of a boost vaccination and highly augmented recruitment of antibodies against all used viruses (figure 3-20 B). An influence on anti-tumor efficacy was however not observed (chapter 3.7). Despite the increase in anti-viral responses, many groups use multiple injections of virus in different intervals to promote therapeutic effects (Boozari et al. 2010, Diaconu et al. 2012, Edukulla et al. 2009, Lee et al. 2006). A method to enable multiple applications of the virus without major increase of anti-viral immune response is the use of heterologous boost-prime regimes. In heterologous boost-prime regimens adenoviruses are applied in combination with other agents like nucleic acids, proteins, or vectors from other viruses (Liu 2010). Additionally, adenoviruses of different serotypes can be used for the priming and for the boosting step (de Gruijl and van de Ven 2012). Even minor changes in the capsids of oncolytic adenoviruses, i.e. application of an unmodified virus, a virus with a RGD motif in the fiber knob, or a virus with the fiber knob from another adenoviral serotype has been shown to result in circumvention of neutralization of the second adenovirus (Raki et al. 2011). This would be a strategy worth testing in the future, since the effort of using an oncolytic YB-1-dependent adenovirus with peptide insertion and one without is minimal and this change might increase therapeutic efficacy.

Moreover, to prevent vector clearance and to favor anti-tumor responses, anti-viral immune responses are often tried to be directly impeded. Notably, the selective replication of a telomerase-specific oncolytic adenovirus alone has been shown to decrease anti-viral innate and adaptive immunity and systemic adenovirus-mediated toxicity in mice (Gurlevik et al. 2010). Additionally, anti-viral immune responses can be impeded by multiple ways of improved delivery and virus shielding (Doronin et al. 2009, Green et al. 2004, Kim et al. 2011a, Thorne et al. 2006), or by general immunosuppression for example by cyclophosphamide (CPA). CPA has been shown to reduce anti-viral cytokine transcription and improve oncolysis (Wakimoto et al. 2004). Nevertheless, it is discussed controversially whether reduction of anti-viral responses is favorable at all or whether high anti-viral immunogenicity rather results in high anti-tumor immune responses. Prestwich et al. describe the situation between benefit and harm of the immune response towards oncolytic virotherapy as a “can’t live with it, can’t live without it” situation that can enhance viral clearance and can in contrast augment anti-tumor efficacy (Prestwich et al. 2009).

#### 4.9. Oncolytic adenovirus treatment enhances anti-tumor immune responses

Oncolytic adenovirus infection reasonably reduced tumor growth *in vivo* (figure 3-16). Whether reductions were caused by direct cytolysis or by immune-mediated effects is not entirely clarified, yet. Other groups reported that limitations of tumor growth can be at least partly attributed to immune-mediated tumor cell killing (Boozari et al. 2010, Diaconu et al. 2012). *In vitro*, apoptosis was identified as important contributor to the cell killing by YB-1-dependent oncolytic adenoviruses (figure 3-8). Moreover, dying cells exposed or released the most important proteins typical for ICD (figures 3-10 and 3-12). The role of ICD in treatment with oncolytic adenoviruses has not been thoroughly investigated so far. However, the immunogenicity of dying tumor cells has been shown to be crucial for chemotherapy (Apetoh et al. 2008), but is gaining more and more attention in the context of virotherapy as well (Boozari et al. 2010, Diaconu et al. 2012). Presence of all ICD parameters indicates immune induction and therapeutic success *in vivo* (Kroemer et al. 2013, Zitvogel et al. 2008b). The two DAMPs ATP and HMGB1 are released from dying cells in the later stages of ICD and are said to trigger DC migration, activation, antigen presentation, and cytokine release (Apetoh et al. 2007, Ghiringhelli et al. 2009, Kroemer et al. 2013). In this study, release of ATP and HMGB1 were measured from serum samples by a luminescence-based ATP assay and by an HMGB1 ELISA, respectively. The release of both ATP and HMGB1 varied strongly between the animals of each group (figure 3-21). This observed *in vivo* variation in the released ICD-related molecules might be the reason, why these parameters are mostly analyzed *in vitro* only (Diaconu et al. 2012, Michaud et al. 2011). Nevertheless, mean serum ATP concentrations were elevated after treatment with Ad-wt or any of the oncolytic viruses (figure 3-21 A). The concentrations were highest for Ad-PSJL-K treatment and consistently with the *in vitro* results also for Ad-Delo3-RGD treatment (figure 3-12 A). Additionally, treatment of tumors with Ad-PSJL-K led to high serum levels of ATP, even though values for Ad-PSJL-K were highly variable (figure 3-21 A). The higher release of ATP after treatment with oncolytic viruses as compared to Ad-wt is consistent with the reduced tumor growth (figure 3-16). The presence of ICD-related DAMPs in the tumor microenvironment or serum shortly after induction of a therapy usually implies therapeutic success. However, ATP, like all other DAMPs has multiple functions, some of which are also contributing to tumor progression and metastasis as well as resistance to anti-cancer therapy (Krysko et al. 2013). Extracellular ATP regulates not only the cell migration of DCs (Elliott et al. 2009, la Sala et al. 2002), but also the migration of cancer cells (Zhang et al. 2010) and may thereby contribute to cancer invasion and metastasis (Krysko et al. 2013). Moreover, extracellular ATP can stimulate cell proliferation (Ryu et al. 2003), can be a source of immunosuppressive adenosine (Krysko et al. 2012, Krysko et al. 2013), and can at low concentrations assist cell survival (Wei et al. 2013). Prolonged release of low amounts of ATP

induces deficient DC maturation and diminishes the ability of mature DCs to induce certain immune responses (la Sala et al. 2001, la Sala et al. 2002). The concentration of extracellular ATP is generally an important determinant of the effect of ATP. Whereas human physiological concentrations of extracellular ATP (1-50 nM) do not affect activated T cells, higher ATP concentrations have a bimodal effect on activated T cells. In contrast to 250 nM extracellular ATP that stimulates T cell proliferation and cytokine release, 1 mM inhibits activated CD4<sup>+</sup> T cell functions and stimulates immunosuppressive regulatory T cell (Treg) proliferation (Trabanelli et al. 2012). In this thesis work, average serum ATP concentrations of about 1.5  $\mu$ M were reached, which, in the case that human and mouse situations would be comparable, would rather indicate a scenario of general T cell activation. The second factor that is released from dying cells and is crucial for the immunogenicity of dying cells is HMGB1 (Apetoh et al. 2007). In order to analyze whether treatment with YB-1-dependent oncolytic adenoviruses resulted in the release of HMGB1 *in vivo*, HMGB1 serum levels were measured by ELISA. Mean HMGB1 serum concentrations were highest after Ad-wt treatment (figure 3-21 B), consistent with the high *in vitro* increase of HMGB1 release of KLN205 cells (figure 3-12 B). Serum HMGB1 concentrations were also elevated after Ad-Delo3-RGD-Flt3L treatment and were lowest after treatment with Ad-dl703 (figure 3-21 B). However, in comparison to PBS treatment, only a slight increase was observed after adenoviral treatment, maybe also due to the high variability in HMGB1 serum levels between animals within each group. The presence of HMGB1 has been associated with several effects besides immunostimulatory effects. For instance, extracellular HMGB1 has been shown to enhance tumor tissue invasion, tumor regrowth, and metastasis formation of cancer cells that have survived chemotherapy (Luo et al. 2013). Furthermore, HMGB1 interaction with T cell Ig domain and mucin domain 3 (TIM-3) on tumor-associated DCs has been shown to decrease anti-tumor immune responses (Chiba et al. 2012). The various functions of HMGB1 can, at least in part, be explained by mutually exclusive redox states of the protein, which make HMGB1 either a chemoattractant, or a proinflammatory cytokine, or a protein without any immunostimulatory properties (Venereau et al. 2012). Redox state distribution of released HMGB1 proteins can be analyzed by liquid chromatography, tandem mass spectrometry, or electrophoretic mobility of HMGB1 in the presence and absence of DTT (Venereau et al. 2012). This could also be an interesting option in the present study to be able to further predict the value of oncolytic virus-mediated HMGB1 release.

Concerning a possible ICD-mediated attraction of immune cells, ATP release was found to be highly increased after Ad-PSJL-K treatment *in vivo* (figure 3-21 A), which is in accordance with high numbers of DCs in the blood after Ad-PSKL-K treatment (figure 3-19) and with the reported ATP-mediated stimulation of DC migration (Elliott et al. 2009, Kroemer et al. 2013). Ad-Delo3-RGD-induced ATP release *in vitro* and *in vivo* (figures 3-12 A and 3-21 A), however, was not reflected by increased recruitment of DCs (figure 3-19). Moreover, HMGB1, which activates DCs and T cells, was highly released after Ad-wt infection *in vitro* and *in vivo* and after Ad-PSJL-K infected cells *in vitro* (figures 3-12 B and 3-21 B), which was in concert with the high numbers of DCs and T cells in the blood after treatment with Ad-wt and Ad-PSJL-K (figure 3-19). Collectively, these findings suggest that YB-1-dependent virotherapy is able to induce ICD in tumor cells and that the suggested connection between ICD and immune cell recruitment is also valid in the context of YB-1-dependent virotherapy.

Efficient virotherapy has shown to initially lyse tumor cells, but in an immunocompetent setting mainly to trigger an immune reaction against the tumor cells that mediates tumor destruction (Boozari et al. 2010, Choi et al. 2011). Following recognition of their cognate antigens, activated cytotoxic cells, mostly CTLs secrete cytokines and kill their target cells by secretion of cytotoxic effector molecules like FasL, perforin, and granzymes (Sanderson et al. 2012, Tau et al. 2001). Several aspects of anti-tumor reactivity of the splenocytes isolated from oncolytic virus treated tumor bearing mice have been investigated in this study. Splenocytes were tested for their ability to secrete IFN $\gamma$  following antigen stimulation, to show degranulation-mediated release of cytotoxic effector molecules, or to directly lyse tumor cells (figure 3-22). IFN $\gamma$  release following *ex vivo* stimulation of splenocytes was elevated in splenocytes of mice treated with YB-1-specific adenoviruses (figure 3-23). IFN $\gamma$  responses were not very high even after treatment, but were comparable to results seen by others after injection of oncolytic adenoviruses as monotherapies in low immunogenic tumor cell models (Choi et al. 2011) like the KLN205 cell model (Woller et al. 2011). If higher *ex vivo* results are desired, antigen-specific immune responses can be artificially enhanced by application of systems that incorporate the use of MHC I model antigens like ovalbumin or hemagglutinin (Edukulla 09). IFN $\gamma$  release from KLN205 tumor cell lysate-stimulated and hTert tumor peptide-stimulated splenocytes was strongest in Ad-PSJL-K treated animals and particularly low in PBS treated animals (figure 3-23). IFN $\gamma$  release after stimulation with tumor cell lysate was generally a bit higher as compared to tumor peptide stimulation, which is probably caused by the heterogeneous antigen mix in the lysate, which triggers immune responses more sensitively but less selectively.

The degranulation of immune effector cells could be stimulated by *ex vivo* tumor cell lysate stimulation (figure 3-24 A). In CTLs isolated from mice after viral treatment, the percentage of CD017a positive cells following tumor cell lysate stimulation was augmented in comparison to CTLs of PBS treated animals (figure 3-24 B), particularly after Ad-wt and Ad-PSJL-K treatment. This observed high degranulation in CTLs after Ad-wt and Ad-PSJL-K treatment was in concert with enhanced recruitment of various immune cell populations, mainly DCs and T cells, which are crucial for therapeutic success, after treatment with these viruses (figures 3-18 and 3-19). Results are furthermore in accordance with the increased IFN $\gamma$  release after Ad-PSJL-K treatment (figure 3-23). NK cell CD107a surface expression was also enhanced after virus treatment with all viruses except for Ad-wt (figure 3-24 C). Finally, also NKT cell surface expression of CD107a was augmented after virus treatment of animals with particularly high cell surface expression levels for replication-competent or conditionally replicating oncolytic viruses. These results were consistent with findings from other groups, who have reported that combined stimulation with the strong immune stimulants PMA and ionomycin results in comparable cell surface expression of CD107a in CTLs and NK cells (Kruschinski et al. 2008, Ratto-Kim et al. 2012). This implies that the KLN205 tumor antigens themselves present quite potent immune stimuli, and that adenovirus treatment of KLN205 tumor bearing animals results in efficient degranulation of isolated splenocytes upon tumor antigen stimulation, at least in this *ex vivo* scenario.

No changes in effector cell-mediated toxicity were seen without *ex vivo* stimulation of the splenocytes, as assessed by a calcein assay (chapter 3.11.2). This observation has also been described by others (Schirmacher et al. 1979) and most researches perform cocultures of splenocytes with tumor cells to enhance the anti-tumor cytotoxicity of the effector cells (Choi et al. 2011, Lee et al. 2006, Schirmacher et al. 1979), even if this represents a rather artificial enhancement of anti-tumor activity. After coculture, the tumor cell lysis potential of all splenocytes was on a relatively high level, also that of splenocytes isolated from mice that had not seen tumor antigens before the coculture (figure 3-25). These findings might indicate a high general activation of the splenocytes following IL-2 stimulation or following tumor cell contact. Cell lysis might have also occurred unspecifically and high resulting so called "specific" cell lysis might be a calculation-dependent artifact due to differences in conditioned versus non-conditioned medium in the null control. Unspecific signals can also be due to calcein release without a cell lysis event, even though the calcein assay was reported to be as stable in signal retention and selective effector-mediated signal release as the  $^{51}\text{Cr}$  release assay (Neri et al. 2001). Due to safety reasons concerning a non-radioactive assay and positive reports though, the calcein assay was favored over the  $^{51}\text{Cr}$  assay. Still, lysis was markedly augmented by addition of cocultured splenocytes from Ad-Delo3-RGD, Ad-Delo3-RGD-Flt3L and Ad-PSJL-K treated mice as



compared to splenocytes from PBS treated mice. These findings imply that the observed increase of splenocyte-mediated tumor cell lysis by 10-20% was directly mediated by the particular, treatment-specific splenocytes and that oncolytic viruses were able to specifically trigger lysis of tumor cells in this *ex vivo* setting. The fact that Ad-wt treatment did not trigger as high tumor cell lysis as the oncolytic viruses is in contrast to the above mentioned stimulation of anti-tumor responses, the high ICD parameter release and the high immune cell recruitment (figures 3-18 to 3-24). However, tumor growth was enhanced (figure 3-16), and MHCII presentation was reduced (figure 3-13) upon treatment with Ad-wt, suggesting that Ad-wt treatment is able to stimulate the immune system, but that Ad-wt-induced downregulation of antigen presentation prevents the recognition of tumor cells by the immune system.

Ad-PSJL-K in contrast has been shown to be able to lyse tumor cells *in vitro* (figure 3-7) and to upregulate all tested ICD parameters *in vitro*, particularly Hsp70 and HMGB1 (figures 3-10 and 3-12) and *in vivo* ATP (figure 3-21). It elicited *in vivo* anti-tumor immune responses as depicted mainly by augmentation of IFN $\gamma$  secretion (figure 3-23) and effector cell degranulation (figure 3-24). Also Ad-Delo3-RGD-Flt3L triggered enhanced IFN $\gamma$  release by immune cells (figure 3-23) and even increased tumor cell lysis by splenocytes isolated from Ad-Delo3-RGD-Flt3L treated mice after coculture (figure 3-25). Especially if results of active reduction of anti-viral immune responses by the Flt3L transgene can be confirmed (figure 3-20), the insertion of the Flt3L transgene into the Ad-PSJL-K genome could present a promising strategy to reduce anti-viral immune response together with triggering of a strong anti-tumor activity.

#### **4.10. Future prospects of oncolytic adenoviral therapy**

Adenoviral therapy alone showed only limited anti-tumor efficacy, as observed in this study and also observed by other groups (Boozari et al. 2010, Woller et al. 2011). The existing direct tumor lysis and the limited anti-tumor immunity are not sufficient to allow effective use of YB-1-dependent virotherapy as single therapy in a weakly immunogenic tumor system like the here employed KLN205 model. Low immunogenicity of tumor cells might also be problematic in the future use of YB-1-dependent virotherapy in clinical practice, facing tumors with naturally highly evolved self immunotolerance (Cavallo et al. 2011, Hanahan and Weinberg 2011). Therefore, the application of animal models with higher immunogenicity for studying the interplay of oncolytic viruses and immune system *in vivo* might be a feasible approach. The use of so called humanized mice might represent a promising alternative to completely non-human systems (Shultz et al. 2012). For the construction of humanized mice, the mice are first rendered immunodeficient and are subsequently engrafted with human primary hematopoietic cells and tissues in order to establish a functional human immune system. The use of humanized mice therefore allows the application of human tumors, in which adenoviral replication and particle formation is much more efficient and closer to the situation found in the natural human host environment than in foreign murine host cells. Despite good progress during the last years, several practical limitations still exist that limit the application of such models to distinct scenarios. These limitations include the lack of human growth factors and of human leukocyte antigen (HLA) molecule expression, problems in lymph node development, the remaining murine innate immune system, and impaired affinity maturation and class-switching of antibodies. Many of these limitations have been addressed in selected humanized mice so far, but models have to be carefully chosen according to the specific application (Macchiarelli et al. 2005, Shultz et al. 2012). The challenge in the choice of an appropriate model is that all arms of the immune system crucial for analysis of the experiments need to be present. In a complex *in vivo* approach consisting of tumor implantation, virus injection, anti-viral and anti-tumoral immunity, including innate and adaptive, cellular and humoral immune interactions, choice or construction of the right humanized model would be a complex challenge. Humanized mice are thus not suitable for the study of immune-aided oncolytic virotherapy yet, but in theory, with further development, would be an ideal approach to study the use of human tumors with human immune environment.

Still, the application of YB-1-dependent oncolytic virotherapy in the existing KLN205 cell model was able to reduce tumor tolerance and to trigger anti-tumor immunity to some degree, possibly by induction of parallel viral and tumor antigen presentation, by viral danger signals like viral nucleic acids, and by induction of ICD parameters. Moreover, oncolytic virotherapy possibly

enhanced tumor cell antigen release by cell killing and induction of inflammatory reactions. All these factors represent very important prerequisites for successful therapy of cancer and therefore, oncolytic adenoviruses can be ideally used in combination therapies. One approach that has proven to be very effective in this context is the combination of virotherapy and DC vaccination. In this experimental concept, isolated DCs are cultured *ex vivo*, stimulated with TLR ligands, and loaded with tumor antigens. DCs are then reinjected into tumor bearing mice with the same genetic background, in combination with virotherapeutic treatment of the tumors (Woller et al. 2011). DC vaccination alone is potentially effective in anti-tumor therapy, but shows very low response rates, so that only a fraction of patients profits from this regimen (Cintolo et al. 2012, Palucka et al. 2011, Rosenberg et al. 2004). Combination therapy reduced anti-viral antibody responses as compared to virotherapy alone and efficiently induced anti-tumor immune effects, tumor reduction, and even reduction of uninfected lung metastases. Efficiency of presentation of phagocytosed antigens by DCs is dependent on the presence of TLR activating ligands within the phagosome (Blander and Medzhitov 2006) and thus only the close interaction of viral TLR stimulating agents and tumor antigens, as observed upon virus infection and lysis of tumor cells, enables efficient tumor antigen presentation. As a consequence, oncolytic adenovirus treatment leads to very effective engulfment and crosspresentation of tumor antigens on the surface of APCs, thus overcoming the established tumor immunotolerance. In addition, virus-mediated inflammation and intratumoral replication of viral DNA have been shown to present an important stimulus for triggering of a strong immune response directed against the tumor, whereas efficient generation of infectious viral progeny was dispensable (Woller et al. 2011). Besides combination of virotherapy with DC vaccination, virotherapy has been combined with other therapeutic approaches like adoptive T cell transfer (Rommelfanger et al. 2012), or cDNA vaccination (Bridle et al. 2010, Kottke et al. 2011) to achieve synergistic or at least additive anti-tumor effects.

In conclusion, YB-1-dependent virotherapy was able to provide all prerequisites, such as effective tumor cell infection, induction of inflammation, as well as initial immune cell recruitment and anti-tumor immune responses, which have been identified to be important for successful application of all these combinatory approaches. However, since virus propagation and host cell lysis were not comparable in murine versus human cells, the real impact of immune responses on YB-1-dependent oncolytic virotherapy and the efficacy of the therapy in humans can only be assumed. Better models need to be established in order to get a more precise notion of the mode of action of YB-1-specific oncolytic adenoviruses as well as the distinct contribution of adenoviral oncolysis and adenovirus-mediated immune stimulation to the therapeutic outcome *in vivo*.

## 5. Appendix

### A. Epitope sequences for the YB-1 N-terminus-specific antibody

The marked N-terminal aa 1-12 sequence of the YB-1 protein plus terminal C was used for immunization for production of the polyclonal rabbit anti-YB-1 antibody used within this thesis.

Human YB-1 protein sequence (324 aa, after UniProtKB/Swiss-Prot: P67809)

**MSSEAETQPPA**APPAAPALSAADTKPGTTGSGAGSGGPGGLTSAAPAGGDKKVIATKVLGTVKWFNVRNGY  
GFINRNDTKEDVVFVHQTAIKKNNPRKYLRSVGDGETVEFDVVEGEKGAEEANVTGPGGVPVQGSKYAADRNH  
YRRYPRRRGPPRNYQQNYQNSESGEKNEGSESAPEGQAQRRPYRRRRFPPYMRPYGRRPQYSNPPVQGE  
VMEGADNQGAGEQGRPVRQNMRYGYRPRFRRGPPRQRQRPREDGNEEDKENQGDDETQGGQPPQRRYRRNF  
FNRRRRPENPKPQDGKETKAADPPAENSSAPEAEQGGAE

Murine YB-1 protein sequence (322 aa, after UniProtKB/Swiss-Prot: P62960)

**MSSEAETQPPA**APAAALSAADTKPGSTGSGAGSGGPGGLTSAAPAGGDKKVIATKVLGTVKWFNVRNGYGF  
INRNDTKEDVVFVHQTAIKKNNPRKYLRSVGDGETVEFDVVEGEKGAEEANVTGPGGVPVQGSKYAADRNHYR  
RYPRRRGPPRNYQQNYQNSESGEKNEGSESAPEGQAQRRPYRRRRFPPYMRPYARRPQYSNPPVQGEV  
MEGADNQGAGEQGRPVRQNMRYGYRPRFRRGPPRQRQRPREDGNEEDKENQGDDETQGGQPPQRRYRRNF  
NYRRRRPENPKPQDGKETKAADPPAENSSAPEAEQGGAE

N-terminal aa sequences and UniProtKB/Swiss-Prot numbers of YB-1 proteins from other species

Rabbit Q28618: **MSSEAETQPPA**APPAAPALSAAEKTP...  
Rat P62961: **MSSEAETQPPA**APAAALSAADTKPGS...  
Neat P67808: **MSSEAETQPPA**APPAAPALSAADTKP...  
Guinea pig B5AB13: **MSSEAETQPPA**APPTAPALSAADTKP...

### B. Predicted sizes of PCR fragments

**Table A-1: Predicted sizes of PCR fragments.**

Virus/PCR	E1A	E1A CR3	E1B19K	E3	RGD
Ad-dl703	-	-	-	1248 bp	-
Ad-wt	1044 bp	548 bp	587 bp	1248 bp	-
Ad-Delo3-RGD	1033 bp	-	378 bp	-	173 bp
Ad-Delo3-RGD-Flt3L	1033 bp	-	378 bp	1394 bp	173 bp
Ad-PSJL-K	-	-	-	646 bp	173 bp

## Abbreviations

”	Inch
°C	Degree Centigrade
A	Ampere
Å	Ångström
aa	Amino acid
Ac-DEVD-amc	Acetyl-Asp-Glu-Val-Asp-7-amino-4-methylcoumarin
ADP	Adenovirus death protein
Ad-wt	Wild type adenovirus
AM	Acetoxymethyl
AP	Activator protein
APC	Antigen-presenting cell
APC	Allophycocyanin
APS	Ammonium persulfate
ATCC	American type culture collection
Atg	Autophagy-related protein
ATP	Adenosine 5' -triphosphate
Bak	Bcl-2 homologous antagonist killer
Bax	Bcl-2-associated X protein
BCA	Bibinochoninic acid
Bcl-2	B-cell lymphoma 2
bp	Base pair
BSA	Albumin bovine fraction V
Ca <sup>2+</sup>	Calcium
CAR	Coxsackie virus and adenovirus receptor
CD(X)	Cluster of differentiation (X=number)
cdc25a	Cell division cycle 25 homolog a
CHX	Cycloheximide
CMV	Cytomegalovirus
CO <sub>2</sub>	Carbon dioxide
CPA	Cyclophosphamide
CPE	Cytopathic effect
CR	Conserved region
CRT	Calreticulin
CsCl	Cesium chloride
ct	Cycle threshold
CTL	Cytotoxic T lymphocyte
Cy	Cyanine
d	Day
Da	Dalton
DAB	3,3'-Diaminobenzidine
DAMP	Damage-associated molecular pattern
DBP	DNA binding protein
DC	Dendritic cell
DMEM	Dulbecco's Modified Eagle's Medium

## Abbreviations

---

DMSO	Dimethyl sulfoxide
DNA	Deoxyribonucleic acid
dNTPs	Deoxynucleoside triphosphate
ds	Double-stranded
DTT	Dithiothreitol
E:T	Effector cell to target cell
E1-4	Adenovirus early region 1-4
EDTA	Ethylenediaminetetraacetic acid
eF	eFluor
eGFP	Enhanced green fluorescent protein
eIF2 $\alpha$	Eukaryotic translation initiation factor 2 subunit $\alpha$
ELISA	Enzyme linked immunosorbent assay
ELISpot	Enzyme linked immuno spot assay
ER	Endoplasmic reticulum
ERK	Extracellular signal-regulated kinase
EtBr	Ethidium bromide
FACS	Fluorescence-activated cell sorting
FasL	Fas ligand
FBS	Fetal bovine serum
FDA	Food and Drug Administration
FITC	Fluorescein isothiocyanate
Flt3L	FMS-like tyrosine kinase-3 ligand
g	Gravitational field strength
g	Gram
G	Gauge
GAF	Gamma-interferon activation factor
GM-CSF	Granulocyte macrophage colony-stimulating factor
GV-SOLAS	Gesellschaft für Versuchstierkunde
h	Hour
H&E	Hematoxylin and eosin
H <sub>2</sub> O	Water
H <sub>2</sub> O <sub>2</sub>	Hydrogen peroxide
HCl	Hydrochloric acid
HLA	Human leukocyte antigen
HMGB1	High mobility group box 1 protein
HNSCC	Head and neck squamous cell carcinoma
HRP	Horseradish peroxidase
Hsp	Heat-shock protein
HSV-1	Herpes simplex virus 1
hTert	Human telomerase reverse transcriptase
ICC	Immunocytochemistry
ICD	Immunogenic cell death
IF	Immunofluorescence
IFN	Interferon
IFU	Infectious Units
Ig	Immunoglobulin

## Abbreviations

---

IHC	Immunohistochemistry
IL	Interleukin
iNOS	Inducible nitric oxide synthase
IRF	Interferon regulatory factor
ISGF	IFN-stimulated gene factor
kb	1000 base pairs
L	Liter
L1-4	Adenovirus late region 1-4
LC3	Light chain 3 protein
LMP	Low molecular mass polypeptide
m	Meter
M	Molar (mol/L)
MAPK	Mitogen-activated protein kinases
MDR1	Multidrug resistance gene 1
MECL1	Multicatalytic endopeptidase complex-like 1
MEM	Minimum Essential Medium
MFI	Median fluorescence intensity
mFlt3L	Murine Fms-like tyrosine kinase-3 ligand
MgCl <sub>2</sub>	Magnesium chloride
MHCI	Major histocompatibility complex class I
min	Minutes
MIP-1a	Macrophage inflammatory protein 1alpha
mM	Millimolar (mmol/L)
MOI	Multiplicity of infection
mRNA	Messenger ribonucleic acid
MRP1	Multidrug resistance related protein 1
MTX	Mitoxantrone
MxA	Myxovirus resistance protein A
NaCl	Sodium chloride
NEAA	Non-essential amino acids
NFκB	Nuclear factor 'κ-light-chain-enhancer' of activated B cells
NK cells	Natural killer cells
NKT cell	Natural killer T cell
NO	Nitric oxide
OD	Optical density
orf	Open reading frame
P-	Phospho-
PAA	Polyacrylamide
PAGE	Polyacrylamide gel electrophoresis
PARP	Poly ADP-ribose polymerase
PBS	Phosphate-buffered saline
PCR	Polymerase chain reaction
PdI	Polydispersity index
PDT	Photodynamic therapy
PE	Phycoerythrin
PE	Phosphatidylethanolamine

## Abbreviations

---

PerCP	Peridinin chlorophyll protein
PERK	Protein kinase RNA-like endoplasmic reticulum kinase
PFA	Paraformaldehyde
PI3K	Phosphoinositide 3-kinase
PKR	RNA-activated protein kinase
PMA	Phorbol 12-myristate 13-acetate
pRb	Retinoblastoma protein
PS	Penicillin and streptomycin
PVDF	Polyvinylidenfluorid
RANTES	Regulated on activation, normal T cell expressed and secreted
RCA	Replication-competed adenoviruses
RDB	Resistant to daunoblastin
RGD	Arginine-glycine-aspartic acid
RNA	Ribonucleic acid
ROS	Reactive oxygen species
rpm	Revolutions per minute
RPMI	Roswell Park Memorial Institute
RSK	Ribosomal S6 kinase
RT	Room temperature
SDS	Sodium dodecyl sulfate
sec	Second
SEM	Standard error of the mean
SRB	Sulforhodamine B
Smad3	SMA (giving the small phenotype in <i>C. elegans</i> )/mothers against decapentaplegic homology 3
Stat	Signal transducer and activator of transcription
TAE	Tris acetate EDTA buffer
TBS	Tris-buffered saline
TCA	trichloroacetic acid
TEMED	Tetramethylethylenediamine
TGF- $\beta$	Transforming growth factor beta
TierSchG	Tierschutzgesetz
TIM-3	T-cell immunoglobulin domain and mucin domain 3
TLR	Toll-like receptor
TMB	3,3',5,5'-Tetramethylbenzidine
TNF	Tumor necrosis factor
TRAIL	Tumor necrosis factors-related apoptosis-inducing ligand
Treg	Regulatory T cell
U	Unit
UniProt	Universal Protein Resource Knowledgebase
UV	Ultraviolet
V	Volt
VA RNAI	Virus-associated RNA molecule I
VP	Viral particles
WB	Western blot
YB-1	Y-box binding protein 1



## Figures

Figure 1-1: Adenovirus assembly. ....	10
Figure 1-2: Adenoviral gene functions. ....	12
Figure 1-3: Concept of tumor specificity of YB-1-dependent adenoviruses. ....	18
Figure 1-4: Therapy-induced induction of ICD elicits potent anti-tumor immune responses. ....	23
Figure 1-5: Interference of adenoviral proteins with anti-viral immune response and cell death	26
Figure 2-1: Mutations in YB-1-dependent oncolytic adenoviruses. ....	43
Figure 3-1: The amplified adenoviruses contain the expected mutations. ....	63
Figure 3-2: Ad-Delo3-RGD-Flt3L effectively releases its transgene Flt3L into the supernatant of infected cells. ....	64
Figure 3-3: Murine KLN205 and CMS-5 cell, as well as Syrian hamster HaK cells are infectable by human adenoviruses. ....	65
Figure 3-4: HaK, KLN205, and CMS-5 cells are able to form infectious progeny. ....	67
Figure 3-5: Cell lines all have efficient YB-1 expression to allow YB-1 dependent adenoviral activity. ....	68
Figure 3-6: YB-1-dependent oncolytic adenoviruses replicate in murine and human tumor cells and form infectious progeny. ....	70
Figure 3-7: YB-1-dependent oncolytic viruses lyse murine and human tumor cells. ....	71
Figure 3-8: Replicating adenoviruses trigger apoptosis in murine and human tumor cells. ....	74
Figure 3-9: No major induction of autophagic activity after infection with adenoviruses. ....	76
Figure 3-10: Adenovirus injection stimulates tumor cell surface exposure of ICD parameters Hsp70 and CRT. ....	77
Figure 3-11: Adenoviruses induce an ER stress response involving phosphorylation of eIF2 $\alpha$ . ....	78
Figure 3-12: Adenoviral treatment is able to elicit release of the ICD parameters ATP and HMGB1. .....	79
Figure 3-13: YB-1-dependent oncolytic adenoviruses do not downregulate MHCI surface exposure in contrast to Ad-wt. ....	81
Figure 3-14: Ad-wt downregulates P-Stat1 expression. ....	82
Figure 3-15: Schematic depiction of <i>in vivo</i> experiments. ....	83
Figure 3-16: Reduced tumor growth after oncolytic virotherapy. ....	85
Figure 3-17: Treatment with replicating adenoviruses triggers infiltration of tumors by innate immune cells. ....	86
Figure 3-18: Adenovirus-mediated increase in spleen weight and blood leukocyte counts. ....	88
Figure 3-19: Adenoviruses, especially Ad-wt and Ad-PSJL-K, trigger recruitment of DCs and immune effector cells. ....	89
Figure 3-20: Replicating adenoviruses trigger efficient humoral and cellular host anti-virus responses. ....	91
Figure 3-21: Adenoviral therapy with replicating viruses elicits release of ICD parameter ATP and HMGB1 <i>in vivo</i> . ....	92
Figure 3-22: Schematic overview over analysis of anti-tumor immune responses. ....	93
Figure 3-23: Ad-PSJL-K treatment augments the anti-tumor immune response. ....	94
Figure 3-24: Adenovirus-mediated degranulation of cytotoxic immune effector cells after stimulation with tumor cell lysate. ....	96
Figure 3-25: YB-1-dependent oncolytic adenoviruses augment effector cell-mediated tumor cell cytotoxicity. ....	97

## Tables

Table 1-1: Overview of selected currently tested virotherapeutics. ....	8
Table 1-2: Summary of important oncogenic roles of nuclear YB-1 as a transcription factor. ....	16
Table 2-1: Laboratory equipment. ....	29
Table 2-2: Software and web portals. ....	31
Table 2-3: Consumables. ....	31
Table 2-4: Chemicals. ....	33
Table 2-5: Commercially available buffers, standards, and other biochemical substances. ....	34
Table 2-6: Prepared buffers and solutions. ....	35
Table 2-7: Kits. ....	36
Table 2-8: Enzymes. ....	36
Table 2-9: Cytokines. ....	38
Table 2-10: Primer sequences. ....	38
Table 2-11: Antibodies. ....	39
Table 2-12: Cell culture media and supplements. ....	40
Table 3-1: Adenoviruses have ideal physical conditions to be used. ....	62
Table A-1: Predicted sizes of PCR fragments. ....	123

## Bibliography

- Aghi M, Martuza RL (2005) Oncolytic viral therapies - the clinical experience. *Oncogene* 24(52): 7802-7816
- Ahn M, Lee SJ, Li X, Jimenez JA, Zhang YP, Bae KH, Mohammadi Y, Kao C, Gardner TA (2009) Enhanced combined tumor-specific oncolysis and suicide gene therapy for prostate cancer using M6 promoter. *Cancer Gene Ther* 16(1):73-82
- Aktas E, Kucuksezer UC, Bilgic S, Erten G, Deniz G (2009) Relationship between CD107a expression and cytotoxic activity. *Cell Immunol* 254(2):149-154
- Alemanly R, Balague C, Curiel DT (2000) Replicative adenoviruses for cancer therapy. *Nat Biotechnol* 18(7):723-727
- Alter G, Malenfant JM, Altfeld M (2004) CD107a as a functional marker for the identification of natural killer cell activity. *Journal of immunological methods* 294(1-2):15-22
- Altomonte J, Marozin S, Schmid RM, Ebert O (2010) Engineered newcastle disease virus as an improved oncolytic agent against hepatocellular carcinoma. *Mol Ther* 18(2):275-284
- Alvarez-Breckenridge CA, Yu J, Kaur B, Caligiuri MA, Chiocca EA (2012a) Deciphering the Multifaceted Relationship between Oncolytic Viruses and Natural Killer Cells. *Adv Virol* 2012:702839
- Alvarez-Breckenridge CA, Yu J, Price R, Wojton J, Pradarelli J, Mao H, Wei M, Wang Y, He S, Hardcastle J, Fernandez SA, Kaur B, Lawler SE, Vivier E, Mandelboim O, Moretta A, Caligiuri MA, Chiocca EA (2012b) NK cells impede glioblastoma virotherapy through NKp30 and NKp46 natural cytotoxicity receptors. *Nat Med* 18(12):1827-1834
- Amgen. Amgen Announces Top-Line Results Of Phase 3 Talimogene Laherparepvec Trial In Melanoma ([http://www.amgen.com/media/media\\_pr\\_detail.jsp?releaseID=1798143](http://www.amgen.com/media/media_pr_detail.jsp?releaseID=1798143), Access Date: 7/19/2013)
- Andersson M, Paabo S, Nilsson T, Peterson PA (1985) Impaired intracellular transport of class I MHC antigens as a possible means for adenoviruses to evade immune surveillance. *Cell* 43(1):215-222
- Apetoh L, Ghiringhelli F, Tesniere A, Obeid M, Ortiz C, Criollo A, Mignot G, Maiuri MC, Ullrich E, Saulnier P, et al (2007) Toll-like receptor 4-dependent contribution of the immune system to anticancer chemotherapy and radiotherapy. *Nat Med* 13(9):1050-1059
- Apetoh L, Tesniere A, Ghiringhelli F, Kroemer G, Zitvogel L (2008) Molecular interactions between dying tumor cells and the innate immune system determine the efficacy of conventional anticancer therapies. *Cancer research* 68(11):4026-4030
- Baca-Estrada ME, Ewen C, Mahony D, Babiuk LA, Wilkie D, Foldvari M (2002) The haemopoietic growth factor, Flt3L, alters the immune response induced by transcutaneous immunization. *Immunology* 107(1):69-76
- Baird SK, Aerts JL, Eddaoudi A, Lockley M, Lemoine NR, McNeish IA (2008) Oncolytic adenoviral mutants induce a novel mode of programmed cell death in ovarian cancer. *Oncogene* 27(22):3081-3090
- Balachandran S, Barber GN (2004) Defective translational control facilitates vesicular stomatitis virus oncolysis. *Cancer Cell* 5(1):51-65
- Barbas CF, 3rd, Burton DR, Scott JK, Silverman GJ (2007) Quantitation of DNA and RNA. *CSH Protoc* 2007:pdb ip47
- Bargou RC, Jurchott K, Wagener C, Bergmann S, Metzner S, Bommert K, Mapara MY, Winzer KJ, Dietel M, Dorken B, Royer HD (1997) Nuclear localization and increased levels of transcription factor YB-1 in primary human breast cancers are associated with intrinsic MDR1 gene expression. *Nat Med* 3(4):447-450
- Barlan AU, Griffin TM, McGuire KA, Wiethoff CM (2011) Adenovirus membrane penetration activates the NLRP3 inflammasome. *Journal of virology* 85(1):146-155

- Basaki Y, Hosoi F, Oda Y, Fotovati A, Maruyama Y, Oie S, Ono M, Izumi H, Kohno K, Sakai K, Shimoyama T, Nishio K, Kuwano M (2007) Akt-dependent nuclear localization of Y-box-binding protein 1 in acquisition of malignant characteristics by human ovarian cancer cells. *Oncogene* 26(19):2736-2746
- Basler M, Kirk CJ, Groettrup M (2013) The immunoproteasome in antigen processing and other immunological functions. *Curr Opin Immunol* 25(1):74-80
- Basu S, Binder RJ, Ramalingam T, Srivastava PK (2001) CD91 is a common receptor for heat shock proteins gp96, hsp90, hsp70, and calreticulin. *Immunity* 14(3):303-313
- Bauer S (2000) Adenovirus Vector Titer Measurements and RCA Levels. FDA Gene Therapy Letter ([http://www.fda.gov/ohrms/dockets/ac/01/briefing/3768b1\\_01.pdf](http://www.fda.gov/ohrms/dockets/ac/01/briefing/3768b1_01.pdf))
- Baumgarth N, Roederer M (2000) A practical approach to multicolor flow cytometry for immunophenotyping. *Journal of immunological methods* 243(1-2):77-97
- Bell CW, Jiang W, Reich CF, 3rd, Pisetsky DS (2006) The extracellular release of HMGB1 during apoptotic cell death. *Am J Physiol Cell Physiol* 291(6):C1318-1325
- Bengtsson M, Karlsson HJ, Westman G, Kubista M (2003) A new minor groove binding asymmetric cyanine reporter dye for real-time PCR. *Nucleic Acids Res* 31(8):e45
- Bergelson JM, Cunningham JA, Droguett G, Kurt-Jones EA, Krithivas A, Hong JS, Horwitz MS, Crowell RL, Finberg RW (1997) Isolation of a common receptor for Coxsackie B viruses and adenoviruses 2 and 5. *Science* 275(5304):1320-1323
- Berhane S, Areste C, Ablack JN, Ryan GB, Blackburn DJ, Mymryk JS, Turnell AS, Steele JC, Grand RJ (2011) Adenovirus E1A interacts directly with, and regulates the level of expression of, the immunoproteasome component MECL1. *Virology* 421(2):149-158
- Berk AJ, Lee F, Harrison T, Williams J, Sharp PA (1979) Pre-early adenovirus 5 gene product regulates synthesis of early viral messenger RNAs. *Cell* 17(4):935-944
- Berk AJ (2005) Recent lessons in gene expression, cell cycle control, and cell biology from adenovirus. *Oncogene* 24(52):7673-7685
- Bernt KM, Ni S, Tieu AT, Lieber A (2005) Assessment of a combined, adenovirus-mediated oncolytic and immunostimulatory tumor therapy. *Cancer research* 65(10):4343-4352
- Bett AJ, Haddara W, Prevec L, Graham FL (1994) An efficient and flexible system for construction of adenovirus vectors with insertions or deletions in early regions 1 and 3. *Proceedings of the National Academy of Sciences of the United States of America* 91(19):8802-8806
- Bieler A, Mantwill K, Holzmüller R, Jurchott K, Kaszubiak A, Stark S, Glockzin G, Lage H, Grosu AL, Gansbacher B, Holm PS (2008) Impact of radiation therapy on the oncolytic adenovirus dl520: implications on the treatment of glioblastoma. *Radiother Oncol* 86(3):419-427
- Binder RJ, Blachere NE, Srivastava PK (2001) Heat shock protein-chaperoned peptides but not free peptides introduced into the cytosol are presented efficiently by major histocompatibility complex I molecules. *The Journal of biological chemistry* 276(20):17163-17171
- Binder RJ, Srivastava PK (2005) Peptides chaperoned by heat-shock proteins are a necessary and sufficient source of antigen in the cross-priming of CD8+ T cells. *Nat Immunol* 6(6):593-599
- Biron CA, Nguyen KB, Pien GC, Cousens LP, Salazar-Mather TP (1999) Natural killer cells in antiviral defense: function and regulation by innate cytokines. *Annu Rev Immunol* 17:189-220
- Blander JM, Medzhitov R (2006) Toll-dependent selection of microbial antigens for presentation by dendritic cells. *Nature* 440(7085):808-812
- Boozari B, Mundt B, Woller N, Struver N, Gurlevik E, Schache P, Kloos A, Knocke S, Manns MP, Wirth TC, Kubicka S, Kuhnel F (2010) Antitumoural immunity by virus-mediated immunogenic apoptosis inhibits metastatic growth of hepatocellular carcinoma. *Gut* 59(10):1416-1426
- Borgland SL, Bowen GP, Wong NC, Libermann TA, Muruve DA (2000) Adenovirus vector-induced expression of the C-X-C chemokine IP-10 is mediated through capsid-dependent activation of NF-kappaB. *Journal of virology* 74(9):3941-3947

- Bortolanza S, Bunuales M, Otano I, Gonzalez-Aseguinolaza G, Ortiz-de-Solorzano C, Perez D, Prieto J, Hernandez-Alcoceba R (2009) Treatment of pancreatic cancer with an oncolytic adenovirus expressing interleukin-12 in Syrian hamsters. *Mol Ther* 17(4):614-622
- Botta G, Passaro C, Libertini S, Abagnale A, Barbato S, Maione AS, Hallden G, Beguinot F, Formisano P, Portella G (2012) Inhibition of autophagy enhances the effects of E1A-defective oncolytic adenovirus dl922-947 against glioma cells in vitro and in vivo. *Hum Gene Ther* 23(6):623-634
- Bowen GP, Borgland SL, Lam M, Libermann TA, Wong NC, Muruve DA (2002) Adenovirus vector-induced inflammation: capsid-dependent induction of the C-C chemokine RANTES requires NF-kappa B. *Hum Gene Ther* 13(3):367-379
- Brabletz T (2012) To differentiate or not--routes towards metastasis. *Nature reviews Cancer* 12(6):425-436
- Bradley RR, Lynch DM, Lampietro MJ, Borducchi EN, Barouch DH (2012) Adenovirus serotype 5 neutralizing antibodies target both hexon and fiber following vaccination and natural infection. *Journal of virology* 86(1):625-629
- Braun SE, Chen K, Blazar BR, Orchard PJ, Sledge G, Robertson MJ, Broxmeyer HE, Cornetta K (1999) Flt3 ligand antitumor activity in a murine breast cancer model: a comparison with granulocyte-macrophage colony-stimulating factor and a potential mechanism of action. *Hum Gene Ther* 10(13):2141-2151
- Bridle BW, Hanson S, Lichty BD (2010) Combining oncolytic virotherapy and tumour vaccination. *Cytokine Growth Factor Rev* 21(2-3):143-148
- Burnett RM (1985) The structure of the adenovirus capsid. II. The packing symmetry of hexon and its implications for viral architecture. *J Mol Biol* 185(1):125-143
- Burnette WN (1981) "Western blotting": electrophoretic transfer of proteins from sodium dodecyl sulfate--polyacrylamide gels to unmodified nitrocellulose and radiographic detection with antibody and radioiodinated protein A. *Anal Biochem* 112(2):195-203
- Butler EB, Zhao Y, Munoz-Pinedo C, Lu J, Tan M (2013) Stalling the engine of resistance: targeting cancer metabolism to overcome therapeutic resistance. *Cancer research* 73(9):2709-2717
- Candolfi M, Curtin JF, Yagiz K, Assi H, Wibowo MK, Alzadeh GE, Foulad D, Muhammad AK, Salehi S, Keech N, Puntel M, Liu C, Sanderson NR, Kroeger KM, Dunn R, Martins G, Lowenstein PR, Castro MG (2011) B cells are critical to T-cell-mediated antitumor immunity induced by a combined immune-stimulatory/conditionally cytotoxic therapy for glioblastoma. *Neoplasia* 13(10):947-960
- Cao W, Bao C, Lowenstein CJ (2003) Inducible nitric oxide synthase expression inhibition by adenovirus E1A. *Proceedings of the National Academy of Sciences of the United States of America* 100(13):7773-7778
- Carmody RJ, Maguschak K, Chen YH (2006) A novel mechanism of nuclear factor-kappaB regulation by adenoviral protein 14.7K. *Immunology* 117(2):188-195
- Carter (1952) COMMITTEE on Standardized Nomenclature for Inbred Strains of Mice. *Cancer research* 12(8):602-613
- Casares N, Pequignot MO, Tesniere A, Ghiringhelli F, Roux S, Chaput N, Schmitt E, Hamai A, Hervas-Stubbs S, Obeid M, Coutant F, Metivier D, Pichard E, Aucouturier P, Pierron G, Garrido C, Zitvogel L, Kroemer G (2005) Caspase-dependent immunogenicity of doxorubicin-induced tumor cell death. *J Exp Med* 202(12):1691-1701
- Cavallo F, De Giovanni C, Nanni P, Forni G, Lollini PL (2011) 2011: the immune hallmarks of cancer. *Cancer Immunol Immunother* 60(3):319-326
- Cerullo V, Seiler MP, Mane V, Brunetti-Pierri N, Clarke C, Bertin TK, Rodgers JR, Lee B (2007) Toll-like receptor 9 triggers an innate immune response to helper-dependent adenoviral vectors. *Mol Ther* 15(2):378-385
- Cerullo V, Pesonen S, Diaconu I, Escutenaire S, Arstila PT, Ugolini M, Nokisalmi P, Raki M, Laasonen L, Sarkioja M, et al (2010) Oncolytic adenovirus coding for granulocyte macrophage colony-stimulating factor induces antitumoral immunity in cancer patients. *Cancer research* 70(11):4297-4309

- Cerullo V, Koski A, Vaha-Koskela M, Hemminki A (2012) Chapter eight--Oncolytic adenoviruses for cancer immunotherapy: data from mice, hamsters, and humans. *Adv Cancer Res* 115:265-318
- Chabner BA, Roberts TG, Jr. (2005) Timeline: Chemotherapy and the war on cancer. *Nature reviews Cancer* 5(1):65-72
- Chatterjee-Kishore M, van Den Akker F, Stark GR (2000) Adenovirus E1A down-regulates LMP2 transcription by interfering with the binding of stat1 to IRF1. *The Journal of biological chemistry* 275(27):20406-20411
- Chavan R, Marfatia KA, An IC, Garber DA, Feinberg MB (2006) Expression of CCL20 and granulocyte-macrophage colony-stimulating factor, but not Flt3-L, from modified vaccinia virus ankara enhances antiviral cellular and humoral immune responses. *Journal of virology* 80(15):7676-7687
- Chekeni FB, Elliott MR, Sandilos JK, Walk SF, Kinchen JM, Lazarowski ER, Armstrong AJ, Penuela S, Laird DW, Salvesen GS, Isakson BE, Bayliss DA, Ravichandran KS (2010) Pannexin 1 channels mediate 'find-me' signal release and membrane permeability during apoptosis. *Nature* 467(7317):863-867
- Chiba S, Baghdadi M, Akiba H, Yoshiyama H, Kinoshita I, Dosaka-Akita H, Fujioka Y, Ohba Y, Gorman JV, Colgan JD, Hirashima M, Uede T, Takaoka A, Yagita H, Jinushi M (2012) Tumor-infiltrating DCs suppress nucleic acid-mediated innate immune responses through interactions between the receptor TIM-3 and the alarmin HMGB1. *Nat Immunol* 13(9):832-842
- Choi IK, Lee JS, Zhang SN, Park J, Sonn CH, Lee KM, Yun CO (2011) Oncolytic adenovirus co-expressing IL-12 and IL-18 improves tumor-specific immunity via differentiation of T cells expressing IL-12Rbeta2 or IL-18Ralpha. *Gene therapy* 18(9):898-909
- Choi KJ, Zhang SN, Choi IK, Kim JS, Yun CO (2012) Strengthening of antitumor immune memory and prevention of thymic atrophy mediated by adenovirus expressing IL-12 and GM-CSF. *Gene therapy* 19(7):711-723
- Cichon G, Boeckh-Herwig S, Schmidt HH, Wehnes E, Muller T, Pring-Akerblom P, Burger R (2001) Complement activation by recombinant adenoviruses. *Gene therapy* 8(23):1794-1800
- Cintolo JA, Datta J, Mathew SJ, Czerniecki BJ (2012) Dendritic cell-based vaccines: barriers and opportunities. *Future Oncol* 8(10):1273-1299
- Coles LS, Lambrusco L, Burrows J, Hunter J, Diamond P, Bert AG, Vadas MA, Goodall GJ (2005) Phosphorylation of cold shock domain/Y-box proteins by ERK2 and GSK3beta and repression of the human VEGF promoter. *FEBS Lett* 579(24):5372-5378
- Condeelis J, Pollard JW (2006) Macrophages: obligate partners for tumor cell migration, invasion, and metastasis. *Cell* 124(2):263-266
- Connell CM, Shibata A, Tookman LA, Archibald KM, Flak MB, Pirlo KJ, Lockley M, Wheatley SP, McNeish IA (2011) Genomic DNA damage and ATR-Chk1 signaling determine oncolytic adenoviral efficacy in human ovarian cancer cells. *The Journal of clinical investigation* 121(4):1283-1297
- Cook JL, Walker TA, Worthen GS, Radke JR (2002) Role of the E1A Rb-binding domain in repression of the NF-kappa B-dependent defense against tumor necrosis factor-alpha. *Proceedings of the National Academy of Sciences of the United States of America* 99(15):9966-9971
- Coux O, Tanaka K, Goldberg AL (1996) Structure and functions of the 20S and 26S proteasomes. *Annu Rev Biochem* 65:801-847
- Curiel DT (2000) The development of conditionally replicative adenoviruses for cancer therapy. *Clin Cancer Res* 6(9):3395-3399
- Curtin JF, Liu N, Candolfi M, Xiong W, Assi H, Yagiz K, Edwards MR, Michelsen KS, Kroeger KM, Liu C, Muhammad AK, Clark MC, Arditi M, Comin-Anduix B, Ribas A, Lowenstein PR, Castro MG (2009) HMGB1 mediates endogenous TLR2 activation and brain tumor regression. *PLoS Med* 6(1):e10
- Dawes KE, Gray AJ, Laurent GJ (1993) Thrombin stimulates fibroblast chemotaxis and replication. *Eur J Cell Biol* 61(1):126-130

- de Gruijl TD, van de Ven R (2012) Chapter six--Adenovirus-based immunotherapy of cancer: promises to keep. *Adv Cancer Res* 115:147-220
- de Jong RN, van der Vliet PC, Brenkman AB (2003) Adenovirus DNA replication: protein priming, jumping back and the role of the DNA binding protein DBP. *Curr Top Microbiol Immunol* 272:187-211
- De Maio A (1999) Heat shock proteins: facts, thoughts, and dreams. *Shock* 11(1):1-12
- Decker P, Muller S (2002) Modulating poly (ADP-ribose) polymerase activity: potential for the prevention and therapy of pathogenic situations involving DNA damage and oxidative stress. *Curr Pharm Biotechnol* 3(3):275-283
- DeLeo AB, Shiku H, Takahashi T, John M, Old LJ (1977) Cell surface antigens of chemically induced sarcomas of the mouse. I. Murine leukemia virus-related antigens and alloantigens on cultured fibroblasts and sarcoma cells: description of a unique antigen on BALB/c Meth A sarcoma. *J Exp Med* 146(3):720-734
- DeNardo DG, Brennan DJ, Rexhepaj E, Ruffell B, Shiao SL, Madden SF, Gallagher WM, Wadhwani N, Keil SD, Junaid SA, Rugo HS, Hwang ES, Jirstrom K, West BL, Coussens LM (2011) Leukocyte complexity predicts breast cancer survival and functionally regulates response to chemotherapy. *Cancer Discov* 1(1):54-67
- Denkert C, Loibl S, Noske A, Roller M, Muller BM, Komor M, Budczies J, Darb-Esfahani S, Kronenwett R, Hanusch C, von Torne C, Weichert W, Engels K, Solbach C, Schrader I, Dietel M, von Minckwitz G (2010) Tumor-associated lymphocytes as an independent predictor of response to neoadjuvant chemotherapy in breast cancer. *J Clin Oncol* 28(1):105-113
- Di Paolo NC, Miao EA, Iwakura Y, Murali-Krishna K, Aderem A, Flavell RA, Papayannopoulou T, Shayakhmetov DM (2009) Virus binding to a plasma membrane receptor triggers interleukin-1 alpha-mediated proinflammatory macrophage response in vivo. *Immunity* 31(1):110-121
- Diaconu I, Cerullo V, Hirvonen ML, Escutenaire S, Ugolini M, Pesonen SK, Bramante S, Parviainen S, Kanerva A, Loskog AS, Eliopoulos AG, Pesonen S, Hemminki A (2012) Immune response is an important aspect of the antitumor effect produced by a CD40L-encoding oncolytic adenovirus. *Cancer research* 72(9):2327-2338
- Dmitriev I, Krasnykh V, Miller CR, Wang M, Kashentseva E, Mikheeva G, Belousova N, Curiel DT (1998) An adenovirus vector with genetically modified fibers demonstrates expanded tropism via utilization of a coxsackievirus and adenovirus receptor-independent cell entry mechanism. *Journal of virology* 72(12):9706-9713
- Donnelly OG, Errington-Mais F, Steele L, Hadac E, Jennings V, Scott K, Peach H, Phillips RM, Bond J, Pandha H, Harrington K, Vile R, Russell S, Selby P, Melcher AA (2013) Measles virus causes immunogenic cell death in human melanoma. *Gene therapy* 20(1):7-15
- Doronin K, Shashkova EV, May SM, Hofherr SE, Barry MA (2009) Chemical modification with high molecular weight polyethylene glycol reduces transduction of hepatocytes and increases efficacy of intravenously delivered oncolytic adenovirus. *Hum Gene Ther* 20(9):975-988
- Douglas JT, Rogers BE, Rosenfeld ME, Michael SI, Feng M, Curiel DT (1996) Targeted gene delivery by tropism-modified adenoviral vectors. *Nat Biotechnol* 14(11):1574-1578
- Dranoff G, Jaffee E, Lazenby A, Golumbek P, Levitsky H, Brose K, Jackson V, Hamada H, Pardoll D, Mulligan RC (1993) Vaccination with irradiated tumor cells engineered to secrete murine granulocyte-macrophage colony-stimulating factor stimulates potent, specific, and long-lasting anti-tumor immunity. *Proceedings of the National Academy of Sciences of the United States of America* 90(8):3539-3543
- Ebert O, Shinozaki K, Huang TG, Savontaus MJ, Garcia-Sastre A, Woo SL (2003) Oncolytic vesicular stomatitis virus for treatment of orthotopic hepatocellular carcinoma in immune-competent rats. *Cancer research* 63(13):3605-3611

- Edukulla R, Woller N, Mundt B, Knocke S, Gurlevik E, Saborowski M, Malek N, Manns MP, Wirth T, Kuhnel F, Kubicka S (2009) Antitumoral immune response by recruitment and expansion of dendritic cells in tumors infected with telomerase-dependent oncolytic viruses. *Cancer research* 69(4):1448-1458
- Egeblad M, Nakasone ES, Werb Z (2010) Tumors as organs: complex tissues that interface with the entire organism. *Dev Cell* 18(6):884-901
- Elliott MR, Chekeni FB, Trampont PC, Lazarowski ER, Kadl A, Walk SF, Park D, Woodson RI, Ostankovich M, Sharma P, Lysiak JJ, Harden TK, Leitinger N, Ravichandran KS (2009) Nucleotides released by apoptotic cells act as a find-me signal to promote phagocytic clearance. *Nature* 461(7261):282-286
- En-Nia A, Yilmaz E, Klinge U, Lovett DH, Stefanidis I, Mertens PR (2005) Transcription factor YB-1 mediates DNA polymerase alpha gene expression. *The Journal of biological chemistry* 280(9):7702-7711
- Evdokimova V, Ovchinnikov LP, Sorensen PH (2006) Y-box binding protein 1: providing a new angle on translational regulation. *Cell Cycle* 5(11):1143-1147
- Evdokimova V, Tognon C, Ng T, Ruzanov P, Melnyk N, Fink D, Sorokin A, Ovchinnikov LP, Davicioni E, Triche TJ, Sorensen PH (2009) Translational activation of snail1 and other developmentally regulated transcription factors by YB-1 promotes an epithelial-mesenchymal transition. *Cancer Cell* 15(5):402-415
- Fattaey AR, Harlow E, Helin K (1993) Independent regions of adenovirus E1A are required for binding to and dissociation of E2F-protein complexes. *Mol Cell Biol* 13(12):7267-7277
- Flint SJ, Gonzalez RA (2003) Regulation of mRNA production by the adenoviral E1B 55-kDa and E4 Orf6 proteins. *Curr Top Microbiol Immunol* 272:287-330
- Fotovati A, Abu-Ali S, Wang PS, Deleyrolle LP, Lee C, Triscott J, Chen JY, Franciosi S, Nakamura Y, Sugita Y, Uchiumi T, Kuwano M, Leavitt BR, Singh SK, Jury A, Jones C, Wakimoto H, Reynolds BA, Pallen CJ, Dunn SE (2011) YB-1 bridges neural stem cells and brain tumor-initiating cells via its roles in differentiation and cell growth. *Cancer research* 71(16):5569-5578
- Freeman AI, Zakay-Rones Z, Gomori JM, Linetsky E, Rasooly L, Greenbaum E, Rozenman-Yair S, Panet A, Libson E, Irving CS, Galun E, Siegal T (2006) Phase I/II trial of intravenous NDV-HUJ oncolytic virus in recurrent glioblastoma multiforme. *Mol Ther* 13(1):221-228
- Frew SE, Sammut SM, Shore AF, Ramjist JK, Al-Bader S, Rezaie R, Daar AS, Singer PA (2008) Chinese health biotech and the billion-patient market. *Nat Biotechnol* 26(1):37-53
- Fridlender ZG, Sun J, Kim S, Kapoor V, Cheng G, Ling L, Worthen GS, Albelda SM (2009) Polarization of tumor-associated neutrophil phenotype by TGF-beta: "N1" versus "N2" TAN. *Cancer Cell* 16(3):183-194
- Frisch SM, Mymryk JS (2002) Adenovirus-5 E1A: paradox and paradigm. *Nat Rev Mol Cell Biol* 3(6):441-452
- Fucikova J, Kralikova P, Fialova A, Brtnicky T, Rob L, Bartunkova J, Spisek R (2011) Human tumor cells killed by anthracyclines induce a tumor-specific immune response. *Cancer research* 71(14):4821-4833
- Galanis E, Markovic SN, Suman VJ, Nuovo GJ, Vile RG, Kottke TJ, Nevala WK, Thompson MA, Lewis JE, Rumilla KM, Roulstone V, Harrington K, Linette GP, Maples WJ, Coffey M, Zwiebel J, Kendra K (2012) Phase II trial of intravenous administration of Reolysin((R)) (Reovirus Serotype-3-dearing Strain) in patients with metastatic melanoma. *Mol Ther* 20(10):1998-2003
- Galluzzi L, Maiuri MC, Vitale I, Zischka H, Castedo M, Zitvogel L, Kroemer G (2007) Cell death modalities: classification and pathophysiological implications. *Cell death and differentiation* 14(7):1237-1243
- Galluzzi L, Kepp O, Morselli E, Vitale I, Senovilla L, Pinti M, Zitvogel L, Kroemer G (2010) Viral strategies for the evasion of immunogenic cell death. *J Intern Med* 267(5):526-542



- Galluzzi L, Vitale I, Abrams JM, Alnemri ES, Baehrecke EH, Blagosklonny MV, Dawson TM, Dawson VL, El-Deiry WS, Fulda S, et al (2012) Molecular definitions of cell death subroutines: recommendations of the Nomenclature Committee on Cell Death 2012. *Cell death and differentiation* 19(1):107-120
- Garber K (2006) China approves world's first oncolytic virus therapy for cancer treatment. *J Natl Cancer Inst* 98(5):298-300
- Garcia-Sastre A, Biron CA (2006) Type 1 interferons and the virus-host relationship: a lesson in detente. *Science* 312(5775):879-882
- Gardai SJ, McPhillips KA, Frasch SC, Janssen WJ, Starefeldt A, Murphy-Ullrich JE, Bratton DL, Oldenborg PA, Michalak M, Henson PM (2005) Cell-surface calreticulin initiates clearance of viable or apoptotic cells through trans-activation of LRP on the phagocyte. *Cell* 123(2):321-334
- Garg AD, Krysko DV, Vandenabeele P, Agostinis P (2012a) Hypericin-based photodynamic therapy induces surface exposure of damage-associated molecular patterns like HSP70 and calreticulin. *Cancer Immunol Immunother* 61(2):215-221
- Garg AD, Krysko DV, Vandenabeele P, Agostinis P (2012b) The emergence of phox-ER stress induced immunogenic apoptosis. *Oncoimmunology* 1(5):786-788
- Garg AD, Krysko DV, Verfaillie T, Kaczmarek A, Ferreira GB, Marysael T, Rubio N, Firczuk M, Mathieu C, Roebroek AJ, Annaert W, Golab J, de Witte P, Vandenabeele P, Agostinis P (2012c) A novel pathway combining calreticulin exposure and ATP secretion in immunogenic cancer cell death. *EMBO J* 31(5):1062-1079
- Garrod LP (1960) Relative antibacterial activity of three penicillins. *British medical journal* 1(5172): 527-529
- Gelebart P, Opas M, Michalak M (2005) Calreticulin, a Ca<sup>2+</sup>-binding chaperone of the endoplasmic reticulum. *Int J Biochem Cell Biol* 37(2):260-266
- Ghiringhelli F, Apetoh L, Tesniere A, Aymeric L, Ma Y, Ortiz C, Vermaelen K, Panaretakis T, Mignot G, Ullrich E, et al (2009) Activation of the NLRP3 inflammasome in dendritic cells induces IL-1 $\beta$ -dependent adaptive immunity against tumors. *Nat Med* 15(10):1170-1178
- Giard DJ, Aaronson SA, Todaro GJ, Arnstein P, Kersey JH, Dosik H, Parks WP (1973) In vitro cultivation of human tumors: establishment of cell lines derived from a series of solid tumors. *J Natl Cancer Inst* 51(5):1417-1423
- Glickman MH, Maytal V (2002) Regulating the 26S proteasome. *Curr Top Microbiol Immunol* 268:43-72
- Glockzin G, Mantwill K, Jurchott K, Bernshausen A, Ladhoff A, Royer HD, Gansbacher B, Holm PS (2006) Characterization of the recombinant adenovirus vector AdYB-1: implications for oncolytic vector development. *Journal of virology* 80(8):3904-3911
- Gluz O, Mengele K, Schmitt M, Kates R, Diallo-Danebrock R, Neff F, Royer HD, Eckstein N, Mohrmann S, Ting E, Kiechle M, Poremba C, Nitz U, Harbeck N (2009) Y-box-binding protein YB-1 identifies high-risk patients with primary breast cancer benefiting from rapidly cycled tandem high-dose adjuvant chemotherapy. *J Clin Oncol* 27(36):6144-6151
- Goldsmith ME, Madden MJ, Morrow CS, Cowan KH (1993) A Y-box consensus sequence is required for basal expression of the human multidrug resistance (mdr1) gene. *The Journal of biological chemistry* 268(8):5856-5860
- Gottesman MM, Fojo T, Bates SE (2002) Multidrug resistance in cancer: role of ATP-dependent transporters. *Nature reviews Cancer* 2(1):48-58
- Graham FL, Smiley J, Russell WC, Nairn R (1977) Characteristics of a human cell line transformed by DNA from human adenovirus type 5. *J Gen Virol* 36(1):59-74
- Green DR, Ferguson T, Zitvogel L, Kroemer G (2009) Immunogenic and tolerogenic cell death. *Nature reviews Immunology* 9(5):353-363
- Green NK, Herbert CW, Hale SJ, Hale AB, Mautner V, Harkins R, Hermiston T, Ulbrich K, Fisher KD, Seymour LW (2004) Extended plasma circulation time and decreased toxicity of polymer-coated adenovirus. *Gene therapy* 11(16):1256-1263

- Grivennikov SI, Greten FR, Karin M (2010) Immunity, inflammation, and cancer. *Cell* 140(6):883-899
- Gross C, Koelch W, DeMaio A, Arispe N, Multhoff G (2003) Cell surface-bound heat shock protein 70 (Hsp70) mediates perforin-independent apoptosis by specific binding and uptake of granzyme B. *The Journal of biological chemistry* 278(42):41173-41181
- Guo ZS, Liu Z, Bartlett DL, Tang D, Lotze MT (2013) Life after death: targeting high mobility group box 1 in emergent cancer therapies. *Am J Cancer Res* 3(1):1-20
- Gurlevik E, Woller N, Struver N, Schache P, Kloos A, Manns MP, Zender L, Kuhnel F, Kubicka S (2010) Selectivity of oncolytic viral replication prevents antiviral immune response and toxicity, but does not improve antitumoral immunity. *Mol Ther* 18(11):1972-1982
- Haase AT, Mautner V, Pereira HG (1972) The immunogenicity of adenovirus type 5 structural proteins. *Journal of immunology* 108(2):483-485
- Halama N, Michel S, Kloor M, Zoernig I, Benner A, Spille A, Pommerencke T, von Knebel DM, Folprecht G, Lubber B, Feyen N, Martens UM, Beckhove P, Gnjatic S, Schirmacher P, Herpel E, Weitz J, Grabe N, Jaeger D (2011) Localization and density of immune cells in the invasive margin of human colorectal cancer liver metastases are prognostic for response to chemotherapy. *Cancer research* 71(17):5670-5677
- Haley KP, Overhauser J, Babiss LE, Ginsberg HS, Jones NC (1984) Transformation properties of type 5 adenovirus mutants that differentially express the E1A gene products. *Proceedings of the National Academy of Sciences of the United States of America* 81(18):5734-5738
- Hallden G, Hill R, Wang Y, Anand A, Liu TC, Lemoine NR, Francis J, Hawkins L, Kirn D (2003) Novel immunocompetent murine tumor models for the assessment of replication-competent oncolytic adenovirus efficacy. *Mol Ther* 8(3):412-424
- Hamid O, Varterasian ML, Wadler S, Hecht JR, Benson A, 3rd, Galanis E, Uprichard M, Omer C, Bycott P, Hackman RC, Shields AF (2003) Phase II trial of intravenous CI-1042 in patients with metastatic colorectal cancer. *J Clin Oncol* 21(8):1498-1504
- Hamilton JA, Anderson GP (2004) GM-CSF Biology. *Growth Factors* 22(4):225-231
- Han J, Sabbatini P, Perez D, Rao L, Modha D, White E (1996) The E1B 19K protein blocks apoptosis by interacting with and inhibiting the p53-inducible and death-promoting Bax protein. *Genes & development* 10(4):461-477
- Hanahan D, Weinberg RA (2011) Hallmarks of cancer: the next generation. *Cell* 144(5):646-674
- Harrington KJ, Hingorani M, Tanay MA, Hickey J, Bhide SA, Clarke PM, Renouf LC, Thway K, Sibtain A, McNeish IA, Newbold KL, Goldsweig H, Coffin R, Nutting CM (2010) Phase I/II study of oncolytic HSV GM-CSF in combination with radiotherapy and cisplatin in untreated stage III/IV squamous cell cancer of the head and neck. *Clin Cancer Res* 16(15):4005-4015
- Harrison SC (2010) Virology. Looking inside adenovirus. *Science* 329(5995):1026-1027
- Hay RT, Freeman A, Leith I, Monaghan A, Webster A (1995) Molecular interactions during adenovirus DNA replication. *Curr Top Microbiol Immunol* 199(Pt 2):31-48
- Heid CA, Stevens J, Livak KJ, Williams PM (1996) Real time quantitative PCR. *Genome Res* 6(10):986-994
- Heink S, Fricke B, Ludwig D, Kloetzel PM, Kruger E (2006) Tumor cell lines expressing the proteasome subunit isoform LMP7E1 exhibit immunoproteasome deficiency. *Cancer research* 66(2):649-652
- Hensley SE, Giles-Davis W, McCoy KC, Weninger W, Ertl HC (2005) Dendritic cell maturation, but not CD8+ T cell induction, is dependent on type I IFN signaling during vaccination with adenovirus vectors. *Journal of immunology* 175(9):6032-6041
- Heo J, Reid T, Ruo L, Breitbach CJ, Rose S, Bloomston M, Cho M, Lim HY, Chung HC, Kim CW, et al (2013) Randomized dose-finding clinical trial of oncolytic immunotherapeutic vaccinia JX-594 in liver cancer. *Nat Med* 19(3):329-336
- Heron M (2012) Deaths: Leading Causes for 2009. U.S. DEPARTMENT OF HEALTH AND HUMAN SERVICES, National Vital Statistics System Vol 61-7 ([http://www.cdc.gov/nchs/data/nvsr/nvsr61/nvsr61\\_07.pdf](http://www.cdc.gov/nchs/data/nvsr/nvsr61/nvsr61_07.pdf))

- Hierholzer JC (1992) Adenoviruses in the immunocompromised host. *Clin Microbiol Rev* 5(3):262-274
- Higashi K, Inagaki Y, Fujimori K, Nakao A, Kaneko H, Nakatsuka I (2003) Interferon-gamma interferes with transforming growth factor-beta signaling through direct interaction of YB-1 with Smad3. *The Journal of biological chemistry* 278(44):43470-43479
- Hirasawa K, Nishikawa SG, Norman KL, Coffey MC, Thompson BG, Yoon CS, Waisman DM, Lee PW (2003) Systemic reovirus therapy of metastatic cancer in immune-competent mice. *Cancer research* 63(2):348-353
- Hirst DG, Brown JM, Hazlehurst JL (1982) Enhancement of CCNU cytotoxicity by misonidazole: possible therapeutic gain. *Br J Cancer* 46(1):109-116
- Hisamatsu H, Shimbara N, Saito Y, Kristensen P, Hendil KB, Fujiwara T, Takahashi E, Tanahashi N, Tamura T, Ichihara A, Tanaka K (1996) Newly identified pair of proteasomal subunits regulated reciprocally by interferon gamma. *J Exp Med* 183(4):1807-1816
- Holm PS, Bergmann S, Jurchott K, Lage H, Brand K, Ladhoff A, Mantwill K, Curiel DT, Dobbstein M, Dietel M, Gansbacher B, Royer HD (2002) YB-1 relocates to the nucleus in adenovirus-infected cells and facilitates viral replication by inducing E2 gene expression through the E2 late promoter. *The Journal of biological chemistry* 277(12):10427-10434
- Holm PS, Lage H, Bergmann S, Jurchott K, Glockzin G, Bernshausen A, Mantwill K, Ladhoff A, Wichert A, Mymryk JS, Ritter T, Dietel M, Gansbacher B, Royer HD (2004) Multidrug-resistant cancer cells facilitate E1-independent adenoviral replication: impact for cancer gene therapy. *Cancer research* 64(1):322-328
- Holzmuller R, Mantwill K, Haczek C, Rognoni E, Anton M, Kasajima A, Weichert W, Treue D, Lage H, Schuster T, Schlegel J, Gansbacher B, Holm PS (2011) YB-1 dependent virotherapy in combination with temozolomide as a multimodal therapy approach to eradicate malignant glioma. *International journal of cancer Journal international du cancer* 129(5):1265-1276
- Hong S, Paulson QX, Johnson DG (2008) E2F1 and E2F3 activate ATM through distinct mechanisms to promote E1A-induced apoptosis. *Cell Cycle* 7(3):391-400
- Hoyert D (2012) 75 Years of Mortality in the United States, 1935–2010. U.S. DEPARTMENT OF HEALTH AND HUMAN SERVICES, NCHS Data Brief Vol 88 (<http://www.cdc.gov/nchs/data/databriefs/db88.pdf>)
- Hu JC, Coffin RS, Davis CJ, Graham NJ, Groves N, Guest PJ, Harrington KJ, James ND, Love CA, McNeish I, Medley LC, Michael A, Nutting CM, Pandha HS, Shorrock CA, Simpson J, Steiner J, Steven NM, Wright D, Coombes RC (2006) A phase I study of OncoVEXGM-CSF, a second-generation oncolytic herpes simplex virus expressing granulocyte macrophage colony-stimulating factor. *Clin Cancer Res* 12(22):6737-6747
- Huang JH, Zhang SN, Choi KJ, Choi IK, Kim JH, Lee MG, Kim H, Yun CO (2010) Therapeutic and tumor-specific immunity induced by combination of dendritic cells and oncolytic adenovirus expressing IL-12 and 4-1BBL. *Mol Ther* 18(2):264-274
- Hwang TH, Moon A, Burke J, Ribas A, Stephenson J, Breitbach CJ, Daneshmand M, De Silva N, Parato K, Diallo JS, Lee YS, Liu TC, Bell JC, Kirn DH (2011) A mechanistic proof-of-concept clinical trial with JX-594, a targeted multi-mechanistic oncolytic poxvirus, in patients with metastatic melanoma. *Mol Ther* 19(10):1913-1922
- Hyogotani A, Ito K, Yoshida K, Izumi H, Kohno K, Amano J (2012) Association of nuclear YB-1 localization with lung resistance-related protein and epidermal growth factor receptor expression in lung cancer. *Clin Lung Cancer* 13(5):375-384
- Igney FH, Krammer PH (2002) Immune escape of tumors: apoptosis resistance and tumor counterattack. *Journal of leukocyte biology* 71(6):907-920
- Ilan Y, Droguett G, Chowdhury NR, Li Y, Sengupta K, Thummala NR, Davidson A, Chowdhury JR, Horwitz MS (1997) Insertion of the adenoviral E3 region into a recombinant viral vector prevents antiviral humoral and cellular immune responses and permits long-term gene expression. *Proceedings of the National Academy of Sciences of the United States of America* 94(6):2587-2592

- Ito H, Aoki H, Kuhnel F, Kondo Y, Kubicka S, Wirth T, Iwado E, Iwamaru A, Fujiwara K, Hess KR, Lang FF, Sawaya R, Kondo S (2006) Autophagic cell death of malignant glioma cells induced by a conditionally replicating adenovirus. *J Natl Cancer Inst* 98(9):625-636
- Janetzki S, Cox JH, Oden N, Ferrari G (2005) Standardization and validation issues of the ELISPOT assay. *Methods Mol Biol* 302:51-86
- Jemal A, Bray F, Center MM, Ferlay J, Ward E, Forman D (2011) Global cancer statistics. *CA Cancer J Clin* 61(2):69-90
- Jiang H, White EJ, Rios-Vicil CI, Xu J, Gomez-Manzano C, Fueyo J (2011) Human adenovirus type 5 induces cell lysis through autophagy and autophagy-triggered caspase activity. *Journal of virology* 85(10):4720-4729
- Jones N, Shenk T (1979) An adenovirus type 5 early gene function regulates expression of other early viral genes. *Proceedings of the National Academy of Sciences of the United States of America* 76(8):3665-3669
- Jurchott K, Bergmann S, Stein U, Walther W, Janz M, Manni I, Piaggio G, Fietze E, Dietel M, Royer HD (2003) YB-1 as a cell cycle-regulated transcription factor facilitating cyclin A and cyclin B1 gene expression. *The Journal of biological chemistry* 278(30):27988-27996
- Kabeya Y, Mizushima N, Ueno T, Yamamoto A, Kirisako T, Noda T, Kominami E, Ohsumi Y, Yoshimori T (2000) LC3, a mammalian homologue of yeast Apg8p, is localized in autophagosome membranes after processing. *EMBO J* 19(21):5720-5728
- Kalvakolanu DV, Bandyopadhyay SK, Harter ML, Sen GC (1991) Inhibition of interferon-inducible gene expression by adenovirus E1A proteins: block in transcriptional complex formation. *Proceedings of the National Academy of Sciences of the United States of America* 88(17):7459-7463
- Kamen A, Henry O (2004) Development and optimization of an adenovirus production process. *J Gene Med* 6(Suppl 1):S184-192
- Kaneko T, LePage GA (1978) Growth characteristics and drug responses of a murine lung carcinoma in vitro and in vivo. *Cancer research* 38(7):2084-2090
- Kanerva A, Nokisalmi P, Diaconu I, Koski A, Cerullo V, Liikanen I, Tahtinen S, Oksanen M, Heiskanen R, Pesonen S, Joensuu T, Alanko T, Partanen K, Laasonen L, Kairemo K, Pesonen S, Kangasniemi L, Hemminki A (2013) Antiviral and antitumor T-cell immunity in patients treated with GM-CSF-coding oncolytic adenovirus. *Clin Cancer Res* 19(10):2734-2744
- Kaufman HL, Bines SD (2010) OPTIM trial: a Phase III trial of an oncolytic herpes virus encoding GM-CSF for unresectable stage III or IV melanoma. *Future Oncol* 6(6):941-949
- Khurana D, Martin EA, Kasperbauer JL, O'Malley BW, Jr., Salomao DR, Chen L, Strome SE (2001) Characterization of a spontaneously arising murine squamous cell carcinoma (SCC VII) as a prerequisite for head and neck cancer immunotherapy. *Head Neck* 23(10):899-906
- Khuri FR, Nemunaitis J, Ganly I, Arseneau J, Tannock IF, Romel L, Gore M, Ironside J, MacDougall RH, Heise C, Randlev B, Gillenwater AM, Bruso P, Kaye SB, Hong WK, Kirn DH (2000) A controlled trial of intratumoral ONYX-015, a selectively-replicating adenovirus, in combination with cisplatin and 5-fluorouracil in patients with recurrent head and neck cancer. *Nat Med* 6(8):879-885
- Kiang A, Hartman ZC, Everett RS, Serra D, Jiang H, Frank MM, Amalfitano A (2006) Multiple innate inflammatory responses induced after systemic adenovirus vector delivery depend on a functional complement system. *Mol Ther* 14(4):588-598
- Kim J, Nam HY, Kim TI, Kim PH, Ryu J, Yun CO, Kim SW (2011a) Active targeting of RGD-conjugated bioreducible polymer for delivery of oncolytic adenovirus expressing shRNA against IL-8 mRNA. *Biomaterials* 32(22):5158-5166
- Kim KH, Ryan MJ, Estep JE, Miniard BM, Rudge TL, Peggins JO, Broadt TL, Wang M, Preuss MA, Siegal GP, Hemminki A, Harris RD, Aurigemma R, Curiel DT, Alvarez RD (2011b) A new generation of serotype chimeric infectivity-enhanced conditionally replicative adenovirals: the safety profile of ad5/3-Delta24 in advance of a phase I clinical trial in ovarian cancer patients. *Hum Gene Ther* 22(7):821-828

- Kim M, Zinn KR, Barnett BG, Sumerel LA, Krasnykh V, Curiel DT, Douglas JT (2002) The therapeutic efficacy of adenoviral vectors for cancer gene therapy is limited by a low level of primary adenovirus receptors on tumour cells. *Eur J Cancer* 38(14):1917-1926
- Kimball KJ, Preuss MA, Barnes MN, Wang M, Siegal GP, Wan W, Kuo H, Saddekni S, Stockard CR, Grizzle WE, Harris RD, Aurigemma R, Curiel DT, Alvarez RD (2010) A phase I study of a tropism-modified conditionally replicative adenovirus for recurrent malignant gynecologic diseases. *Clin Cancer Res* 16(21):5277-5287
- Kitajewski J, Schneider RJ, Safer B, Munemitsu SM, Samuel CE, Thimmappaya B, Shenk T (1986) Adenovirus VAI RNA antagonizes the antiviral action of interferon by preventing activation of the interferon-induced eIF-2 alpha kinase. *Cell* 45(2):195-200
- Klionsky DJ, Emr SD (2000) Autophagy as a regulated pathway of cellular degradation. *Science* 290(5497):1717-1721
- Klionsky DJ, Abeliovich H, Agostinis P, Agrawal DK, Aliev G, Askew DS, Baba M, Baehrecke EH, Bahr BA, Ballabio A, et al (2008) Guidelines for the use and interpretation of assays for monitoring autophagy in higher eukaryotes. *Autophagy* 4(2):151-175
- Klionsky DJ, Abdalla FC, Abeliovich H, Abraham RT, Acevedo-Arozena A, Adeli K, Agholme L, Agnello M, Agostinis P, Aguirre-Ghiso JA, et al (2012) Guidelines for the use and interpretation of assays for monitoring autophagy. *Autophagy* 8(4):445-544
- Kohno K, Izumi H, Uchiumi T, Ashizuka M, Kuwano M (2003) The pleiotropic functions of the Y-box-binding protein, YB-1. *Bioessays* 25(7):691-698
- Koike K, Uchiumi T, Ohga T, Toh S, Wada M, Kohno K, Kuwano M (1997) Nuclear translocation of the Y-box binding protein by ultraviolet irradiation. *FEBS Lett* 417(3):390-394
- Kolk A, Jubitz N, Mengele K, Mantwill K, Bissinger O, Schmitt M, Kremer M, Holm PS (2011) Expression of Y-box-binding protein YB-1 allows stratification into long- and short-term survivors of head and neck cancer patients. *Br J Cancer* 105(12):1864-1873
- Koski A, Kangasniemi L, Escutenaire S, Pesonen S, Cerullo V, Diaconu I, Nokisalmi P, Raki M, Rajecki M, Guse K, et al (2010) Treatment of cancer patients with a serotype 5/3 chimeric oncolytic adenovirus expressing GMCSF. *Mol Ther* 18(10):1874-1884
- Kottke T, Errington F, Pulido J, Galivo F, Thompson J, Wongthida P, Diaz RM, Chong H, Ilett E, Chester J, Pandha H, Harrington K, Selby P, Melcher A, Vile R (2011) Broad antigenic coverage induced by vaccination with virus-based cDNA libraries cures established tumors. *Nat Med* 17(7):854-859
- Kovesdi I, Reichel R, Nevins JR (1987) Role of an adenovirus E2 promoter binding factor in E1A-mediated coordinate gene control. *Proceedings of the National Academy of Sciences of the United States of America* 84(8):2180-2184
- Krishnamurthy S, Takimoto T, Scroggs RA, Portner A (2006) Differentially regulated interferon response determines the outcome of Newcastle disease virus infection in normal and tumor cell lines. *Journal of virology* 80(11):5145-5155
- Kroemer G, Levine B (2008) Autophagic cell death: the story of a misnomer. *Nat Rev Mol Cell Biol* 9(12):1004-1010
- Kroemer G, Galluzzi L, Kepp O, Zitvogel L (2013) Immunogenic cell death in cancer therapy. *Annu Rev Immunol* 31:51-72
- Kruschinski A, Moosmann A, Poschke I, Norell H, Chmielewski M, Seliger B, Kiessling R, Blankenstein T, Abken H, Charo J (2008) Engineering antigen-specific primary human NK cells against HER-2 positive carcinomas. *Proceedings of the National Academy of Sciences of the United States of America* 105(45):17481-17486
- Krysko DV, Garg AD, Kaczmarek A, Krysko O, Agostinis P, Vandenabeele P (2012) Immunogenic cell death and DAMPs in cancer therapy. *Nature reviews Cancer* 12(12):860-875
- Krysko O, Love Aaes T, Bachert C, Vandenabeele P, Krysko DV (2013) Many faces of DAMPs in cancer therapy. *Cell Death Dis* 4:e631
- Kuroda Y, Furuyama J (1963) Physiological and biochemical studies of effects of mitomycin C on strain HeLa cells in cell culture. *Cancer research* 23:682-687

- Kwon TK, Park JW (2002) Intramuscular co-injection of naked DNA encoding HBV core antigen and Flt3 ligand suppresses anti-HBc antibody response. *Immunol Lett* 81(3):229-234
- la Sala A, Ferrari D, Corinti S, Cavani A, Di Virgilio F, Girolomoni G (2001) Extracellular ATP induces a distorted maturation of dendritic cells and inhibits their capacity to initiate Th1 responses. *Journal of immunology* 166(3):1611-1617
- la Sala A, Sebastiani S, Ferrari D, Di Virgilio F, Idzko M, Norgauer J, Girolomoni G (2002) Dendritic cells exposed to extracellular adenosine triphosphate acquire the migratory properties of mature cells and show a reduced capacity to attract type 1 T lymphocytes. *Blood* 99(5):1715-1722
- Laemmli UK (1970) Cleavage of structural proteins during the assembly of the head of bacteriophage T4. *Nature* 227(5259):680-685
- Lal R, Harris D, Postel-Vinay S, de Bono J (2009) Reovirus: Rationale and clinical trial update. *Curr Opin Mol Ther* 11(5):532-539
- Lapteva N, Aldrich M, Weksberg D, Rollins L, Goltsova T, Chen SY, Huang XF (2009) Targeting the intratumoral dendritic cells by the oncolytic adenoviral vaccine expressing RANTES elicits potent antitumor immunity. *J Immunother* 32(2):145-156
- Lasham A, Moloney S, Hale T, Homer C, Zhang YF, Murison JG, Braithwaite AW, Watson J (2003) The Y-box-binding protein, YB1, is a potential negative regulator of the p53 tumor suppressor. *The Journal of biological chemistry* 278(37):35516-35523
- Lee C, Dhillon J, Wang MY, Gao Y, Hu K, Park E, Astanehe A, Hung MC, Eirew P, Eaves CJ, Dunn SE (2008) Targeting YB-1 in HER-2 overexpressing breast cancer cells induces apoptosis via the mTOR/STAT3 pathway and suppresses tumor growth in mice. *Cancer research* 68(21):8661-8666
- Lee CT, Wu S, Ciernik IF, Chen H, Nadaf-Rahrov S, Gabrilovich D, Carbone DP (1997) Genetic immunotherapy of established tumors with adenovirus-murine granulocyte-macrophage colony-stimulating factor. *Hum Gene Ther* 8(2):187-193
- Lee YS, Kim JH, Choi KJ, Choi IK, Kim H, Cho S, Cho BC, Yun CO (2006) Enhanced antitumor effect of oncolytic adenovirus expressing interleukin-12 and B7-1 in an immunocompetent murine model. *Clin Cancer Res* 12(19):5859-5868
- Leonard GT, Sen GC (1996) Effects of adenovirus E1A protein on interferon-signaling. *Virology* 224(1):25-33
- Leopold PL, Kreitzer G, Miyazawa N, Rempel S, Pfister KK, Rodriguez-Boulan E, Crystal RG (2000) Dynein- and microtubule-mediated translocation of adenovirus serotype 5 occurs after endosomal lysis. *Hum Gene Ther* 11(1):151-165
- Levine B, Klionsky DJ (2004) Development by self-digestion: molecular mechanisms and biological functions of autophagy. *Dev Cell* 6(4):463-477
- Levine B, Deretic V (2007) Unveiling the roles of autophagy in innate and adaptive immunity. *Nature reviews Immunology* 7(10):767-777
- Levy JM, Thorburn A (2011) Targeting autophagy during cancer therapy to improve clinical outcomes. *Pharmacol Ther* 131(1):130-141
- Li JL, Liu HL, Zhang XR, Xu JP, Hu WK, Liang M, Chen SY, Hu F, Chu DT (2009) A phase I trial of intratumoral administration of recombinant oncolytic adenovirus overexpressing HSP70 in advanced solid tumor patients. *Gene therapy* 16(3):376-382
- Lichtenfels R, Biddison WE, Schulz H, Vogt AB, Martin R (1994) CARE-LASS (calcein-release-assay), an improved fluorescence-based test system to measure cytotoxic T lymphocyte activity. *Journal of immunological methods* 172(2):227-239
- Lichtenstein DL, Krajcsi P, Esteban DJ, Tollefson AE, Wold WS (2002) Adenovirus RIDbeta subunit contains a tyrosine residue that is critical for RID-mediated receptor internalization and inhibition of Fas- and TRAIL-induced apoptosis. *Journal of virology* 76(22):11329-11342

- Liikanen I, Ahtiainen L, Hirvonen ML, Bramante S, Cerullo V, Nokisalmi P, Hemminki O, Diaconu I, Pesonen S, Koski A, Kangasniemi L, Pesonen SK, Oksanen M, Laasonen L, Partanen K, Joensuu T, Zhao F, Kanerva A, Hemminki A (2013) Oncolytic adenovirus with temozolomide induces autophagy and antitumor immune responses in cancer patients. *Mol Ther* 21(6):1212-1223
- Liu C, Hermann TE (1978) Characterization of ionomycin as a calcium ionophore. *The Journal of biological chemistry* 253(17):5892-5894
- Liu H, Jin L, Koh SB, Atanasov I, Schein S, Wu L, Zhou ZH (2010) Atomic structure of human adenovirus by cryo-EM reveals interactions among protein networks. *Science* 329(5995):1038-1043
- Liu MA (2010) Immunologic basis of vaccine vectors. *Immunity* 33(4):504-515
- Liu Q, White LR, Clark SA, Heffner DJ, Winston BW, Tibbles LA, Muruve DA (2005a) Akt/protein kinase B activation by adenovirus vectors contributes to NFkappaB-dependent CXCL10 expression. *Journal of virology* 79(23):14507-14515
- Liu TC, Hallden G, Wang Y, Brooks G, Francis J, Lemoine N, Kirn D (2004) An E1B-19 kDa gene deletion mutant adenovirus demonstrates tumor necrosis factor-enhanced cancer selectivity and enhanced oncolytic potency. *Mol Ther* 9(6):786-803
- Liu TC, Wang Y, Hallden G, Brooks G, Francis J, Lemoine NR, Kirn D (2005b) Functional interactions of antiapoptotic proteins and tumor necrosis factor in the context of a replication-competent adenovirus. *Gene therapy* 12(17):1333-1346
- Liu Y, Shevchenko A, Shevchenko A, Berk AJ (2005c) Adenovirus exploits the cellular aggresome response to accelerate inactivation of the MRN complex. *Journal of virology* 79(22):14004-14016
- Lomonosova E, Subramanian T, Chinnadurai G (2005) Mitochondrial localization of p53 during adenovirus infection and regulation of its activity by E1B-19K. *Oncogene* 24(45):6796-6808
- Lorence RM, Roberts MS, O'Neil JD, Groene WS, Miller JA, Mueller SN, Bamat MK (2007) Phase 1 clinical experience using intravenous administration of PV701, an oncolytic Newcastle disease virus. *Curr Cancer Drug Targets* 7(2):157-167
- Lowe SW, Ruley HE (1993) Stabilization of the p53 tumor suppressor is induced by adenovirus 5 E1A and accompanies apoptosis. *Genes & development* 7(4):535-545
- Lundin A, Thore A (1975) Analytical information obtainable by evaluation of the time course of firefly bioluminescence in the assay of ATP. *Anal Biochem* 66(1):47-63
- Luo Y, Chihara Y, Fujimoto K, Sasahira T, Kuwada M, Fujiwara R, Fujii K, Ohmori H, Kuniyasu H (2013) High mobility group box 1 released from necrotic cells enhances regrowth and metastasis of cancer cells that have survived chemotherapy. *Eur J Cancer* 49(3):741-751
- Lynch DH, Andreasen A, Maraskovsky E, Whitmore J, Miller RE, Schuh JC (1997) Flt3 ligand induces tumor regression and antitumor immune responses in vivo. *Nat Med* 3(6):625-631
- Macchiarelli F, Manz MG, Palucka AK, Shultz LD (2005) Humanized mice: are we there yet? *J Exp Med* 202(10):1307-1311
- Maciejczyk A, Szelachowska J, Ekiert M, Matkowski R, Halon A, Lage H, Surowiak P (2012) Elevated nuclear YB1 expression is associated with poor survival of patients with early breast cancer. *Anticancer Res* 32(8):3177-3184
- Maizel JV, Jr., White DO, Scharff MD (1968) The polypeptides of adenovirus. II. Soluble proteins, cores, top components and the structure of the virion. *Virology* 36(1):126-136
- Malvern\_Instruments. DYNAMIC LIGHT SCATTERING - COMMON TERMS DEFINED ([http://www.biophysics.bioc.cam.ac.uk/wp-content/uploads/2011/02/DLS\\_Terms\\_defined\\_Malvern.pdf](http://www.biophysics.bioc.cam.ac.uk/wp-content/uploads/2011/02/DLS_Terms_defined_Malvern.pdf), Access Date: 7/20/2013)
- Mantwill K, Kohler-Vargas N, Bernshausen A, Bieler A, Lage H, Kaszubiak A, Surowiak P, Dravits T, Treiber U, Hartung R, Gansbacher B, Holm PS (2006) Inhibition of the multidrug-resistant phenotype by targeting YB-1 with a conditionally oncolytic adenovirus: implications for combinatorial treatment regimen with chemotherapeutic agents. *Cancer research* 66(14):7195-7202

- Maraskovsky E, Brasel K, Teepe M, Roux ER, Lyman SD, Shortman K, McKenna HJ (1996) Dramatic increase in the numbers of functionally mature dendritic cells in Flt3 ligand-treated mice: multiple dendritic cell subpopulations identified. *J Exp Med* 184(5):1953-1962
- Marenstein DR, Ocampo MT, Chan MK, Altamirano A, Basu AK, Boorstein RJ, Cunningham RP, Teebor GW (2001) Stimulation of human endonuclease III by Y box-binding protein 1 (DNA-binding protein B). Interaction between a base excision repair enzyme and a transcription factor. *The Journal of biological chemistry* 276(24):21242-21249
- Martin SJ, Lennon SV, Bonham AM, Cotter TG (1990) Induction of apoptosis (programmed cell death) in human leukemic HL-60 cells by inhibition of RNA or protein synthesis. *Journal of immunology* 145(6):1859-1867
- Martins I, Tesniere A, Kepp O, Michaud M, Schlemmer F, Senovilla L, Seror C, Metivier D, Perfettini JL, Zitvogel L, Kroemer G (2009) Chemotherapy induces ATP release from tumor cells. *Cell Cycle* 8(22):3723-3728
- Martins I, Kepp O, Galluzzi L, Senovilla L, Schlemmer F, Adjemian S, Menger L, Michaud M, Zitvogel L, Kroemer G (2010) Surface-exposed calreticulin in the interaction between dying cells and phagocytes. *Ann N Y Acad Sci* 1209:77-82
- Martins I, Kepp O, Schlemmer F, Adjemian S, Tailler M, Shen S, Michaud M, Menger L, Gdoura A, Tajeddine N, Tesniere A, Zitvogel L, Kroemer G (2011) Restoration of the immunogenicity of cisplatin-induced cancer cell death by endoplasmic reticulum stress. *Oncogene* 30(10):1147-1158
- Martins I, Michaud M, Sukkurwala AQ, Adjemian S, Ma Y, Shen S, Kepp O, Menger L, Vacchelli E, Galluzzi L, Zitvogel L, Kroemer G (2012) Premortem autophagy determines the immunogenicity of chemotherapy-induced cancer cell death. *Autophagy* 8(3):413-415
- Matsumura N, Mandai M, Hamanishi J, Yamaguchi K, Fukuhara K, Yagi H, Higuchi T, Takakura K, Fujii S (2008) Immunostimulatory effect of Fms-like tyrosine kinase 3 ligand on peripheral monocyte-derived dendritic cells and natural killer cells: utilization for ovarian cancer treatment. *Oncol Rep* 19(2):505-515
- Matza D, Badou A, Jha MK, Willinger T, Antov A, Sanjabi S, Kobayashi KS, Marchesi VT, Flavell RA (2009) Requirement for AHNK1-mediated calcium signaling during T lymphocyte cytolysis. *Proceedings of the National Academy of Sciences of the United States of America* 106(24):9785-9790
- Mazerski J, Martelli S, Borowski E (1998) The geometry of intercalation complex of antitumor mitoxantrone and ametantrone with DNA: molecular dynamics simulations. *Acta Biochim Pol* 45(1):1-11
- McCormick F (2011) Mutant onco-proteins as drug targets: successes, failures, and future prospects. *Curr Opin Genet Dev* 21(1):29-33
- McGuire KA, Barlan AU, Griffin TM, Wiethoff CM (2011) Adenovirus type 5 rupture of lysosomes leads to cathepsin B-dependent mitochondrial stress and production of reactive oxygen species. *Journal of virology* 85(20):10806-10813
- McKenna HJ, Stocking KL, Miller RE, Brasel K, De Smedt T, Maraskovsky E, Maliszewski CR, Lynch DH, Smith J, Pulendran B, Roux ER, Teepe M, Lyman SD, Peschon JJ (2000) Mice lacking flt3 ligand have deficient hematopoiesis affecting hematopoietic progenitor cells, dendritic cells, and natural killer cells. *Blood* 95(11):3489-3497
- McSharry BP, Burgert HG, Owen DP, Stanton RJ, Prod'homme V, Sester M, Koebernick K, Groh V, Spies T, Cox S, Little AM, Wang EC, Tomasec P, Wilkinson GW (2008) Adenovirus E3/19K promotes evasion of NK cell recognition by intracellular sequestration of the NKG2D ligands major histocompatibility complex class I chain-related proteins A and B. *Journal of virology* 82(9):4585-4594
- Meier O, Greber UF (2004) Adenovirus endocytosis. *J Gene Med* 6 Suppl 1:S152-163
- Melcher A, Parato K, Rooney CM, Bell JC (2011) Thunder and lightning: immunotherapy and oncolytic viruses collide. *Mol Ther* 19(6):1008-1016



- Mertens C, Zhong M, Krishnaraj R, Zou W, Chen X, Darnell JE, Jr. (2006) Dephosphorylation of phosphotyrosine on STAT1 dimers requires extensive spatial reorientation of the monomers facilitated by the N-terminal domain. *Genes & development* 20(24):3372-3381
- Mertens PR, Harendza S, Pollock AS, Lovett DH (1997) Glomerular mesangial cell-specific transactivation of matrix metalloproteinase 2 transcription is mediated by YB-1. *The Journal of biological chemistry* 272(36):22905-22912
- Mertens PR, Alfonso-Jaume MA, Steinmann K, Lovett DH (1998) A synergistic interaction of transcription factors AP2 and YB-1 regulates gelatinase A enhancer-dependent transcription. *The Journal of biological chemistry* 273(49):32957-32965
- Michaud M, Martins I, Sukkurwala AQ, Adjemian S, Ma Y, Pellegatti P, Shen S, Kepp O, Scoazec M, Mignot G, Rello-Varona S, Tailler M, Menger L, Vacchelli E, Galluzzi L, Ghiringhelli F, di Virgilio F, Zitvogel L, Kroemer G (2011) Autophagy-dependent anticancer immune responses induced by chemotherapeutic agents in mice. *Science* 334(6062):1573-1577
- Miyamoto S, Inoue H, Nakamura T, Yamada M, Sakamoto C, Urata Y, Okazaki T, Marumoto T, Takahashi A, Takayama K, Nakanishi Y, Shimizu H, Tani K (2012) Coxsackievirus B3 is an oncolytic virus with immunostimulatory properties that is active against lung adenocarcinoma. *Cancer research* 72(10):2609-2621
- Mizuno NS, Zakis B, Decker RW (1975) Binding of daunomycin to DNA and the inhibition of RNA and DNA synthesis. *Cancer research* 35(6):1542-1546
- Mizushima N, Yoshimori T (2007) How to interpret LC3 immunoblotting. *Autophagy* 3(6):542-545
- Molinier-Frenkel V, Prevost-Blondel A, Hong SS, Lengagne R, Boudaly S, Magnusson MK, Boulanger P, Guillet JG (2003) The maturation of murine dendritic cells induced by human adenovirus is mediated by the fiber knob domain. *The Journal of biological chemistry* 278(39):37175-37182
- Mollenhauer HH, Morre DJ, Rowe LD (1990) Alteration of intracellular traffic by monensin; mechanism, specificity and relationship to toxicity. *Biochim Biophys Acta* 1031(2):225-246
- Msaouel P, Iankov ID, Dispenzieri A, Galanis E (2012) Attenuated oncolytic measles virus strains as cancer therapeutics. *Curr Pharm Biotechnol* 13(9):1732-1741
- Multhoff G, Botzler C, Wiesnet M, Muller E, Meier T, Wilmanns W, Issels RD (1995) A stress-inducible 72-kDa heat-shock protein (HSP72) is expressed on the surface of human tumor cells, but not on normal cells. *International journal of cancer Journal international du cancer* 61(2):272-279
- Muruve DA, Barnes MJ, Stillman IE, Libermann TA (1999) Adenoviral gene therapy leads to rapid induction of multiple chemokines and acute neutrophil-dependent hepatic injury in vivo. *Hum Gene Ther* 10(6):965-976
- Muruve DA, Petrilli V, Zaiss AK, White LR, Clark SA, Ross PJ, Parks RJ, Tschopp J (2008) The inflammasome recognizes cytosolic microbial and host DNA and triggers an innate immune response. *Nature* 452(7183):103-107
- Nemerow GR, Stewart PL, Reddy VS (2012) Structure of human adenovirus. *Curr Opin Virol* 2(2):115-121
- Nemunaitis J, Khuri F, Ganly I, Arseneau J, Posner M, Vokes E, Kuhn J, McCarty T, Landers S, Blackburn A, Romel L, Randlev B, Kaye S, Kirn D (2001) Phase II trial of intratumoral administration of ONYX-015, a replication-selective adenovirus, in patients with refractory head and neck cancer. *J Clin Oncol* 19(2):289-298
- Nemunaitis J, Tong AW, Nemunaitis M, Senzer N, Phadke AP, Bedell C, Adams N, Zhang YA, Maples PB, Chen S, Pappen B, Burke J, Ichimaru D, Urata Y, Fujiwara T (2010) A phase I study of telomerase-specific replication competent oncolytic adenovirus (telomelysin) for various solid tumors. *Mol Ther* 18(2):429-434
- Neri S, Mariani E, Meneghetti A, Cattini L, Facchini A (2001) Calcein-acetyoxymethyl cytotoxicity assay: standardization of a method allowing additional analyses on recovered effector cells and supernatants. *Clinical and diagnostic laboratory immunology* 8(6):1131-1135
- Nettelbeck DM (2003) Virotherapeutics: conditionally replicative adenoviruses for viral oncolysis. *Anticancer Drugs* 14(8):577-584

- Nicholson DW, Ali A, Thornberry NA, Vaillancourt JP, Ding CK, Gallant M, Gareau Y, Griffin PR, Labelle M, Lazebnik YA, et al. (1995) Identification and inhibition of the ICE/CED-3 protease necessary for mammalian apoptosis. *Nature* 376(6535):37-43
- Niedel JE, Kuhn LJ, Vandenbark GR (1983) Phorbol diester receptor copurifies with protein kinase C. *Proceedings of the National Academy of Sciences of the United States of America* 80(1):36-40
- Nociari M, Ocheretina O, Schoggins JW, Falck-Pedersen E (2007) Sensing infection by adenovirus: Toll-like receptor-independent viral DNA recognition signals activation of the interferon regulatory factor 3 master regulator. *Journal of virology* 81(8):4145-4157
- Norman JT, Lindahl GE, Shakib K, En-Nia A, Yilmaz E, Mertens PR (2001) The Y-box binding protein YB-1 suppresses collagen alpha 1(I) gene transcription via an evolutionarily conserved regulatory element in the proximal promoter. *The Journal of biological chemistry* 276(32):29880-29890
- Obeid M, Panaretakis T, Joza N, Tufi R, Tesniere A, van Endert P, Zitvogel L, Kroemer G (2007a) Calreticulin exposure is required for the immunogenicity of gamma-irradiation and UVC light-induced apoptosis. *Cell death and differentiation* 14(10):1848-1850
- Obeid M, Tesniere A, Ghiringhelli F, Fimia GM, Apetoh L, Perfettini JL, Castedo M, Mignot G, Panaretakis T, Casares N, Metivier D, Larochette N, van Endert P, Ciccosanti F, Piacentini M, Zitvogel L, Kroemer G (2007b) Calreticulin exposure dictates the immunogenicity of cancer cell death. *Nat Med* 13(1):54-61
- Oda Y, Ohishi Y, Saito T, Hinoshita E, Uchiumi T, Kinukawa N, Iwamoto Y, Kohno K, Kuwano M, Tsuneyoshi M (2003) Nuclear expression of Y-box-binding protein-1 correlates with P-glycoprotein and topoisomerase II alpha expression, and with poor prognosis in synovial sarcoma. *J Pathol* 199(2):251-258
- Oda Y, Ohishi Y, Basaki Y, Kobayashi H, Hirakawa T, Wake N, Ono M, Nishio K, Kuwano M, Tsuneyoshi M (2007) Prognostic implications of the nuclear localization of Y-box-binding protein-1 and CXCR4 expression in ovarian cancer: their correlation with activated Akt, LRP/MVP and P-glycoprotein expression. *Cancer Sci* 98(7):1020-1026
- Okada H, Mak TW (2004) Pathways of apoptotic and non-apoptotic death in tumour cells. *Nature reviews Cancer* 4(8):592-603
- Okamoto T, Izumi H, Imamura T, Takano H, Ise T, Uchiumi T, Kuwano M, Kohno K (2000) Direct interaction of p53 with the Y-box binding protein, YB-1: a mechanism for regulation of human gene expression. *Oncogene* 19(54):6194-6202
- Palucka K, Ueno H, Roberts L, Fay J, Banchereau J (2011) Dendritic cell subsets as vectors and targets for improved cancer therapy. *Curr Top Microbiol Immunol* 344:173-192
- Panaretakis T, Kepp O, Brockmeier U, Tesniere A, Bjorklund AC, Chapman DC, Durchschlag M, Joza N, Pierron G, van Endert P, Yuan J, Zitvogel L, Madeo F, Williams DB, Kroemer G (2009) Mechanisms of pre-apoptotic calreticulin exposure in immunogenic cell death. *EMBO J* 28(5):578-590
- Parato KA, Senger D, Forsyth PA, Bell JC (2005) Recent progress in the battle between oncolytic viruses and tumours. *Nature reviews Cancer* 5(12):965-976
- Park BH, Hwang T, Liu TC, Sze DY, Kim JS, Kwon HC, Oh SY, Han SY, Yoon JH, Hong SH, Moon A, Speth K, Park C, Ahn YJ, Daneshmand M, Rhee BG, Pinedo HM, Bell JC, Kirn DH (2008) Use of a targeted oncolytic poxvirus, JX-594, in patients with refractory primary or metastatic liver cancer: a phase I trial. *Lancet Oncol* 9(6):533-542
- Pelka P, Ablack JN, Fonseca GJ, Yousef AF, Mymryk JS (2008) Intrinsic structural disorder in adenovirus E1A: a viral molecular hub linking multiple diverse processes. *Journal of virology* 82(15):7252-7263
- Pesonen S, Kangasniemi L, Hemminki A (2011) Oncolytic adenoviruses for the treatment of human cancer: focus on translational and clinical data. *Mol Pharm* 8(1):12-28

- Pesonen S, Diaconu I, Cerullo V, Escutenaire S, Raki M, Kangasniemi L, Nokisalmi P, Dotti G, Guse K, Laasonen L, et al (2012a) Integrin targeted oncolytic adenoviruses Ad5-D24-RGD and Ad5-RGD-D24-GMCSF for treatment of patients with advanced chemotherapy refractory solid tumors. *International journal of cancer Journal international du cancer* 130(8):1937-1947
- Pesonen S, Diaconu I, Kangasniemi L, Ranki T, Kanerva A, Pesonen SK, Gerdemann U, Leen AM, Kairemo K, Oksanen M, Haavisto E, Holm SL, Karioja-Kallio A, Kauppinen S, Partanen KP, Laasonen L, Joensuu T, Alanko T, Cerullo V, Hemminki A (2012b) Oncolytic immunotherapy of advanced solid tumors with a CD40L-expressing replicating adenovirus: assessment of safety and immunologic responses in patients. *Cancer research* 72(7):1621-1631
- Prestwich RJ, Errington F, Diaz RM, Pandha HS, Harrington KJ, Melcher AA, Vile RG (2009) The case of oncolytic viruses versus the immune system: waiting on the judgment of Solomon. *Hum Gene Ther* 20(10):1119-1132
- Querido E, Blanchette P, Yan Q, Kamura T, Morrison M, Boivin D, Kaelin WG, Conaway RC, Conaway JW, Branton PE (2001) Degradation of p53 by adenovirus E4orf6 and E1B55K proteins occurs via a novel mechanism involving a Cullin-containing complex. *Genes & development* 15(23):3104-3117
- Radke JR, Siddiqui ZK, Miura TA, Routes JM, Cook JL (2008) E1A oncogene enhancement of caspase-2-mediated mitochondrial injury sensitizes cells to macrophage nitric oxide-induced apoptosis. *Journal of immunology* 180(12):8272-8279
- Raki M, Sarkioja M, Escutenaire S, Kangasniemi L, Haavisto E, Kanerva A, Cerullo V, Joensuu T, Oksanen M, Pesonen S, Hemminki A (2011) Switching the fiber knob of oncolytic adenoviruses to avoid neutralizing antibodies in human cancer patients. *J Gene Med* 13(5):253-261
- Ratto-Kim S, Currier JR, Cox JH, Excler JL, Valencia-Micolta A, Thelian D, Lo V, Sayeed E, Polonis VR, Earl PL, Moss B, Robb ML, Michael NL, Kim JH, Marovich MA (2012) Heterologous prime-boost regimens using rAd35 and rMVA vectors elicit stronger cellular immune responses to HIV proteins than homologous regimens. *PLoS One* 7(9):e45840
- Rawle FC, Tollefson AE, Wold WS, Gooding LR (1989) Mouse anti-adenovirus cytotoxic T lymphocytes. Inhibition of lysis by E3 gp19K but not E3 14.7K. *Journal of immunology* 143(6):2031-2037
- Reddy VS, Natchiar SK, Stewart PL, Nemerow GR (2010) Crystal structure of human adenovirus at 3.5 Å resolution. *Science* 329(5995):1071-1075
- Rekosh DM, Russell WC, Bellet AJ, Robinson AJ (1977) Identification of a protein linked to the ends of adenovirus DNA. *Cell* 11(2):283-295
- Riske F, Berard N, Albee K, Pan P, Henderson M, Adams K, Godwin S, Spear S (2013) Development of a platform process for adenovirus purification that removes human SET and nucleolin and provides high purity vector for gene delivery. *Biotechnol Bioeng* 110(3):848-856
- Robinson CM, Singh G, Henquell C, Walsh MP, Peigue-Lafeuille H, Seto D, Jones MS, Dyer DW, Chodosh J (2011) Computational analysis and identification of an emergent human adenovirus pathogen implicated in a respiratory fatality. *Virology* 409(2):141-147
- Robinson CM, Singh G, Lee JY, Dehghan S, Rajaiya J, Liu EB, Yousuf MA, Betensky RA, Jones MS, Dyer DW, Seto D, Chodosh J (2013) Molecular evolution of human adenoviruses. *Sci Rep* 3:1812
- Rodriguez-Rocha H, Gomez-Gutierrez JG, Garcia-Garcia A, Rao XM, Chen L, McMasters KM, Zhou HS (2011) Adenoviruses induce autophagy to promote virus replication and oncolysis. *Virology* 416(1-2):9-15
- Rognoni E, Widmaier M, Haczek C, Mantwill K, Holzmüller R, Gansbacher B, Kolk A, Schuster T, Schmid RM, Saur D, Kaszubiak A, Lage H, Holm PS (2009) Adenovirus-based virotherapy enabled by cellular YB-1 expression in vitro and in vivo. *Cancer Gene Ther* 16(10):753-763

- Rommelfanger DM, Wongthida P, Diaz RM, Kaluza KM, Thompson JM, Kottke TJ, Vile RG (2012) Systemic combination virotherapy for melanoma with tumor antigen-expressing vesicular stomatitis virus and adoptive T-cell transfer. *Cancer research* 72(18):4753-4764
- Rosenberg SA, Yang JC, Restifo NP (2004) Cancer immunotherapy: moving beyond current vaccines. *Nat Med* 10(9):909-915
- Rovere-Querini P, Capobianco A, Scaffidi P, Valentinis B, Catalanotti F, Giazson M, Dumitriu IE, Muller S, Iannacone M, Traversari C, Bianchi ME, Manfredi AA (2004) HMGB1 is an endogenous immune adjuvant released by necrotic cells. *EMBO Rep* 5(8):825-830
- Rowe WP, Huebner RJ, Gilmore LK, Parrott RH, Ward TG (1953) Isolation of a cytopathogenic agent from human adenoids undergoing spontaneous degeneration in tissue culture. *Proc Soc Exp Biol Med* 84(3):570-573
- Russell SJ, Peng KW, Bell JC (2012) Oncolytic virotherapy. *Nat Biotechnol* 30(7):658-670
- Russell WC (2000) Update on adenovirus and its vectors. *J Gen Virol* 81(Pt 11):2573-2604
- Russell WC (2009) Adenoviruses: update on structure and function. *J Gen Virol* 90(Pt 1):1-20
- Rygaard J, Povlsen CO (1969) Heterotransplantation of a human malignant tumour to "Nude" mice. *Acta Pathol Microbiol Scand* 77(4):758-760
- Ryu JK, Choi HB, Hatori K, Heisel RL, Pelech SL, McLarnon JG, Kim SU (2003) Adenosine triphosphate induces proliferation of human neural stem cells: Role of calcium and p70 ribosomal protein S6 kinase. *J Neurosci Res* 72(3):352-362
- Sadler AJ, Williams BR (2008) Interferon-inducible antiviral effectors. *Nature reviews Immunology* 8(7):559-568
- Salinovich O, Montelaro RC (1986) Reversible staining and peptide mapping of proteins transferred to nitrocellulose after separation by sodium dodecylsulfate-polyacrylamide gel electrophoresis. *Anal Biochem* 156(2):341-347
- Samuel S, Twizere JC, Bernstein LR (2005) YB-1 represses AP1-dependent gene transactivation and interacts with an AP-1 DNA sequence. *Biochem J* 388(Pt 3):921-928
- Samuel S, Beifuss KK, Bernstein LR (2007) YB-1 binds to the MMP-13 promoter sequence and represses MMP-13 transactivation via the AP-1 site. *Biochim Biophys Acta* 1769(9-10):525-531
- Sanderson NS, Puntel M, Kroeger KM, Bondale NS, Swerdlow M, Iranmanesh N, Yagita H, Ibrahim A, Castro MG, Lowenstein PR (2012) Cytotoxic immunological synapses do not restrict the action of interferon-gamma to antigenic target cells. *Proceedings of the National Academy of Sciences of the United States of America* 109(20):7835-7840
- Sarkar D, Su ZZ, Vozhilla N, Park ES, Randolph A, Valerie K, Fisher PB (2005) Targeted virus replication plus immunotherapy eradicates primary and distant pancreatic tumors in nude mice. *Cancer research* 65(19):9056-9063
- Sauthoff H, Heitner S, Rom WN, Hay JG (2000) Deletion of the adenoviral E1b-19kD gene enhances tumor cell killing of a replicating adenoviral vector. *Hum Gene Ther* 11(3):379-388
- Scaffidi P, Misteli T, Bianchi ME (2002) Release of chromatin protein HMGB1 by necrotic cells triggers inflammation. *Nature* 418(6894):191-195
- Schagen FH, Ossevoort M, Toes RE, Hoeben RC (2004) Immune responses against adenoviral vectors and their transgene products: a review of strategies for evasion. *Crit Rev Oncol Hematol* 50(1):51-70
- Scherer WF, Syverton JT, Gey GO (1953) Studies on the propagation in vitro of poliomyelitis viruses. IV. Viral multiplication in a stable strain of human malignant epithelial cells (strain HeLa) derived from an epidermoid carcinoma of the cervix. *J Exp Med* 97(5):695-710
- Schierer S, Hesse A, Knippertz I, Kaempgen E, Baur AS, Schuler G, Steinkasserer A, Nettelbeck DM (2012) Human dendritic cells efficiently phagocytose adenoviral oncolysate but require additional stimulation to mature. *International journal of cancer Journal international du cancer* 130(7):1682-1694

- Schirmmacher V, Bosslet K, Shantz G, Clauer K, Hubsch D (1979) Tumor metastases and cell-mediated immunity in a model system in DBA/2 mice. IV. Antigenic differences between a metastasizing variant and the parental tumor line revealed by cytotoxic T lymphocytes. *International journal of cancer Journal international du cancer* 23(2):245-252
- Schnizlein-Bick CT, Spritzler J, Wilkening CL, Nicholson JK, O'Gorman MR (2000) Evaluation of TruCount absolute-count tubes for determining CD4 and CD8 cell numbers in human immunodeficiency virus-positive adults. Site Investigators and The NIAID DAIDS New Technologies Evaluation Group. *Clinical and diagnostic laboratory immunology* 7(3):336-343
- Senzer NN, Kaufman HL, Amatruda T, Nemunaitis M, Reid T, Daniels G, Gonzalez R, Glaspy J, Whitman E, Harrington K, Goldsweig H, Marshall T, Love C, Coffin R, Nemunaitis JJ (2009) Phase II clinical trial of a granulocyte-macrophage colony-stimulating factor-encoding, second-generation oncolytic herpesvirus in patients with unresectable metastatic melanoma. *J Clin Oncol* 27(34):5763-5771
- Serano RD, Pegram CN, Bigner DD (1980) Tumorigenic cell culture lines from a spontaneous VM/Dk murine astrocytoma (SMA). *Acta Neuropathol* 51(1):53-64
- Sester M, Ruzsics Z, Mackley E, Burgert HG (2013) The transmembrane domain of the adenovirus E3/19K protein acts as an endoplasmic reticulum retention signal and contributes to intracellular sequestration of major histocompatibility complex class I molecules. *Journal of virology* 87(11):6104-6117
- Shibahara K, Sugio K, Osaki T, Uchiumi T, Maehara Y, Kohno K, Yasumoto K, Sugimachi K, Kuwano M (2001) Nuclear expression of the Y-box binding protein, YB-1, as a novel marker of disease progression in non-small cell lung cancer. *Clin Cancer Res* 7(10):3151-3155
- Shiota M, Izumi H, Onitsuka T, Miyamoto N, Kashiwagi E, Kidani A, Yokomizo A, Naito S, Kohno K (2008) Twist promotes tumor cell growth through YB-1 expression. *Cancer research* 68(1):98-105
- Shiota M, Yokomizo A, Tada Y, Uchiumi T, Inokuchi J, Tatsugami K, Kuroiwa K, Yamamoto K, Seki N, Naito S (2010) P300/CBP-associated factor regulates Y-box binding protein-1 expression and promotes cancer cell growth, cancer invasion and drug resistance. *Cancer Sci* 101(8):1797-1806
- Shultz LD, Brehm MA, Garcia-Martinez JV, Greiner DL (2012) Humanized mice for immune system investigation: progress, promise and challenges. *Nature reviews Immunology* 12(11):786-798
- Singh B, Mitchison DA (1954) Bactericidal activity of streptomycin and isoniazid against tubercle bacilli. *British medical journal* 1(4854):130-132
- Skehan P, Storeng R, Scudiero D, Monks A, McMahon J, Vistica D, Warren JT, Bokesch H, Kenney S, Boyd MR (1990) New colorimetric cytotoxicity assay for anticancer-drug screening. *J Natl Cancer Inst* 82(13):1107-1112
- Smith JG, Wiethoff CM, Stewart PL, Nemerow GR (2010) Adenovirus. *Curr Top Microbiol Immunol* 343:195-224
- Smith PK, Krohn RI, Hermanson GT, Mallia AK, Gartner FH, Provenzano MD, Fujimoto EK, Goeke NM, Olson BJ, Klenk DC (1985) Measurement of protein using bicinchoninic acid. *Anal Biochem* 150(1):76-85
- Sohn SY, Hearing P (2011) Adenovirus sequesters phosphorylated STAT1 at viral replication centers and inhibits STAT dephosphorylation. *Journal of virology* 85(15):7555-7562
- Soop T, Nashchekin D, Zhao J, Sun X, Alzhanova-Ericsson AT, Bjorkroth B, Ovchinnikov L, Daneholt B (2003) A p50-like Y-box protein with a putative translational role becomes associated with pre-mRNA concomitant with transcription. *J Cell Sci* 116(Pt 8):1493-1503
- Spisek R, Charalambous A, Mazumder A, Vesole DH, Jagannath S, Dhodapkar MV (2007) Bortezomib enhances dendritic cell (DC)-mediated induction of immunity to human myeloma via exposure of cell surface heat shock protein 90 on dying tumor cells: therapeutic implications. *Blood* 109(11):4839-4845

- Spitkovsky D, Jansen-Durr P, Karsenti E, Hoffman I (1996) S-phase induction by adenovirus E1A requires activation of cdc25a tyrosine phosphatase. *Oncogene* 12(12):2549-2554
- Spurgeon ME, Ornelles DA (2009) The adenovirus E1B 55-kilodalton and E4 open reading frame 6 proteins limit phosphorylation of eIF2alpha during the late phase of infection. *Journal of virology* 83(19):9970-9982
- Stagg J, Smyth MJ (2010) Extracellular adenosine triphosphate and adenosine in cancer. *Oncogene* 29(39):5346-5358
- Stangl S, Gehrman M, Riegger J, Kuhs K, Riederer I, Sievert W, Hube K, Mocikat R, Dressel R, Kremmer E, Pockley AG, Friedrich L, Vigh L, Skerra A, Multhoff G (2011) Targeting membrane heat-shock protein 70 (Hsp70) on tumors by cmHsp70.1 antibody. *Proceedings of the National Academy of Sciences of the United States of America* 108(2):733-738
- Stark GR, Kerr IM (1992) Interferon-dependent signaling pathways: DNA elements, transcription factors, mutations, and effects of viral proteins. *J Interferon Res* 12(3):147-151
- Steel JC, Morrison BJ, Mannan P, Abu-Asab MS, Wildner O, Miles BK, Yim KC, Ramanan V, Prince GA, Morris JC (2007) Immunocompetent syngeneic cotton rat tumor models for the assessment of replication-competent oncolytic adenovirus. *Virology* 369(1):131-142
- Stein U, Jurchott K, Walther W, Bergmann S, Schlag PM, Royer HD (2001) Hyperthermia-induced nuclear translocation of transcription factor YB-1 leads to enhanced expression of multidrug resistance-related ABC transporters. *The Journal of biological chemistry* 276(30):28562-28569
- Stevenson SC, Rollence M, Marshall-Neff J, McClelland A (1997) Selective targeting of human cells by a chimeric adenovirus vector containing a modified fiber protein. *Journal of virology* 71(6):4782-4790
- Stojdl DF, Lichty B, Knowles S, Marius R, Atkins H, Sonenberg N, Bell JC (2000) Exploiting tumor-specific defects in the interferon pathway with a previously unknown oncolytic virus. *Nat Med* 6(7):821-825
- Stratford AL, Fry CJ, Desilets C, Davies AH, Cho YY, Li Y, Dong Z, Berquin IM, Roux PP, Dunn SE (2008) Y-box binding protein-1 serine 102 is a downstream target of p90 ribosomal S6 kinase in basal-like breast cancer cells. *Breast Cancer Res* 10(6):R99
- Sutherland BW, Kucab J, Wu J, Lee C, Cheang MC, Yorida E, Turbin D, Dedhar S, Nelson C, Pollak M, Leighton Grimes H, Miller K, Badve S, Huntsman D, Blake-Gilks C, Chen M, Pallen CJ, Dunn SE (2005) Akt phosphorylates the Y-box binding protein 1 at Ser102 located in the cold shock domain and affects the anchorage-independent growth of breast cancer cells. *Oncogene* 24(26):4281-4292
- Swaminathan S, Thimmapaya B (1995) Regulation of adenovirus E2 transcription unit. *Curr Top Microbiol Immunol* 199 (Pt 3):177-194
- Takeichi T, Mocevicius P, Deduchovas O, Salnikova O, Castro-Santa E, Buchler MW, Schmidt J, Ryschich E (2012) alphaL beta2 integrin is indispensable for CD8+ T-cell recruitment in experimental pancreatic and hepatocellular cancer. *International journal of cancer* 130(9):2067-2076
- Tamanini A, Nicolis E, Bonizzato A, Bezzeri V, Melotti P, Assael BM, Cabrini G (2006) Interaction of adenovirus type 5 fiber with the coxsackievirus and adenovirus receptor activates inflammatory response in human respiratory cells. *Journal of virology* 80(22):11241-11254
- Tau GZ, Cowan SN, Weisburg J, Braunstein NS, Rothman PB (2001) Regulation of IFN-gamma signaling is essential for the cytotoxic activity of CD8(+) T cells. *Journal of immunology* 167(10):5574-5582
- Ternovoi VV, Le LP, Belousova N, Smith BF, Siegal GP, Curiel DT (2005) Productive replication of human adenovirus type 5 in canine cells. *Journal of virology* 79(2):1308-1311
- Tesniere A, Schlemmer F, Boige V, Kepp O, Martins I, Ghiringhelli F, Aymeric L, Michaud M, Apetoh L, Barault L, Mendiboure J, Pignon JP, Jooste V, van Endert P, Ducreux M, Zitvogel L, Piard F, Kroemer G (2010) Immunogenic death of colon cancer cells treated with oxaliplatin. *Oncogene* 29(4):482-491

- Thaci B, Ulasov IV, Wainwright DA, Lesniak MS (2011) The challenge for gene therapy: innate immune response to adenoviruses. *Oncotarget* 2(3):113-121
- Thirukkumaran C, Morris DG (2009) Oncolytic viral therapy using reovirus. *Methods Mol Biol* 542:607-634
- Thomas MA, Spencer JF, La Regina MC, Dhar D, Tollefson AE, Toth K, Wold WS (2006) Syrian hamster as a permissive immunocompetent animal model for the study of oncolytic adenovirus vectors. *Cancer research* 66(3):1270-1276
- Thorburn J, Horita H, Redzic J, Hansen K, Frankel AE, Thorburn A (2009) Autophagy regulates selective HMGB1 release in tumor cells that are destined to die. *Cell death and differentiation* 16(1):175-183
- Thorne SH, Negrin RS, Contag CH (2006) Synergistic antitumor effects of immune cell-viral biotherapy. *Science* 311(5768):1780-1784
- To K, Fotovati A, Reipas KM, Law JH, Hu K, Wang J, Astanehe A, Davies AH, Lee L, Stratford AL, Raouf A, Johnson P, Berquin IM, Royer HD, Eaves CJ, Dunn SE (2010) Y-box binding protein-1 induces the expression of CD44 and CD49f leading to enhanced self-renewal, mammosphere growth, and drug resistance. *Cancer research* 70(7):2840-2851
- Tollefson AE, Scaria A, Hermiston TW, Ryerse JS, Wold LJ, Wold WS (1996) The adenovirus death protein (E3-11.6K) is required at very late stages of infection for efficient cell lysis and release of adenovirus from infected cells. *Journal of virology* 70(4):2296-2306
- Tollefson AE, Hermiston TW, Lichtenstein DL, Colle CF, Tripp RA, Dimitrov T, Toth K, Wells CE, Doherty PC, Wold WS (1998) Forced degradation of Fas inhibits apoptosis in adenovirus-infected cells. *Nature* 392(6677):726-730
- Tomko RP, Johansson CB, Totrov M, Abagyan R, Frisen J, Philipson L (2000) Expression of the adenovirus receptor and its interaction with the fiber knob. *Exp Cell Res* 255(1):47-55
- Trabanelli S, Ocadlikova D, Gulinelli S, Curti A, Salvestrini V, Vieira RP, Idzko M, Di Virgilio F, Ferrari D, Lemoli RM (2012) Extracellular ATP exerts opposite effects on activated and regulatory CD4+ T cells via purinergic P2 receptor activation. *Journal of immunology* 189(3):1303-1310
- Uchiumi T, Fotovati A, Sasaguri T, Shibahara K, Shimada T, Fukuda T, Nakamura T, Izumi H, Tsuzuki T, Kuwano M, Kohno K (2006) YB-1 is important for an early stage embryonic development: neural tube formation and cell proliferation. *The Journal of biological chemistry* 281(52):40440-40449
- Uramoto H, Izumi H, Ise T, Tada M, Uchiumi T, Kuwano M, Yasumoto K, Funa K, Kohno K (2002) p73 Interacts with c-Myc to regulate Y-box-binding protein-1 expression. *The Journal of biological chemistry* 277(35):31694-31702
- Vaha-Koskela MJ, Heikkila JE, Hinkkanen AE (2007) Oncolytic viruses in cancer therapy. *Cancer Lett* 254(2):178-216
- Vellinga J, Van der Heijdt S, Hoeben RC (2005) The adenovirus capsid: major progress in minor proteins. *J Gen Virol* 86(Pt 6):1581-1588
- Venereau E, Casalgrandi M, Schiraldi M, Antoine DJ, Cattaneo A, De Marchis F, Liu J, Antonelli A, Preti A, Raeli L, Shams SS, Yang H, Varani L, Andersson U, Tracey KJ, Bachi A, Ugucioni M, Bianchi ME (2012) Mutually exclusive redox forms of HMGB1 promote cell recruitment or proinflammatory cytokine release. *J Exp Med* 209(9):1519-1528
- Viney JL, Mowat AM, O'Malley JM, Williamson E, Fanger NA (1998) Expanding dendritic cells in vivo enhances the induction of oral tolerance. *Journal of immunology* 160(12):5815-5825
- Wakimoto H, Fulci G, Tyminski E, Chiocca EA (2004) Altered expression of antiviral cytokine mRNAs associated with cyclophosphamide's enhancement of viral oncolysis. *Gene therapy* 11(2):214-223
- Walsh MP, Seto J, Jones MS, Chodosh J, Xu W, Seto D (2010) Computational analysis identifies human adenovirus type 55 as a re-emergent acute respiratory disease pathogen. *J Clin Microbiol* 48(3):991-993

- Wang H, Dai J, Hou S, Qian W, Li B, Ma J, Fan X, Zhao J, Yang S, Sang H, Yang Q, Wang R, Guo Y (2005) Treatment of hepatocellular carcinoma with adenoviral vector-mediated Flt3 ligand gene therapy. *Cancer Gene Ther* 12(9):769-777
- Wang H, Wei F, Zhang J, Wang F, Li H, Chen X, Xie K, Wang Y, Li C, Huang Q (2012) A novel immunocompetent murine tumor model for the evaluation of RCAd-enhanced RDAd transduction efficacy. *Tumour Biol* 33(4):1245-1253
- Wang M, Chen PW, Bronte V, Rosenberg SA, Restifo NP (1995) Anti-tumor activity of cytotoxic T lymphocytes elicited with recombinant and synthetic forms of a model tumor-associated antigen. *J Immunother Emphasis Tumor Immunol* 18(3):139-146
- Wang Y, Hallden G, Hill R, Anand A, Liu TC, Francis J, Brooks G, Lemoine N, Kirn D (2003) E3 gene manipulations affect oncolytic adenovirus activity in immunocompetent tumor models. *Nat Biotechnol* 21(11):1328-1335
- Wei Q, Zhang Y, Sun L, Jia X, Huai W, Yu C, Wan Z, Han L (2013) High dose of extracellular ATP switched autophagy to apoptosis in anchorage-dependent and anchorage-independent hepatoma cells. *Purinergic Signal* [Epub ahead of print]
- Weitzman MD (2005) Functions of the adenovirus E4 proteins and their impact on viral vectors. *Front Biosci* 10:1106-1117
- White E (2001) Regulation of the cell cycle and apoptosis by the oncogenes of adenovirus. *Oncogene* 20(54):7836-7846
- Wickham TJ, Mathias P, Cheresch DA, Nemerow GR (1993) Integrins alpha v beta 3 and alpha v beta 5 promote adenovirus internalization but not virus attachment. *Cell* 73(2):309-319
- Wildner O, Blaese RM, Morris JC (1999) Therapy of colon cancer with oncolytic adenovirus is enhanced by the addition of herpes simplex virus-thymidine kinase. *Cancer research* 59(2):410-413
- Wirth B. Charakterisierung adenoviraler Vektoren zur regulierten Expression der BS-RNase ([http://edoc.ub.uni-muenchen.de/11393/1/Wirth\\_Bianca.pdf](http://edoc.ub.uni-muenchen.de/11393/1/Wirth_Bianca.pdf), Access Date: 7/19/2013)
- Wold WS, Toth K (2012) Chapter three--Syrian hamster as an animal model to study oncolytic adenoviruses and to evaluate the efficacy of antiviral compounds. *Adv Cancer Res* 115:69-92
- Woller N, Knocke S, Mundt B, Gurlevik E, Struver N, Kloos A, Boozari B, Schache P, Manns MP, Malek NP, Sparwasser T, Zender L, Wirth TC, Kubicka S, Kuhnel F (2011) Virus-induced tumor inflammation facilitates effective DC cancer immunotherapy in a Treg-dependent manner in mice. *The Journal of clinical investigation* 121(7):2570-2582
- Wollmann G, Davis JN, Bosenberg MW, van den Pol AN (2013) Vesicular stomatitis virus variants selectively infect and kill human melanomas but not normal melanocytes. *Journal of virology* 87(12):6644-6659
- Wu J, Lee C, Yokom D, Jiang H, Cheang MC, Yorida E, Turbin D, Berquin IM, Mertens PR, Iftner T, Gilks CB, Dunn SE (2006) Disruption of the Y-box binding protein-1 results in suppression of the epidermal growth factor receptor and HER-2. *Cancer research* 66(9):4872-4879
- Wu J, Stratford AL, Astanehe A, Dunn SE (2007) YB-1 is a Transcription/Translation Factor that Orchestrates the Oncogenome by Hardwiring Signal Transduction to Gene Expression. *Transl Oncogenomics* 2:49-65
- Xu W, Zhou L, Qin R, Tang H, Shen H (2009) Nuclear expression of YB-1 in diffuse large B-cell lymphoma: correlation with disease activity and patient outcome. *Eur J Haematol* 83(4):313-319
- Yang Y, Xiang Z, Ertl HC, Wilson JM (1995) Upregulation of class I major histocompatibility complex antigens by interferon gamma is necessary for T-cell-mediated elimination of recombinant adenovirus-infected hepatocytes in vivo. *Proceedings of the National Academy of Sciences of the United States of America* 92(16):7257-7261
- Younghusband HB, Tyndall C, Bellett AJ (1979) Replication and interaction of virus DNA and cellular DNA in mouse cells infected by a human adenovirus. *J Gen Virol* 45(2):455-467
- Zaiss AK, Machado HB, Herschman HR (2009) The influence of innate and pre-existing immunity on adenovirus therapy. *J Cell Biochem* 108(4):778-790



- Zamarin D, Palese P (2012) Oncolytic Newcastle disease virus for cancer therapy: old challenges and new directions. *Future Microbiol* 7(3):347-367
- Zhang Y, Gong LH, Zhang HQ, Du Q, You JF, Tian XX, Fang WG (2010) Extracellular ATP enhances in vitro invasion of prostate cancer cells by activating Rho GTPase and upregulating MMPs expression. *Cancer Lett* 293(2):189-197
- Zhou F (2009) Molecular mechanisms of IFN-gamma to up-regulate MHC class I antigen processing and presentation. *International reviews of immunology* 28(3-4):239-260
- Zhu J, Huang X, Yang Y (2007) Innate immune response to adenoviral vectors is mediated by both Toll-like receptor-dependent and -independent pathways. *Journal of virology* 81(7):3170-3180
- Zhu J, Huang X, Yang Y (2008) A critical role for type I IFN-dependent NK cell activation in innate immune elimination of adenoviral vectors in vivo. *Mol Ther* 16(7):1300-1307
- Zhu W, Wei L, Zhang H, Chen J, Qin X (2012) Oncolytic adenovirus armed with IL-24 inhibits the growth of breast cancer in vitro and in vivo. *J Exp Clin Cancer Res* 31:51
- Zitvogel L, Apetoh L, Ghiringhelli F, Andre F, Tesniere A, Kroemer G (2008a) The anticancer immune response: indispensable for therapeutic success? *The Journal of clinical investigation* 118(6):1991-2001
- Zitvogel L, Apetoh L, Ghiringhelli F, Kroemer G (2008b) Immunological aspects of cancer chemotherapy. *Nature reviews Immunology* 8(1):59-73
- Zitvogel L, Kepp O, Kroemer G (2011) Immune parameters affecting the efficacy of chemotherapeutic regimens. *Nat Rev Clin Oncol* 8(3):151-160
- Zong WX, Thompson CB (2006) Necrotic death as a cell fate. *Genes & development* 20(1):1-15

## Acknowledgements

First of all I would like to thank PD Dr. Per Sonne Holm for giving me the chance to do my dissertation work in his group and for providing the interesting topic. Thank you for your confidence in me, the good working environment, and the helpful scientific support and discussion.

Moreover, I would like to thank Prof. Dr. Bernd Gänsbacher for giving me the chance to work in his institute.

I especially thank Prof. Dr. Gabriele Multhoff and PD Dr. Oliver Ebert for the support and helpful discussion within my Ph.D. committee.

I thank the members of the executive committee of the Ph.D. program Medical Life Science and Technology for admitting me into the program, and especially Dr. Katrin Offe and Desislava Zlatanova for the organizational help within the Ph.D. program.

For financial support, I thank the commission for clinical research of the medical faculty of the Technical University Munich (KKF) for admission to my scholarship.

I thank Prof. Dr. Christian Plank, PD Dr. Ulrike Naumann, and Prof. Dr. Jürgen Schlegel for giving me the chance to do the Ph.D. program lab rotations in their laboratories and for their support.

PD Dr. Florian Kühnel and Dr. Norman Woller from the Hannover Medical School I would like to thank for their kind help with planning of the *in vivo* experiments and answering all upcoming immunological and experimental questions.

I would like to thank Prof. Dr. Gabriele Multhoff and Dr. Daniela Schilling for admission and introduction to their ELISpot reader, and Prof. Dr. Axel Walch and Andreas Voss from the Institute of Pathology Helmholtz Zentrum for admission to their fluorescence microscope.

I would like to thank Dirk Weinspach, Youlia Kostova, Barbara Grünwald, Haissi Cui, Julia Kobuch, Dr. Ulrike Schillinger, and Edelburga Hammerschmidt from the Institute of Experimental Oncology a lot for their help, friendship, and support.

Furthermore, I thank the present and former members of the AG Holm, especially Savoula Michailidou, Hilde Kalvelage, Klaus Mantwill, Elisabeth Mitterwallner, Dr. Regina Holzmüller, and Dr. Dialekti Vlaskou for their help and the positive working environment.

A special thank goes to my friends and to my brother for always supporting and encouraging me. I especially thank my parents for their unlimited support and for always being there for me.

## Statutory Declaration

I solemnly declare that I have written the dissertation entitled

Immunological aspects of YB-1-dependent oncolytic virotherapy

and submitted it to the Faculty of Medicine of the Technical University Munich for doctoral examination at the

Institute of Experimental Oncology and Therapy Research

under the guidance and supervision of

PD Dr. Per Sonne Holm

without other help and, while writing it, only used aids in accordance with the academic and examination regulations of the Ph.D. program in Medical Life Science and Technology.

- I have not involved any organization that offers doctoral advisors for a fee or partially or entirely fulfills examination obligations required of me on my behalf.
- I have submitted the dissertation in this or a similar form in no other examination procedure as an examination achievement.
- The complete dissertation was published in

\_\_\_\_\_.

The Faculty of Medicine has approved the advance publication.

- I have not yet acquired the Doctor of Philosophy and I have not definitely failed in a previous doctoral procedure for the Doctor of Philosophy.
- I have already submitted a dissertation with the subject

\_\_\_\_\_

at the Faculty of \_\_\_\_\_

of the university \_\_\_\_\_

on \_\_\_\_\_ to apply for admission to the doctoral examination with the result:

\_\_\_\_\_

I am familiar with the academic and examination regulations of the Ph.D. program in Medical Life Science and Technology of the Technical University Munich.

Munich, 7/31/13

\_\_\_\_\_  
Signature

## Curriculum Vitae

**Name** Vroni Girbinger  
**Date of birth** 9/25/1984  
**Place of birth** Starnberg  
**Nationality** German  
**Address** Daiserstr. 22, 81371 Munich  
**Email** vroni.girbinger@gmx.de  
**Marital status** Single

### School Education

1991-1995 Grundschule Süd Moosburg  
1995-2004 Karl-Ritter-von-Frisch Gymnasium Moosburg

### Academic education

2004-2007 Bachelor of Science in Molecular Biotechnology at the TU Munich  
Bachelor`s Thesis at the Institute of Pharmacology and Toxicology,  
laboratory of Dr. Andrea Welling; Topic: "Die Wirkung von Antiepileptika auf  
Natriumkanäle muriner Pankreasinseln"

2007-2009 Master of Science in Molecular Biotechnology at the TU Munich  
Subjects: Molecular Medicine; Molecular Infection Biology;  
Protein Engineering and Biochemistry; Genetics  
10 months studies at the Uppsala University, Sweden (ERASMUS program)  
Master`s Thesis at the Institute of Experimental Oncology and Therapy Research,  
laboratory of PD Dr. Per Holm; Topic: "Does Adenovirus wild type induce  
posttranslational modifications in the YB-1 protein?"

2009-2013 Ph.D. program Medical Life Science and Technology  
Ph.D. Thesis at the Institute of Experimental Oncology and Therapy Research,  
laboratory of PD Dr. Per Holm; Topic: "Immunological aspects of YB-1-dependent  
oncolytic virotherapy"